ALMA MATER STUDIORUM
UNIVERSITÀ DI BOLOGNA

DOTTORATO DI RICERCA IN

SCIENZE BIOMEDICHE E NEUROMOTORIE

Ciclo 37

Settore Concorsuale: 06/A2 - PATOLOGIA GENERALE E PATOLOGIA CLINICA

Settore Scientifico Disciplinare: MED/04 - PATOLOGIA GENERALE

LACTATE SIGNALLING IN CHEMORESISTANCE: FROM A POTENTIAL THREAT TO A THERAPEUTIC OPPORTUNITY

Presentata da: Valentina Rossi

Coordinatore Dottorato:

Matilde Yung Follo

Supervisore:

Giuseppina Di Stefano

Co-supervisore:

Paolo Caraceni

Esame finale anno 2025

ALMA MATER STUDIORUM
UNIVERSITÀ DI BOLOGNA

Ph.D. PROGRAMME IN

BIOMEDICAL AND NEUROMOTOR SCIENCES

Cycle 37th

Academic recruitment field: 06/A2 - GENERAL PATHOLOGY AND CLINICAL PATHOLOGY

Academic discipline: MED/04 - GENERAL PATHOLOGY

LACTATE SIGNALLING IN CHEMORESISTANCE: FROM A POTENTIAL THREAT TO A THERAPEUTIC OPPORTUNITY

Ph.D. student: Valentina Rossi

Coordinator of the Ph.D. program:

Matilde Yung Follo

Supervisor:

Giuseppina Di Stefano

Co-supervisor:

Paolo Caraceni

Final exam, 2025

[This page is intentionally left blank]

TABLE OF CONTENTS

[This page is intentionally left blank]

ABSTRACT

Cancer cells are characterized by high glucose consumption, leading to increased lactate production. Once considered a waste product, lactate was recently shown to take part in the epigenetic regulation of gene expression, in promoting the unlimited growth of cancer cells and in facilitating metastasis. Furthermore, aberrant metabolism of cancer cells emerged as significant factor affecting drug efficacy and several evidences correlated some therapeutic failures with changes in cell metabolic asset.

My Ph.D. project is focused at characterizing the effects of lactate signalling in cancer cells, with special attention to the potential role of this metabolite in modifying the response of cancer cells to chemotherapeutic treatments and in promoting the onset of drug resistance. In particular, this thesis describes how lactate influences the response of cancer cells to some commonly used chemotherapeutic drugs, such us cisplatin, doxorubicin and tamoxifen, while also highlighting the potential role of lactate in promoting the activated state of the EGFR receptor. The investigation was conducted using different cancer cell lines, with special attention on colon and breast adenocarcinomas. Overall, the described experiments have elucidated that lactate can induce drug resistance through pathways that may differ according to cancer cell histology.

In agreement with our findings, it would be essential to develop strategies to obtain the inhibition of lactate production. A direct way for achieving this goal is through the inhibition of LDHA, the primary enzyme isoform responsible for lactate production in cancer cells. In this context, I collaborated in a study coordinated by Professors Alejandro Hochkoeppler and Luca Gentilucci, (University of Bologna) who designed peptides with potential inhibition on LDHA activity. The conclusive section of this thesis describes experiments aimed at evaluating the efficacy of these peptides in cancer cell cultures.

KEYWORDS

Lactate, cancer cell metabolism, drug resistance, LDH inhibitors.

ABBREVIATIONS

AB: abasic sites

Acetyl-CoA: acetyl-coenzyme A

ADP: adenosine diphosphate

AKT: protein kinase B

ALDH1: aldehyde Dehydrogenase

ANT: adenine nucleotide translocase

ATCC: American Type Culture Collection

ATP: adenosine triphosphate

cAMP: cyclic adenosine monophosphate

CCNE2: cyclin E2

CDK1: cyclin dependent kinase 1

CPL: cisplatin

CRM197: cross reacting material 197

DCF: fluorescent dichlorofluorescin

DCF-DA: 2′,7′-dichlorofluorescin diacetate

D-H9c2: differentiated H9c2 cultures

DMEM: Dulbecco's minimal essential medium

DMSO: dimethyl sulfoxide

DOXO: doxorubicin

ECACC: European Collection of Authenticated Cell Cultures

E-CAD: epithelial cadherin

EGF: epidermal growth factor

EGFR: epidermal growth factor receptor

EMT: epithelial-mesenchymal transition

ERα: oestrogen alpha-receptor

ER-positive breast cancer: ER+ breast cancer

FANC-A: Fanconi anaemia complementation group A

FBS: fetal bovine serum

FDA: Food and Drug Administration

FEN1: flap structure-specific endonuclease 1 gene

GDH: glutamate dehydrogenase enzyme

GRP81: G-protein coupled receptor 81

GRP94: glucose-regulated protein 94

GSTP-1: glutathione S-Transferase π1

HATs: histone acetyltransferases

HBEGF: heparin-binding EGF

HDACs: histone deacetylases

HGF: hepatocyte growth factor

HMGB1: high mobility group box 1

HIF-1α: hypoxia-inducible-factor1-alpha

H2AFX: H2AX variant histone

HSP70: inducible heat shock protein 70

HSC70: constitutive heat shock 70

HK: hexokinase

HK2: hexokinase-2

HR: homologous recombination

KEGG: Kyoto Encyclopedia of Genes and Genomes

Km: Michaelis constant

Kla: histone lysine lactylation

K388: lysine 388

LDH: lactate dehydrogenase

lactyl-CoA: lactyl coenzyme A

LIG1:DNA Ligase 1

MCTs: monocarboxylate transporters

MRP: multidrug resistance proteins

MMPs: metalloproteinases

NADH: nicotinamide adenine dinucleotide + hydrogen

NAD: nicotinamide adenine dinucleotide

NSCLC: non-small cell lung cancer

NBS1: Nibrin

NR: neutral red

N-CAD: neural cadherin

OXPHOS: oxidative phosphorylation

OAA: oxaloacetate

OXA: oxamate

PDH: pyruvate dehydrogenase

PET: positron emission tomography

PKA: activates protein kinase A

PCNA: proliferating cell nuclear antigen

PD-L1: programmed death-ligand 1

PI3K: phosphatidylinositol 3-kinase

PKM2: pyruvate kinase M2

ROS: reactive oxygen species

RFC4: replication factor C subunit 4

siRNAs: small interfering RNAs

SIRT1-3: sirtuins 1-3

SMUG1: selective monofunctional uracil DNA glycosylase

SOD1: superoxide dismutase 1

SOD2: superoxide dismutase 2

STRING: Search Tool for the Retrieval of Interacting Genes

TAM: Tamoxifen

TAZ: taffazin

TCA: tricarboxylic acid cycle

TGF-β/SMAD2: transforming growth factor β

TOP2: topoisomerase-2

TP73: tumour protein p73

Tregs: regulatory T cells

TRAP1: receptor-associated protein 1

VEGF: vascular endothelial growth factor

Y10: tyrosine 10

Y83: tyrosine 83

α-MHC: α-myosin heavy chain

β-GAL: β-galactosidase

γ-H2AX: phosphorylated H2AX

8-OHdG: 8-hydroxy-2-deoxy guanosine

^{18}F-FDG: ^{18}F-Fluorodeoxyglucose

[This page is intentionally left blank]

1. INTRODUCTION

1.1 Glycolytic metabolism and Warburg effect

Glucose serves as the primary cellular fuel for energy generation through a sequence of enzymatic reactions. The key stages in this process include glycolysis, the tricarboxylic acid cycle (TCA) and oxidative phosphorylation (OXPHOS)[1,2].

Within glycolysis, a single glucose molecule yields four adenosine triphosphate (ATP), two NADH and two molecules of pyruvate[3]. The fate of pyruvate differs based on the presence of oxygen: under aerobic conditions, it enters in mitochondria for OXPHOS and this process is define as oxidative metabolism; while under anaerobic conditions, pyruvate remains in the cytoplasm and it transformed to lactate by lactate dehydrogenase (LDH), a process named anaerobic metabolism[4] (Figure 1). Normal cells would primarily use oxidative metabolism, which involves glycolysis followed by TCA cycle (Krebs cycle) and OXPHOS to efficiently produce ATP, the cell's energy currency[5]. Nucleotides, amino acids and lipids are supplied by intermediate metabolites from these pathways; for instance, glycolytic intermediates are used for non-essential amino acids, acetyl-coenzyme A (acetyl-CoA) contributes to fatty acid synthesis, and ribose is utilized for nucleotide production[6].

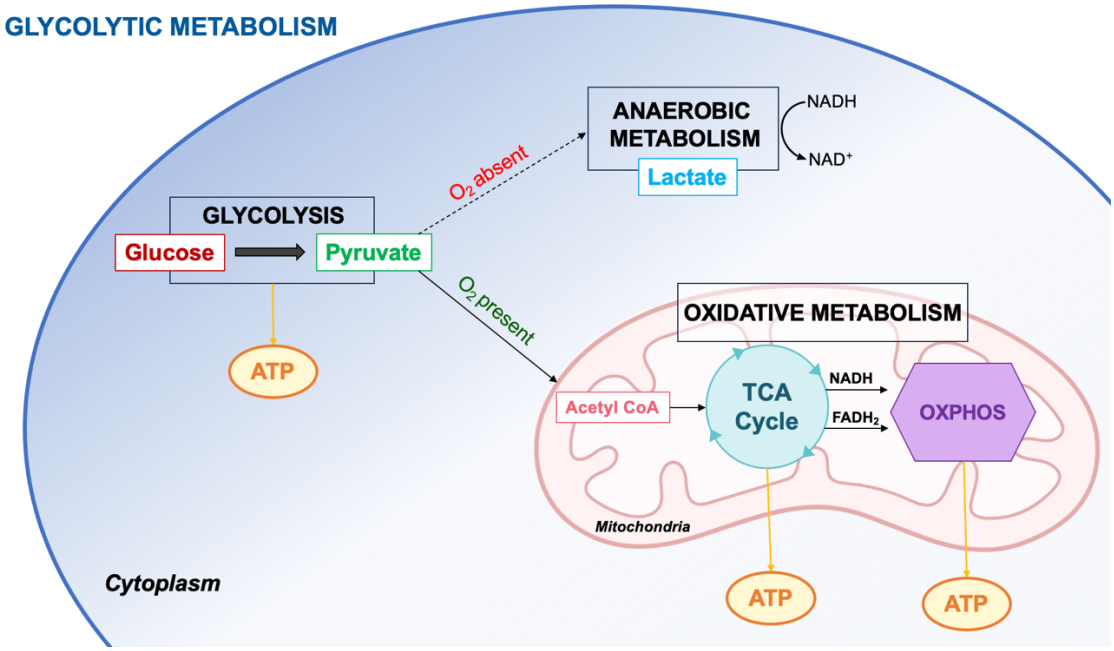

Figure 1. Schematic representation of glycolytic metabolism.

In oxidative metabolism, the production of 36 ATP molecules starting from a single glucose molecule[7]. However in highly glycolytic cells such us tumour cells, pyruvate molecules produced from glycolysis, are transformed into lactate via LDHs rather than entering the TCA cycle and from this process are generated only two ATP molecules[8].

Cancer cells are characterized by an uncontrolled cell proliferation and it has widely recognized as one of hallmarks of cancer[9,6]. An adjustment in cellular energy metabolism is required to fuel this common feature of oncological diseases[9].

Tumour cells exhibit metabolic features similar to those of rapidly proliferating normal cells; however, they also possess a high degree of plasticity, enabling them to rewire their metabolism to support increased cellular growth in variable microenvironmental conditions[6]. Specifically, cancer cells are characterized by an energy metabolism based on increased glucose uptake and lactate production and this phenomenon is called "aerobic glycolysis" or "Warburg effect". This definition comes from a century ago, when Otto H. Warburg observed that tumour cells metabolize glucose to lactic acid even in aerobic conditions[10]. This metabolic reprogramming of cancer cells leads to accumulation of lactate, even in the presence of sufficient oxygen[11]. Unlike normal cells, cancer cells are characterized by unrestricted proliferation and have metabolic needs that are both quantitatively and qualitatively distinct from those of normal cells[12]. For this reason, cancer cells predominantly depend on glycolysis over OXPHOS, since this metabolic pathway allows rapid energy supply and produces the precursors of macromolecules necessary to support cell proliferation[1]. Initially, Warburg suggested that aerobic glycolysis could be linked to defective mitochondria, which makes oxidative metabolism ineffective[13]. However, Warburg's explanation has been challenged and ultimately disproven because both the TCA cycle and the cytochromes involved in OXPHOS are typically intact and function correctly in cancer cells[14]. Some studies have shown that certain cancer cells possess the ability to reversibly alternate between anaerobic metabolism and oxidative metabolism, depending on the availability of glucose. In the absence of glucose, where it replaced by galactose, cells shift towards oxidative phosphorylation. Conversely, in the presence of high amounts of glucose, they revert to a glycolytic, anaerobic metabolism[15].

It was acknowledged that cancer cells opted for less efficient way of obtaining energy from glucose (2 ATP molecules from glycolysis compared to 36 ATP from OXPHOS) in order to acquire essential intermediates crucial for anabolic reactions necessary to fast cell growth[16]. Warburg's research demonstrated that, in terms of energy production, cancer cells actually generated 10% more ATP than normal cells[17]. Cancer cells have the ability to perform both glycolysis and mitochondrial respiration concurrently[18]. Even in the absence of oxygen, the significant glycolytic activity led to an increase in ATP produce by normal cells through oxidative metabolism[17]. Typically, cancer cells

derive 60% of their energy from glycolysis, and the other portion is produced into mitochondria through OXPHOS[19].

The altered metabolic state of cancer cell is considered a core of the hallmarks of cancer and has implications for cancer diagnosis and treatment strategies[1].

As described before, in tumour cells there is enhanced production of lactate from glucose. In this way tumour cells have different advantages:

1. They have high levels of glycolysis and low levels of OXPHOS and in particular ~85% of the glucose uptake in converted into lactate and only ~5% of glycolysis-derived pyruvate enters in mitochondria (OXPHOS) to promote rapid production of ATP in the cytoplasm[20].
2. Several intermediate metabolites are produced during glycolysis and they support the biosynthesis of lipids, amino acids and nucleotides even in absences of oxygen[21].
3. A reduction in oxidative stress caused by lower production of reactive oxygen species (ROS) was observed[22].
4. Lactate is produced in large quantities in cancer cells and this induce its accumulation in the extracellular space contributing to the acidification of cellular microenvironmental. This phenomenon has significant effects on tumour behaviour and progression[23].

Initially lactate was considered only as a waste product from anaerobic glycolysis[24]. After years of study, became evident that this metabolite served a more significant role[12]. Increased lactate levels, caused by Warburg effect, are associated with typical features of cancer such as increased of cell proliferation and acquisition of replicative immortality, evasion of immune system and of growth inhibitory factors, stimulation of invasion, metastasis and angiogenesis[25] (Figure 2).

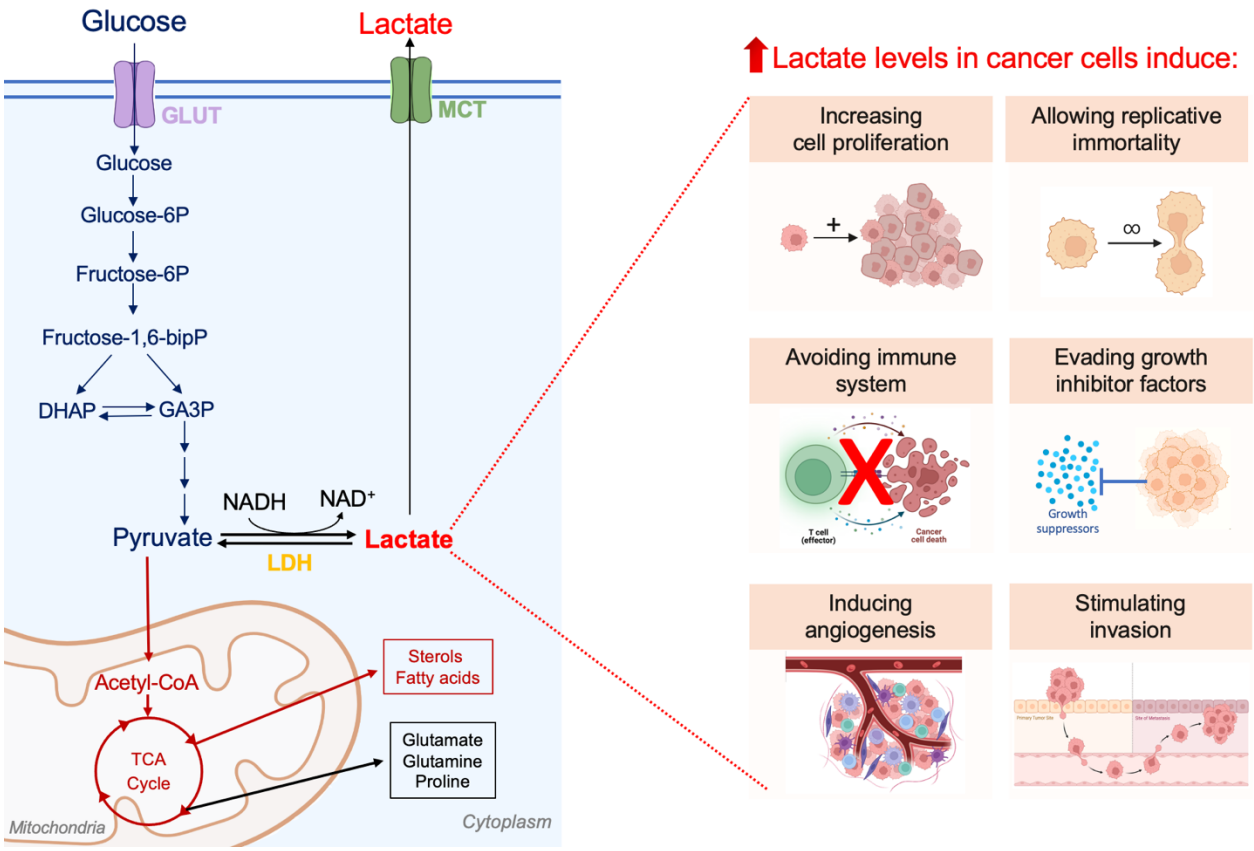

Figure 2. Schematic representation of Warburg effect and its outcomes on cancer cells. *Warburg effect (or Aerobic glycolysis) is characterized by augmented lactate levels. Lactate can induce cell proliferation, replicative immortality capacity, angiogenesis, invasion, escape from immune system and evade from growth inhibitor factors.*

1.2 Lactate

Carl Wilhelm Scheele was the first to isolate the lactate from sour milk in 1780[26]. Lactate serves as a crucial signalling molecule and it is a hydroxy monocarboxylic acid anion. It is the conjugated base of lactic acid[24]. Lactic acid has a low dissociation constant (pKa, ~ 3.86) and for this reason it can dissociate rapidly into lactate and hydrogen ion within a normal physiological pH range (~ 6.5-7.2). This means that lactate is the primary form present in living organism[27]. There are two stereoisomers of lactate: L-lactate and D-lactate, defined as left-handed and right-handed, respectively[28]. L-lactate is the most common physiological enantiomer detected in tissues[29].

Generally, in humans at rest, plasma lactate concentration is 1-3 mM; it can increase to 15 mM after intense exercise[30] and may reach 30 mM in different cancer microenvironments[31]. Some tissues generate lactate daily, including muscles, brain, skin and intestines[32]. This metabolite undergoes a rapid exchange across the body to maintain a stable concentration within the physiological range[33]. Lactate has a very high circulatory turnover, higher than glucose[8]. 60% - 70% of lactate clearance is in the liver, the remaining 30% - 40% can be attributed to the work of kidney, heart and skeletal muscle[34] (Figure 3).

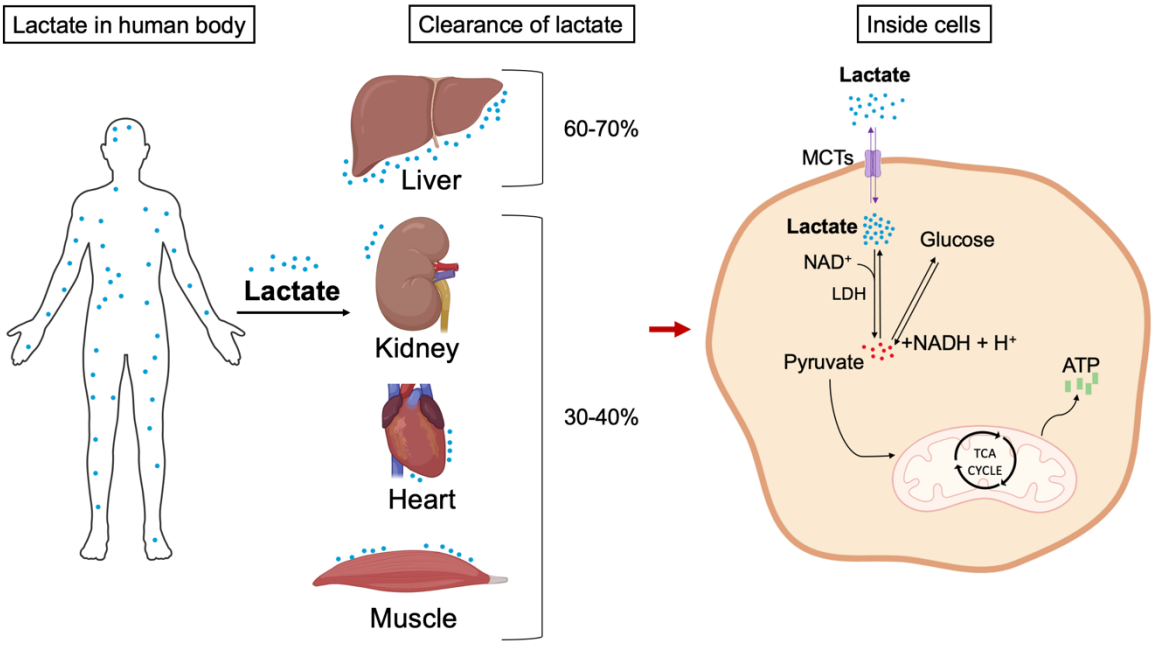

Figure 3. The flux of lactate in human body. *Lactate is the end product of glycolysis in metabolically active human cells. Lactate can enter cells through the monocarboxylate transports (MCTs). Inside the cells, it can be re-oxidized to pyruvate by lactate dehydrogenase (LDH) and enter in TCA cycle.*

In the cytoplasm, LDH catalyses the conversion of pyruvate to lactate by oxidizing NADH to NAD+ in a thermodynamically favourable and reversible reaction[35]. This process does not require oxygen. By regenerating NAD+, the enzyme LDH allows glycolysis to proceed even in low oxygen conditions[36]. Thanks to glycolysis, glucose is the primary source of lactate production in several solid tumours. Additionally, alanine and glutamine contribute to a small levels of lactate produced in cancer cells[9]. Glutamine is an L-α-amino acid containing five carbons and it is the most abundant amino acid in the blood, with a concentration of ~500μM. Glutamine represents 20% of all amino acids in blood circulation and 40% in muscle[37]. Glutamine, like glucose, is metabolized by high proliferating cells to be used in several pathways as a support for rapid bioenergetics process and biosynthesis. As well known a tumour cells culture needs at least 10 times more glutamine than any other amino acid[38]. Through various reactions, glutamine is transformed into α-ketoglutarate due to glutamate dehydrogenase enzyme (GDH). This metabolite enters TCA cycle, generating malate. Malate is transported to the cytosol and transformed in pyruvate by the malic enzyme. In the last part of this process, pyruvate is converted into lactate by LDH[39] (Figure 4). For example, DeBerardinis et al. have observed that glutamine produces lactate in proliferating glioblastoma cells[38].

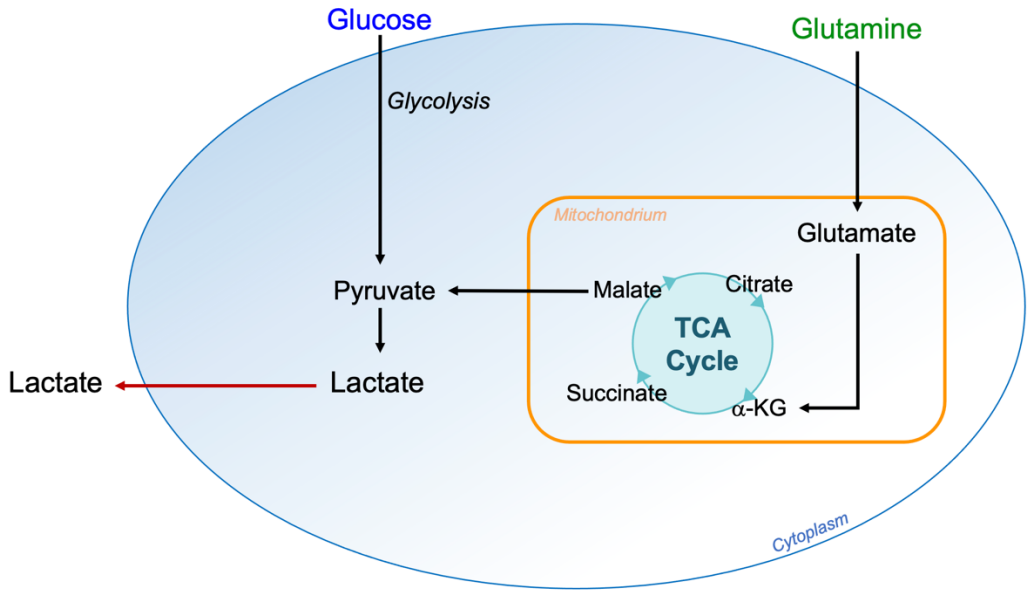

Figure 4. Metabolic pathways of lactate production. *Lactate can be generated from glucose or from glutamine. Glucose is metabolized through glycolysis to produce lactate, while glutamine can also be converted into lactate through a shortened TCA cycle via a process named glutaminolysis.*

1.2.1 Lactate metabolism

Lactate accumulation in human is very dangerous and increase serum lactate can lead to lactic acidosis[40]. Thus, lactate must be rapidly removed from tissues. Irreversible removal of lactate is carried out by pyruvate dehydrogenase (PDH)[41], which converts lactate to pyruvate, subsequently forming a two-carbon compound called acetyl-CoA or a four-carbon compound called oxaloacetate (OAA). Both these two compounds, can be enter into TCA cycle to produce citrate. In the TCA cycle, acetyl-CoA serves as a two-carbon unit. Therefore, the systemic balance between glycolysis and PDH flux is crucial in determining lactate levels. PDH is part of a catalytically active complex regulated by the phosphorylation status of the E1α subunit and NADH, both of which inhibit PDH activity, leading to increased lactate levels when mitochondrial activity or oxidative metabolism are compromised[42]. Additionally, high levels of lactate can trigger gluconeogenesis in the liver and skeletal muscle cells, converting lactate to glucose, which is released into the blood to support further glucose consumption[43]. In addition to being a primary energy source, lactate is also a significant oncometabolite, playing crucial roles in extracellular and intracellular signalling that collectively aid in cancer progression[44].

Lactate functions as both a metabolic fuel and a signalling oncometabolite, driving complex interactions between cancer cells and their surrounding microenvironment. Through monocarboxylate transporter-mediated shuttle, lactate is exchanged among cancer cells or between cancer cells and associated stromal cells, providing metabolic support. Additionally, lactate acts as an intracellular signalling molecule, activating pathways that promote cancer progression. Outside of cells, lactate binds to the lactate receptor GPR81, further contributing to tumour aggressiveness. This multifaced role of lactate culminates in the enhancement of several cancer hallmarks, including proliferation, migration, invasion, extracellular matrix degradation, angiogenesis, immune invasion and resistance to therapy[45] (Figure 5).

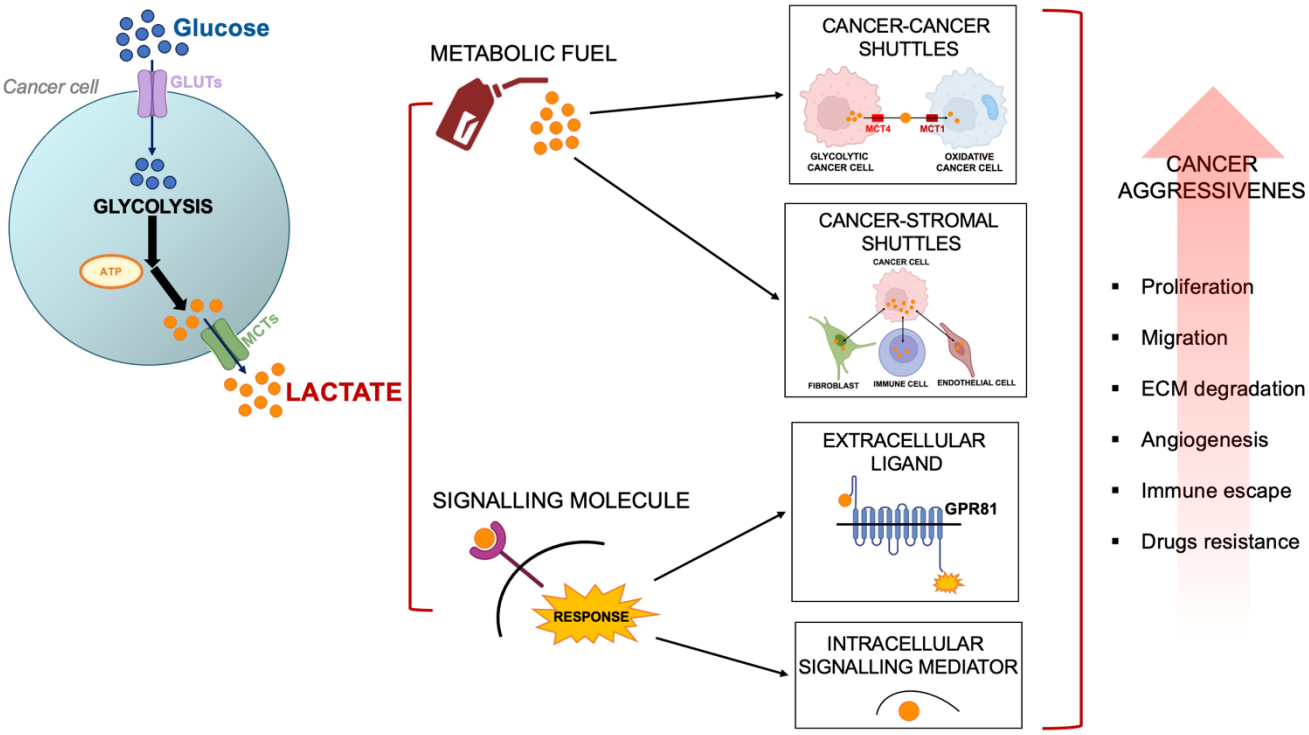

Figure 5. Lactate roles in the tumour microenvironment. *Lactate serves as both a metabolic fuel and a signalling oncometabolite, facilitating complex interactions between cancer cells and their microenvironment. It is exchanged among cancer cells and associated stromal cells via monocarboxylate transporters. Additionally, lactate functions as an intracellular signalling molecule that activates different pathways. Extracellularly, lactate binds to the GPR81 receptor, further enhancing tumour aggressiveness. This multifaceted role of lactate contributes to the amplification of various cancer hallmarks, including proliferation, migration, extracellular matrix degradation, angiogenesis, immune evasion, and resistance to therapy.*

1.2.2 LDHs and their role in cancer

As mentioned above, lactate is generated by LDH. LDH is a oxidoreductase enzyme composed by four protein subunits[46]. The *ldha, ldhb* and *ldhc* genes encode the protein subunits M, H and C respectively[9] (Figure 6). The subunits M and H can combine to form five different homo- or hetero-tetramers in human tissues: LDH-1 (4H), LDH-2 (3H1M), LDH-3 (2H2M), LDH-4 (1H3M), and LDH-5 (4M). The subunit C can form an homo-tetramers called LDHC, a specific isoform present only in the testis[47]. The formation of tetramers is regulated by the availability of the substrate and by post-translational modifications[48].

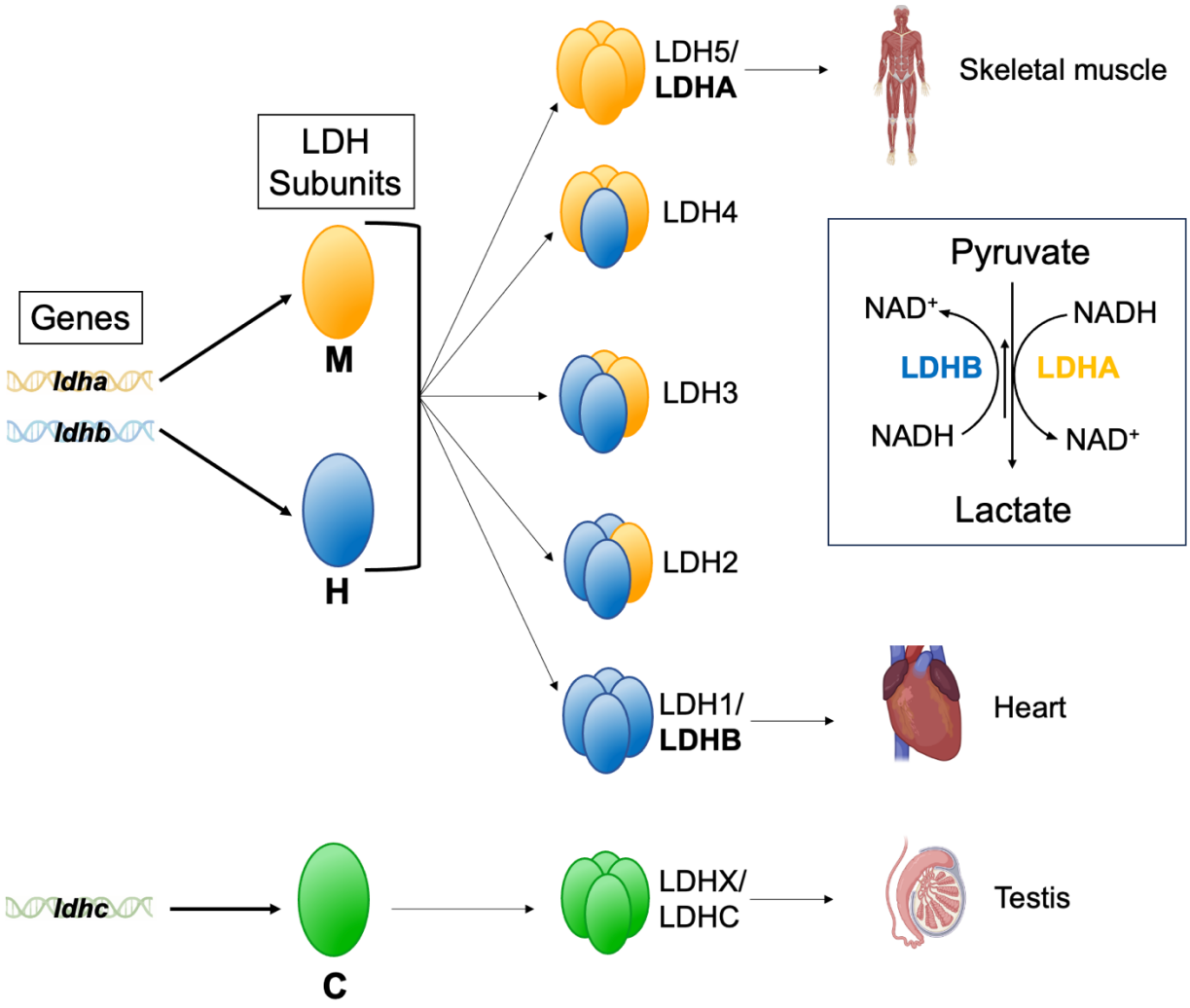

Figure 6. Schematic representation of LDH isoforms and their distribution. *Subunits forming LDH are encoded by three different genes: ldha, ldhb and ldhc. The ldha, ldhb and ldhc genes encode the protein subunits M (yellow), H (blue) and C (green) respectively. Each subunit can form different LDH isoform. From the top there is homo-tetramer LDH5 or LDHA composed by 4M; hetero-tetramer LDH-4 composed by 1H and 3M; LDH-3 composed by 2H and 2M; LDH-2 composed by 3H and 1M, LDH1 or LDHB composed by 4H and the last is homo-tetramer LDHX or LDHC is composed by 4C. On the right there is the most frequent localization of LDHA (skeletal muscles), LDHB (Hearts) and LDHC (testis). At the end there is a schematic representation of LDHA and LDHB role in cellular metabolism.*

The two most relevant tetramers of LDH are LDHA (LDH5) and LDHB (LDH1). They have different kinetic properties and these differences of LDHA and LDHB are primarily due to their distinct roles in cellular metabolism. LDHA has a higher affinity for pyruvate, indicated by a lower Michaelis Constant (Km) value, which allows it to efficiently convert pyruvate to lactate during glycolysis[49]. Indeed the principal role of LDHA is to reduce pyruvate to lactate by oxidating NADH to NAD+. In contrast, LDHB exhibits a higher affinity for lactate, enabling it to preferentially convert

lactate back to pyruvate during oxidative metabolism[50] (Figure 6). The tissue distribution of these enzymes further highlights their differences. LDHA is predominantly expressed in tissues with high glycolytic activity, such as skeletal muscle and tumour cells, while LDHB is more abundant in tissues that rely on oxidative metabolism, like cardiac muscle and liver. LDHB facilitates the transformation of lactate to pyruvate in cells that perform oxidative metabolism and gluconeogenesis by using lactate as a nutrient[51].

Although the function of LDHA is mainly cytoplasmatic, it has been found that this enzyme can be located in the nucleus of cell and act by modifying gene expression[52] (see paragraph 1.2.7).

It was shown that, abnormal activation and expression of LDHA is correlates with neoplastic changes and tumour progression[53]. For this reason and for its proprieties, this enzyme, is considered as an interesting target for cancer treatments[46]. For example, high LDHA levels are considered a negative factor in breast cancers since increased levels of this protein are detected in the most aggressive forms of this neoplastic disease[54]. Increased levels of LDHA are also negatively associated with other tumours such as pancreatic[55], hepatocellular[56] and prostate carcinoma[57]. Furthermore it was found that inhibiting LDHA results in the reduction of cancer angiogenesis, migration, invasion and immune escape[58,59]. Additionally, the inhibition of LDHA enhances the sensitivity of resistant cancer cells to chemotherapy and radiotherapy[60,61,62]. Similarly to other enzymes, LDHA was shown to undergo translational modifications (acetylation and phosphorylation); the most commonly detected were the phosphorylation of two specific tyrosine: tyrosine 10 (Y10) and tyrosine 83 (Y83)[9]. Y10 phosphorylation of LDHA enhances the catalytic activity of the enzyme and has been associated to both promotion of cell invasion and enhanced *anoikis* resistance in breast cancer[63]. By increasing the activity of LDHA, this modification promotes the Warburg effect and the invasive and metastatic potential of cancer cells[63].

As stated above, LDHA is considered a potential therapeutic target, and for this reason, there is an active research into its potential inhibitors[25]. Oxamate (OXA) is the best characterized LDH inhibitor. It is a pyruvate analogue that inhibits the enzyme by competing with pyruvate[64] and creating an inactive complex with LDH. As a consequence of LDH inhibition, OXA was found to induce reactive oxygen species production and mitochondrial apoptosis of cancer cells[65]. In preclinical studies, it was also found that OXA hindered the cell proliferation of different brain tumours including medulloblastomas[66], glioblastomas[67] and pituitary adenomas[68]. OXA was also tested in association with others drugs. Some studies verified that OXA can enhance the antineoplastic activity of paclitaxel in breast cancer cells[69]. Moreover, Balboni et al. suggest that the inhibition of LDH through OXA can affect the DNA repair system of cancer cells, in

particular the homologous recombination repair. In that way OXA can increase the antitumoral activity of Olaparib or other drugs[61]. Other studied LDH inhibitors were Gossypol[70], FX11[71], quinoline 3-sulhonamides[72] , galloflavin[73] and NC1-006 the first compound potentially active in *vivo*[74,75]. In the last year small interfering RNAs (siRNAs) able to inhibit LDH have also been discovered[76].

All these molecules showed the ability to reduce cell proliferation in different types of tumours such as breast, pancreatic, colon cancer and melanoma[77]. This and other studies allowed to highlight the potential of LDH inhibition. Unfortunately, despite many studies, the identification of an LDH inhibitor potentially applicable in clinical settings is proving to be a difficult task[25].

1.2.3 MCTs-mediated lactate transports and shuttle

Lactate can be transported across the cell membrane by different ways. A small amount of lactate can passively diffuse across the cell membrane due to its concentration gradient[43], but the most common way is through monocarboxylate transporters (MCTs)[32]. This transport mechanism can be modulated by pH gradient, concentration gradient and redox state[78]. MCTs are membrane proteins formed by 12 transmembrane domains, with intracellular NH_2 and COOH termini and a cytosolic loop located between the 6th and 7th transmembrane domains[79]. MCTs can operate "lactate shuttle", a process in which lactate can be transported in the extracellular microenvironment and can subsequently to be able to enter nearby cells[24]. There are 14 well-identified MCTs and all these transporters are a part of the SLC16 gene family[24]. Between these 14 different types, MCTs 1 - 4 are the better characterized and are encoded by *slc16a1, slc16a7, slc16a8* and *slc16a3* genes, respectively[80]. In normal conditions, MCTs 1 - 4 have synergistic activity that promotes lactate shuttling between glycolytic and oxidizing cells. These transporters are a key factor to maintain lactate homeostasis within different tissues[43]. Among them, the most commonly present are MCT1 and MCT4[81], which have been detected in all tissues. As shown by several published works, MCT1 and MCT4 are the most expressed forms, also in cancer cells[24]; MCT1 is linked to lactate import, whereas MCT4 is involved to lactate export[81] (Table 1).

In cancer cells, the MCT4-mediated lactate shuttle is an essential process for lactate signalling. The efflux of lactate contributes to the microenvironment acidification because lactate accumulates outside of the cell and it increases the concentration of hydrogen ions, lowering the pH in the

surrounding area[82]. This phenomenon promotes cancer growth through multiple mechanisms. These include activation of metalloproteinases (MMPs) that promotes extracellular matrix remodelling[83]. The low pH can directly induce conformational changes in pro-MMPs, exposing their catalytic domain and leading to their activation[84]. Moreover the acidic environment can inactivate endogenous MMP inhibitors, such as tissue inhibitors metalloproteinases, allowing MMPs to remain active[85]. Once activated, MMPs can degrade various components of the extracellular matrix leading to a consequences that promote growth and metastasis. Another mechanism associated with lactate efflux is the increase of cancer cell motility[86]. The addition of exogenous lactate has been shown to increase cell motility and random migration in various cancer cells lines in a concentration-dependent-manner[87]. In particular, acidosis can promote the release of growth factors and cytokines that stimulate cell migration[82]. The acidic environment caused by lactate efflux can impair the function of various immune cells, including T cells and dendritic cells[88]. This can contribute to inhibit the immune response to cancer antigens[89,90]. The accumulation of lactate in the tumour microenvironment leads to acidification which can influence cellular signalling and behaviour through the increase of infiltration and angiogenesis via the release of vascular endothelial growth factor (VEGF)[91]. Specifically, lactate has been shown to stimulate the production and release of VEGF, a key factor in angiogenesis. The mechanism by which lactate induces VEGF release may involve the activation of hypoxia-inducible-factor1-alpha (HIF-1α). Lactate can stabilize HIF-1α leading to increased VEGF expression. As a consequence there will be elevated levels of VEGF in the tumour microenvironment that promote the infiltration of endothelial cells, which are essential for forming new blood vessels[92].

On the contrary, influx of lactate can have different outcomes. The uptake of lactate via MCT1, was found to protect hepatocellular carcinoma cells from ferroptosis by increasing the level of monounsaturated fatty acids[93]. Particularly, ferroptosis is a form of regulated cell death characterized by the accumulation of lipid peroxides to lethal levels and is associated with iron metabolism and oxidative stress[94]. Cancer cells often develop resistance to ferroptosis, allowing them to survive[95]. Lactate uptake via MCT1 can influence lipid metabolism within the cell. When lactate is taken up by hepatocellular carcinoma cells through MCT1, it can be converted into other metabolites that contribute to lipid synthesis, including monounsaturated fatty acids. This metabolic shift helps to maintain membrane integrity and prevent the accumulation of lipid peroxides. Consequently, by increasing monounsaturated fatty acids levels, lactate uptake via MCT1 provides a protective effect against ferroptosis, allowing cancer cells to survive under conditions that would otherwise induce cell death[96]. Another research has been shown that the inactivation of MTC1 in cancer cells reduces lactate uptake and slows down the growth of tumours[97,98]. In particular, because of MCT1 is the main

transporter responsible for the uptake of lactate into cancer cells, its inactivation or inhibition leads to a reduction in lactate uptake. When lactate uptake is impaired, it may limit the availability of this energy substrate, thereby slowing tumour growth[98]. In addition to its role in tumour metabolism, lactate has been shown to enhance the suppressive function of the regulatory T cells (Tregs), a type of immune cell that infiltrates the tumour microenvironment[97]. Tregs have the ability of suppress the activity of other immune cells, contributing to an immunosuppressive environment that allows tumours to evade immune detection and destruction[99]. By reducing lactate uptake through MCT1 inactivation, the suppressive activity of Tregs within the tumour may be weakened. This weakening of Tregs function can lead to an enhanced response to immunotherapy, which aims to stimulate the immune system to recognized and eliminate cancer cells[97]. Thus, the inactivation of MCT1 not only impacts tumour metabolism but also has significant implications for the immune landscape of the tumour, highlighting a potential therapeutic strategy to enhance the efficacy of cancer immunotherapy[100,101].

In summary, the lactate shuttle, operated by monocarboxylate transporters, establishes inter-cellular connections and supports cooperative metabolism between glycolytic and oxidative tumour cells, thereby promoting tumour initiation and progression[43].

For its property of involving different cell type in tumour microenvironment, lactate shuttle, has garnered significant interest from scientists in recent years. Lactate is an energy-rich metabolite that is used for both gluconeogenesis and ATP synthesis[102]. For these reasons, it is essential for this metabolite to reach all cells within the tumour mass, starting from the internal cells that are low in oxygen and reaching the external cells that are in aerobic conditions due to their proximity to blood vessels. In the tumour mass, hypoxic cells produce lactate through the action of LDHA. This metabolite is imported from nearby cells under aerobiosis conditions that convert it into pyruvate, a substrate used to obtain energy. In this specific lactate shuttle, the role of MCT1 and MCT4 is crucial: MCT4 mediates the release of lactate from hypoxic tumour cells, meanwhile MCT1 allows its entry into normoxic cancer cells. This process is essential to understand the mutual relationship and metabolic symbiosis between cancer cells[43].

Transporter	Gene	Direction of lactate	Tissue distributions	References
MCT1	SLC16A1	Influx and efflux	Ubiquitous	103
MCT2	SLC16A7	Efflux	Skeletal muscle, blood, brain	101,104
MCT3	SLC16A8	Efflux	Retinal pigment, choroid plexus epithelial of the eye	105,106
MCT4	SLC16A3	Efflux	Kidney, skeletal muscle, intestine, heart, lung	107

Table 1. MCTs distribution*. The expression, lactate transporting pattern and different tissue distribution of 1-4 MCTs.*

1.2.4 The GPR81 lactate receptor

Recently, it has become evident that metabolites can act like hormones or neurotransmitters, serving as extracellular signalling molecules through G-protein-coupled receptors. In particular, lactate can function like a signal molecule through G-protein coupled receptor 81 (GRP81)[108]. GPR81 was discovered in 2001[109], it is the first recognized lactate receptor and is commonly present in human tissues[110]. GPR81 is encoded by *hcar1* gene. It is highly expressed in white adipose tissue and, to a lesser extent, in brain, parathyroid, spleen, colon including cancer cells[111],[112]. GPR81 is composed by seven transmembrane domains coupled to a heterotrimeric G-protein. When lactate binds its receptor, the transduction of different intracellular signals are activated through the G-protein[110]. Activation of GPR81 by lactate leads to the downregulation of cyclic adenosine monophosphate (cAMP), resulting in reduced intracellular cAMP levels. Considering the high levels of lactate in the cancer microenvironment, it was hypothesized that lactate-induced activation of GPR81is involved in the regulation of cancer cell progression. Roland et al. have highlighted the crucial role of GPR81 in tumour. They observed a correlation between GPR81 expression and both tumour growth and metastasis in pancreatic cancer[113]. In breast cancer cells, GPR81 enhance cell proliferation and angiogenesis via the PI3K/Akt/cAMP pathway[114]. Specifically, when GPR81 is activated by lactate, it can lead to the activation of PI3K , which subsequently activates Akt. This signalling cascade promotes cell proliferation by enhancing metabolic processes that support rapid cell division and

growth. The activation of the PI3K/Akt pathway is associated with the upregulation of VEGF, a critical factor in angiogenesis[114]. In addition, Ishihara et al. discovered that GPR81 is commonly highly expressed in breast cancer cells, and silencing GPR81 expression reduced the proliferation and migration of these cells in vitro and inhibited tumour growth in vivo[115]. Moreover, glycolysis and ATP production decreased in GPR81-silenced cells. These findings indicate that activation of GPR81 mediated by lactate plays a crucial role in breast cancer aggressiveness, suggesting that GPR81 could be a promising therapeutic target for this tumour[115].

Researcher discovered a complex mechanism by which lactate receptor GPR81 influences immune evasion in lung cancer cells through the regulation of programmed death-ligand 1 (PD-L1) expression[116]. Lactate activation of GPR81 leads to a decrease in intracellular cAMP levels. cAMP is a signalling molecule that typically activates protein kinase A (PKA). By reducing cAMP levels, GPR81 inhibits PKA activity. The inhibition of PKA activity results in the activation of Taffazin (TAZ), a transcriptional coactivator. TAZ plays a crucial role in regulating gene expression, including PD-L1. When TAZ is activated, it promotes the transcription of PD-L1, a gene associated with immune evasion. In conclusion, by increasing PD-L1 expression on the surface of lung cancer cells through this signalling pathway, lactate helps to protect cancer cells from immune cells. This mechanism illustrates how metabolic changes in tumours can influence immune responses, linking metabolic reprogramming to immune evasion[116].

All these findings suggest that lactate may function as a signalling molecule by binding to GPR81, and this mechanism significantly impacts cancer progression.

1.2.5 Lactate and epigenetics

Epigenetics is a term initially used to describe the intricate connections between the genome and the environment that contribute to development and differentiation in organism[117]. From recent years, epigenetics is defined as the heritable and stable changes in gene expression that do not involve alterations in the DNA sequence but involve mainly chromosome[118]. Precisely, epigenetics mechanisms can change gene expression by modifying the chromosomal structure without changing DNA sequence[119].

Epigenetic modifications change DNA accessibility and chromatin structure, regulating gene expression patterns. There are different type of epigenetic modifications involved in cancers: DNA methylation, histone modification, chromatin re-modelling, RNA modification and non-coding RNA associated gene silencing[120]. For many years, cancer biology has primarily focused on oncogenic

mutations. Recently, has been focalized on the connection between metabolism and gene expression[121]. Cancer cells adapt their metabolism to support rapid growth and proliferation under various stress conditions, demonstrating metabolic plasticity[122]. Specifically, metabolites can act as substrates and co-factors for epigenetic enzymes to facilitate post-translational modifications of DNA and histones. Oncometabolites are metabolites that are abnormally accumulated in cancer cells due to genetic or epigenetic alterations, and play a crucial role in promoting cancer progression and malignancy[123]. Evidence suggests that the epigenome is correlated to cancer metabolism, while epigenetic dysfunction can alter metabolic enzymes, contributing to tumorigenesis. The relationship between epigenetics and metabolism can influence the vision that the researchers have on cancer[124].

Lactate is one of the oncometabolites showing the potential of altering gene expression[31]. Although the discovery of the Warburg effect is dating back to one century ago[21], for many years, lactate was only considered a waste product from anaerobic glycolysis[125]. Evidences showing a direct correlation between enhanced glycolytic metabolism and changes in gene expression have only been obtained recently. During these studies, the glycolysis-based metabolic reprogramming was found to impact on distinct morphological features of cancer cell nucleus[126]. At present, several evidences have been obtained concerning the role of lactate in regulating gene expression and in promoting the unlimited growth of cancer cells through different mechanism including epigenetic modifications[25].

1.2.6 Lactate and histone acetylation

Histones are essential proteins that take part in chromatin structure. They are divided into core histones (H2A, H2B, H3 and H4) and linker histones (H1 and H5), according to their function and position on chromatin[127]. Histones are the proteins around which DNA is coiled to form chromatin and chromosomes. Nucleosome is the elementary unit of a chromosome and includes a histone octamer with 200 base pairs of DNA wrapped around it[128]. As mentioned above, core histones can undergo modifications. Specifically, histones undergo posttranslational modifications in the protruding C-terminal and N-terminal regions and these kind of modifications are a part of epigenetic[129]. Various histones' modifications have been known for many years, among these are acetylation, methylation and phosphorylation[130]. Histones' acetylation is a key epigenetic mechanism involved in various chromatin-dependent processes, including DNA replication, damage and repair, transcriptional activation, cell cycle progression and gene regulation[131]. Histones' acetylation is operated by two classes of enzymes: histone acetyltransferases (HATs) and histone deacetylases (HDACs). In general, higher levels of histone acetylation (hyperacetylation) lead to open and

transcriptionally active chromatin structure, while lover levels of acetylation (hypoacetylation) result in a more compressed and transcriptionally repressed chromatin[132] (Figure 7).

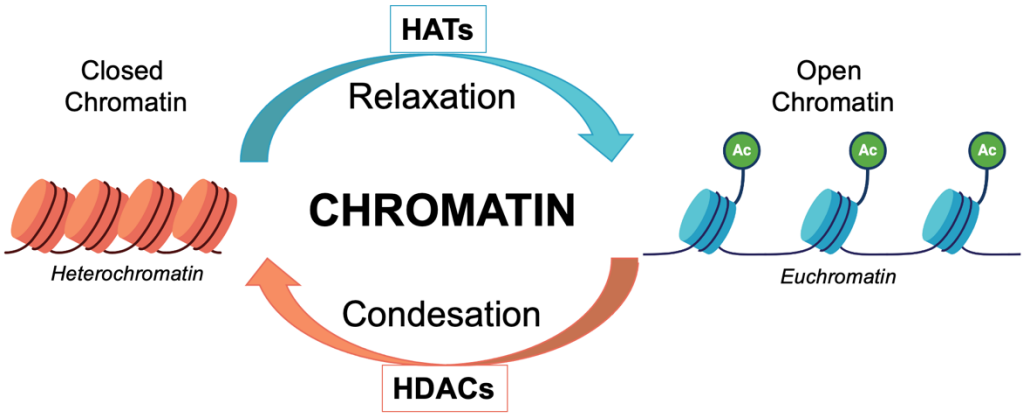

Figure 7. Schematic representation of histone acetylation mechanism. *Histone' acetylation is an epigenetic modification that plays a pivotal role in regulating chromatin structure and gene expression. It involves the addition of acetyl group (in green) to the specific lysine residues of histone proteins. This process is catalysed by histone acetyltransferase enzyme (HAT, in blue) and can be reversed by histone deacetylase enzyme (HDAC, in orange). Histone acetylation is generally associated with transcriptional activation and an open permissive chromatin state (euchromatin). Conversely, the removal of acetyl groups by HDACs leads to a more condensed chromatin structure (heterochromatin), which is typically associated with transcriptional repression.*

Metabolites originating during glycolysis have been shown to inhibit HDAC and stimulate HAT, which promotes an open chromatin structure[133]. This chromatin change can facilitate the transcriptional and replication machineries triggered by oncogenes activation. Interestingly, elevation of glycolysis was also found to facilitate DNA repair and confer cancer cells resistance to ionizing radiation[134]. Moreover, considerable amounts of evidences suggest that inhibition of glycolysis leads to compromised DNA repair which is accompanied by energy depletion[135]. Taken together, these data suggest a metabolic control on gene transcription and DNA integrity, mediated by epigenetic mechanisms.

Specifically, the product of the pyruvate dehydrogenase reaction, acetyl-COA, is a substrate for HATs; this enzyme can actually transfer the acetyl moiety of acetyl-CoA to the lysine residues of histone proteins[136].

Sunghyouk Park et al. have shown that lactate serves as a significant carbon source for the acetylation of histones, particularly histone H4[125]. This process occurs through oxidation-dependent metabolism, where lactate is converted into acetyl-CoA in the nucleus. Using isotopically labelled

lactate, the researchers found that up to 60% of the carbons from lactate can be integrated into histone H4. The incorporation of lactate into histones depends on the presence of nucleus-localized LDHA. Specifically, inside the nucleus, LDH can facilitate the conversion of lactate into pyruvate intermediate that is subsequently converted to acetyl-CoA by PDH. In that way lactate-derived carbons can contribute to the level of acetyl-CoA in cells[125].

These metabolic reactions create an important functional connection between lactate and histones' acetylation (Figure 8). The resulting opening of chromatin structure induce enhanced transcription of genes involved in different cellular pathways, including proliferation and DNA repair[137,138].

Lactate was also found to be a natural inhibitor of HDAC, the enzymes that remove acetyl groups from histones. As mentioned above, this process promotes the creation of a more relaxed, open and transcriptionally active chromatin[139]. Wagner et al. have shown that higher levels of lactate such as those detected in the uterine cervix can inhibit HDACs, inducing the hyperacetylation of H3 and H4 histones[138]. The consequent increase in accessible chromatin was found to enhance DNA repair activity in cervical cancer cells[138]. As a consequence, the survival of some cervical cancer cells after chemotherapeutic treatment is facilitated[138].

In addition, researchers discovered that increased protein acetylation (including histones) is significantly influenced by pH levels[140], since it may also occur under higher pH conditions through a non-enzymatic process[141].

In conclusion, lactate can be utilized as a carbon substrate for the acetylation of histones. The increased histones' acetylation typically promotes cell proliferation, a very common characteristic in tumour cells[108].

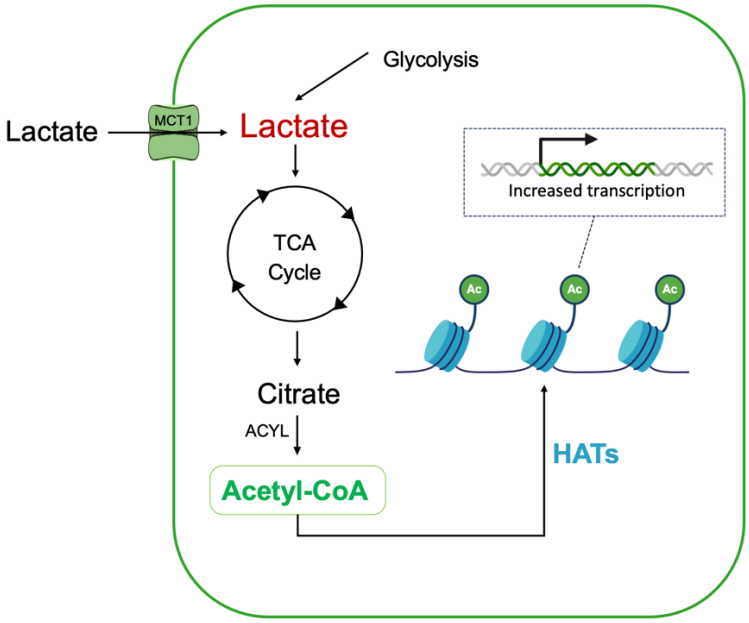

Figure 8. Lactate as a carbon source for histone acetylation. *Lactate plays an important role in histone acetylation, serving as a key metabolic link between cellular metabolism and epigenetic regulation. This figure shown that lactate can be used as a carbon source to produce acetyl-CoA. HATs used Acetyl-CoA as a substrate to add acetyl groups to the histone proteins generating open chromatin and resulting in increases transcription of genes.*

1.2.7 Lactate and protein lactylation

Few years ago, Zhang et al. discovered a new important modification of histones produced by lactate[142]. They found that lactate could be converted to lactyl coenzyme A (lactyl-CoA), subsequently transferred to lysine residues on histones. This epigenetics modification is called histone lysine lactylation (Kla). This discovery unveiled a direct link between cellular metabolism and epigenetic regulation of genes expression[129].

In 2019, during their studies, Zhang and his collaborators discovered a mass shift caused by the addition of lactyl group (CH3-CH(OH)-CO-) to the ε-amino group of lysine residues in proteins of human breast cancer cells[129]. To demonstrate that this phenomenon was caused by lactate they performed several experiments. They used synthetic peptides to verify whether, after cell penetration, these peptides shared any chemical characteristics with the in vivo peptide exhibiting the mass change. Taken together the results of their experiments suggested that exogenous and endogenous lactate is a crucial factor in causing lysine lactylation of histones. In addition, they found that knockdown of LDH completely abrogated lysine lactylation, which further demonstrated the dependence of this modification on lactate. They discovered 28 different lactylation sites on histones

of human and mouse cells. Another important observation made by Zhang et al. is that lysine lactylation differs from lysine acetylation in terms of kinetics: lactylation takes a long time (about 24 h) to reach a stable state, while acetylation only takes 6h. This finding suggests that lactylation and acetylation are different process and happen at different times[129,142].

Like other modifications, such us acetylation, lactylation requires enzymatic activities that add or remove the lactyl group from lysine residues. Interestingly, these modifications were found to be operated by HATs and some HDACs[143] (Figure 9). One of the HATs involved in lactylation is the p300 enzyme; this HAT was found to display an additional activity: the ability to transfer of lactyl group from lactyl-CoA to specific lysine residues in different proteins[129,144]. This activity was demonstrated by inducing p300 overexpression and knockdown in pancreatic cancer cells. Remarkably, these modifications resulted in increased or decreased levels of histone Kla, respectively, which confirmed the involvement of p300 in this process. Furthermore, in bone marrow-derived macrophages obtained from mice[145], a notable reduction in histones' Kla was observed when the expression of p300 was suppressed. Inhibition of p300 using siRNA or the C&46 p300 inhibitor impaired histones' lactylation in various cell types[81,146]. Taken together, these and other studies provided evidence that the histone acetyltransferase p300 can catalyse the lactylation of histones, thereby regulating gene expression and cellular process depending on this modification[81,147].

Removal of lactyl groups from histones was found to be catalysed by two families of deacetylase: HDAC1-3 (histone deacetylases 1-3), SIRT1-3 (sirtuins 1-3). These enzymes were identified during a series of experiments, which included overexpression and knockdown of specific enzymes in cultured living cells[129,148]. These studies revealed that HDAC1 and HDAC3, but not HDAC2, play a distinct and specialized role in the removal of lactyl groups from histones[143]. Instead, SIRT1 can delactylate α-myosin heavy chain (α-MHC), while SIRT3 can mediate delactylation of cyclin E2 (CCNE2)[149].

Histones' modifications activate transcriptional signals that are interpreted by effector "readers" proteins, which give rise to downstream signalling pathways and initiate different biological process[150]. At present, the identity of "readers" proteins specifically identifying lactylation sites, is still unknown[151].

While the exact mechanisms underlying these phenomena are still being investigated, the cited enzymes are believed to play crucial roles in regulating the presence of lactyl groups, thereby modulating gene expression and various biological processes. However, it is important to note that the identification of the enzymes involved in lactylation is an ongoing area of research and further studies are needed to fully elucidate the complete set of enzymatic activities involved in this protein modification and their specific substrates.

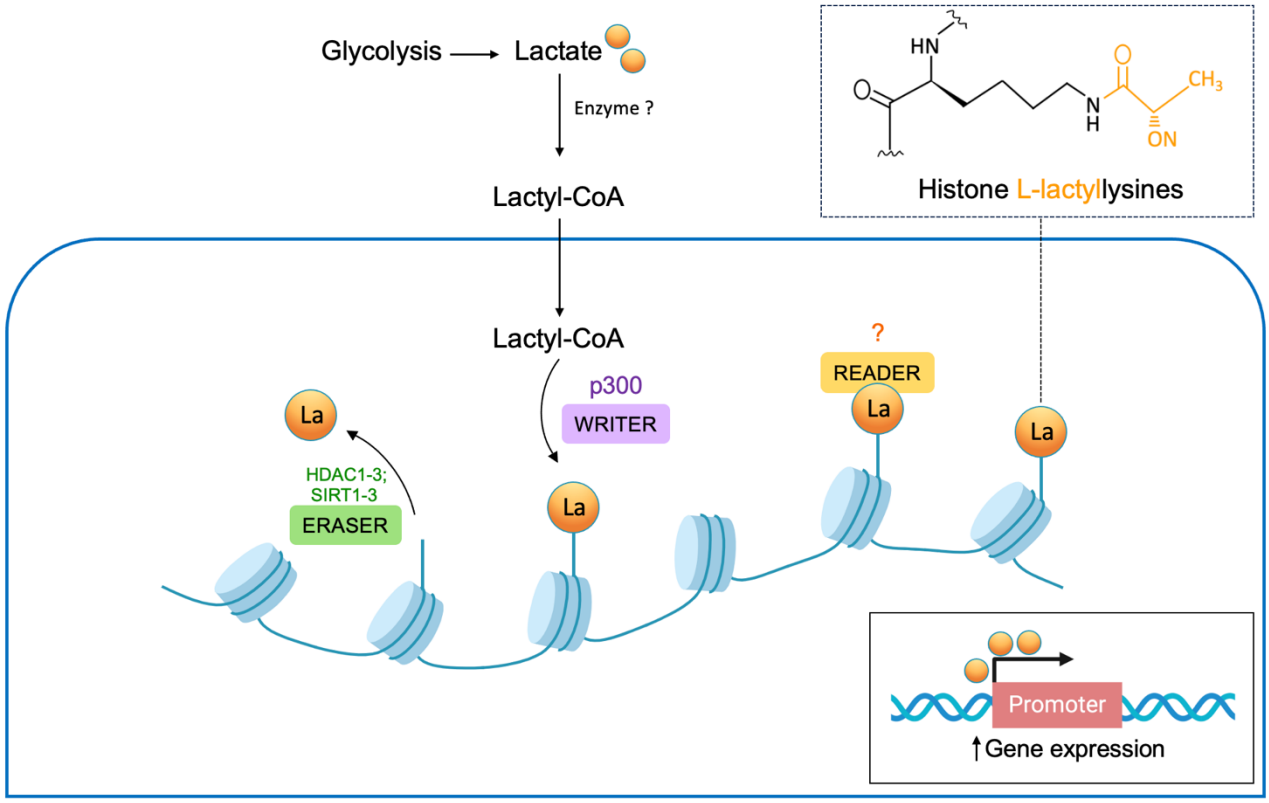

Figure 9. Schematic representation of histone lactylation and of the involved enzymes. *Histone lactyl transferases (in violet), like p300, that can catalyse the addition of lactyl group from lactyl-CoA to specific lysine residues; histone de-lactylases (in green), like HDAC 1-3 / SIRT 1-3 that are able to remove lactyl group from histones; the "reader" proteins (in yellow) that specifically identify the lactylation and translate it into various functional effects within the cell are unknown.*

1.2.7.1 Sites of lactylation

Protein acylation was a recognized phenomenon for more than half a century. It was initially observed on histone proteins, where it plays a fundamental role in regulating transcription[152,153]. Subsequent findings revealed that numerous other proteins can also undergo acylation on their lysine residues[154]. Like other acylation reactions, lactylation has been observed not only on histones but also on non-histone proteins in multiple organisms. This discovery highlighted the widespread nature of lactylation as a post-translational modification, extending its potential regulatory functions beyond the chromatin structure and transcriptional control[81].

Several studies have identified specific lysine residues on core histones that can undergo lactylation, highlighting the role of metabolic changes in epigenetic regulation[155,142,156]. Five years ago, Zhang and colleagues identified several Kla sites on the core histones H2A, H2B, H3 and H4

from human HeLa cells and mouse bone marrow-derived macrophages[142]. Thereafter these specific histone lactylation sites were identified across different cell types, organisms and experimental conditions including mammals, protozoans, fungi and plants. These discoveries underscore the importance of these post-translational modifications in regulating chromatin structure and gene expression through diverse biological systems[155,157].

K18 is a major lactylation site on histone H3. H3K18 lactylation has been linked to gene activation, macrophage polarization and cellular reprogramming[158,159]. K23 and K27 on histone H3 can also undergo lactylation[81].

Four different lysine have been identified as lactylation sites on H4: K5, K8, K12 and K16[158]. K199, K16 and K34 are lysine can undergo lactylation on H2A and H2B respectively[81].

The identification of these lactylation sites on histones can provide insights into the potential roles of lactylation in regulating chromatin structure, gene expression and various biological processes such as embryonic development, immune response and cancer progression[81,159].

Several studies have also identified non-histone lactylation sites on different proteins distributed in different cellular compartments including cytoplasmatic, nuclear, mitochondrial, ribosomal and membrane proteins[81].

During their studying, Gaffney et al. recognized 350 lactylated proteins in HEK293T cells. Many of lactylated proteins identified were enzymes involved in the glycolytic pathway such us hexokinase 1, aldolase A/C, phosphoglycerate kinase 1, enolase 1 and pyruvate kinase M[160]. These finding suggest that enzymes involved in the glycolytic pathway are frequent targets of lactylation, which could serve as a mechanism to regulate glycolytic flux and metabolic reprogramming[136]. Moreover, some specific lactylated proteins were found to play critical roles in regulating cellular activities.

Yang et al. discovered that the nuclear protein high mobility group box 1 (HMGB1) can undergo direct lactylation upon lactate stimulation, through a mechanism dependent on the p300 acetyltransferase. The lactylation of HMGB1 was found to trigger its translocation from the nucleus to the cytoplasm. Specifically, the cytoplasmatic translocation of lactylated HMGB1 was proposed to play a role in regulating different cellular processes, such us inflammation, immunity and proliferation[161].

The identification of the exact sites of Kla is a crucial step for understanding the molecular mechanisms underlying lactylation. Some scientists also developed the on-line application called FSL-Kla, which serves as a prediction model for Kla sites[162].

The recent discovery of Kla hights the importance of histone lactylation as a mechanism through which lactate can influence transcriptional regulation thereby impacting on many cellular processes including metabolic rewiring, immune modulation, cell fate determination, cancer stemness and

senescence[25] (Figure 10). Similar to the other histone modifications, Kla plays an essential role in regulating transcriptional activation[25]. Thus far, scientists have uncovered the importance of histone lactylation in several key process[163–165].

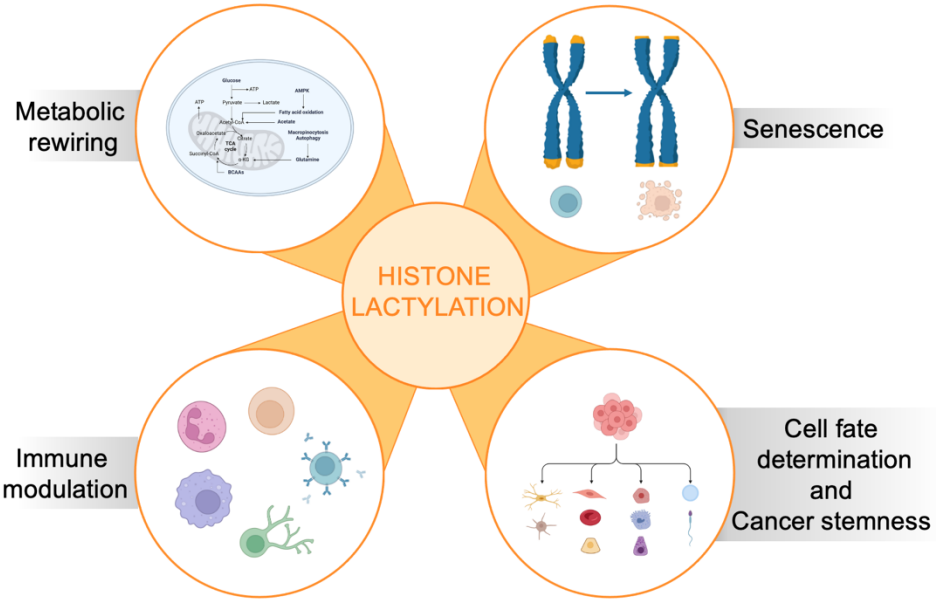

Figure 10. Implication of histone lactylation in cellular processes. *Histone lactylation is a process that can influence different important cellular mechanism such us: metabolic rewiring, senescence, immune modulation, cell fate determination and cancer stemness. In this way, lactylation, can modify the fate of cells.*

1.2.7.2 Lactylation and cancer

Histone lactylation plays a crucial role in mediating the metabolic reprogramming which is a hallmark of cancer cells and involves alterations in cellular metabolism to support rapid proliferation[159]. As mentioned above, cancer cells are characterized by increased glycolysis and enhanced lactate production[166,167]. Lactate accumulation leads the increase of lysine lactylation of histones[25]. Importantly, Kla is closely associated with enzymes that regulate key metabolic pathways including TCA cycle, carbohydrate, amino acid, fatty acid and nucleotide metabolism[168]. These interactions can lead to changes in gene expression patterns that are critical for cellular functions and adaptation to metabolic demands[25]. This suggests that lactylation may play a significant role in the regulation of cellular metabolism[25].

Emerging evidence suggests that histone lactylation may contribute to the regulation of cancer stem cells as well as of cellular senescence, which are critical factors in tumour initiation, progression and therapeutic resistance[158].

Another important aspect is that cancer microenvironment is characterised by immunosuppressive and pro-tumorigenic molecules and often it shows elevated levels of senescence associated factors across various cancer types[169]. Although numerous studies have demonstrated that aging plays a significant role in the development of cancer, the exact mechanisms by which histone lactylation contributes to this process remain unclear and require additional research[25].

It has been shown that in samples of human ocular melanoma elevated levels of histone lactylation, specifically H3K19la, are identified as a poor prognosis factors in patients and are correlated with worse outcomes[163]. Wei et al. found that elevated histone lactylation in endometrial cancer stimulates malignant progression by enhancing USP39 expression, which in turn activates the PI3K/AKT/HIF-1α signalling cascade. This epigenetic modification plays a crucial role in driving the aggressive behaviour of endometrial carcinoma through its effects on significant cellular pathways[170]. Furthermore, a recent study discovered that lactate has a multifaceted role in non-small cell lung cancer (NSCLC) cells, demonstrating its capacity to simultaneously suppress glycolysis and preserve mitochondrial homeostasis. In this study the authors observed that lactate exposure led to decreased transcription of some glycolytic enzymes, specifically hexokinase 1 and pyruvate kinase M. Conversely, lactate treatment resulted in increased expression of crucial mitochondrial enzymes. These findings suggest that lactate may induce a metabolic reprogramming in NSCLC cells, potentially shifting the balance from glycolysis towards enhanced mitochondrial activity[171].

Another important role of lactylation is its ability to alter the immunological environment. Lactylation has been shown to modulate the immune response, specifically in the context of macrophage polarization and inflammation[172]. Elevated histone lactylation in tumours facilitates immune evasion during cancer progression by promoting the polarization of M2 tissue-associated macrophages[173]. Recent research has discovered that histone lactylation plays a role in the response to immunotherapy[25]. Increased lactate production promotes the nuclear translocation of E3BP, a component of pyruvate dehydrogenase complex. E3BP has been shown to interact with lactylated histone. This results in increased histone lactylation and induces transcription of PD-L1[174]. This finding highlights the link between cellular metabolism, epigenetic regulation and immune evasion in cancer. It suggests that lactate-induced histone lactylation can modulate the expression of immune checkpoint molecules like PD-L1, potentially influencing the efficacy of immunotherapy[175].

Moreover, Zhang et al. observed elevated levels of histone lysine lactylation in tumour-associated macrophages extracted from mice with B16F10 melanoma and with LLC1 lung cancer tumours[142,176]. This increased of Kla was related with the polarization of tumour-associated macrophages towards a tumour promoting M2 phenotype. Consequently, this pattern were found to substantially contribute to tumour initiation and progression[142].

Lactylation was also found to be implicated in the first steps of tumorigenesis[177] and in the epithelial-mesenchymal transition (EMT), a crucial process in both cancer initiation and metastasis[178]. By examining lactylation and EMT under hypoxic conditions, a recent study has offered valuable insights into the relationship between the initiation of tumorigenesis, cancer metastasis and histone lactylation. In tissue, hypoxic conditions trigger a significant increase in glycolytic metabolism with a result of elevated lactate production[179]. As a consequence, there was an increase of histone lactylation, which directly promotes the expression of Snail1, a key transcription factor. Snail1, in turn, drives EMT through the transforming growth factor β/SMAD2 (TGF-β/SMAD2) signalling pathway[179]. This finding has important implications for understanding the potential role of histone lactylation in cancer progression. The study highlights how microenvironment factors, such us hypoxia, can influence epigenetic states and cellular behaviour, potentially contributing to the initiation and progression of cancer[158].

Another study suggested that the inhibition of H3K9 and H3K14 lactylation could potentially reduce the onset of hepatocellular carcinoma[180]. These researches unlock new opportunities for exploring the role of histone lactylation in cancer development and may inform future strategies for cancer prevention and treatment.

1.2.8 Lactate and drug resistance

One of the primary challenges hindering the effectiveness of cancer treatments is the development of intrinsic or acquired resistance. Several evidences have established a connection between treatment failures and alterations in cellular metabolism[181]. In line with these findings, recent research has highlighted the significant role of lactate accumulation in promoting drugs tumour resistance[182].

Lactate plays a significant role in enhancing chemoresistance of tumour cells. In almost all human cancer cells, there is an elevated activation of phosphatidylinositol 3-kinase (PI3K). As a consequence, it is observed the stimulation of protein kinase B (AKT) and its downstream signalling pathways[183]. The activation of this pathway leads to high glucose uptake and increased aerobic glycolysis[184]. For this reason, the development of PI3K inhibitors represents a significant and important challenge for researchers. PI3K inhibitors are a class of targeted cancer therapies that block the activity of this protein. Several PI3K inhibitors have been developed and investigated in clinical trials for various cancers[185]. For example, Alpelisib was the first PI3K inhibitor approved by the U.S.

Food and Drug Administration (FDA) in 2019 for the treatment of hormone receptor-positive, human epidermal growth factor 2-negative, PIK3CA-mutated advance or metastatic breast cancer in postmenopausal women and men, in combination with the endocrine therapy fulvestrant[186]. However, while PI3K inhibitors have shown promising results in haematological malignancies, their efficacy in solid tumours appears more limited[185]. Therapeutic failure arise from a narrow therapeutic window due to on-target toxicities, which necessitates the development of more specific and potent inhibitors, as well as addressing resistance mechanisms. About the development of resistance, it was shown that oestrogen receptor positive breast cancer cells appeared resistance to PI3K and dual PI3K/mTOR inhibitors[187]. Moreover, through *in vitro* experiments it has been demonstrated that, the supplementation of lactate can induce resistance to AKT inhibitors in colon cancer cells[188]. This phenomenon can be mitigated by inhibiting MCT activity OXPHOS[188]. This finding suggests that cancer cells exhibit significant metabolic plasticity, since they can evade the effects of targeted therapies by shifting their metabolic preference towards oxidative processes. By adapting their metabolism to utilize lactate as an energy substrate, these cells can overcome the inhibitory effects of specific cancer treatments targeting glycolytic metabolism[187].

Corso et. al revealed that lactate is a critical factor that stimulates cancer-associated fibroblast to produce hepatocyte growth factor (HGF) through a nuclear factor kB-dependent mechanism. The elevated levels of HGF were found to activate signalling mechanisms which contribute to sustained resistance against tyrosine kinase inhibitors, a class of anticancer drugs[189]. The same drug resistance phenomenon was observed in lung cancer patients, which underscores the clinical importance of these findings and suggests new strategies to fight drug resistance in cancer[189].

Moreover, Dong et. al discovered that the chemotherapeutic agent etoposide promotes a shift to aerobic glycolysis in non-small cell lung cancer cell lines[190]. They found that elevated levels of lactate in the extracellular environment significantly contribute to etoposide resistance by upregulating the expression of multidrug resistance proteins (MRP). At the molecular level, lactate was found to orchestrate the TGF-β1/Snail and Taz/Ap-1 signalling pathways, leading to the assembly of a Snail/TAZ/AP-1 complex on the promoter region of the MRP gene. The resulting upregulation of MRP expression was found to counteract DNA-damage and cell death. These mechanisms can inhibit the effects of chemotherapeutic agents by enhancing the expulsion of these drugs from cancer cells[190].

The above-described data suggest that, by increasing the lactylation of histone and of other proteins, high levels of lactate might contribute to changes in gene expression supporting drug resistance. In agreement with this idea, recent research has uncovered a crucial role for lactate-induced lactylation in DNA repair and chemotherapy resistance. Specifically, lactylation of the Nibrin (NBS1) protein at lysine 388 (K388) was found to be essential for forming the MRE11-RAD50-

NBS1 (MRN) complex and recruiting homologous recombination (HR) repair proteins to DNA double-strand breaks[191]. High levels of NBS1 K388 lactylation correlate with poor outcomes in patients receiving neoadjuvant chemotherapy. Importantly, reducing lactate levels, by using LDHA inhibitor, decreases the lactylation of this protein and this impairs DNA repair efficiency, helping to overcome chemotherapy resistance[191]. These researches suggest that targeting lactate production could be a promising strategy for enhancing cancer treatment efficacy.

In addition, it was shown that a high level of lactate promotes the expression of methyltransferase-like 3 in tumour infiltrating myeloid cells through H3K18 lactylation, and this effect is correlated with a poor prognosis in patients with colon cancer[176]. Another study suggested that inhibition of H3 histone lactylation can reduce the tumorigenicity of liver cancer stem cells by interfering with their ability to promote tumour growth and metastasis[192]. By blocking this modification, the metabolic and epigenetic pathways that contribute to the aggressive behaviour of liver cancer stem cells are disrupted, leading to decreased proliferation and increased apoptosis in these cells[192].

These findings highlight the complex relationship between lactate metabolism and drug resistance in cancer cells, suggesting potential strategies for overcoming chemoresistance through the modulation of lactate.

[This page is intentionally left blank]

2. AIM OF THE THESIS

Intrinsic or acquired drug resistance is one of the major problems compromising the success of antineoplastic treatments. This phenotype can be manifested through various mechanisms: alteration of drug efflux or delivery, apoptosis suppression, activated intracellular survival signalling, enhanced DNA repair, epithelial-mesenchymal transition (EMT) mediated chemoresistance, epigenetic alteration, aberrant metabolism[193]. In recent years, aberrant metabolism of cancer cells emerged as significant factor affecting drug efficacy and several evidences correlated some therapeutic failures with changes in cell metabolic asset[194]. In line with these findings, hindering the glycolytic metabolism of cancer cells via LDH inhibition was found to overcome the resistance to chemotherapeutic agents[195]. While there is great interest in targeting LDH, research on effective LDH inhibitors is still in early stages. Various small molecules have been developed to inhibit LDH; however, none have yet received FDA approval for the clinical use in cancer treatment[196].

As detailed explained in the Introduction, lactate (the end product of glycolysis in cancer cells) was recently shown to play a role in regulating gene expression, in promoting the unlimited growth of cancer cells and in facilitating metastasis.

My Ph.D. project was aimed at characterizing the effects of lactate signalling in cancer cells, with special attention to the potential role of this metabolite in modifying the response of cancer cells to chemotherapeutic treatments and in promoting the onset of drug resistance. This project was based on the observation that increased lactate production is a common hallmark in several neoplastic conditions showing acquired resistance to the applied anticancer treatment.

For my study, different model of cancer culture cells were used. My work can be structured in five sections.

Preliminary experiments described in Section I were aimed at evaluating the impact of lactate on the cellular response to cisplatin-induced DNA damage. For these experiments, to discriminate between the effects potentially caused by the enhanced glycolytic metabolism of cancer cells from those directly referable to lactate, we selected cancer cell lines able to grow in glucose deprived conditions (L15 medium): SW620 (a model of colorectal adenocarcinoma) and HepG2 (a model of hepatocellular carcinoma).

Section II describes a study exploring the effects of increased lactate levels on the anticancer efficacy of doxorubicin. After exposing cancer cells to a lactate concentration similar to that characterizing the microenvironment of neoplastic tissue, we examined whether this metabolite could interfere with the principal mechanisms responsible for the doxorubicin antineoplastic effect.

Experiments of Section III were devoted to highlight the potential role of lactate in reducing the response of ER-positive breast cancer (ER+ breast cancer) cells to tamoxifen treatment. Tamoxifen is a widely used oestrogen receptor inhibitor, whose clinical success is frequently limited by the development of acquired resistance. To test this hypothesis, we used the MCF7 cell line (a model of human breast cancer cell line oestrogen receptor positive, progesterone receptor positive and HER2 negative) together with a tamoxifen resistant derived sub-culture (MCF7-TAM) .

Section IV describes experiments aimed at investigating on a possible role of lactate in fostering the constitutive activation of EGFR pathway. For this study, we used two human cell lines: MDA-MB-231 (a model of triple-negative breast cancer) and HT-29 (a model of colon adenocarcinoma).

Section V describes a study performed in collaboration with Professor Alejandro Hochkoeppler, (Department of Pharmacology and Biotechnologies, FaBiT, University of Bologna) and Professor Luca Gentilucci, (Department of Chemistry, CHIM, University of Bologna), aimed at improving the knowledge of LDH kinetic properties. This study allowed the design of peptides with specific inhibition activity on LDHA (the major enzyme isoform in cancer cells). My contribution in this project was to study the effects of the peptide inhibitors on the lactate production in cultured cancer cells.

[This page is intentionally left blank]

3. SECTION I – Preliminary data:

Lactate Upregulates the Expression of DNA Repair Genes, Causing Intrinsic Resistance of Cancer Cells to Cisplatin.

3.1 Introduction

The activated glucose metabolism of cancer cells is functional in coping with their increased energy demand and need of metabolic intermediates, required to build-up new macromolecules[197,198].

As described in the Introduction, evidences showing a direct correlation between enhanced glycolysis and changes in gene expression have been obtained. Indeed, the metabolic reprogramming of cancer cells was found to impact on distinct morphological features of cancer cell nucleus[126].

Interestingly, elevation of glycolysis seems to confer cancer cells resistance to ionizing radiation[134], while its inhibition results in compromised DNA repair[135].

Predictably, facilitated DNA repair could also impact on the response of cancer cells to chemotherapeutic agents, as suggested by several evidences correlating therapeutic failures with changes in cell metabolic asset[199].

LDH activity is a nodal point for the maintenance of the glycolytic flux of cancer cells[200]. By reducing pyruvate to lactate, LDH rapidly restores NAD+, which is needed for the first steps of glucose metabolism. As mentioned above, this enzyme is considered an interesting therapeutic target for developing new antineoplastic treatments and accumulating evidences show that its inhibition or reduced expression can be successful in increasing the efficacy of chemotherapeutic agents[195,201,202]. A possible explanation to these results resides in the block of energy metabolism potentially caused by LDH inhibition, which hinders the highly ATP consuming reactions involved in DNA repair. A further mechanism could be linked to the non-metabolic functions of this enzyme; in fact, LDHA was found to be located also in cell nucleus, where it takes part in transcription complexes regulating gene expression[203].

With the experiments described in this preliminary study, we explored a possible direct role of lactate in reducing the response of cancer cells to cisplatin, a chemotherapeutic treatment that induces DNA damage. To this aim, we also verified the effect of lactate on the expression of a panel of genes involved in DNA repair, predicting a functional interaction network between the proteins encoded by the upregulated genes. We used cultured human cancer cells maintained in conditions allowing to highlight a possible direct effect of lactate, ruling out interferences from other glycolytic intermediates.

3.2 Materials and methods

3.2.1 Cell cultures and treatments

For this study two cancer cell lines were used: SW620 and HepG2 cells. Cells were cultured in L-15 medium supplemented with 100 U/ml penicillin/streptomycin, 4 mM glutamine and 10% dialyzed fetal bovine serum (FBS). This medium does not contain glucose. For some experiments, cells were also maintained in low-glucose (1 g/l) Dulbecco's minimal essential medium (DMEM), with standard supplementations. All the materials used for cell culture and all the reagents were obtained from Merck unless otherwise specified. Lactate (L-isomer) was always used at a 10 mM concentration and was administered in L-15 medium 48–72 h before experiments. Both cell cultures were found to express the MCT1 carrier for lactate uptake[204,205]. Cultures were routinely tested for Mycoplasma contamination and found to be free.

3.2.2 Cell viability experiments

The effect of cisplatin (CPL, 0–50 μM) on cell viability was assessed at 24 h, in cultures maintained in L-15 medium with or without 10 mM lactate. Results were evaluated with the neutral red assay (NR), which allows a precise estimate of cell number[206]. Before each experiment, a plot reporting the NR absorbance values of scalar amounts of cells was obtained. These data were fitted by using the linear regression analysis; the resulting mathematical equation was used to calculate the number of cells at the end of experiments. SW620 and HepG2 cells (1.0×10^4/well) were seeded in 96-multiwell plates. After 24 h treatment with CPL, they were maintained 3 h at 37°C with the NR dye, dissolved in medium at the final concentration of 30 μg/ml. Medium was then removed and the cells were solubilized with 200 μl of 1% acetic acid in 50% ethanol. Absorbance of the solutions was measured at λ540.

3.2.3 Evaluation of abasic DNA site

The amount of abasic (AB) sites on DNA after CPL treatment was evaluated using a commercially available assay from Cell Biolabs. This assay is based on the use of a probe (ARP) which specifically reacts with the aldehyde group on the open ring form of AB sites[207]. SW620 cells maintained in L-15 with or without 10 mM lactate were exposed for 90 min to CPL (0–50 μM). Genomic DNA was isolated using the phenol/chloroform/isoamyl alcohol extraction procedure[208].

The recovered, water-soluble material was then treated with 2 μg RNase (Thermo-Fisher Scientific) for 75 min at room temperature, after which the enzyme was removed by an additional step of phenol extraction. Finally, DNA was purified by ethanol precipitation. It was dissolved in a 10 mM Tris buffer, pH 7.5, containing 1 mM EDTA at a concentration of 100 μg/ml. Reaction with ARP was performed following the instructions of the assay's manufacturer and the quantification of AB sites in the experimental samples was obtained by generating a standard curve using an ARP-DNA reference sample included in the assay. Experiment was repeated twice, with duplicate samples.

3.2.4 Immunoblotting experiments

These experiments were performed in SW620 and HepG2 cells cultured in L-15 with or without 10 mM lactate; immunoblotting was used to assess the level of H3 acetylation, H2AX phosphorylation (γ-H2AX, a marker of DNA damage[209]), TP73 and GSTP1. To assess DNA damage, cells were exposed to 12.5 μM CPL for 1 h; medium was then removed and cultures were maintained for additional 16, 24 and 40 h γ-H2AX level was evaluated at the end of each time interval. For immunoblotting, cells (9×10^5 in T25 flasks) were harvested and lysed in 60 μl RIPA buffer containing protease and phosphatase inhibitors. Proteins (30–50 μg) were loaded onto 4–12% precast polyacrylamide gel for electrophoresis and run at 170 V. Gels were blotted on a low fluorescent PVDF membrane (GE Healthcare) using a standard apparatus for wet transfer. The blotted membrane was blocked with 5% BSA in TBS-TWEEN and probed with the primary antibodies: rabbit anti-H3 (Cell Signaling); rabbit anti-Panacetyl-H3 (Active Motif), rabbit anti-γ-H2AX (phospho-S139) (Abcam); rabbit anti-TP73 and anti-GSTP1 (Thermo-Fisher Scientific); rabbit anti-β-actin, (Sigma-Aldrich). Binding was revealed by a Cy5-labelled secondary antibody (goat anti rabbit-IgG, GE Healthcare). Fluorescence of the blots was assayed with the Pharos FX Scanner (Bio-Rad) at a resolution of 100 μm.

3.2.5 Study of episomal plasmid recombination

The rate of episomal plasmid recombination in SW620 and HepG2 cells maintained in L-15 with or without 10mM lactate was assessed by using a commercially available kit (Norgen Biotek). This assay is based on cell transfection with two plasmids that recombine upon entry. Recombination efficiency can be assessed by real-time PCR, using the primer mixtures included in the assay kit, which allow discriminating between the original plasmid backbones and their recombination product.

Cells were seeded in a 24-well plate (2×10^5 cells/well, in duplicate) and allowed to adhere overnight. Co-transfection with the two plasmids was performed in Lipofectamine 2000 (Thermo-Fisher Scientific) for 5 h at 37°C. At the end of incubation, cells were washed with PBS and harvested; DNA was isolated using the QIAamp DNA mini kit (Qiagen). 25 ng of purified DNA was used for the real-time PCR, which was performed according to the protocol indicated by the manufacturer.

Data analysis was based on the $^{\Delta\Delta}$Ct method and compared the level of recombination assessed in cells to that measured in control cultures.

3.2.6 Real-Time PCR Array of DNA repair genes

This experiment was performed on SW620 and HepG2 cultures, maintained in L-15 with or without 10 mM lactate (72 h). For comparison, a similar experiment was also performed on cultures grown in DMEM (a medium allowing glycolytic metabolism), exposed for 16 h to 40–80mM oxamate (OXA), a LDH inhibitor hindering glucose metabolism[210]. RNA was extracted from exponentially growing cells seeded in T75 flasks, using an RNA isolation kit (Merck) and was quantified spectrophotometrically (ONDA Nano Genius Photometer). For each sample, 2 µg RNA was retro-transcribed with the iScript gDNA Clear cDNA Synthesis kit (Bio-Rad). The expression of DNA damage and repair genes was analysed using the DNA Damage Tier 1 H96 PrimePCR™ Assay (Bio-Rad). Real-time PCR was conducted as indicated by the manufacturer, in a CFX96 real-time cycler (Bio- Rad). The validation data for this array are available online at: https://www.bio-rad.com/en-uk/prime-pcr-assays/predesignedplate/syber-green-dna-damage-tier-1-h96. The same experimental conditions were followed also for the additional PCR assays reported in figure 14D. The primers' sequences used for assessing the expression of the genes reported in figure 14D.

3.2.7 Statistical analyses

All data were analysed by using the GraphPad Prism software. All results were obtained from at least two independent experiments, performed with triplicate samples. They are expressed as mean values ± SE and have been calculated using all the data obtained from the independent experiments; the significance level was set at $p < 0.05$.

3.3 Results and discussion

3.3.1 Lactate-exposed SW620 cells showed reduced response to cisplatin

CPL was selected as a representative chemotherapeutic agent for the experiments since the pattern of DNA damage produced by this drug has been extensively studied. CPL appeared to potentially trigger all the principal DNA repair pathways: nucleotide excision repair, mismatch repair, homologous recombination and non-homologous end joining[211]. Reduced response to chemotherapeutic agents has been often correlated with increased glycolytic metabolism[199]. In order to evidence a direct contribute of lactate in this phenomenon, we searched human cancer cell lines able to grow in glucose deprived conditions (L-15 medium). According to the American Type Culture Collection (ATCC) and European Collection of Authenticated Cell Cultures (ECACC) indications, L-15 is the optimal medium for culturing the SW620 colon adenocarcinoma cells and, for this, they were used in all the reported experiments. SW620 cells were maintained in L-15 and probed with 0–50 μM CPL for 24 h, with or without a supplementation of 10 mM lactate. This dose of lactate was chosen on the basis of previously published works, suggesting that in cancer cells and extracellular milieu the concentration of this metabolite easily reaches or even overcomes this level[138]. The obtained results are reported in Figure 11A. Data were analysed by two-way ANOVA; according to Bonferroni's post-test, lactate in medium significantly reduced the antiproliferative effect of 50 μM CPL ($p < 0.05$).

3.3.2 The reduced response to cisplatin caused by lactate was associated with decreased signatures of DNA damage and upregulated DNA recombination competence

To explain the data of Figure 11A, we estimated the extent of DNA damage caused by CPL in SW620 cells grown in L-15, with or without 10 mM lactate. In the first experiment, DNA damage was evaluated by quantifying the presence of AB sites[207]. For this assay, cells were exposed for 90 min to 0–50 μM CPL. Results are shown in Figure 11B; they were statistically analysed using two way ANOVA. Lactate in medium was found to significantly decrease the number of AB sites, with $p = 0.0016$. This experiment showed that initial evidences of DNA damage are obtained starting from 12.5 μM CPL; for this reason, this dose was also applied for assessing γ-H2AX levels[209] (Figures 11C,D). In the different samples, the γ-H2AX band intensity was normalized on β-actin; the results of the densitometric reading are reported in the bar graph (Figure 11D). Data were analysed by two-

way ANOVA; Bonferroni's post-test indicated a significantly reduced γ-H2AX level in lactate-exposed cells at the 40-h time interval ($p < 0.001$). Taken together, these findings suggested enhanced competence in managing DNA damage in cells exposed to lactate. Interestingly, these cells also displayed improved DNA recombination, which was observed independently of CPL exposure.

SW620 cultures were transfected with a couple of plasmids reproducing the LacZ sequence as a result of their recombination. This sequence can be detected by real-time PCR. As shown in Figure 1E, lactate-exposed SW620 cells revealed an almost doubled capacity of generating the LacZ sequence, which suggests enhanced activity of enzymes involved in the DNA recombination process.

The data of Figure 1E were obtained from three independent experiments and were analysed by applying the paired t-test, which compared the increase measured in lactate-exposed SW620 cultures to the recombination level measured in their respective control cultures, set to 1; *p* value was 0.0389.

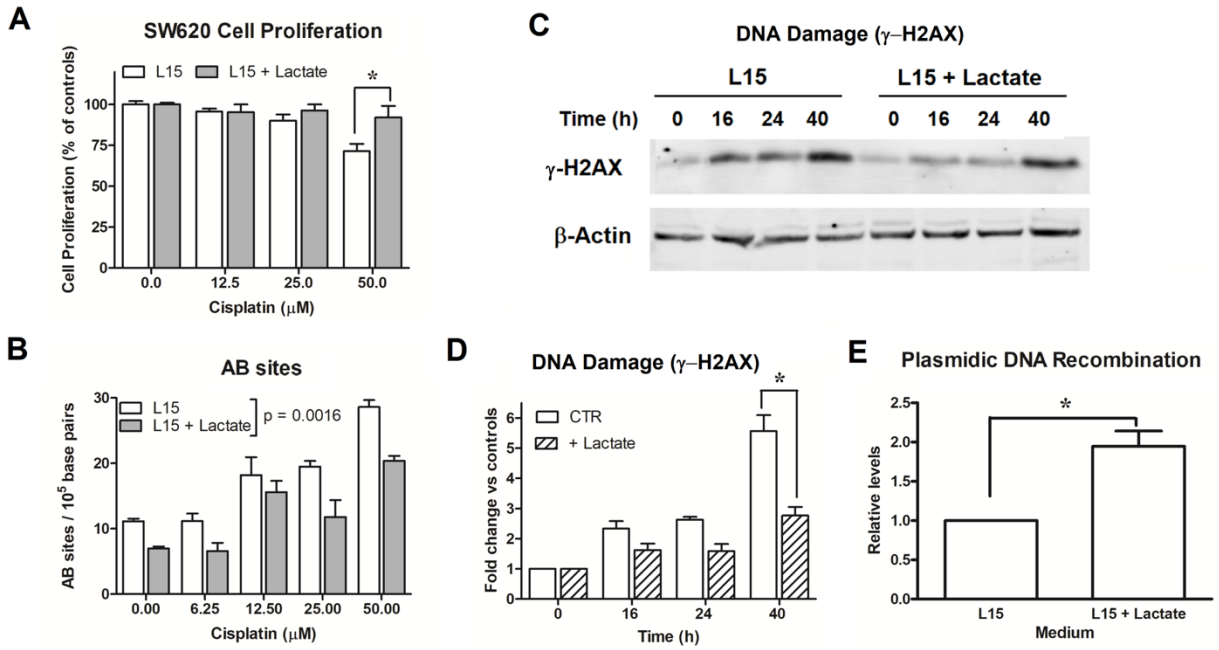

Figure 11. Experiments on SW620 cells. (A)*: Antiproliferative effects caused by cisplatin on SW620 cultures maintained in L-15. *, p < 0.05.* ***(B)****: Evaluation of AB sites in cultures exposed to scalar doses of cisplatin (0–50 μM) for 90 min, with or without 10 mM lactate. Lactate in medium was found to significantly reduce AB sites (p=0.001).* ***(C)****: Evaluation of DNA damage (γ-H2AX) in cells maintained with or without 10 mM lactate and exposed to cisplatin (12.5 μM). The densitometric reading of band intensities is shown in* ***(D)****. *, p < 0.001, compared to control cultures.* ***(E)****: DNA recombination competence assessed in cultures exposed to lactate. *, p < 0.05, compared to control cultures.*

3.3.3 Real-Time PCR array of DNA repair genes

To identify the DNA repair genes upregulated by lactate, we applied to SW620 cells a real-time PCR array specifically developed to study DNA damage and repair (Tier1 H-96 Prime PCR Array).

Experiment was repeated twice and the obtained results were processed with the aid of a dedicated software. The complete list of genes included in this array, together with the internal controls of the PCR reaction, is available at: https://www.bio-rad.com/en-uk/prime-pcr-assays/predesigned-plate/sybr-green-dna-damage-tier-1-h96.

In evaluating the obtained results, a lower threshold at 25%-increased expression was set, since comparable effects have been reported in previous studies examining the epigenetic effects of lactate in different experimental settings[212]. Among the 88 genes included in the array, 12 showed a >25% upregulation following lactate exposure; they are reported in the bar graph of Figure 12A. Results were analysed using the column statistics' function of the GraphPad software by applying the one-sample t-test, which computes whether the mean of each data set is different from a given hypothetical value (0, i.e., no change, compared to untreated cultures). All the reported data were found to be statistically significant with the exception of the genes for Cyclin Dependent Kinase 1 (CDK1) and for H2AX variant Histone (H2AFX). The statistically significant changes showed *p* values ranging from 0.045 to 0.009.

To confirm the findings of Figure 12A, additional PCR array experiments were performed on SW620 cells grown in DMEM. Contrary to L-15, DMEM contains glucose and allows the proceeding of glycolytic flux up to lactate. For these PCR experiments we exposed glycolyzing SW620 cells to 40mM OXA for 16 h. As describe in the Introduction, OXA is a pyruvate analogue which specifically inhibits LDH[66]; in preliminary experiments (data not shown), we found that a 40 mM dose of this inhibitor almost completely prevents lactate production in glycolyzing SW620 cells, without reducing their ATP level and viability. Figure 12B shows that when glycolyzing SW620 cells were exposed to OXA, all the 12 genes identified in the previous PCR array (Figure 12A) reduced their expression below the levels measured in untreated, glycolyzing cells. With the exception of Flap structure-specific Endonuclease 1 gene (FEN1), all the observed reductions were found to be statistically significant; *p* values ranged from 0.039 to < 0.0001. Interestingly, in lactate deprived cultures a statistically significant reduction was observed also for CDK1 and H2AFX.

To extend our observations, we wondered whether the changes in gene expression caused by lactate could differ among cell types. For this reason, we searched a second culture able to grow in the same glucose-deprived condition as SW620 cells, but from a different tissue. The HepG2 hepatoma cell line was found to tolerate the glucose-deprived L-15 medium and was then used for

additional PCR array experiments, aimed at evaluating the expression of DNA repair genes after lactate exposure. Results are shown in Figure 12C. In this case, we found a >25% upregulation in 9 genes and, interestingly, 6 of them were in common with SW620 cells. Results were analysed as described for SW620 cells. In HepG2 cells, the observed upregulation reached the level of statistical significance for all genes; *p* values ranged from 0.048 to < 0.0001. When these cells were maintained in DMEM and exposed to the OXA dose preventing lactate production (80 mM) all the observed changes were reversed, except for CDK1NA, which was further increased. The *p* values ranged from 0.039 to < 0.0001. The antiproliferative effect caused by OXA in DMEM-cultured HepG2 cells could explain the finding concerning CDK1NA (a cell cycle regulator).

Figure 12E shows that lactate-exposed SW620 and HepG2 cells displayed a significantly increased level of H3 acetylation, suggesting inhibition of HDAC as the mechanism underlying the effects observed in Figures 12A,C.

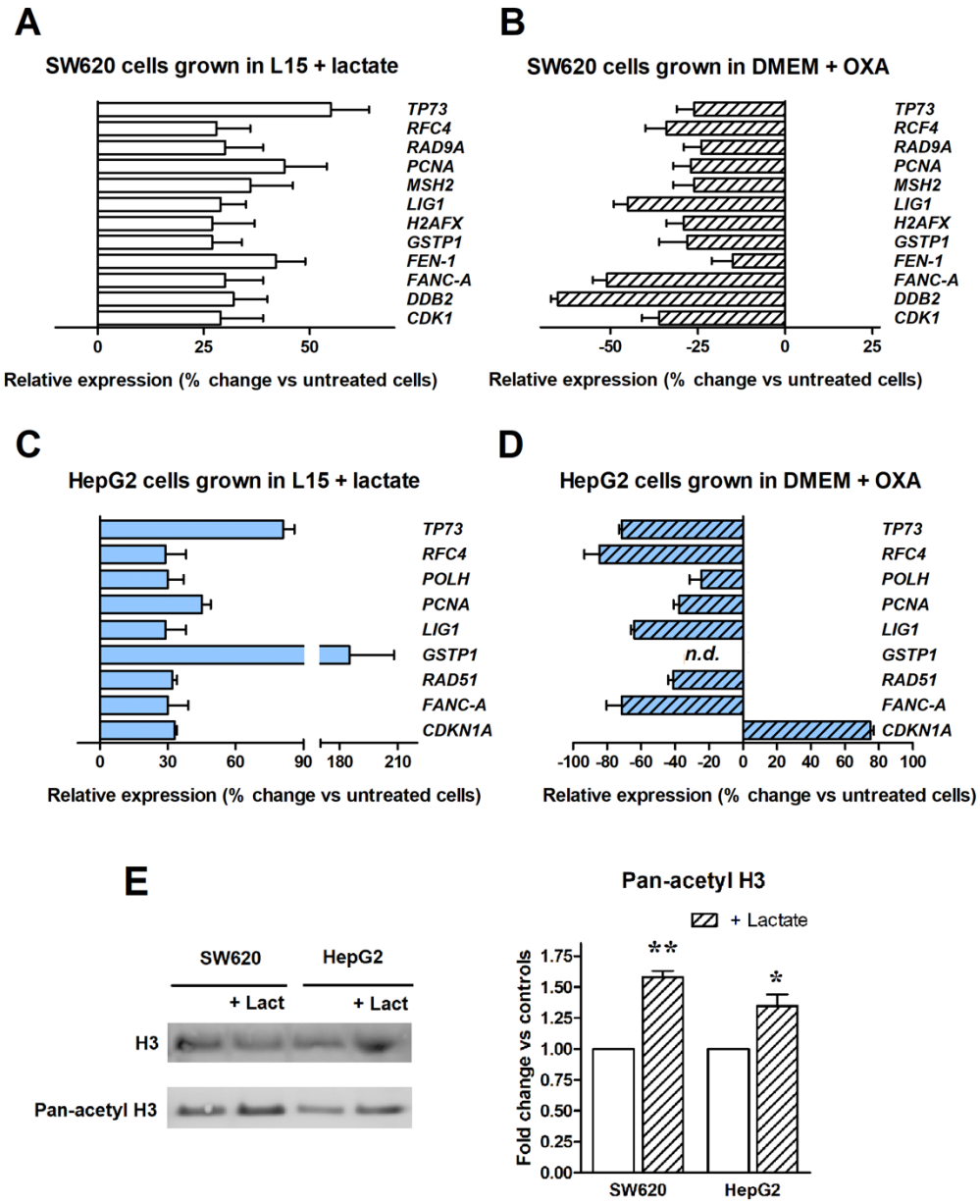

Figure 12. Real-time PCR array of DNA repair genes. *The bar graphs display genes showing a >25%-increased expression.* ***(A)****: Experiment performed in SW620 cells maintained in L-15 medium and exposed to lactate. All the reported data were found to be statistically significant, with the exception of H2AFX and CDK1.* ***(B)****: Experiment performed in glycolyzing SW620 cells exposed to OXA. Lactate depletion caused by OXA significantly reduced the expression of all the genes, with the exception of FEN1.* ***(C)****: Experiment performed in HepG2 cultures maintained in L-15 medium and exposed to lactate. All the reported data were found to be statistically significant. The used statistical analysis and the obtained p values are reported in the text.* ***(D)*** *Experiment performed in glycolyzing HepG2 cells exposed to OXA. Lactate depletion caused by OXA significantly reduced the expression of all the genes, with the exception of CDK1NA. n.d.: GSTP1 expression was not detected in OXA exposed cells.* ***(E)*** *Level of H3 acetylation assessed in lactate-exposed cultures. * and **, $p < 0.05$ and <0.01, compared to control cultures, respectively.*

3.3.4 Experiments on lactate-exposed HepG2 cells

Following these results, we also investigated whether a different susceptibility to DNA damage could also be detected in lactate-exposed HepG2 cultures, as observed for SW620 cells. Due to the compromised proliferation shown by these cells in L-15; the obtained results are reported in Figure 13. The data of Figures 13A,B were in line with those previously observed in SW620 cells. They were statistically analysed as described for the corresponding experiments in Figures 11A, E. In the experiment of Figure 13A, lactate was found to significantly reduce the efficacy of 25 and 50 μM CPL ($p < 0.05$, according to Bonferroni's post-test). In the experiment of Figure 13B, the plasmidic DNA recombination detected in lactate-exposed cells was significantly increased ($p = 0.045$). The study of γ-H2AX (Figure 13C) showed in HepG2 cells a DNA damage signalling pattern different from that observed in SW620 cultures (Figures 11C,D). A γ-H2AX level constantly increasing over time was observed in control cells. Lactate exposed cultures showed a constitutively higher γ-H2AX signal, which after CPL treatment peaked at 16 h. However, when compared to T = 0, its further increase over time (fold change) was significantly lower than that measured in control cultures not exposed to lactate: at 40 h, a 2-fold increased signal was detected in control cultures, while a 1.3-fold increase was measured in lactate-exposed cells. Data of Figure 13C were statistically analysed as described for the similar experiment performed on SW620 cells (Figure 11C). The increase of γ-H2AX signal (fold change) in lactate-exposed cultures was significantly lower at 24 and 40 h ($p <$ 0.05 and 0.01, respectively, according to Bonferroni's post-test).

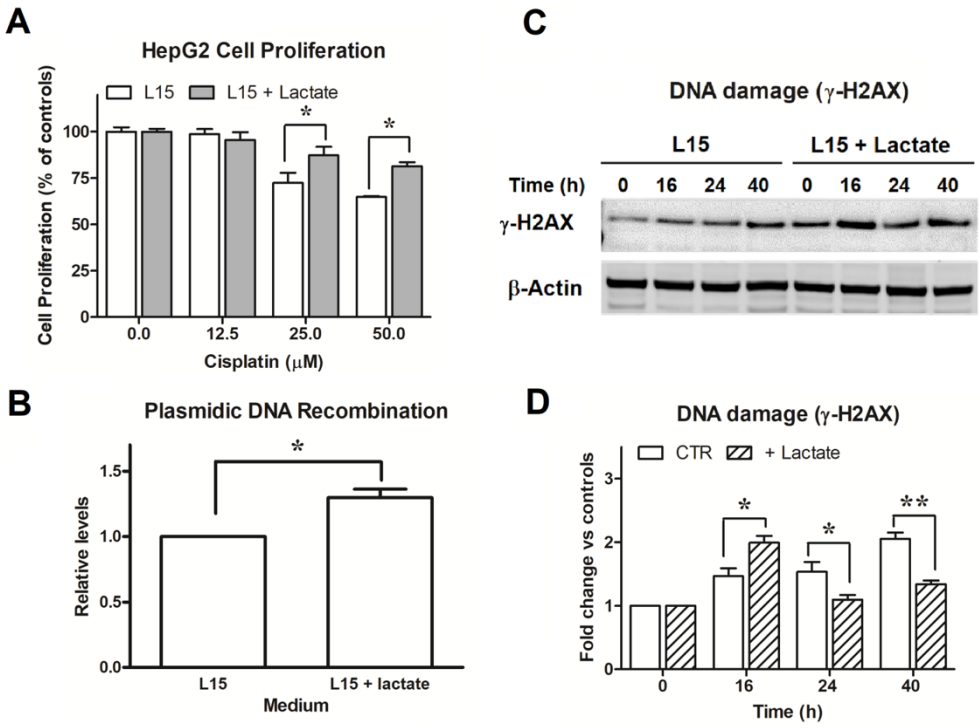

Figure 13. Experiments on HepG2 cells. (A)*: Antiproliferative effects caused by cisplatin on HepG2 maintained in L-15 and exposed to 10 mM lactate. *, p < 0.05, compared to control cultures.* ***(B)****: DNA recombination competence, assessed as described for SW620 cells. *, p < 0.05.* ***(C)****: Evaluation of DNA damage following CPL exposure in cells maintained with or without 10 mM lactate and assessed by immunoblotting evaluation of γ-H2AX. The densitometric reading of band intensities is shown in* ***(D)****. Lactate-exposed cells showed a constitutively higher γ-H2AX signal which, after CPL treatment, peaked at T = 16 h. At later time intervals, the γ-H2AX signal increase referred to T = 0 (fold change) was significantly lower in lactate-exposed cells, when compared to control cultures. *, p < 0.05; **, p < 0.01.*

3.3.5 Functional interaction network of upregulated genes

The PCR array experiments allowed us to identify a cluster of 6 genes which in both SW620 and HepG2 cells appeared to be potentially regulated through the level of this metabolite: Proliferating Cell Nuclear Antigen (PCNA), Tumor Protein p73 (TP73), Replication Factor C subunit 4 (RFC4), Fanconi Anemia complementation group A (FANC-A), DNA Ligase 1 (LIG1), Glutathione S-Transferase π1 (GSTP-1). To identify the functional connections between the corresponding proteins, we used the Search Tool for the Retrieval of Interacting Genes (STRING) database, a resource which can be reached at: http://string-db.org. The STRING database is able to construct interaction networks among genes, also providing a confidence score; moreover, by applying the Kyoto Encyclopaedia of

Genes and Genomes (KEGG) analysis, it identifies their related biochemical pathways and cellular functions. Figures 14A, B show the obtained results. In building the interaction network, the edges representing gene-gene associations have been set on the highest confidence interaction score (0.9), to increase the strength of data support. This setting resulted in the identification of a functional network involving four of the analysed genes, which gave an interaction enrichment p value = 7.35×10^{-05}. Accordingly, three of the four identified KEGG pathways showed very low false discovery rates, reported in the scheme of Figure 14B. All of them concern the interaction between LIG1, PCNA and RFC4. Interestingly, the identified pathways include mismatch and nucleotide excision DNA repair, which were found to be involved in cellular response to CPL damage[211]. These data can give a mechanistic explanation to the results obtained in lactate-exposed SW620 and HepG2 cells, treated with CPL; together with the data of Figures 11–13, they suggest that the increased gene expression caused by lactate can result in enhanced protein function, leading to modified cell response to DNA damaging agents. According to Figure 14A, TP3 and GSTP1 cannot be included in the gene network involved in the response to CPL. For this reason, we analysed the level of the corresponding proteins by immunoblotting. Results (Figure 14C) showed increased level of TP73 in both lactate-exposed cultures, while GSTP1 protein appeared to be unchanged. GSTP1 belongs to the family of phase II detoxification enzymes, the activity of which is commonly induced by exposition to xenobiotics[213]; for this reason, it can be hypothesized that the upregulated GSTP1 gene expression caused by lactate is not sufficient for obtaining enhanced protein levels.

Finally, we focused our attention on the two genes showing the highest increased expression in lactate-exposed cells: PCNA and TP73 (Figures 12A,C). PCNA is a DNA polymerase accessory factor playing a regulatory role in both DNA repair and replication[214,215]. It was found to be preferentially expressed in actively proliferating human cancer cells and in transformed normal cells; moreover, it has also been widely used as a tumour marker. TP73 is a member of the TP53 family showing prognostic significance[216]. TP73 can be translated into different isoforms with opposite functions; in particular, the A isoform (TAp73) shows tumour-suppressor activity, while the Dominant-Negative isoform (ΔNTP73) fails to induce apoptosis and cell cycle arrest. It negatively regulates TP53 and TAp73 by acting as negative dominant. The primer sequences used for the DNA-damage PCR assay did not allow to discriminate between the TP73 isoforms. For these reasons, an additional PCR study was performed to characterize the phenotypic changes induced in both SW620 and HepG2 cells by lactate exposure. We analysed the expression of representative genes associated with proliferative potential and stem cell properties. Results are shown in Figure 14D. Unfortunately, in HepG2 cultures the only detectable genes were those of the epithelial and neural cadherins (E- and N-CAD)[217] and Ki67[218]. No significant changes were observed concerning E- and N-CAD; a

significant increase was detected for Ki67 expression ($p < 0.05$). An upregulation of this proliferation marker was also found in SW620 cells; in both cell lines, the increased expression of Ki67 fits well with the data of PCNA expression. In SW620 cells, lactate was found to markedly increase E-CAD levels and to cause reduced ΔNTP73. Together with the unchanged levels of the colon cancer stem markers NANOG, SLUG and SNAIL[219], these effects suggest that the increased trend in cell proliferation usually associated with Ki67 and PCNA is not characterized by phenotypic traits suggesting cancer progression, at least in this cell model. This idea is in line with the markedly upregulated expression of GSTP1, primarily observed in HepG2 cells (Figure 12C); the clinical significance of this parameter was repeatedly investigated in hepatocellular carcinoma and was found to correlate with a favourable prognosis[220]. Notably, in lactate-exposed SW620 cultures a doubled level of Aldehyde Dehydrogenase (ALDH1) was observed, suggesting that the increased resistance of these cells to CPL could also be linked to their higher capacity to cope with oxidative stress[221].

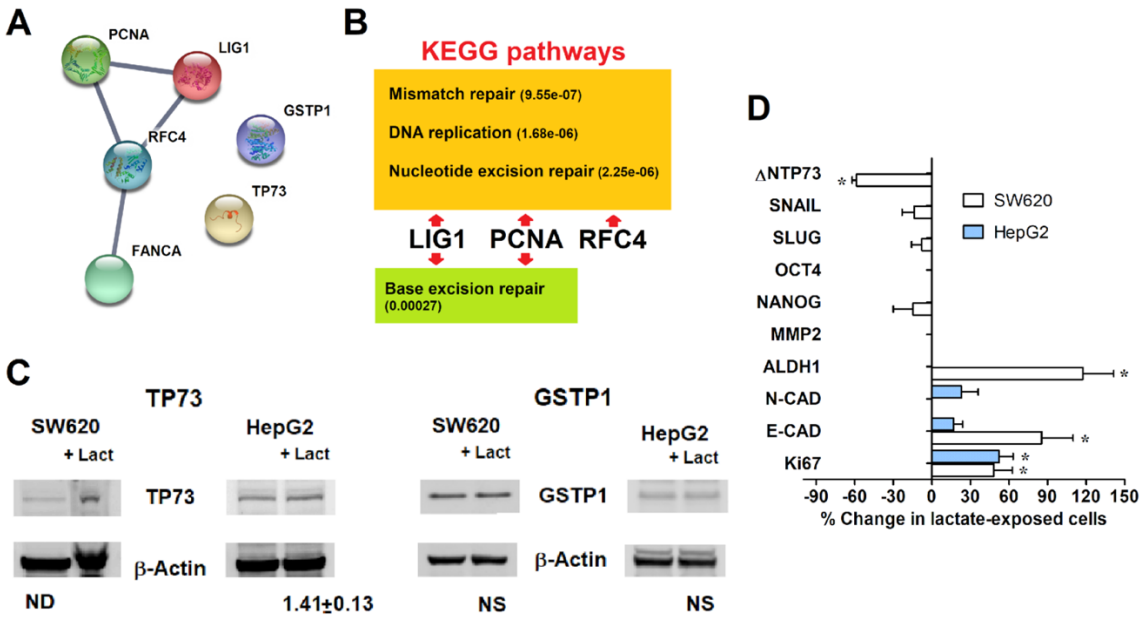

***Figure 14. (A)**: Functional interaction network among the genes identified using the real-time PCR array; downloaded from http://string-db.org. The edge thickness between protein nodes is indicative of a 0.9 confidence score. **(B)**: Biochemical pathways identified by the KEGG analysis. In parentheses, false discovery rates. **(C)**: Immunoblotting evaluation of the proteins not included in the identified DNA repair pathways. The level of TP73 was found to be increased in both lactate exposed cultures. **(D)**: Expression of representative genes associated with proliferative potential and stem properties, assessed in lactate-exposed SW620 and HepG2 cells. Data were analysed using the column statistics function of the Prism software, as described for the PCR array of DNA repair genes; *, statistically significant changes; p values ranged from 0.040 to 0.004. Missing bars in the graph denote undetectable mRNA.*

3.4 Conclusion – SECTION I – Preliminary data

As described in the Introduction, lactate has an important role in linking the metabolic state of the cell to gene expression[14,138,222].

Lactate has been defined a "mirror and motor" of tumour malignancy[9,44,223], since the metabolic program characterized by increased glycolysis and lactate production supports neoplastic change and tumour progression. Increased glycolysis is also associated with one of the most serious problems complicating cancer treatment, the increased drug resistance[199].

A better understanding of the linkages between the drug resistant phenotype and glycolytic metabolism is complicated by the difficulty of discriminating between a possible effect of lactate from that of other intermediates originating from glucose metabolism, for which a role in transcriptional regulation has also been suggested[126,133].

The experiments described in this preliminary Section attempted to address this issue. To our knowledge, our experiments showed for the first time a direct effect of this metabolite increasing the expression of genes needed for mismatch and nucleotide excision DNA repair, which appeared to compromise the antineoplastic efficacy of cisplatin. Our data suggest that the increased lactate production of cancer cells could facilitate the onset of chemotherapy resistance.

For this preliminary study, to explore a possible direct role of lactate on cancer cells, we used cell lines able to grow in glucose-deprived conditions (L-15 medium). Since only a few cell lines can tolerate these specific growth conditions, for the subsequent studies, we utilized alternative models (see Section II).

[This page is intentionally left blank]

4. SECTION II

Lactate Can Modulate The Antineoplastic Effects Of Doxorubicin And Relieve The Drug's Oxidative Damage On Cardiomyocytes

Following the preliminary data obtained with cisplatin, we focused our attention on investigating the potential role of lactate in modifying the response of cancer cells to doxorubicin.

4.1 Introduction

To improve neoplastic disease treatment, recent efforts have mainly focused on the development of new-generation drugs, targeting critical pathways involved in cancer cell proliferation and survival. However, despite the unquestionable progress achieved with these studies, the currently applied anticancer therapeutic regimens very often continue to maintain the use of old, conventional chemotherapeutic agents. In this context, the enduring use of doxorubicin (DOXO) in the fight against disparate cancer diseases is exemplificative[224,225].

DOXO belongs to the family of anthracyclines and is probably one of the most effective antineoplastic drugs ever developed, even though its potential side effects (heart muscle damage) can limit the success of treatment[226]. DOXO and its variants are currently administered as the first-choice therapy for a variety of solid and hematologic malignancies and have also been evaluated in combination treatments[225,226].

Concurrently with this extensive and long-lasting clinical use, the molecular targets of DOXO action have been actively investigated and a number of potential antineoplastic mechanisms have been proposed for this drug. Some of these postulated mechanisms are probably not relevant for the antineoplastic effects observed in clinics since they were documented at DOXO concentrations far above those reached in the blood circulation of treated patients. Others were observed at clinically relevant drug doses[227–229]. Among these, the best characterized are topoisomerase-2 (TOP2) poisoning, free radical generation, ceramide overproduction and histone eviction. In addition to contributing to DOXO antineoplastic action[230], free radical generation is also considered to be involved in heart muscle damage[231], often hindering an adequately lasting treatment. Histone eviction from nucleosomes results from the well-documented capacity of DOXO to intercalate between DNA bases[229]; DOXO intercalation causes torsional stress in the DNA helix, leading to H2A/H2B

dissociation. This event could be involved in the antineoplastic effects and could also explain the extensive alteration in transcriptome observed in cells exposed to DOXO or to its variants[232].

Changes in cell transcriptome can also be linked to cellular metabolic asset since intermediates originating from energy metabolism reactions have been found to alter histone acetylation and chromatin structure[203]. As mentioned before, lactate is one of the most studied metabolite showing the potential of altering gene expression. Through histone lactylation, lactate can function as a sensor able to transduce metabolic changes into stable gene expression patterns[142]. As described in Section I, preliminary experiments showed that lactate has the potential to reduce the antineoplastic efficacy of cisplatin, an effect linked to the increased expression of genes involved in repair pathways typically associated with managing DNA alterations caused by this drug.

The experiments reported in this Section investigated whether lactate could interfere with the principal mechanisms responsible for the DOXO antineoplastic effect, considering the transcriptional changes potentially caused by the joint action of both compounds. The experimental outline is summarized in the following Scheme 1:

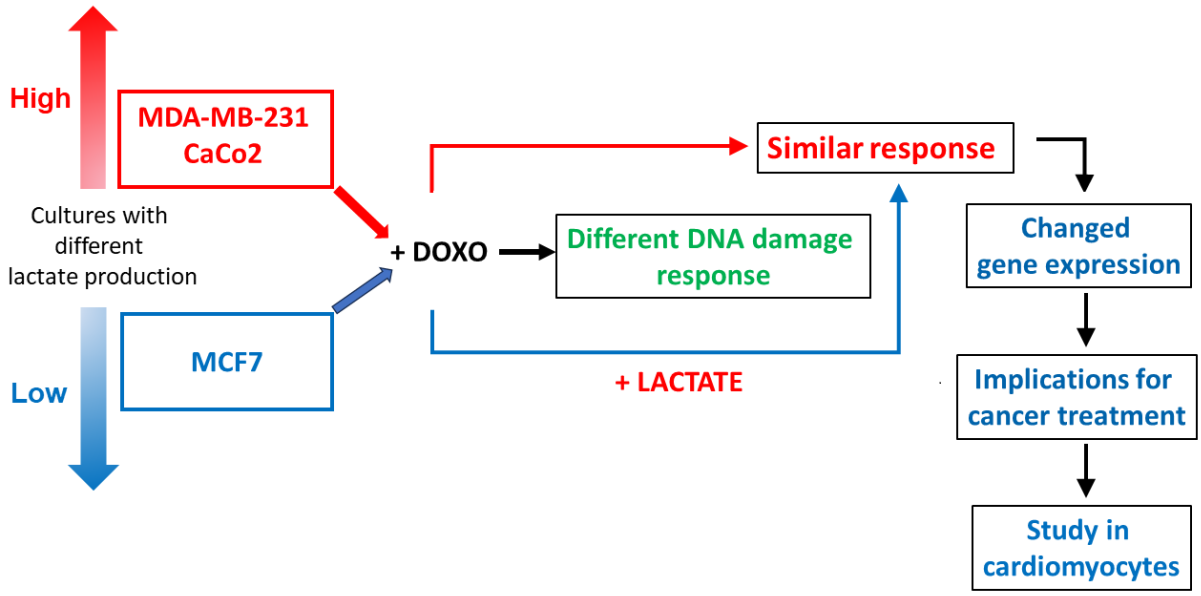

***Scheme 1**. Experimental outline.*

4.2 Materials and methods

4.2.1 Cell cultures and treatments

For this study four different cell lines were use: MCF7, MDA-MB-231, CaCo2 and H9c2 cells (ATCC, Manassas, VA, USA). All these cell lines were grown in low-glucose (1 g/l) DMEM, supplemented with 100 U/mL penicillin/streptomycin, 2 mM glutamine and 10% FBS. All the materials used for cell culture and all the reagents were obtained from Merck unless otherwise specified. Lactate (L-isomer) was dissolved in the culture medium at a 20 mM concentration; before DOXO treatment, MCF7 and H9c2 cell cultures were exposed to 20 mM lactate for 72 h. DOXO (Selleckchem) was dissolved in dimethyl-sulfoxide (DMSO). In DOXO including experiments, the culture medium was supplemented with 0.6% DMSO.

Differentiation of H9c2 cardiomyocytes was induced when cells reached 80% confluence; to this aim, cells were maintained for 10–11 days in DMEM with 1% FBS and supplemented daily with 10 nM retinoic acid (Enzo Life Sciences). Mycoplasma contamination and found to be free.

4.2.2 Assay of lactate levels

Cells (5×10^5/well) were plated in triplicate in 6-well plates and left to adhere overnight. The medium was then replaced with Krebs–Ringer buffer and the released lactate was measured after 2–4 h incubation at 37 °C. In particular, at the end of incubation, 200–400 µL of Krebs–Ringer buffer was withdrawn, brought to 1 mL with H2O and mixed with 200 µL of 20% $CuSO_4$; 200 mg di $Ca(OH)_2$ were then added, and the tubes were maintained for 30 min at room temperature. After a 5 min centrifugation at 4000 rpm, 200 µL of the supernatant was placed in conical glass tubes containing 1.25 mL of 96% H_2SO_4, vortexed and boiled for 5 min at 100 °C. The samples were then placed on ice and added with 6.4 µL of 4% $CuSO_4$ and 5 µL of phenyl–phenol. After 30 min incubation at 37 °C and 1.5 min of boiling, they were left to cool at room temperature. The absorbance was read at λ 565, and the amount of lactic acid in the samples was calculated with the aid of a calibration curve prepared with known amounts of sodium lactate.

4.2.3 Immunoblotting experiments

Immunoblotting was used (a) to evidence DOXO-induced DNA damage, which was assessed with histone 2AX phosphorylation (γ-H2AX, an established marker of DNA damage[209]); (b) to evaluate, in treated cells, the levels of LDHA, glucose-regulated protein 94 (GRP94, also known as heat shock protein 90B), superoxide dismutase 1 and 2 (SOD1, SOD2) and single-strand selective monofunctional uracil DNA glycosylase (SMUG1); (c) to assess the level of acetylated histone 3 in lactate-exposed MCF7 cells.

For evidencing γ-H2AX, LDHA and GRP94 proteins, the cell cultures were exposed to 1 μM DOXO from 0 to 24 h. SOD1, SOD2 and SMUG1 proteins were evaluated in control and lactate-exposed MCF7 cells treated with 1 μM DOXO for 4 h, followed by a 16 h recovery time.

In all immunoblotting experiments, at the indicated times after treatment, cell cultures (T-25 flasks, at 80% confluence) were harvested and lysed in 50 μL RIPA buffer containing protease and phosphatase inhibitors. Then, 60 μg of protein (measured according to Bradford) was loaded onto precast 4–12% polyacrylamide gels for electrophoresis and run at 170 V. The separated proteins were blotted on low-fluorescent PVDF membranes (Cytiva Life Sciences, Milano, Italy) using a standard apparatus for wet transfer with an electrical field of 60 mA for 16 h. The blotted membranes were blocked with 5% BSA in TBS-Tween and probed with the primary antibody. Actin was used as a loading control in all experiments, with the exception of those performed in MCF7 cultures and requiring long exposure times (≥6 h) to DOXO. In agreement with published data[233], we observed that long DOXO exposures changed the actin level in MCF7 cells; in these cases, constitutive heat shock 70 (HSC70) was the selected internal control protein. For each immunoblotting experiment, the used internal control protein can be verified from the Figures (Figures 15, 17, 18, 20 and 21) by referring to the indicated molecular weights (38–49 kDa and 62–98 kDa for actin and HSC70, respectively). The used antibodies were: rabbit anti-human γ-H2AX (phospho-S139) (Abcam); rabbit anti-rat γ-H2AX (phospho-S139) (Cell Signaling); rabbit anti-LDH-A (Cell Signaling); rabbit anti-GRP94 (Cell Signaling); rabbit anti-histone-3 (Cell Signaling); rabbit anti-panacetyl-histone-3 (Active Motif); rabbit anti- human and rat SOD1 (Cohesion Bioscience); rabbit anti-human and rat SOD2 (Cohesion Bioscience); rabbit anti-SMUG1 (Cohesion Bioscience); rabbit anti-Actin (Merck); and rabbit anti-HSC70 (Enzo Life Sciences). Binding was revealed using a Cy5-labelled secondary antibody (goat anti-rabbit-IgG, Cytiva Life Sciences). The fluorescence of the blots was assessed with the Pharos FX Scanner (Bio-Rad) at a resolution of 100 μm. The intensity of the bands was evaluated using the ImageJ software methods.

4.2.4 Evaluation of oxidative stress

Oxidative stress was evaluated using a 2′,7′-dichlorofluorescin diacetate (DCF-DA) assay. After cell entry, in the presence of ROS, this probe is oxidized to highly fluorescent dichloro-fluorescein (DCF)[234].

Control and lactate-exposed MCF7 cells were grown on coverslips in 6-well plates and treated for 2 h with 1 μM DOXO. After washing with PBS two times, the cells were incubated at room temperature in the dark for 25 min with 10 μM DCF-DA dissolved in PBS. Cultures were then quickly washed with PBS and mounted with a solution of Hoechst/DABCO (1:200). The samples were observed using a Nikon epifluorescence microscope equipped with filters for Hoechst and FITC. Cells showing a bright and intense fluorescence were counted as positive, whereas cells having no or low fluorescence were counted as negative. For each sample, 500–700 cells were counted by two independent observers. A similar experiment was performed using proliferating and differentiated H9c2 (D-H9c2) cells. In this case, the control and lactate-exposed cells were treated with 1 μM DOXO for 16 h.

In a further experiment, oxidative stress in DOXO-treated MCF7 cells was evaluated by measuring 8-hydroxy-2-deoxy guanosine (8-OHdG), a marker of DNA oxidative damage, generated by reactive oxygen and nitrogen species[235]. A commercially available competitive ELISA test was used (Abcam) following the manufacturer's protocol. Control and lactate-exposed MCF7 cells were treated with 1 μM DOXO for 2 h. Genomic DNA was isolated using the phenol/chloroform/isoamyl alcohol extraction procedure[208]. DNA was digested using Nuclease P1 (New England BioLabs) in 50 mM sodium acetate pH 5.5; the pH was then adjusted to 7.5–8.5 using 1 M TRIS. For each sample, 100 μg of DNA was incubated at 37 °C for 30 min with 1 unit of alkaline phosphatase. Samples were then boiled for 10 min and placed on ice until used. For the ELISA procedure, they were diluted to a final DNA concentration of 500 ng/mL, and 25 ng samples were used for the assay. At the end of the procedure, absorbance was measured using a Victor plate reader (PerkinElmer) with a wavelength of 450 nm.

4.2.5 Real-Time PCR

This experiment was performed in control and lactate-exposed MCF7, MDA-MB-231 and CaCo2 cells to evaluate the expression of inducible heat shock protein 70 (HSP70), GRP94 and TNF receptor-associated protein 1 (TRAP1, the mitochondrial form of HSP90). Exponentially growing cells from T25 flasks were used. In a further, different experiment, control and lactate-exposed MCF7

cells were treated with 1 µM of DOXO for 4 h followed by a 16 h recovery. RNA was extracted using a RNA isolation kit (Merck) and was quantified spectrophotometrically (ONDA Nano Genius Photometer). Retro-transcription to cDNA was performed using a Revert Aid First Strand cDNA Synthesis Kit (ThermoFisher) in different steps: 5 min denaturation at 65°C, 5 min annealing at 25°C, 1 h retro-transcription at 42°C and 5 min at 70°C. A real-time PCR (RT-PCR) analysis was performed using 20 ng cDNA, SsoAdvanced Universal SYBR Green Supermix (Bio-Rad) and different primer mixtures. All the primers used for the PCR experiments were predesigned and obtained from Merck. For all genes, the annealing temperature of the primers was 60°C, and the thermal cycler (CFX96 TM Real-Time System, Bio-Rad) was programmed as follows: 30 s at 95°C, 40 cycles of 15 s at 95 °C and 30s at 60°C. The data from RT-PCR experiments were analysed by applying the $2^{-\Delta\Delta CT}$ method[236].

4.2.6 Quantification of TOP2A:DNA covalent complexes

To assess a possible increase in TOP2A:DNA complexes after DOXO treatment, the in vivo complex of the enzyme assay[237] was followed, with some modifications. Specifically, control and lactate-exposed MCF7 cells (T-25 flasks, at 80% confluence) were treated with 1 µM DOXO for 24 h. After treatment, the medium was removed and 3 mL of 1% Sarkosyl in 1X TE pH 7.5 (10 mM Tris HCl pH 7.5, 1 mM EDTA) was added to the flasks. The addition of the anionic detergent caused cell lysis and stabilization of the DNA–protein complexes, which became measurable. Cell lysates were sheared with a syringe equipped with a 25G gauge needle, and the final volumes were then increased to 10 mL with 1% Sarkosyl solution. Sheared lysates were gently stratified onto 3 mL of 9 M CsCl, dissolved in H2O in 13.5 mL Quick-Seal centrifuge tubes (Beckman Coulter, Pasadena, CA, USA) and centrifuged (121,900× g for 21 h at 25°C). The pelleted material containing DNA and bound proteins was washed once with 500 µL of 70% ethanol, air-dried to remove ethanol, dissolved again in 200 µL 1X TE buffer pH 7.5, left overnight at 4°C and then incubated in a water bath at 65°C for 5 min to complete resuspension.

The DNA concentration of the samples was measured; scalar amounts of DNA (0–5 µg) were diluted to a final volume of 200 µL with 1X TE buffer and applied on a PVDF membrane (Cytiva Life Science) using a dot-blot apparatus (Bio-Rad). The blotted membrane was blocked with 5% BSA (in TBS-TWEEN) for 1 h and probed with the primary antibody (rabbit-anti-topoisomerase II alpha, Abcam). Binding was revealed using a Cy5-labelled secondary antibody (goat anti-rabbit-IgG, Cytiva Life Sciences). The fluorescence of the blots was assessed with the Pharos FX Scanner (Bio-Rad) at a resolution of 100 µm. The results were evaluated with densitometry using the Protein Array

Analyzer in ImageJ software with the aid of the Gilles Carpentier's Dot-Blot-Analyzer macro. This macro is available at http://rsb.info.nih.gov/ij/macros/toolsets/Dot%20Blot%20Analyzer.txt.

4.2.7 Cell proliferation

These experiments were performed in control and lactate-exposed MCF7 cultures and in an MCF7 subclone grown in the presence of 20 mM lactate for at least 6 months (LAC-MCF7). Cells (20×10^4 cells/well) were plated in clear bottom 96-well white plates, left to adhere overnight and then exposed to scalar doses of DOXO (0–8 μM) for 24–48 h. At the end of treatment, cell proliferation was assessed with the detection of ATP levels using the CellTiter-Glo Assay (Promega). A Fluoroskan Ascent FL reader was used to evaluate the plates' luminescence.

4.2.8 Statistical analyses

All data were analysed as described in paragraph 3.2.7 in Materials and methods of Section I.

4.3 Results and discussion

4.3.1 Enhanced lactate levels modified the DNA damaging effects caused by DOXO

The primary model used for our study was the MCF7 breast cancer cell line. Chemotherapeutic treatments based on DOXO are a frequent therapeutic option for patients diagnosed with breast cancer[238], and MCF7 cultures are among the most studied models for this neoplasm. These cells are characterized by moderate-level glycolysis, which allows to easily evidence lactate-induced cell changes following exogenous administration of increased amounts of this metabolite. To highlight a possible role of lactate in modifying DOXO antineoplastic action, MCF7 cultures were routinely grown with 5 mM glucose and exposed to 20 mM lactate, added to the medium 72 h before experiments. This lactate concentration fits well with the level of metabolite usually assessed in the microenvironment of neoplastic tissues[138]. The data obtained from MCF7 cultures exposed to lactate and treated with DOXO were compared with results obtained for the MDA-MB-231 and CaCo2 cultures. MDA-MB-231 cells are a widely used model of drug-resistant breast cancer[239]. The CaCo2 culture was selected as representative of a neoplastic disease from a different tissue, for which DOXO-based treatment is a frequent therapeutic option[240]. As shown in Figure 15A, both these cultures were characterized by significantly increased levels of glycolysis and lactate production compared to MCF7 cells ($p < 0.01$ at both 2 and 4 h).

In the first experiment, the three cell cultures, together with lactate-exposed MCF7 cells, were treated with 1 μM DOXO, and the drug-induced DNA damage was assessed at different times using an immunoblotting evaluation of γ-H2AX[209]. The results are shown in Figure 15B, C. Interestingly, all the cultures exposed to higher lactate levels (derived from either constitutively increased glycolysis rate or exogenous administration) appeared to respond similarly to DOXO treatment. In contrast, they showed an appreciably reduced DNA damage signal compared to MCF7 cultures at 2 and 6 h. In lactate-exposed MCF7 cells, the increase in γ-H2AX band intensities measured at these time intervals after DOXO treatment was 2.4- and 1.8-fold lower than that measured in DOXO-treated control MCF7 cells ($p < 0.01$ and < 0.05 at 2 and 6 h, respectively). Conversely, the fold increase in the DNA damage signal assessed at 16 and 24 h appeared to be significantly higher in the lactate-exposed MCF7 culture (2.2-fold at 24 h with $p < 0.05$) (Figure 15C).

The immunoblotting experiment shown in Figure 15B,C also investigated the changes in LDHA level during the phase of DOXO treatment. As well known, DNA damage triggers glycolysis[134] since increased ATP levels are required for the repair reactions. Interestingly, parental MCF7 and MDA-MB-231 cells showed progressively enhanced LDHA levels, in relation to the timing of DOXO

exposure: in the case of MCF7 cells, a ≈2.3-fold increase was measured at both 16 and 24 h ($p < 0.05$). This increase appeared to be linked to lactate levels since it was undetected in lactate-exposed MCF7 cells and in CaCo2, the cell line showing the highest rate of lactate production (Figure 15A). This result could be interpreted as a feedback regulation mechanism induced by elevated lactate levels in the medium. Increased LDHA is expected to lead to higher lactate production, which could potentially affect cell response to DOXO. The viability experiments described below (see Section 4.3.5) showed no difference between lactate-exposed MCF7 cells and their parental culture treated with DOXO for 24–48 h. This result suggests that the evidenced glycolytic flare (Figure 15B, C) could play a role in equalizing the drug response of the two cell cultures in the long term.

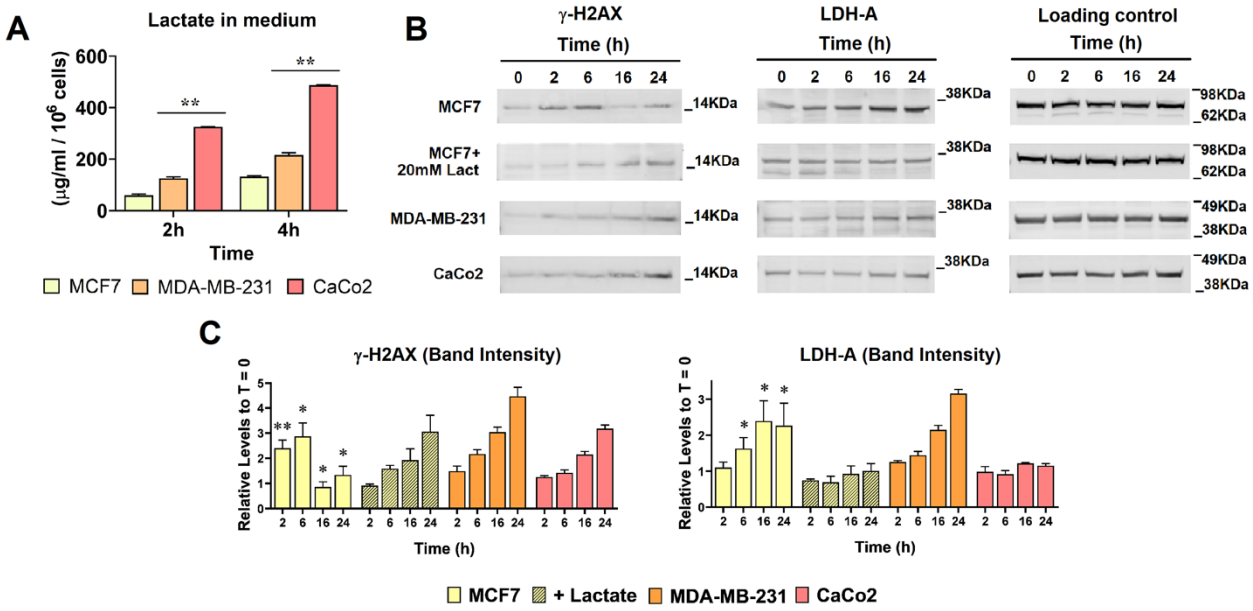

Figure 15. (A) *Assay of lactate levels. Lactate released in the medium was assessed as described in the Materials and Methods section. Data were analysed using ANOVA. A statistically significant difference was confirmed by comparing MDA-MB-231 and CaCo2 cells with MCF7 cells. **, $p < 0.01$.* ***(B)*** *Time course showing DNA damage and LDHA expression caused by DOXO in the cell cultures. DNA damage was assessed with γ-H2AX. The densitometric reading of the bands is shown in* ***(C)****. For both the evaluation of DNA damage and LDHA levels, we compared the data of parental MCF7 cells with those obtained in lactate-exposed cultures using the multiple t-test analysis in GraphPad. For γ-H2AX, a statistically significant difference was found at all the examined intervals. *, $p < 0.05$; **, $p < 0.01$. The level of LDHA was found to be increased in parental MCF7 cultures from 6 h onwards, with $p < 0.05$.*

4.3.2 Enhanced lactate levels reduced free radical generation caused by DOXO

According to the data shown in Figure 15B, lactate exposure appeared to reduce the early DNA damage (2–6 h) caused by DOXO. For their rapid onset, the DNA damage signatures detected in parental MCF7 cells at this time could be attributed to drug-induced oxidative stress, a mechanism mainly accounting for the detrimental side effects of DOXO[230]. This hypothesis is also in agreement with the notion that cancer cells with activated glycolysis (such as MDA-MB-231 and CaCo2 cells) usually show protection against oxidative stress[241]. This was verified with the experiments shown in Figure 16.

Non treated and lactate-exposed MCF7 cells were grown on glass slides and treated with 1 μM DOXO for 2 h, and ROS generation was visualized after applying a DCFH-DA probe. The labelled cells were identified on pictures taken using a microscope after merging the fluorescent DCF signal with Hoechst nuclear staining (Figure 16A). In agreement with the data obtained with the immunoblotting evaluation of γ-H2AX, the bar graph in Figure 16B shows that lactate exposure resulted in a significantly dampened ROS generation in DOXO-treated MCF7 cells: the percentage of labelled cells in control cultures was reduced to about one-third by lactate (42 % vs. 14%, $p < 0.01$).

Additional evidence for the reduced ROS generation in lactate-exposed cells was achieved with the experiment shown in Figure 16C. As well documented, ROS can modify guanine bases in DNA, giving rise to 8-OHdG. This modified guanine is considered an oxidative stress biomarker[235].

Moreover, 8-OHdG easily forms base pairs with thymidine, and this property could contribute to the mutagenic activity of DOXO[235]. The bar graph in Figure 16C shows that DOXO treatment caused a ≈38% increased level of 8-OHdG in parental MCF7 cells, while only an ≈11% increase was detected following lactate exposure. The subsequent step in our experiment was aimed at identifying possible molecular mechanisms underlying the oxidative damage protection effect observed in lactate-exposed cells.

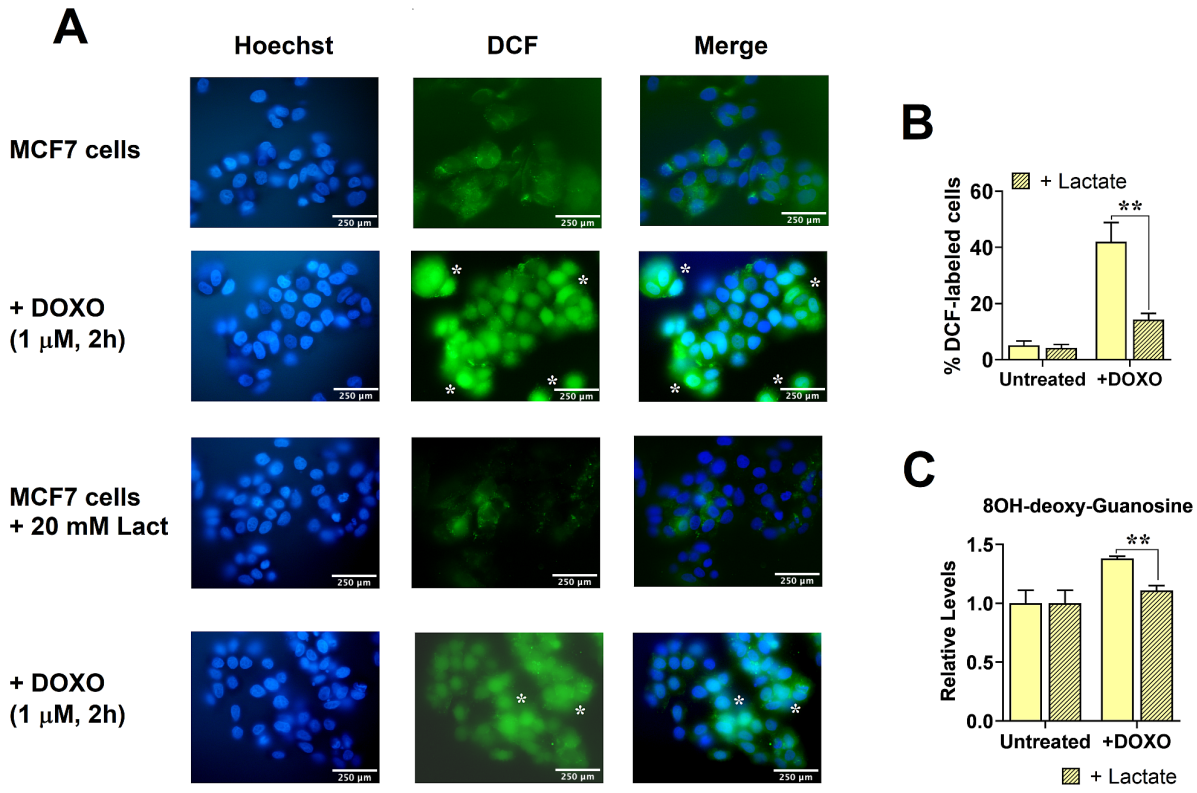

Figure 16. Oxidative stress evaluation in control and lactate-exposed MCF7 cells. ***(A)*** *Microscopic view of DOXO-treated cells exposed to DCF-DA; original magnification: 600×. In these cells, DCF-DA treatment resulted in a diffuse cytoplasmic fluorescence, and lactate exposure caused a dampened, but still diffuse fluorescence. For this reason, labelled cells were identified in merged pictures, as indicated with white asterisks. The percentage of labelled cells is shown in the bar graph* ***(B)****. A statistically significant difference was found between control and lactate-exposed MCF7 cells.* ***(C)*** *Results of the ELISA assay performed to evaluate 8OH-deoxyguanosine in the DNA of DOXO-treated cells; this oxidative stress marker appeared to be significantly reduced in lactate-exposed cells. **, $p < 0.0$.*

4.3.3 Involvement of the stress response

Recently published studies showed that in tumour cells, high lactate production is often associated with stress protein overexpression and radio-resistance[242,243]; on the contrary, depletion of lactate by LDH inhibition or knockout was found to impair stress response and promote cell sensitivity to ionizing radiation[244]. The application of ionizing radiation in tissues is typically followed by the induction of oxidative stress and ROS generation[245]; therefore, we hypothesized that the results observed in lactate-exposed MCF7 cells (Figures 15 and 16) would be mediated by a

lactate-induced stress response. For this reason, we verified whether the increased lactate levels in MCF7 cells could promote the expression of three stress proteins, for which a role in the protection from DNA damage induced by oxidants is well documented: inducible HSP70 and two members of the HSP90 family, GRP94 and TRAP1[246–248]. Furthermore, in previous studies, HSP70 and GRP94 were found to be linked with glycolytic metabolism, and their increased levels were associated with poor survival and worse prognosis in breast cancer[249,250].

Figure 17A shows the mRNA level of the selected stress proteins as assessed using RT-PCR for all cultures used in the experiments shown in Figures 15 and 16. No difference was observed between the used cell lines concerning HSP70 and TRAP1. In the cultures characterized by high lactate levels, the only observed upregulation was in GRP94 mRNA, for which a ≈3-fold increased expression was measured in MDA-MB-231 and CaCo2 cells compared to the MCF7 culture. A modest but statistically significant increase was also observed in lactate-exposed MCF7 cells compared to their parental culture. However, when GRP94 levels were evaluated using immunoblotting (Figure 17B), the differences between the cell lines appeared to be clearly decreased, and no statistically significant finding was observed in lactate-exposed MCF7 compared to their parental culture. Since stress protein mRNAs are expected to be translated mainly as a consequence of harmful stimuli, the immunoblotting evaluation of GRP94 was repeated in DOXO-treated cells using the same conditions applied in the experiments shown in Figure 15B. The results are shown in Figure 17C,D. Again, no evident difference was observed between lactate-exposed and parental MCF7 cells. This was also shown by the levels of band intensities measured after 24 h of DOXO exposure, which, for all four cell cultures, were related to the GRP94 band intensity measured at T = 0 (Figure 17D).

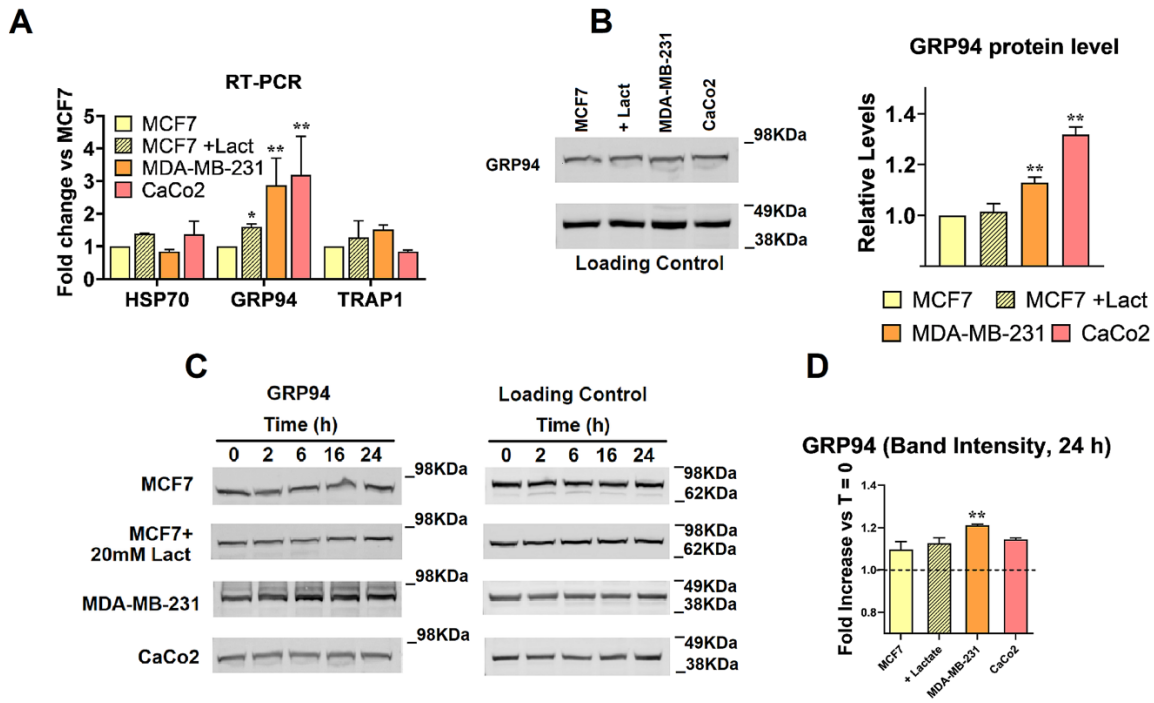

Figure 17. Evaluation of the stress-mediated response in DOXO-treated cell cultures. ***(A)*** *mRNA expression level of three stress proteins involved in the protection against oxidative DNA damage. Compared to MCF7 cells, GRP94 mRNA was found to be significantly increased in MDA-MB-231 and CaCo2 cells, as evaluated using the multiple t-test analysis in GraphPad. A lower extent increase was also observed in GRP94 lactate-exposed MCF7 cultures.* ***(B)*** *Level of GRP94 protein as assessed using immunoblotting. No direct effect of lactate was observed.* ***(C,D)*** *Level of the GRP94 protein assessed in DOXO-treated cells. Again, no direct effect of lactate was observed. * and **, $p < 0.05$ and 0.01, respectively, compared with MCF7 cells.*

Taken together, the experiments shown in Figure 17B, D suggest that, compared to MCF7 cells, the highly glycolyzing cultures express a slight but statistically significant level of the GRP94 protein. However, the data obtained from lactate-exposed MCF7 cultures suggest that this finding cannot be simply explained by the increased lactate level.

From all the experiments shown in Figure 17, we concluded that the three considered stress proteins are not involved in the oxidative damage protection observed in DOXO-treated and lactate-exposed MCF7 cells (Figure 16) or in the different time courses of DOXO-induced DNA damage shared by all the cultures characterized by increased lactate levels (Figure 15B, C).

4.3.4 Changes in gene expression following lactate and DOXO administration in MCF7 cells

Both lactate and DOXO have the potential to modify gene expression[14,142,203,222,229]. Lactate was originally shown to increase histone acetylation[14], and, as shown in Figure 18A, this effect was also evidenced in lactate-exposed MCF7 cells. On the other hand, for its capacity to intercalate between DNA bases, DOXO was shown to cause the dissociation of histones/DNA complexes[229]. For these properties, the combined action of these two molecules can be expected to have a significant impact on cell transcriptome. As a following step, to explain the results shown in Figures 15 and 16, we next verified whether lactate could modify the expression of a number of genes involved in the oxidative stress response in MCF7 exposed to DOXO treatment. Figure 18B, C shows the results of RT-PCR experiments aimed at evaluating the expression levels for a panel of genes involved in both oxidative damage repair (B) and protection (C). For these experiments, control and lactate-exposed MCF7 cells were treated with 1 μM DOXO for 4 h; mRNA extraction for RT-PCR was performed after an additional 16 h rescue time. As expected, both DOXO and lactate appeared to affect gene expression levels, sometimes in opposite ways. When evaluating these results, we only considered genes showing upregulation caused by both lactate and DOXO and for which the combination of the two compounds resulted in a statistically significant increased gene expression. This criterion, designed to provide stronger evidence of the combined effect of the two compounds, was satisfied by three genes: SMUG1, SOD1 and SOD2. The level of these proteins was further analysed in treated cells using immunoblotting; the results are shown in Figure 18D, E. When given to MCF7 cells independently, lactate and DOXO did not affect SOD1 and SOD2 protein levels, which, however, appeared to be significantly increased in cells receiving the combined treatment (≈1.5 fold compared to control MCF7 cultures). After the immunoblotting evaluation, SMUG1 appeared to be split into two bands, compatible with two of the five isoforms described for this protein[251]. The higher molecular weight band is compatible with isoform 1 (NCBI Reference Sequence: NP_055126.1), whereas the lower is compatible with isoform 3 (NCBI Reference Sequence: NP_001338187.1). Isoform 3 originates from an alternative mRNA splicing and is missing part of the terminal sequence of SMUG1. Interestingly, the missing region contains amino acids found to participate in the catalytical reaction of SMUG1. For this reason, this protein isoform is expected to have compromised catalytic activity. When the band intensities of the two isoforms were analysed together, no significant difference was observed between untreated and lactate/DOXO exposed cultures. After evaluating the relative abundance of the two SMUG1 isoforms, for the cells exposed to DOXO single treatment, we found a marked increase in the isoform 1 band, which reached 42% of the total protein signal, a value ≈7-fold higher than that observed in untreated cultures. Lactate was found to counteract the effect of

DOXO on SMUG1 isoforms, and in cells exposed to the combined treatment, the more functional isoform of SMUG1 was ≈3-fold lower than measured in DOXO-treated cultures.

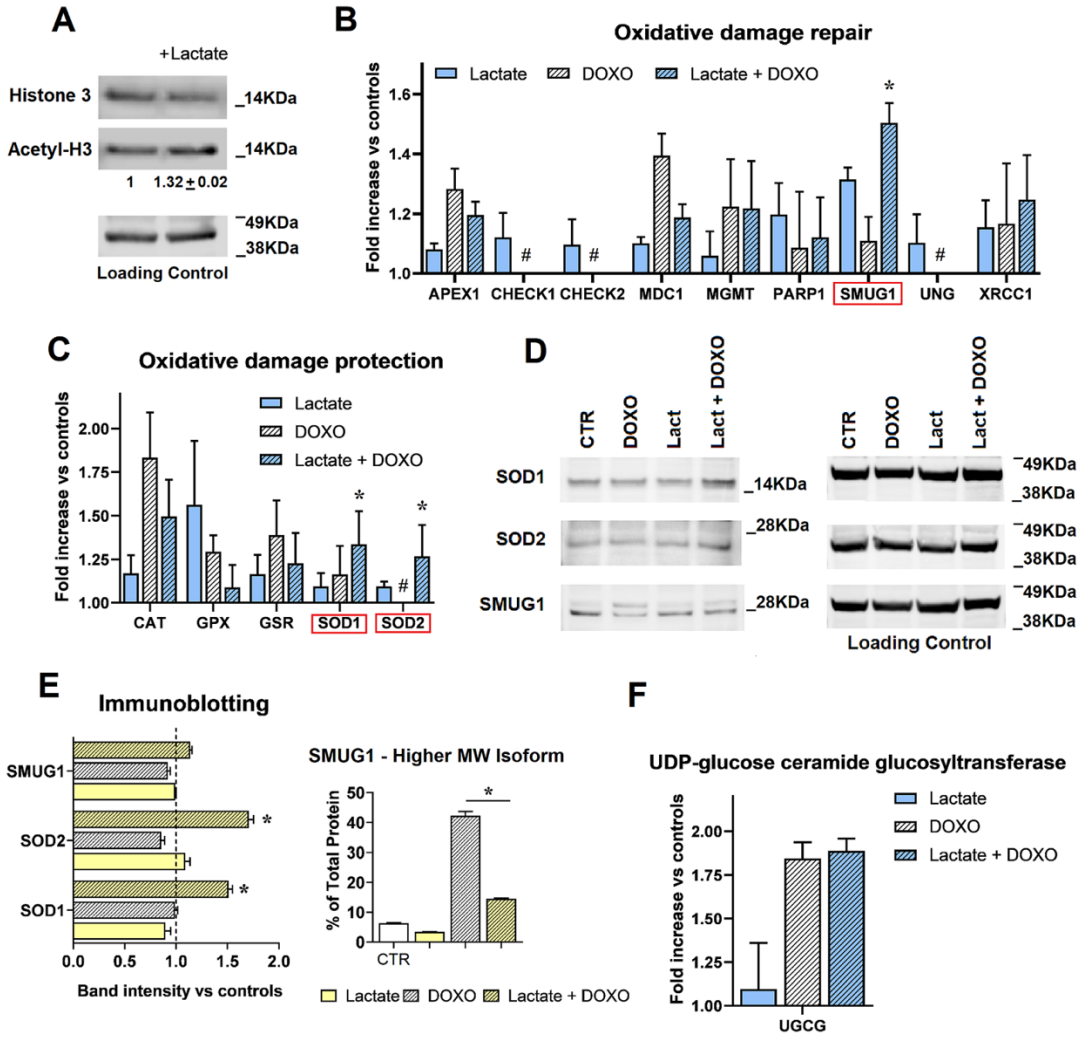

Figure 18. Changes in gene expression caused by the combined treatment lactate/DOXO in MCF7 cultures. (A) *Lactate-exposed MCF7 cells showed a 30% increased level of histone-3 acetylation, suggesting changes in gene expression. The expression of a group of genes involved in oxidative damage repair* ***(B)*** *and protection* ***(C)*** *was then assessed in MCF7 exposed to lactate/DOXO. Statistically significant changes were evaluated using the multiple t-test analysis in GraphPad. (#) indicates a reduced gene expression following DOXO treatment compared to the untreated cultures: a result excluding a contribution of these genes to the effects shown in Figures 15B,C and 16. SMUG1, SOD1 and SOD2 mRNA (red boxes) were found to be significantly increased with the combined lactate/DOXO treatment, and the levels of the corresponding proteins were analysed using immunoblotting (D,E). A statistically significant increase caused by the combination lactate/DOXO was confirmed for SOD1 and SOD2* ***(D)*** *(*, $p < 0.05$, compared to lactate and DOXO single treatments). In the case of SMUG1, a change in the protein isoforms caused by DOXO was observed, which was significantly counteracted by lactate (*, $p < 0.05$).* ***(F)*** *The level of UGCG mRNA was significantly increased by DOXO, but no effect of lactate was observed for this marker of DOXO resistance. *, $p < 0.05$.*

This observation suggests that despite the evidently increased SMUG1 mRNA expression found in cells exposed to the lactate/DOXO treatment, this protein should not be relevant to the oxidative damage protection observed in the cultures exposed to the combined treatment. In conclusion, and on the basis of our results, the observed protective effect can be only ascribed to the increased levels of SOD1 and SOD2. These findings provide a mechanistic explanation for the results observed in the experiments shown in Figures 15B, C and 16.

Finally, the bar graph in Figure 18F shows a RT-PCR experiment aimed at evaluating the combined effect of DOXO and lactate on UDP-glucose ceramide glucosyltransferase (UGCG). UGCG (also cited as glucosylceramide synthase, GCS) is a rate-limiting enzyme in the synthesis of glycosylated sphingolipids[252], and its increased expression correlates with resistance to DOXO and other chemotherapeutic agents[253]. Figure 18F shows that DOXO treatment caused a ≈75% increased expression of UGCG; lactate did not affect the expression of this gene either when given as a single treatment or in combination with DOXO. From this experiment, we concluded that lactate should not impact the UGCG-based mechanism underlying DOXO resistance.

4.3.5 DOXO-induced TOP2 poisoning in lactate-exposed MCF7 cells

TOP2 poisoning inhibition is considered the main antineoplastic mechanism of DOXO. TOP2 corrects DNA tangles that occur during replication and transcription by cleaving and resealing the filaments[254]. DOXO intercalates in DNA strands and prevents the resealing of cleaved sites, thus causing DNA double-strand breaks[255]. Specifically, TOP2A is the enzyme isoform found to be essential for cell proliferation, while TOP2B is mainly required for nervous tissue development. In DOXO resistance, an involvement of TOP1 was also described[256], and this form is also engaged in removing DNA supercoils during transcription and replication[257]. To assess whether lactate and DOXO can affect the expression of topoisomerase genes, an RT-PCR assay was performed using the same treatment schedule used for the experiments shown in Figure 18. The results (Figure 19A) showed a significantly increased expression of all three cited topoisomerase forms in DOXO-treated cells; no contribution related to lactate emerged in this experiment. To confirm that lactate does not affect the primary antineoplastic mechanism of DOXO, a dot-blot assay was performed to evaluate DNA-TOP2A complexes in control and lactate-exposed MCF7 cultures treated for 24 h with 1μM DOXO. The results are shown in Figure 19B, C. For this experiment, samples containing scalar doses of DNA were used. The dot fluorescence was analysed with ImageJ software using the built-in dot-blot-analyser macro (see paragraph 4.2.6), which allowed us to obtain the heatmap shown in Figure 19C. For each DNA sample, the signal given by the DNA-trapped TOP2A in DOXO-treated cells

was normalized on the respective untreated control and plotted on a graph. As shown in the graph in Figure 19C, the values for the fluorescence intensity ratios measured in control and lactate-exposed MCF7 cells did not show significant differences, suggesting that the level of TOP2A inhibition caused by DOXO in lactate-exposed cultures is superimposable to that observed in control MCF7 cells.

Finally, we performed cell viability experiments to evaluate the anti-proliferative effect of DOXO in control and lactate-exposed MCF7 cells. Again, no difference was observed between the two cultures at either 24 or 48 h (Figure 19D).

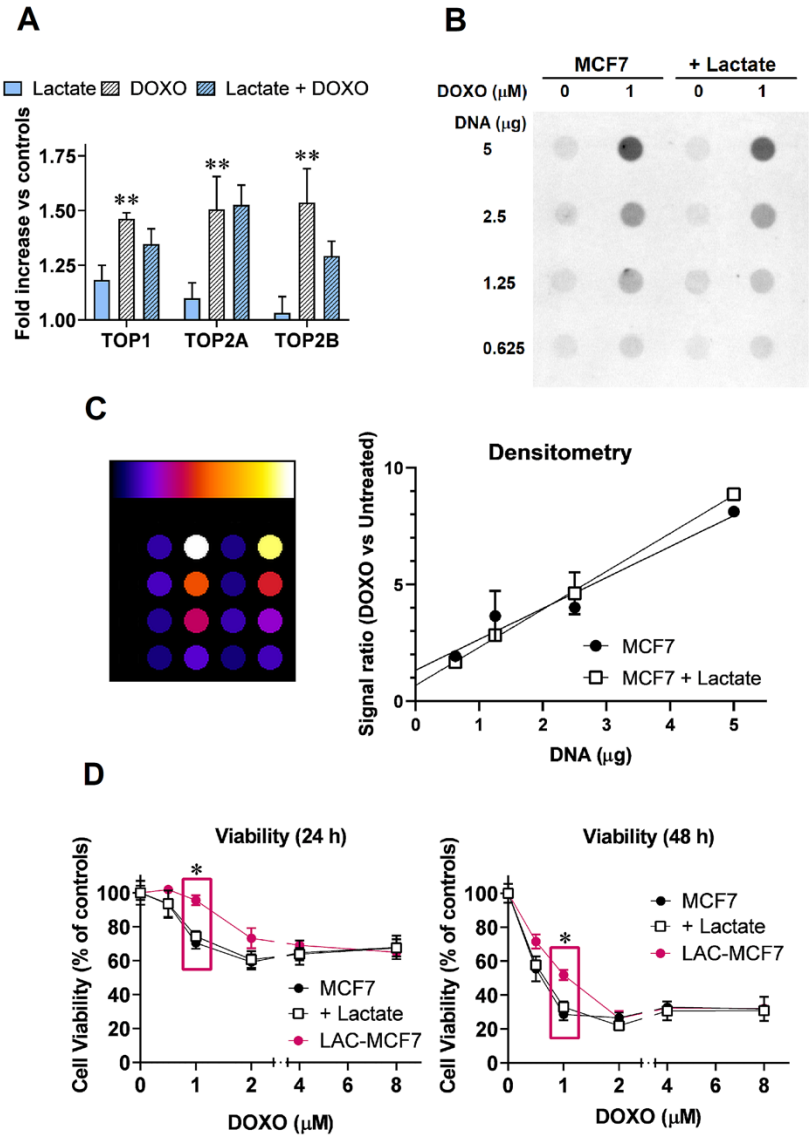

Figure 19. TOP2A inhibition assay. (A) *The level of mRNA in three topoisomerase isoforms was assessed in MCF7 cells exposed to lactate/DOXO treatment. When administered singularly, DOXO caused a statistically significant increased expression of the mRNAs (**, $p < 0.01$, as evaluated using the multiple t-test analysis in GraphPad). Lactate co-administration did not significantly change the effects of DOXO.* ***(B)*** *Dot-blot image obtained using a functional TOP2A assay;* ***(C)*** *heatmap showing dot fluorescence obtained with the aid of ImageJ software. The built-in dot-blot-analyser macro in ImageJ allowed us to obtain the densitometric evaluation shown in the graph.* ***(D)*** *Cell viability assay performed on control and lactate-exposed MCF7 cells treated with scalar doses of DOXO for 24 and 48 h. In this experiment, a clone of MCF7 cells grown with 20 mM lactate for ≥ 6 months was also used (LAC-MCF7). The short exposure to lactate did not affect the antiproliferative activity of DOXO, which appeared significantly reduced in LAC-MCF7 cultures. *, $p < 0.05$, as assessed using multiple t-test analysis.*

Taken together, the described experiments suggest that lactate should not impair the primary antineoplastic mechanism of DOXO, at least when lactate is administered using a short-term exposure

before DOXO treatment. Interestingly, for the experiments shown in Figure 19D, we also used an MCF-7 sub-culture that was adapted to grow in the presence of 20 mM lactate for about 6 months (LAC-MCF7). As shown in the Figure 19D, LAC-MCF7 cells showed a significantly reduced response to 1 μM DOXO. We hypothesize that this finding could reflect a phenomenon of neoplastic progression triggered by a continuative exposure to lactate[258], which would not be expected in the case of sporadic administrations of this metabolite.

4.3.6 Experiments on H9c2 cardiomyocytes

While the contribution of DOXO-induced oxidative damage is considered secondary to its antineoplastic effect, there is consolidated evidence that it plays a major role in the cardiac toxicity caused by the drug[228,259]. Following the results obtained for lactate-exposed MCF7 cells, we wondered whether a similar protective effect against DOXO-induced oxidative damage could be exerted by lactate in cardiomyocytes. For this experiment, we used rat H9c2 cells, a validated model for studying DOXO cardiotoxicity and developing potential cardioprotective strategies[260]. The combined effects of DOXO and lactate on oxidative damage were studied in both proliferating and differentiated H9c2 cells (Figures 20 and 21, respectively). For these experiments, H9c2 cells were exposed to 20 mM lactate for 72 h, following the same schedule used for lactate-exposed MCF7 cells. Figure 20A shows the results from the immunoblotting evaluation of γ-H2AX performed on proliferating H9c2 cells treated with 1 μM DOXO.

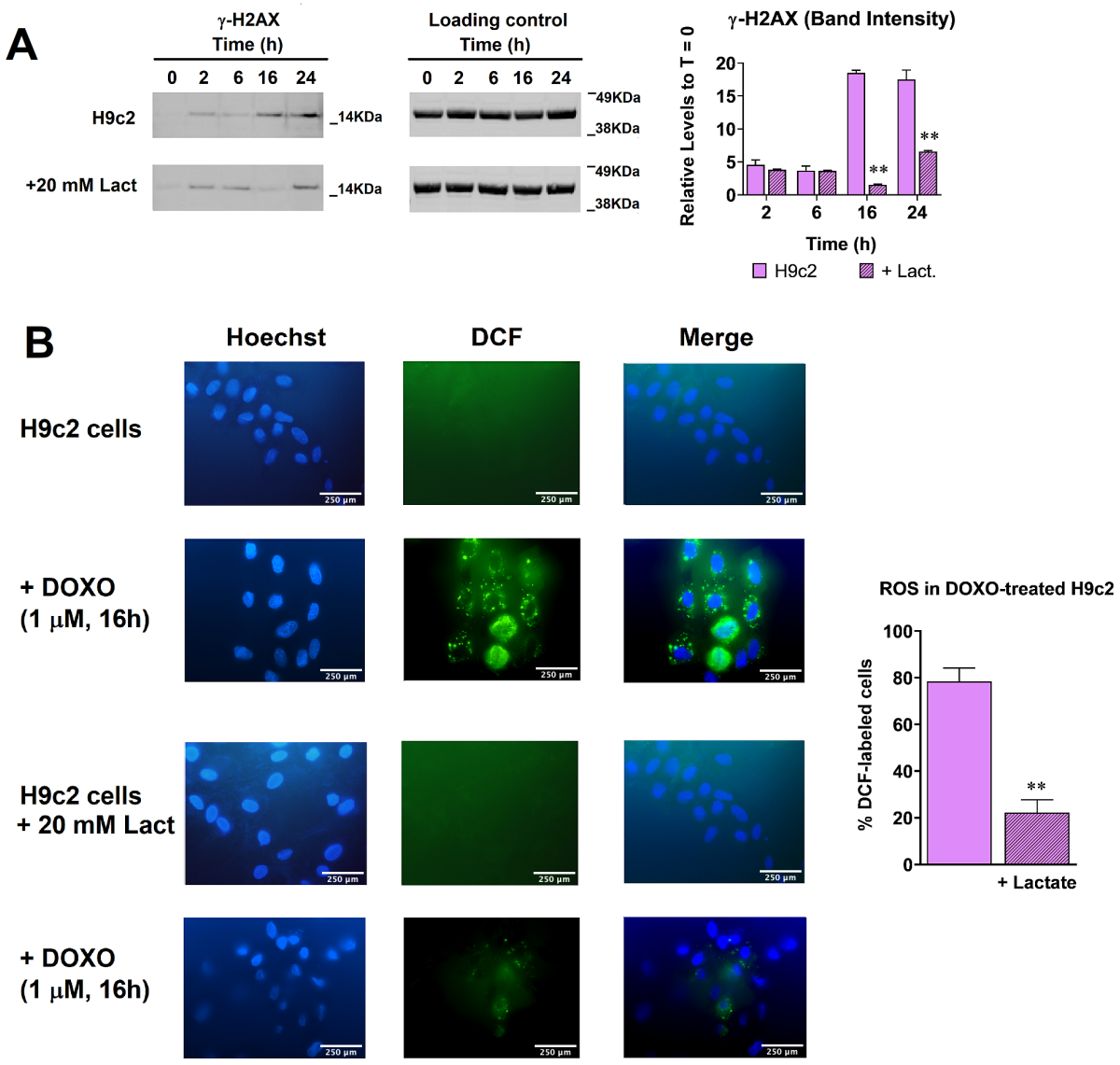

Figure 20. Evaluation of DNA damage and oxidative stress in DOXO-treated and lactate-exposed H9c2 cells. ***(A)*** *Time course of DNA damage observed in proliferating H9c2 cells. The untreated cells showed a barely detectable γ-H2AX signal, and DNA damage became evident 16–24 h after DOXO treatment. Lactate successfully reduced the extent of DNA damage. The quantitative differences between parental and lactate-exposed H9c2 cells are shown in the bar graph **, $p < 0.01$, compared to parental cells treated with DOXO.* ***(B)*** *Microscopic view showing DOXO-treated H9c2 cells exposed to DCF-DA; original magnification: 600×. Compared to MCF7 cells (Figure 16), in untreated H9c2 cells, no sign of oxidative stress was evidenced with DCF-labelling, and in DOXO-treated cultures, fluorescence showed a less diffuse and more spotted pattern. The percentage of labelled cells is shown in the bar graph. A statistically significant difference was found between control and lactate-exposed H9c2 cells (**, $p < 0.01$, as assessed with a t-test).*

In these cells, evidence of DNA damage was observed at later times when compared with the MCF7 cultures (Figure 15B). These results are in complete agreement with previously published data that showed oxidative damage in H9c2 cells only after ≈24 h of DOXO exposure[261]. As shown in the immunoblotting images and the bar graph reporting the relative levels of band intensities, exposure to lactate caused a marked and statistically significant reduction in DNA damage.

This effect was remarkable at 16 h, when, in lactate-exposed cultures, the γ-H2AX band intensity became barely detectable; however, it also remained evident at 24 h, when the γ-H2AX band was reduced to about one-third compared with the control cultures. In agreement with these results, ROS evaluation in H9c2 cells treated with 1 μM DOXO for 16 h showed a marked reduction in lactate-exposed cells (Figure 20B); the extent of the effect (≈70% reduction) is in line with the results from the γ-H2AX immunoblotting evaluation in Figure 20A.

The same experiments were performed on differentiated H9c2 cultures (D-H9c2). The results are shown in Figure 21. The immunoblotting evaluation in Figure 21A shows that, compared to their un- differentiated parental cultures, D-H9c2 appeared to be more prone to oxidative stress: the γ-H2AX band was more evident in untreated cultures, and its increase in response to DOXO treatment was already observed at 2 h. However, lactate exposure also successfully reduced DNA damage in D-H9c2 cells, and the extent of the protective effect measured at 16 and 24 h was found to be very similar to that observed in the parental culture (≈70% reduction in γ-H2AX band intensity). The higher level of oxidative stress in untreated D-H9c2 was confirmed with the experiments in Figure 21B, which showed ROS detection also in ≈10% of cells in the control cultures. Despite this increased vulnerability to oxidative damage, the coadministration of lactate successfully reduced DOXO-associated ROS (65% vs. 25% ROS-labelled cells in DOXO-exposed cultures, compared to cultures exposed to lactate/DOXO).

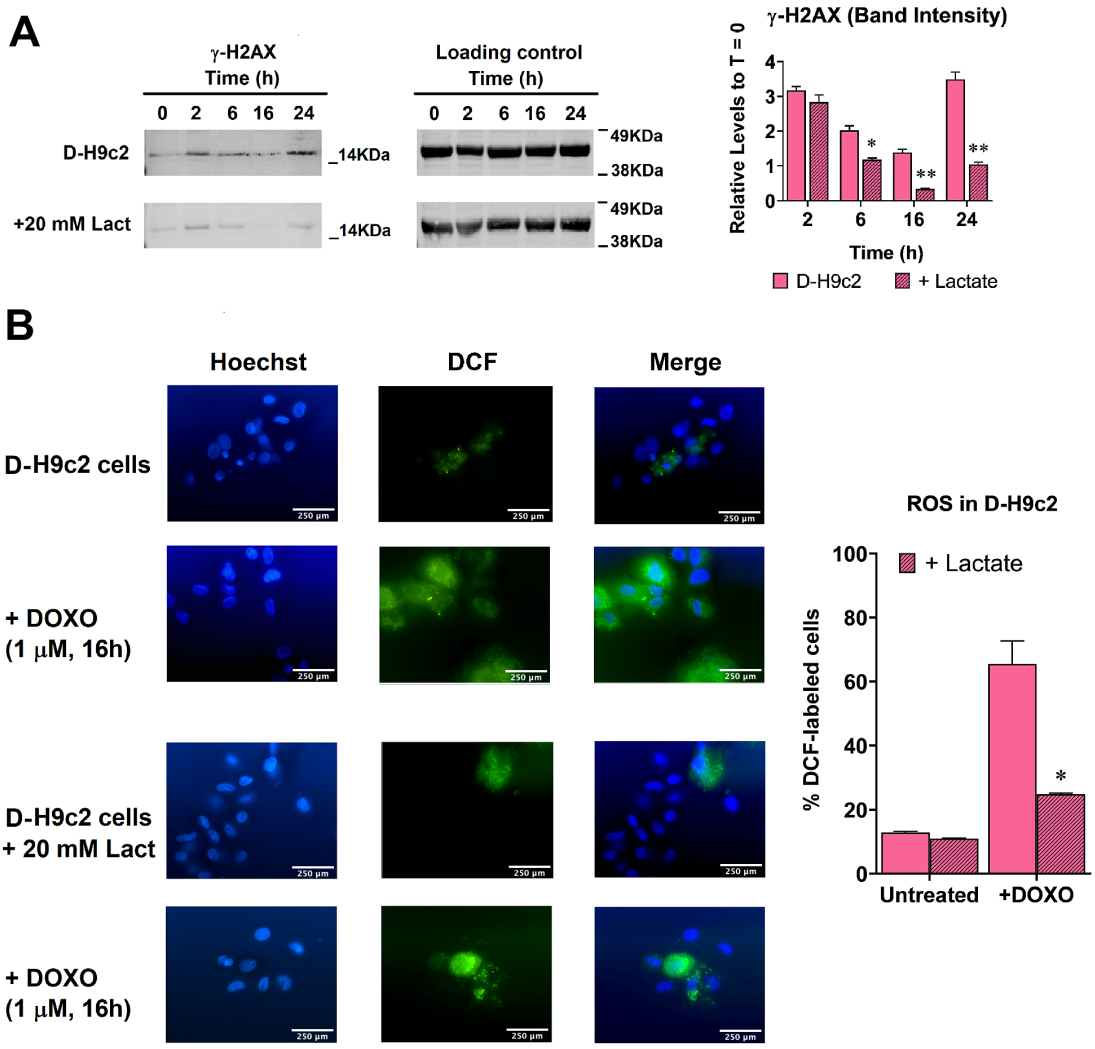

Figure 21. Evaluation of DNA damage and oxidative stress in DOXO-treated and lactate-exposed D-H9c2 cells. ***(A)*** *Time course of DNA damage observed in D-H9c2 cells. Untreated cells showed a more detectable γ-H2AX signal, and DOXO-induced DNA damage became evident even after short-time exposures. Again, lactate successfully reduced the extent of DNA damage. The quantitative differences between parental and lactate-exposed D-H9c2 cells are shown in the bar graph. * and **, $p < 0.05$ and 0.01, respectively, when compared to parental cells treated with DOXO.* ***(B)*** *Microscopic view showing DOXO-treated H9c2 cells exposed to DCF-DA; original magnification: 600×. The percentage of labelled cells is shown in the bar graph. A statistically significant difference was found between control and lactate-exposed D-H9c2 cells (*, $p < 0.05$, as assessed using a t-test).*

The increased vulnerability to oxidative stress of D-H9c2 could be explained by the metabolic switch (oxidative metabolism instead of glycolysis) that characterizes the differentiation process of normal cells and leads to reduced lactate production[262]. This hypothesis was confirmed with the experiment shown in Figure 22A. Compared to proliferating H9c2 cells, the differentiated culture showed a 40% reduction in lactate production.

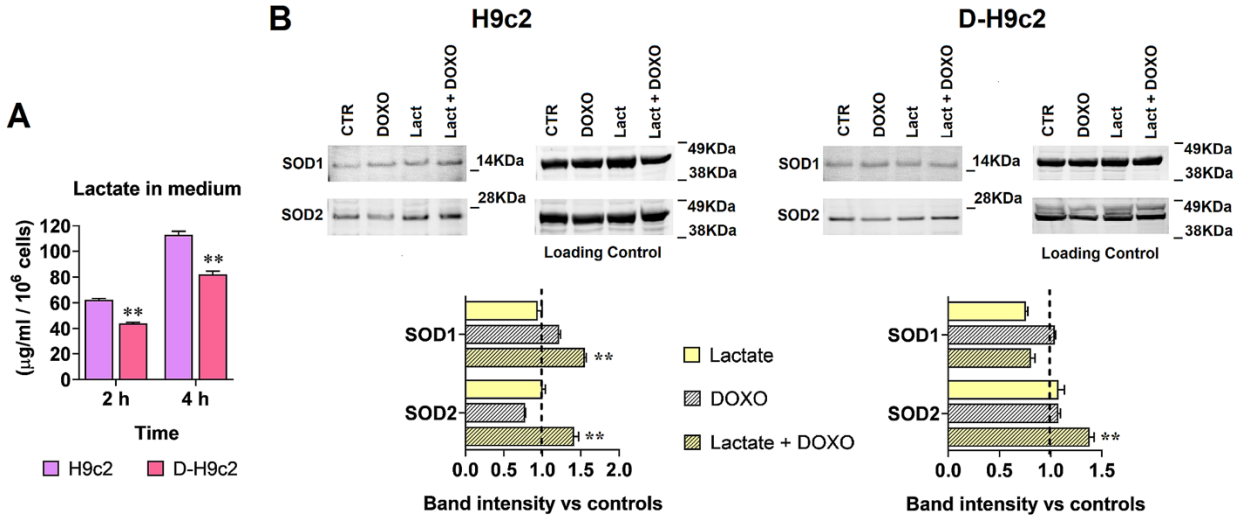

Figure 22. Evaluation of lactate production and SOD1 and SOD2 levels in cardiomyocytes. (A) *Assay of lactate levels. Lactate released in the medium was assessed as described in the Materials and Methods section. Data were analysed using ANOVA. A statistically significant difference was observed between H9c2 and D-H9c2. **, $p < 0.01$.* ***(B)*** *Immunoblotting evaluation of SOD1 and SOD2. In proliferating H9c2 cells, a statistically significant increase caused by the combination lactate/DOXO was confirmed for both SOD1 and SOD2; in the differentiated culture, the lactate-induced protective effect could be ascribed only to SOD2. **, $p < 0.01$, compared to lactate and DOXO single treatments.*

Finally, for the cardiomyocyte cultures exposed to the combined lactate/DOXO treatment, we verified whether the observed oxidative damage protection (Figures 20 and 21) could be ascribed to SOD1 and SOD2 proteins, as already demonstrated for MCF7 cells. The control and lactate-exposed H9c2 and D-H9c2 cells were treated with 1 µM DOXO for 16 h, the time-interval with the most evident reduction in oxidative damage in lactate-exposed cells (Figures 20 and 21).The cells were then lysed, and the SOD1 and SOD2 levels were detected using immunoblotting. As shown in Figure 22B, in DOXO-treated H9c2 cells, both SOD1 and SOD2 proteins exhibited a 40–50% increased level when these cultures were previously exposed to 20 mM lactate. In D-H9c2 cells, the protective effect of lactate could be ascribed only to the SOD2 protein. This difference between the proliferating and differentiated culture can be explained by previous studies showing that in mature cardiomyocytes, the level of SOD1 is quite low and that, in these cells, the enzyme isoform primarily involved in oxidative damage protection is SOD2[263]. From these experiments, we can conclude that the molecular mechanism underlying the oxidative damage protection induced by lactate is similar in both MCF7 cells and in cardiomyocyte cultures.

4.4 Conclusion – SECTION II

DOXO and its analogues are widely used as a first-line chemotherapeutic treatment for different solid and hematologic malignancies. It was estimated that about 1 million cancer patients receive DOXO treatment every year[224,225]. The broad-spectrum activity of DOXO reflects the multiplicity of the identified intracellular targets for this drug. In addition to accounting for antineoplastic action, these targets are also involved in heavy DOXO side effects. Among these, cardiotoxicity proved to be the most relevant since it often leads to therapy exclusion or discontinuation for patients with compromised heart function[264]. A number of mechanisms have been hypothesized to contribute to the pathogenesis of DOXO-induced cardiotoxicity; among them, oxidative stress received by far the most attention since it can easily explain the mitochondrial damage and cardiomyocyte apoptosis frequently observed in experimental models used to characterize the molecular mechanisms underlying DOXO side effects[228,259,265]. Oxidative stress was found to be derived by metabolic processing of the DOXO molecule, which produces a semi-quinone derivative able to transfer its unpaired electrons to molecular oxygen, giving rise to ROS[266]. It is well known that ROS can cause membrane damage and mitochondrial dysfunction, leading to cell apoptosis. Recent studies also identified some molecular targets involved in DOXO-induced oxidative damage and confirmed the beneficial effects of antioxidant compounds in alleviating cardiotoxicity[267,268].

One of the most recently characterized mechanisms underlying DOXO action is its capacity to damage the chromatin structure and cause histone eviction, which results in transcriptome alterations[229,266]. This observation prompted studies aimed at evaluating the effect of the co-administration of DOXO with other compounds affecting gene expression, such as HDAC inhibitors.

Neoplastic diseases are the most clinically relevant conditions characterized by activated glycolytic metabolism and increased lactate production; therefore, increased histone lactylation can be reasonably hypothesized to contribute to the growth and invasiveness of cancer cells[81]. The protective effects exerted by lactate on DNA integrity are coherent with the role of glycolytic metabolism in embryonic tissues[269]. For the treatment of cancer diseases, these effects could reduce the efficacy of chemotherapy. However, the results obtained from cultured cardiomyocytes suggest that when the antineoplastic mechanisms of the drug are not affected, the gene regulatory properties of lactate could be exploited to protect normal tissues from chemotherapy-associated damage.

In conclusion, we explored the effect of lactate on DOXO antineoplastic mechanisms and found that when MCF7 cells are exposed to DOXO in the presence of increased lactate levels, TOP2A poisoning (the main antineoplastic mechanism of the drug) is not affected. Interestingly, lactate-

exposed MCF7 cells showed upregulated levels of SOD1 and SOD2 proteins and appeared to be protected from drug-induced oxidative damage. Oxidative damage plays a major role in cardiac toxicity caused by a drug. When the effect of lactate was evaluated on both proliferating and differentiated cardiomyocytes exposed to DOXO (Figures 20 and 21), this metabolite succeeded in significantly reducing ROS generation and the DNA damage signatures caused by the drug.

Taken together, the results of the experiments described in Section II suggest that, by relieving the oxidative damage in cardiomyocytes without significantly affecting the antineoplastic effect on cancer cells, short-term exposure to lactate prior to DOXO treatment could be considered as a possible attempt to increase the chemotherapeutic index of the drug.

[This page is intentionally left blank]

5. SECTION III

Lactate Is a Potential Promoter Of Tamoxifen Resistance In MCF7 Cells

Subsequent to the results described in Section II, we further investigated ER+ breast cancer (MCF7 cells), specifically focusing on the potential role of lactate in inducing resistance to tamoxifen.

5.1 Introduction

Tamoxifen (TAM) is a competitive inhibitor of the transcriptional activity of estrogen alpha-receptor (ERα); it was discovered about fifty years ago and was subsequently introduced in the clinical practice for the treatment of ER+ breast cancer, the most common form of this tumor[270,271]. During its long-lasting clinical use, this pioneering compound proved to reduce disease recurrence and mortality rate by 50% and 30%, respectively. Furthermore, it appeared to be devoid of relevant side effects in the majority of patients. For its efficacy and tolerability, after so many years TAM is still considered the first-choice medication in the adjuvant therapy of pre- and post-menopausal women and has also been evaluated in the chemoprevention of breast cancer.

Unfortunately, the success of this lifesaving compound can be undermined by the development of acquired resistance, which was found to occur in about 30% treated patients[272,273]. The possible mechanisms underlying this phenomenon have been extensively investigated and a number of complex pathways leading to a reduced response to TAM have been identified in resistant breast cancer cells cultured in vitro.

Altered expression of ERα and/or ERβ and change in co-regulatory proteins are frequent causes of TAM resistance[274]; furthermore, genetic polymorphisms involved in the compound metabolism have been identified[275]. Different miRNA expression profiles have also been observed in TAM resistant and sensitive breast cancer cell lines, by microarray analysis[276]. By using this technique, 97 miRNAs differentially expressed in MCF7 endocrine-sensitive versus resistant LY2 breast cancer cells have been identified.

A number of studies reported the upregulation of growth factor receptors (HER2, EGFR, FGFR, IGF1R) and the consequent activation of the PI3K-PTEN/AKT/mTOR pathway to be closely related to acquired TAM resistance[277].

Interestingly, in spite of the varied mechanisms potentially involved in the onset of TAM resistance, several studies showed that breast cancer cells with acquired resistance to TAM seem to

display a similarly up-regulated glycolytic metabolism and increased lactate production[278,279]. Furthermore, inhibition of glycolysis was found to hinder some of the pathways leading to TAM resistance and to restore the cell response to this compound[280].

Actively pursued studies aimed at characterizing additional properties of TAM molecular structure also evidenced for this compound ER-independent effects. In particular, one of these seems to be strictly related to the lipophilic nature of the molecule, which facilitates its partition into membrane lipid bilayers[281]. This feature could explain the inhibition of mitochondrial respiratory rate observed in cells exposed to TAM, probably exerted at the level of complex I. In particular, Daurio et al. showed for TAM a pronounced, ER-independent effect on cancer cell metabolism, consisting in increased glycolysis and lactate production[282]. Interestingly, this observation could have clinical relevance: breast neoplastic lesions of patients undergoing FDG-PET scans after TAM administration often show a "metabolic flare", a picture that could be easily explained by the increased glucose consumption caused by the drug mitochondrial inhibition[283].

Based on all the above cited data, it can be hypothesized that the increased glycolysis and lactate production which characterize TAM resistant cells, but is also observed early after the drug administration, could not only be epiphenomena of TAM resistance, but might also play an active role in the onset of this detrimental condition. The experiments described in this Section were aimed at shedding light on this question.

5.2 Materials and methods

5.2.1 Cell cultures and treatments

For this study we have used: MCF7, MDA-MB- 231 and MCF10A cells. Cells were grown in low-glucose (1 g/l) DMEM medium, supplemented with 100 U/ml penicillin/streptomycin, 2 mM glutamine and 10% FBS. Medium of MCF10A cultures also contained 0.5 μg/ml hydrocortisone and 100 ng/ml cholera toxin. MCF7-TAM^{284} were maintained in α-MEM without phenol red, supplemented with 10% charcoal-stripped FBS, 100 U/ml penicillin/streptomycin, 2 mM glutamine, 1 mM sodium pyruvate and 10^{-7} M 4-hydroxy-tamoxifen. All the materials used for cell culture and all the reagents were obtained from Merck, unless otherwise specified. For the experiment shown in Figure 29C, MCF7-TAM were grown in L15 medium; this medium does not contain glucose and is supplemented with 10% dialyzed FBS and 4 mM glutamine. For of its formulation, L15 medium does not allow glycolysis and lactate production. In TAM including experiments, media were supplemented with 0,6% DMSO. Lactate (L-isomer) was dissolved in culture medium at a 20 mM concentration; MCF7 cultures were exposed to 20 mM lactate for both conditional (72 h) and sustained (≥ 4 months) treatments. In these experiments, the 20 mM lactate supplement was directly added to the medium; medium was changed every 72 h since in preliminary testing we found that lactate concentration was not significantly affected within this time interval. Cultures were routinely tested for Mycoplasma contamination and found to be free.

5.2.2 Assay of lactate levels

Cells (5×10^5 / well) were plated in triplicate in 6-wells plates and let to adhere overnight. Medium was then replaced with Krebs-Ringer buffer and released lactate was measured after 1–6 h incubation at 37°C using the method described in paragraph 4.2.2 of Materials and methods of Section II. The same procedure was adopted to evaluate released lactate in the presence of 1 μM TAM.

5.2.3 Cell proliferation

These experiments were performed in MCF7 cultures to both identify the TAM lowest active concentration and study the proliferation dynamics in lactate-exposed cells. In both experiments, cell proliferation was assessed through the detection of ATP levels, by using the CellTiter-Glo Assay (Promega). A Fluoroskan Ascent FL reader was used to evaluate luminescence. For the TAM

experiments, 15–20 × 10^4 cells/well, plated in triplicate in clear bottom 96-well white plates were incubated with 1 μM TAM for 24–120 h. For studying the proliferation dynamics of lactate-exposed cells, 20 × 10^4 cells, were plated as described above; they were let to adhere for 16 h, after which the number of living cells was detected in three wells by applying the CellTiter-Glo Assay (Time = 0). Plated cells were then grown for 24–48 h in a medium with different FBS concentration (10, 2 and 1%).

5.2.4 Real-time PCR

MCF7 cells were seeded in T25 flasks and allowed to adhere overnight. Exponentially growing cultures were conditionally exposed to 20 mM lactate (72 h). RNA was extracted using an RNA isolation kit (Merck) and was quantified spectrophotometrically (ONDA Nano Genius Photometer). Retro-transcription to cDNA was performed as describe in paragraph 4.2.5 of Materials and methods of Section II. RT-PCR and analyses of data were performed as describe in 4.2.5 of Materials and methods of Section II.

For comparison, the same experiment was also performed on lactate-exposed MCF10A cells and on MCF7-TAM cultures, maintained in their routinely growth medium.

5.2.5 Immunoblotting experiments

These experiments were performed on MCF7 cells after the conditional (72 h) exposure to lactate, to assess histone acetylation and expression level of some proteins identified following the RT-PCR experiments. A similar experiment was performed in cells with sustained (≥ 4 months) lactate exposure to obtain evidence on the activation of the EGFR pathway. For both experiments, control and treated MCF7 cultures were harvested and lysed in 50 μl RIPA buffer containing protease and phosphatase inhibitors. To evidence the activation of EGFR pathway, a 3-h pretreatment with 10 μg/ml Insulin was applied to cells with sustained lactate exposure and their untreated controls before culture harvesting.

80 μg of protein (measured according to Bradford) was loaded into 4–12% polyacrylamide gel for electrophoresis and run at 170 V. The separated proteins were blotted on a low fluorescent PVDF membrane (GE Lifescience) using a standard apparatus for wet transfer with an electrical field of 60 mA for 16 h. The blotted membrane was blocked with 5% BSA in TBS-TWEEN and probed with the primary antibody. The antibodies used were: rabbit anti-H3 (Cell Signaling); rabbit anti-Panacetyl-H3 (Active Motif); rabbit anti-TAZ (Cohesion Biosciences); rabbit anti-LDH-A (Cell

Signaling); rabbit anti-(Tyr10)-phospho-LDH-A (Cell Signaling); rabbit anti-c-Myc (Abcam); rabbit Ab-21 polyclonal anti-EGFR (Neomarkers/Labvision Inc.); rabbit anti-phospho-(Tyr1068)-EGFR (Novex); rabbit anti-AKT (Cell Signaling); rabbit anti-phospho-(Ser473)-AKT (Cell Signaling). Binding was revealed by a Cy5-labelled secondary antibody (goat anti rabbit-IgG, Cytiva Life Sciences). Fluorescence of the blots was assayed with the Pharos FX Scanner (Bio-Rad) at a resolution of 100 μm, using the Quantity One software (Bio-Rad).

5.2.6 Telomerase assay

Telomerase activity in control and conditionally (72 h) lactate-exposed MCF7 cells was measured using a quantitative real-time telomeric repeat amplification protocol (RTQ-TRAP)[285,286].

For this experiment, cultures were scraped-off and washed with cold PBS. Subsequently, 1–2 × 10^6 cells were lysed in 50 μl CHAPS buffer, left on ice for 30 min and sonicated for 15 s in an ice-submerged tube. A Heat System Model XL2020 sonicator was used, applying a power of 50–60 W for 5 s, with 15 s intervals.

Lysates were centrifuged at 14000g for 20 min at 4 °C; surnatant was recovered, aliquoted and stored at –80 °C until used. Proteins of the lysates were quantified using the Bradford method.

The RTQ-TRAP assay mixture contained 0.25 μM TS primer (5'-AATCCGTCGAGCAGAGTT-3′), 0.25 μM ACX primer (5'-GCGCGG (CTTACC)3CTAACC-3′), 1× SsoAdvanced Universal SYBR Green Supermix (Bio-Rad) and 2–5 μl of cell lysate, in a final volume of 25 μl. Mixture was incubated 20 min at 25°C to allow TS primer elongation with TTAGGG repeats by the telomerase enzyme in cell lysates. Quantification of the added telomeric sequences was assessed by RT-PCR using the following conditions: 10 min denaturation at 95°C and 40 amplification cycles (20 s at 95°C, 30 s at 50°C, 90 s at 72°C). PCR reactions were performed in a CXF96 Real Time System (Bio-Rad). Negative controls (2–5 μl lysis buffer) and telomerase-negative controls (2–5 μl heat-inactivated cellular lysates) were used in each experiment.

5.2.7 Wound healing assay

Control and conditionally (72 h) lactate-exposed MCF7 cells were seeded in triplicate in 6-well plates (1.5 × 10^6 /well) and cultured until they had reached 100% confluence. Artificial wounds were then created using a 10 μl pipette tip. The detached cells were washed away with PBS and cultures were exposed to a medium supplemented with a lowered serum content (1 and 2%). 20 mM lactate was also added to the medium of lactate-exposed cultures. The wound areas were captured with an

inverted microscope at 0, 24 and 36 h and their repopulation was analysed by using the ImageJ software.

5.2.8 Senescence associated β-galactosidase staining

This experiment was performed in MCF7 cultures exposed to a sustained (≥ 4 months) 20 mM lactate treatment. Control and lactate-exposed cells (1×10^5 /well) were seeded in triplicate in 6-well plates and treated with 1 μM TAM for 7 days. After treatment, cells were washed twice with PBS and fixed with a 2% formalin / 0.2% glutaraldehyde solution, for 5 min at room temperature. After fixation, they were washed again with PBS and incubated overnight at 37°C with X-gal (1 mg/ml), dissolved in a staining solution containing 40 mM citric acid pH 6, 5mM potassium ferrocyanide II, 5mM potassium ferrocyanide III, 150 mM NaCl and 2mM $MgCl_2$. After a 16-h incubation, pictures of each condition were captured using an inverted microscope. The development of a perinuclear blue colour was indicative of senescent cells.

5.2.9 Statistical analyses

All data were analysed as described in paragraph 3.2.7 in Materials and methods of Section I.

5.3 Results and discussion

5.3.1 Short-term exposure to TAM causes enhanced lactate release by MCF7 cells

To establish a correlation between lactate-induced changes and reduced TAM response in MCF7 cells, we took advantage of a TAM-resistant clone of this line (MCF7-TAM), obtained by the Professor Fulvia Farabegoli (FaBit, University of Bologna)[287]. MCF7-TAM cells are routinely cultured in the presence of TAM and differ from their parental line in a markedly higher level of released lactate (> 1.5-fold in 4 h, Figure 23A); furthermore, in agreement with previous studies showing upregulated glycolysis as a hallmark of poor pharmacological response, they show a pattern of metabolite production superimposable to that of MDA-MB-231 cells, a well-studied model of triple-negative, drug resistant breast cancer that we used for the experiments in Section II.

In a following experiment, parental MCF7 cells were exposed to scalar doses of TAM (0–4 μM) for 120 h in order to identify the lowest drug concentration able to reduce cell viability. As shown in Figure 23B, a statistically significant effect was observed with 1 μM TAM, only after the 120h treatment. Interestingly, when this dose was applied to both MCF7 and MDA-MB-231 cultures a rapid increase (2–6 h) in the lactate production rate was detected (Figure 23C, D); in TAM-exposed MCF7 cells, the curve elevation of lactate production rate resulted significantly higher ($p = 0.0034$) with a 27%-increased slope, compared to the untreated cultures. Even more marked effects were measured in MDA-MB-231 cells, which do not express ER. These results suggest that the metabolic changes caused by TAM definitely forestall the emergence of its antiproliferative effects, paving the way to phenotypic adaptations, which could potentially interfere with the drug antineoplastic action.

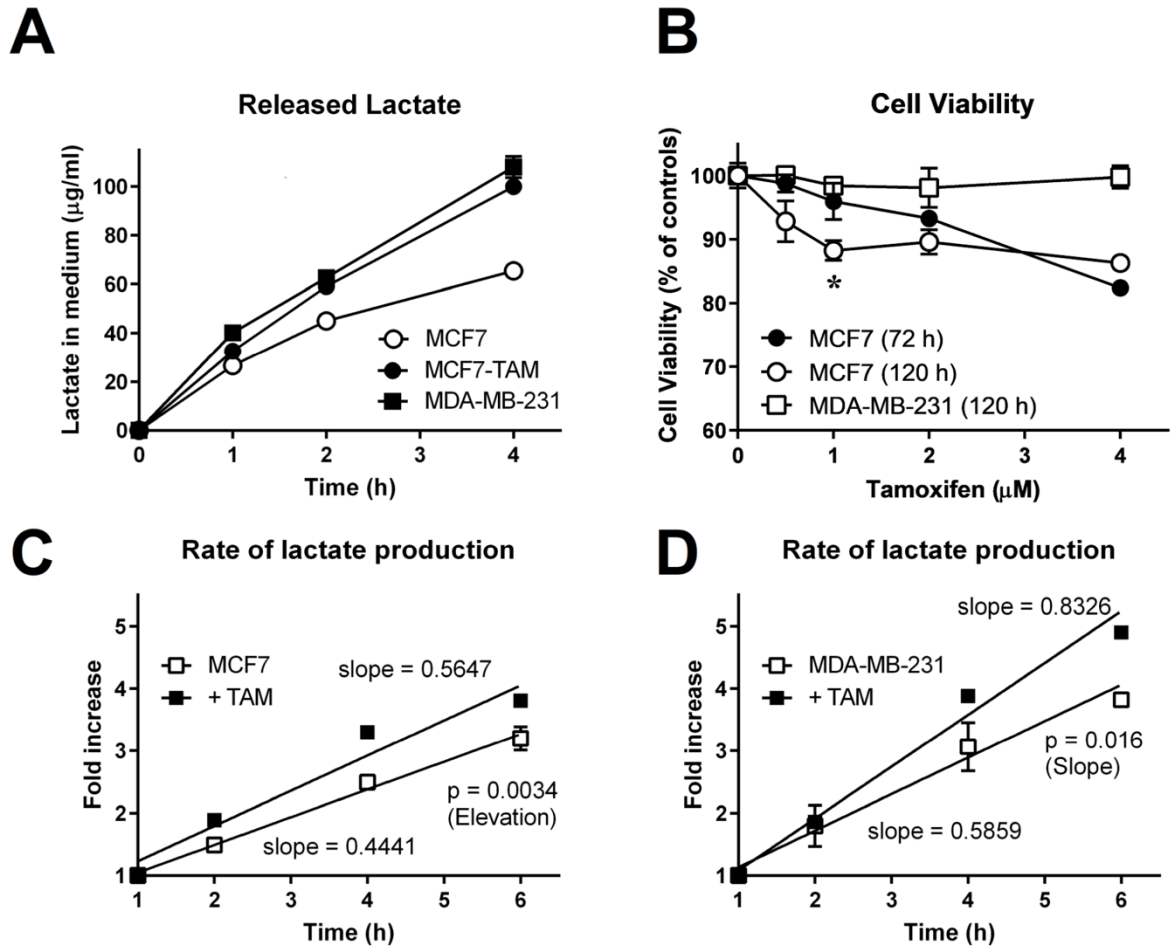

Figure 23. Assay of lactate levels. (A)*: Lactate released in medium was assessed as described in Materials and Methods. Data were analysed by applying the linear regression; the curve slopes measured in MCF7-TAM and MDA-MB-231 cells were significantly higher ($p < 0.05$) than that shown by MCF7 cells.* ***(B)****: Effect of TAM on the viability of MCF7 and MDA-MB-231 cells. Data were analysed by multiple t-test; no statistically significant effect was evidenced in MDA-MB-231 cells, which do not express ER. In MCF7 cells, a statistically significant reduction of cell viability was observed at 120 h with 1 μM TAM, the dose used for the experiments shown in (C) and (D).* ***(C),(D)****: Rate of lactate production assessed in MCF7 (C) and MDA-MB-231 (D) cells exposed to 1 μM TAM. Data were analysed by linear regression; curves' slopes and statistically significant parameters are shown in the graphs.*

5.3.2 Conditional exposure of MCF7 cells to lactate leads to gene expression changes similar to those constitutively observed in MCF7-TAM cells

To explore whether lactate is involved in the transcriptional regulation of genes potentially leading to TAM resistance, we conditionally exposed MCF7 cells to increased level of this metabolite (72 h). In planning this experiment, we referred to the linear regression curve obtained from the data of lactate levels released into the medium by MCF7- TAM cells (Figure 23A). The equation obtained

from the data regression analysis (μg/ml Lact =(26.20 ± 0.86) × h) indicated that the lactate level released in medium from these cultures could reach a concentration of about 7 mM in 24 h, theoretically growing up to 20 mM in 72 h. As mentioned in Section II, 20 mM lactate is the concentration that characterised the microenvironment of different tumour tissues; for this reasons, the experiments aimed at evaluating upregulated gene expression were then performed by exposing the parental MCF7 cultures to this lactate concentration for 72 hours.

RT-PCR assays examined a number of genes selected among those with a documented relationship with TAM resistance or having prognostic significance in breast cancer.

Genes with a statistically significant up-regulation induced by lactate are shown in Figure 24A, grouped by their relevance in biological processes. Interestingly, the gene cluster shown in the "Proliferative Potential" graph was found to be involved in the control of cancer cells' stem properties. In particular, TAZ, a transducer of the Hippo pathway, was shown to sustain self-renewal and tumour-initiation capacities in breast cells[288]. Together with its partner protein YAP, it was also found to be involved in metabolism regulation and glycolysis promotion, suggesting a role in coordinating nutrient availability with cell proliferation[289]. The marked up-regulation of LDHA observed in lactate-exposed MCF7 cells (Figure 24A, "Metabolism" graph) is in line with this idea.

Figure 24A also shows that some statistically significant up-regulations were also found in genes related to infiltrative growth; however, these findings were not completely confirmed by the analysis of some prognostic markers with consolidated value in breast cancer: E- and N-CAD[290]; CD24 and CD44[291,292]. In lactate-exposed MCF7 cells, E-CAD was found to be increased, CD44 decreased. These inconsistent results did not allow relating the enhanced self-renewal potential induced by lactate with features suggesting cancer progression, at least in the short time. This finding is in line with the results described in Section I – preliminary data.

Following these results, we wondered whether lactate exposure could in the same way affect the gene expression of non-cancerous cells. As a model of non-neoplastic breast cells, we adopted the MCF10A line[293]; in this culture, the 72h treatment with 20 mM lactate resulted in fewer gene expression changes. When the lactate responsive genes identified in the MCF7 culture were evaluated in MCF10A cells, only TAZ and the telomerase complex genes (TERC, TERT) were found to be significantly up-regulated by lactate (Figure 24B). This finding poses a clinically relevant question on the effects potentially induced by the metabolites released by highly glycolyzing cancer cells on the surrounding normal tissue.

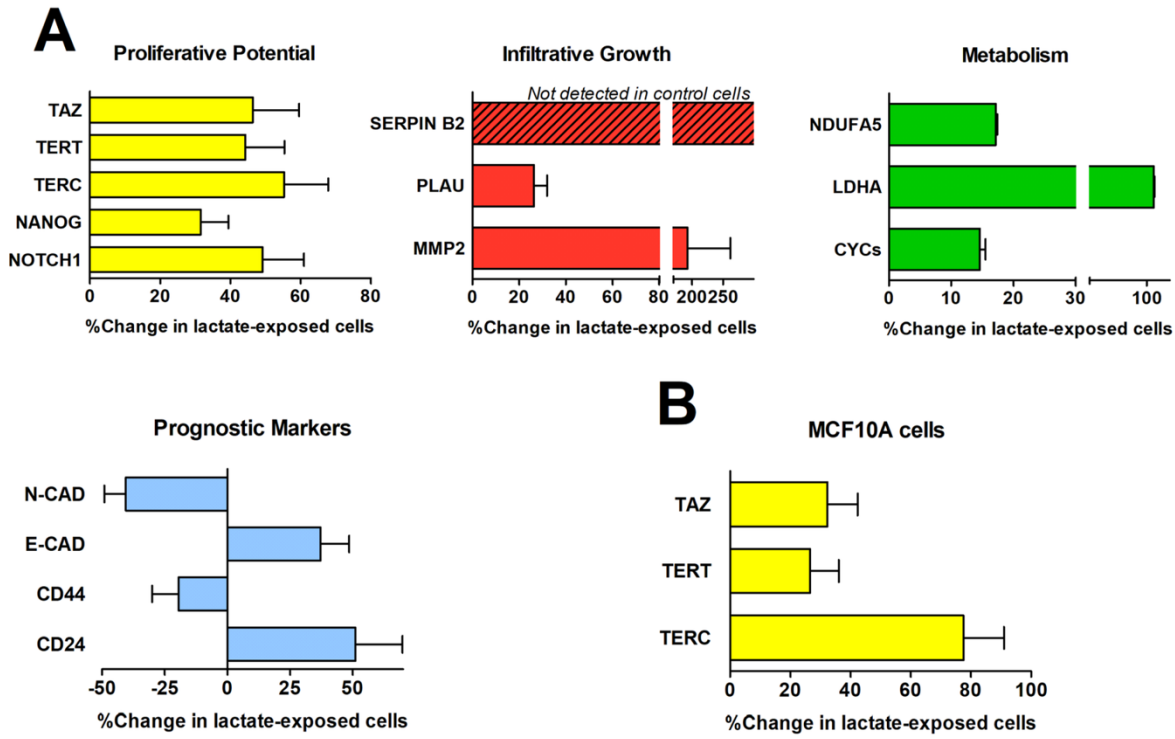

Figure 24. Real-time PCR experiments performed in MCF7 and MCF10A cells after a conditional (72 h) lactate exposure. (A)*: Experiments performed in MCF7 cells; genes have been grouped in graphs according to their biological function.* ***(B)****: Experiments performed in MCF10A cells; in these cultures, only three genes were found to be upregulated. Results were evaluated one sample t-test and calculates whether the mean of each data set is different from a given hypothetical value (0, i.e. no change, compared to untreated cultures). The graphs show only the statistically significant changes; p values ranged from 0.04 to <0.0001.*

Figure 25 shows a comparison between MCF7-TAM and its parental culture, concerning the expression of lactate-upregulated genes identified with the RT-PCR experiments shown in Figure 24A.

The upregulated gene expression pattern observed in lactate-exposed MCF7 cells was confirmed in the TAM resistant line. In these actively glycolyzing cells, which produce elevated lactate levels (Figure 23A), the genes upregulation was markedly higher than that observed in the parental culture exposed to 20 mM lactate. Interestingly, in MCF7-TAM cells the considered prognostic parameters appeared to be markedly worsened. Taken together, the results of Figure 24A and 25 warranted further experiments to highlight the role of lactate in the onset of neoplastic progression and TAM resistance.

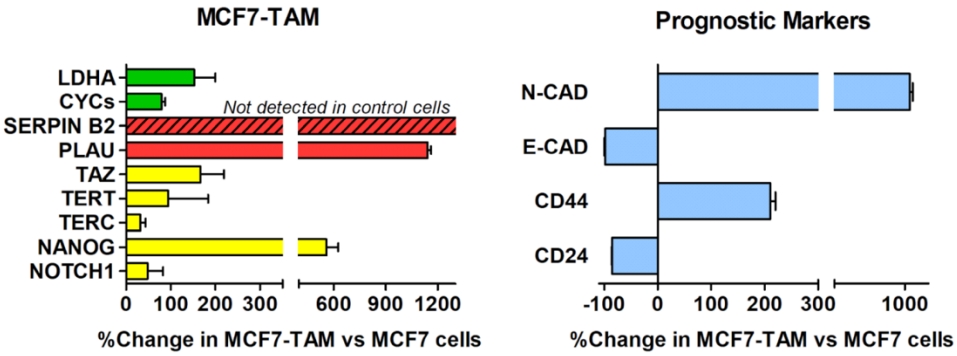

Figure 25. Real-time PCR experiments performed in MCF7-TAM. *In these experiments the expression of the lactate-upregulated genes (Figure 24A) was evaluated in MCF7- TAM and compared to their parental culture. The increased expression shown by lactate-exposed cells was found further enhanced in MCF7-TAM culture and prognostic markers appeared worsened. Results were statistically evaluated as described for Figure 24; the level of statistical significance was reached for all genes, with the exception of NOTCH1 and TERT; p values ranged from 0.03 to <0.0001.*

5.3.3 Conditional exposure to lactate increases the proliferative potential of MCF7 cells

The next step of our study was aimed at exploring whether the observed gene expression changes could also be evidenced at protein and/or functional level.

Because of the negative results, the genes related to prognosis and infiltrative growth were not furtherly considered. We hypothesized that some changes in the metabolism-related genes could be linked to the upregulation of TAZ function[289], instead of a direct effect of lactate. For these reasons, among the results obtained with the RT-PCR experiments, we mainly focused our attention on the lactate-dependence shown by genes correlated with proliferative potential.

As a first step, we verified whether the observed upregulated genes affect histone 3 (H3) acetylation, and whether it also resulted in increased protein levels, as assessed by immunoblotting experiments or by functional assays. Unfortunately, among the "Proliferative Potential" proteins, NANOG and NOTCH1 were not evidenced in the immunoblotting experiments, both in control and in lactate-exposed cells; the low-level expression of these genes in the RT-PCR assay ($Ct \geq 28$) could account for this result.

Figure 26 showed that the adopted conditional exposure to lactate caused a ≈ 30% increased level of H3 pan-acetylation and that this effect resulted in a similarly increased level of TAZ protein. HDAC inhibition and increased H3 acetylation are recognized mechanisms underlying the epigenetic effects of lactate[14]. Results were statistically evaluated by multiple t-test; *, $p < 0.05$, compared to control cultures.

The increased level/function of the transcriptional co-activator TAZ was confirmed; it was accompained by a higher levels of target proteins MYC and LDHA. MYC is a well know target of the Hippo pathway[294] and is known to directly activate the transcription of the LDHA gene[295]. Concerning LDHA, we also measured the levels of its phosphorylation on Tyr10, a post-translational modification enhancing the enzymatic activity of the protein and promoting cancer cell invasion and *anoikis* resistance[63]. According to the data of Figure 26A, B, the increased level of (Tyr10)-phosphorylation fits well with the increased level of the total protein, which suggested that the lactate-triggered effects did not affect post-translational LDHA changes.

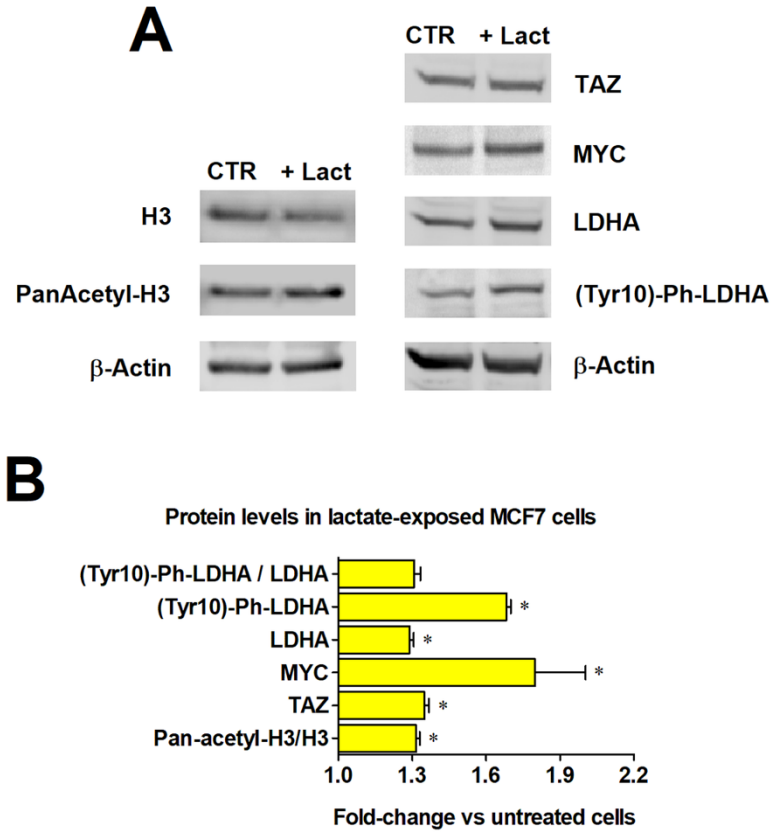

Figure 26. Immunoblotting evaluation of the lactate-upregulated proteins. ***(A)*** *Immunoblotting images.* ***(B)*** *Protein level changes, assessed through bands' densitometric reading.*

For the two identified telomerase complex gene components TERC and TERT (Figure 24A), only a functional assay was adopted, since only one of them (the reverse transcriptase TERT) is translated into a protein, while the other (TERC) encodes for the RNA component of the enzymatic complex. The assay of telomerase activity was performed using scalar amount of cells proteins (1–20 μg); it measured, in control and lactate-exposed MCF7 cells, the elongation with TTAGGG repeats operated by the cell TERT enzyme on a primer sequence added in the reaction mix (TS primer).

Results (Figure 27A-D) showed no difference between the two cultures when the experiment was performed with 1 µg proteins. However, when the telomerase reaction assay was repeated with higher amounts of cell lysates, a progressively increasing difference in the reaction yield was observed between the two cultures, suggesting a higher-level activation of the telomerase complex in lactate-exposed cells.

As shown in Figure 27C, D, the telomerase activity of lactate-exposed cells appeared to be 2-fold higher when the assay was performed with 20 µg cell proteins. Previous studies showed TAM to be involved in the control of TERT expression with opposite functions, both involving ERs: in endometrial cells it acts as a receptor agonist, stimulating proliferation and activating TERT expression [296], whereas in breast cancer cells it may suppress TERT by functioning as a receptor antagonist[297]. The results of Figure 24A and 27 suggest that the off-target metabolic effects of TAM can contribute to hinder one of the effects of its primary mechanism of action.

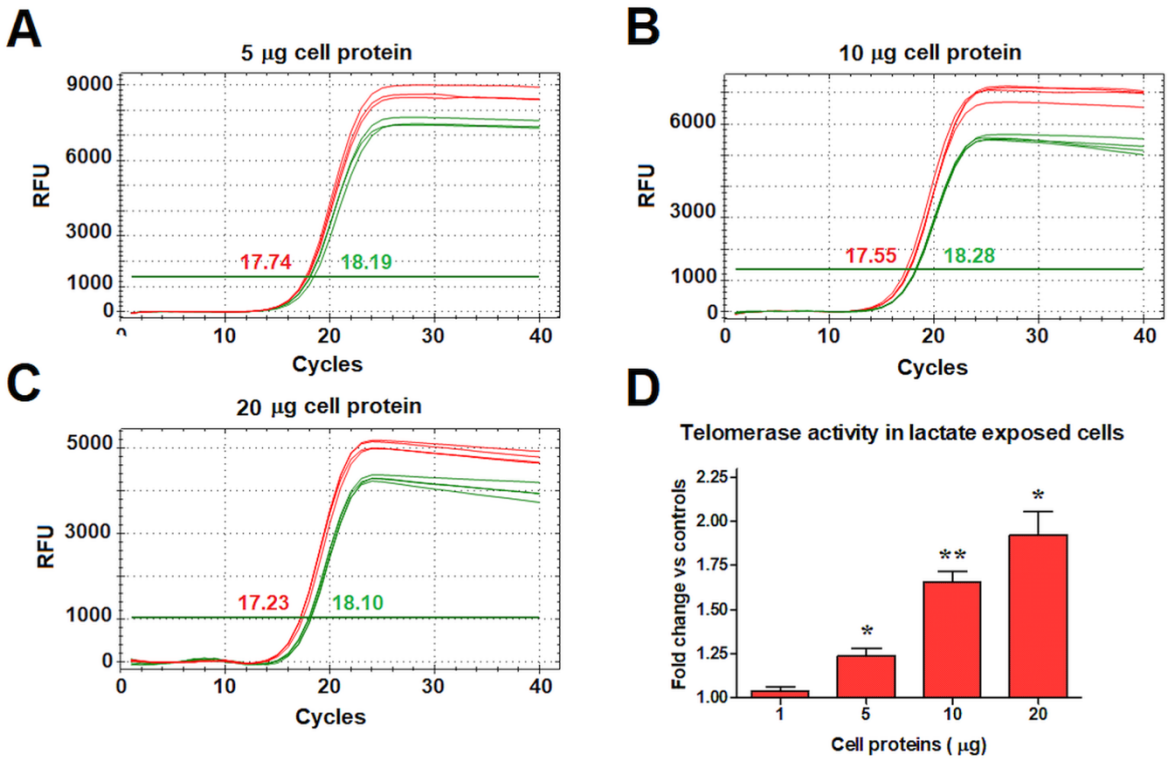

Figure 27. Assay of telomerase activity. *Telomerase complex activity was assessed using scalar amounts of protein extracts from control and lactate-exposed MCF7 cells.* ***(A-C)*** *Exemplificative plots showing the PCR amplification curves obtained from control (green) and lactate-exposed (red) cells. The numbers reported in plot images show the Ct mean values. Differences were evaluated by applying the* $2^{-\Delta Ct}$ *method and are shown in* ***(D)****; * and **, p < 0.05 and 0.01 compared to control cultures, as evaluated by multiple t-test.*

To gain further confirmation about the lactate-induced enhancement of replicative potential, which was suggested by the results of Figure 24, 26 and 27, other assays were performed (Figure 28). The proliferation of lactate-exposed MCF7 cells was compared to that of the parental culture by applying a wound healing assay (Figure 28A) and by measuring the increase in cell number through the detection of ATP levels (Figure 28B). Both experiments were performed by maintaining the cultures in a medium with low serum levels (1–2%), to reduce stimulation by growth factors. Figure 28A shows that in lactate-exposed cells maintained at 2% FBS the percentage of repopulated wound area was significantly higher at 24 h; in this condition, the advantage of lactate treatment disappear at 36 h, when, however, the proliferative advantage observed in lactate-exposed cells became more evident and reached statistical significance in cultures maintained at 1% FBS. The experiments of Figure 28B showed that after 24 h culture in the conventional medium supplemented with 10% FBS, cell number was 30% higher in lactate-exposed cells; furthermore, when both cultures were maintained in serum-deprived conditions, the proliferation of lactate-exposed cells showed a significantly lower level of inhibition.

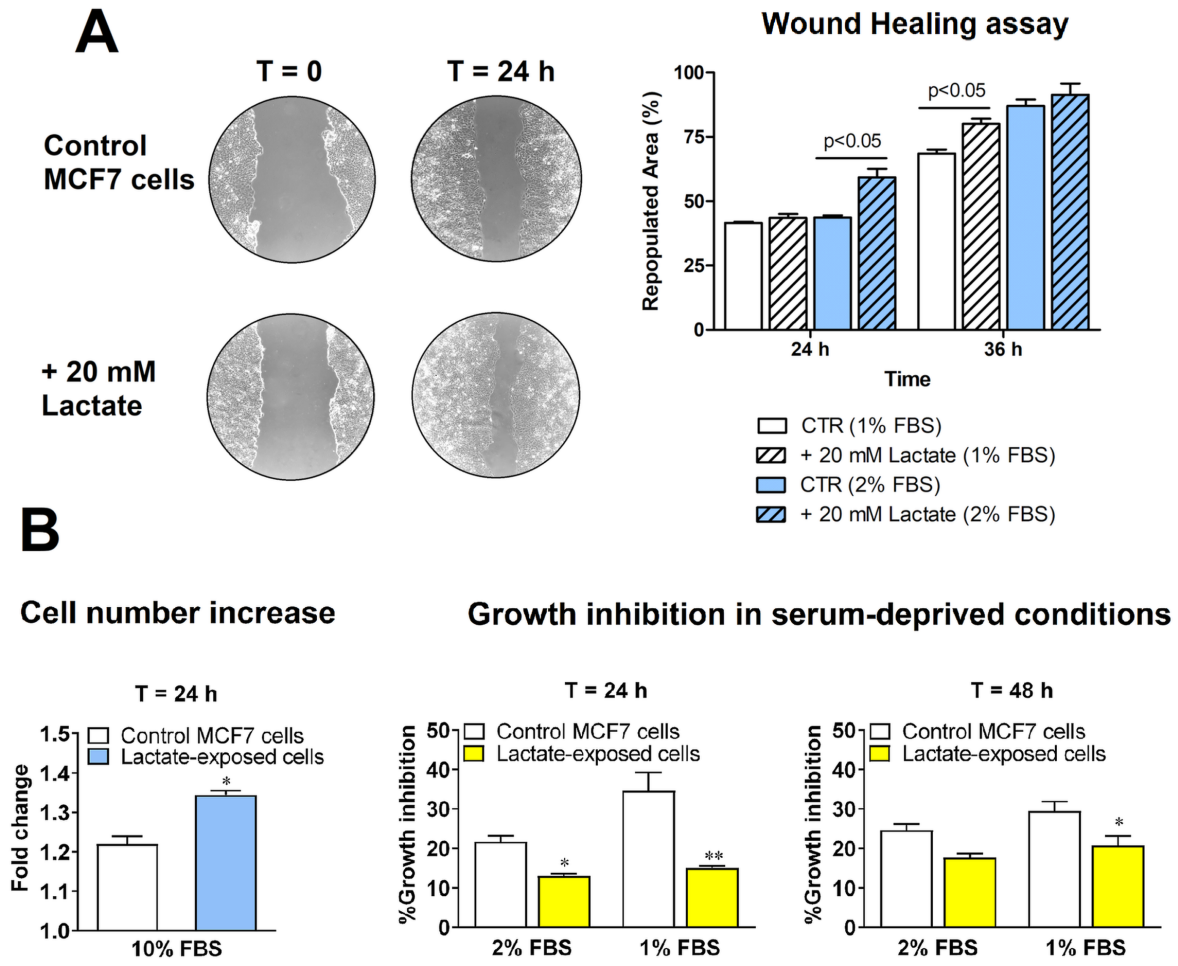

Figure 28. Evaluation of proliferative potential in lactate-exposed MCF7 cells. ***(A)*** *Wound healing assay; the percentage of wound repopulated area was evaluated using the ImageJ software. Data were statistically analysed using two-way ANOVA followed by Bonferroni post-test.* ***(B)*** *When maintained in the conventional culture medium, lactate-exposed MCF7 cells showed a 30% increased proliferation at 24 h. The growth inhibition caused by serum deprivation was significantly reduced by lactate. Data were evaluated by multiple t-test; * and **, p < 0.05 and 0.01, respectively.*

5.3.4 Sustained lactate-exposure reduces the senescence of MCF7 cells treated with TAM

The conclusive section of this study was aimed at evidencing signs of a subsiding response to TAM in lactate-grown MCF7 cells. For these experiments, MCF7 cultures were adapted to grow in a medium containing 20 mM lactate for ≥4 months. No evident morphological changes were observed in cells after sustained lactate exposure. To compare the antineoplastic effect of TAM at 1 µM in control and lactate-exposed cultures, we tried to evidence a p53-mediated response, by an immunoblotting evaluation of p53 levels, followed by a RT-PCR detection of p21 mRNA. No

significant difference was observed between the two cultures, up to a 7-days TAM treatment (data not shown). We hypothesized that this missing result could be a linked to the ER-mediated p53 regulation[298]; as a consequence of the antagonism between anti-oestrogens and p53, these compounds were previously found to reduce both breast cancer cell proliferation and their p53 levels[139]. In agreement with this hypothesis, a marked difference between the two treated cultures was observed when the effect of TAM was evaluated by assessing senescence-associated β-galactosidase (SA β-GAL) activity, a widely used biomarker of replicative senescence. Figure 29A shows SA β-GAL activity of control and lactate-exposed MCF7 cultures. Untreated cultures did not show appreciable differences; however, after the 7-days exposure to 1 μM TAM, marked and diffuse β-GAL staining was clearly more evident in control MCF7 cells. This result suggested that the lactate-awarded proliferative advantage, together with the activated telomerase function can impact on the cellular response to TAM and foster drug resistance.

Several studies highlighted progressive activation of the EGFR pathway as a salvage mechanism adopted by TAM-exposed breast cancer cells in which the ER functions are repressed[299]. Expression of EGFR was found to slightly increase shortly after the beginning of TAM treatment and to become markedly increased in resistant tumours[300].

Figure 29B shows an immunoblotting evaluation of EGFR pathway activation, performed in MCF7 cells after the sustained exposure to lactate and in their parental culture. Phosphorylation on Tyr1068 was shown to positively regulate EGFR signalling[301] and promote AKT activation, evidenced by phosphorylation on Ser473. As shown in Figure 29B, both these phosphorylation events appeared to be significantly increased by lactate exposure. Activation of EGFR pathway has been shown to promote glycolytic metabolism[302,303]. Interestingly, it can be concluded that in our experiments lactate exposure appeared to trigger a cell response that, by promoting glycolysis, should lead to further increased lactate levels.

Finally, the experiment shown in Figure 29C attempted to verify whether lactate deprivation in MCF7-TAM cells could recover, at least in part, their response to TAM. To impede lactate production, MCF7-TAM cells were cultured in L15 medium, which does not allow glycolysis and lactate production. In this medium the proliferation rate of MCF7-TAM appeared to be compromised, but cells maintained their viability. The bar graph shown in Figure 29C compares the effect caused by 1 μM TAM administered for 120 h (dose and time used for the experiment of Figure 23B) to MCF7- TAM and MCF7 cells maintained in their conventional medium and to MCF7-TAM maintained in L15 medium. This dose of TAM did not compromise the viability of MCF7-TAM cells when they were grown in their conventional medium, allowing glycolysis and lactate production. On the contrary, when this culture was maintained in L-15 medium, TAM was found to significantly

affect cell proliferation, causing an inhibitory effect very similar to that observed in the parental MCF7 cell culture. This result can be considered a further confirmation of the role of lactate in maintaining the TAM-resistant cell phenotype.

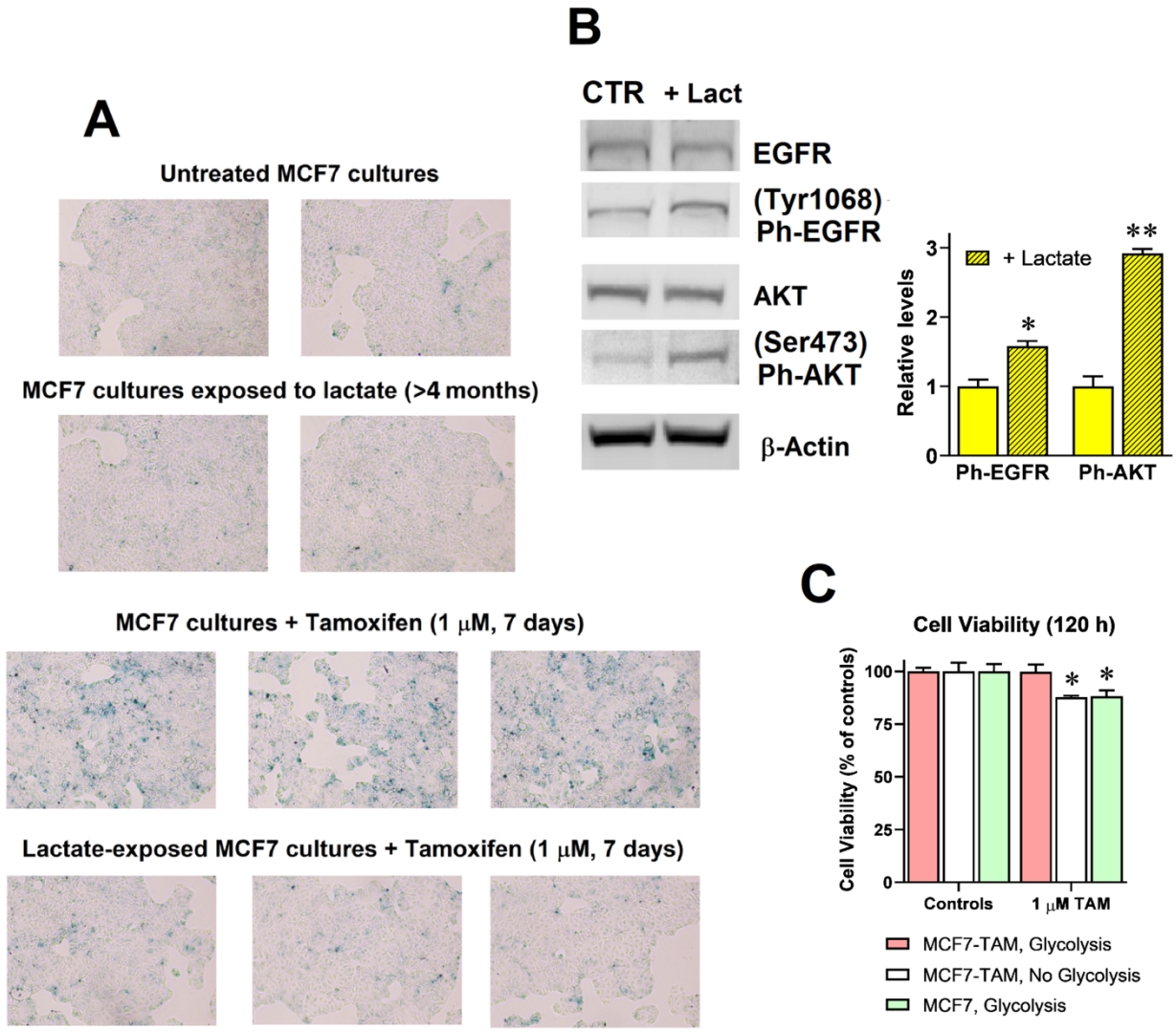

Figure 29. Experiments performed in MCF7 cells after a sustained exposure (≥ 4 months) to lactate and restoration of TAM response after lactate deprivation. ***(A)*** *Pictures showing parental and lactate-exposed MCF7 cells treated for 7 days with 1 μM TAM and stained for β-galactosidase activity. Lactate-exposed cells showed a markedly lower development of the β-galactosidase reaction product.* ***(B)*** *Immunoblotting evaluation of activated EGFR pathway. The level of (Tyr1068)-phospho-EGFR and (Ser473)-phospho-AKT appeared to be significantly enhanced in lactate-exposed cells. Differences were assessed by multiple t-test; * and **, $p < 0.05$ and 0.01 compared to control cultures.* ***(C)*** *Lactate deprivation in MCF7-TAM cells leads to a restored TAM response. Lactate deprivation was obtained by culturing the cells in L15 medium, which does not allow glycolysis. TAM was administered for 120 h at 1 μM, which are the same conditions used in the experiment of Fig. 1B. Differences were assessed by multiple t-test; *, $p < 0.05$ compared to the untreated cultures.*

5.4 Conclusion – SECTION III

The results of Section III showed that a lactate level potentially achievable in cancer cell microenvironment could affect gene expression in a way that might lead to reduced TAM response. According to our data, the contribution of lactate in reducing TAM efficacy could derive from its capacity to enhance the proliferative potential of cells and, as a consequence of the activation of the telomerase complex, to reduce their attitude to undergo senescence. The same features can be expected to impact also on the response of cancer cells to different antineoplastic agents. Our data are in complete agreement with the findings of Hamadneh et al.[304], who showed that the development of TAM resistance in MCF7 cells correlates with upregulated LDHA/B expression and increased lactate concentration in cell culture medium. Our data support this study by suggesting that the product of LDH reaction (either deriving from the basal cancer cell metabolism, or from the TAM side-effects) can by itself play a direct role in promoting a reduced drug response. Furthermore, as also proposed by Das et al.[305], our results suggest that targeting LDHA could open a novel strategy to interrupt TAM resistance in breast cancer.

Interestingly, experiment shown in Figure 24B suggested that tumour released lactate could also exert phenotypic modifications on normal bystander breast cells. The observed phenotypic modifications caused by lactate in both cancer and normal cells are completely coherent with the role of glycolytic metabolism in embryonal development and in the maintenance of stem compartment in normal tissues[269]. Cancer promoters are defined as agents that, without changing DNA sequence, influence cell proliferation, also inhibiting programmed cell death; this epigenetic process ultimately results in the generation of neoplastic cell foci[306]. In line with this concept, our results suggest that lactate could be viewed as a promoter of TAM resistance in the MCF7 breast cancer model. In MCF7 cultures exposed to lactate for ≥4 months, we obtained evidence of EGFR activation, which has been previously documented as a crucial pathway controlling the proliferation of TAM-resistant cells[277]. A direct correlation between the epigenetic effects caused by lactate and EGFR activation, is suggested by previously published data showing that in breast cancer, but also in different neoplastic cells, TAZ overexpression promotes EGFR signalling, leading to AKT/ERK activation and increased cell proliferation[307,308]. The increased AKT phosphorylation also shown in Figure 29B is a further evidence of activated EGFR pathway. Because of the promoting effect on aerobic glycolysis of EGFR-mediated signalling[302,303], on the basis of our results we can speculate that the increased lactate levels in the microenvironment of TAM-exposed breast cancer cells can fire up a self-feeding loop where a metabolic product (lactate) promotes epigenetic changes ultimately resulting in the

amplification of its generation (Figure 30). In the long term, the cell phenotypic changes induced by the activation of this self-supporting cycle could lead to TAM resistance.

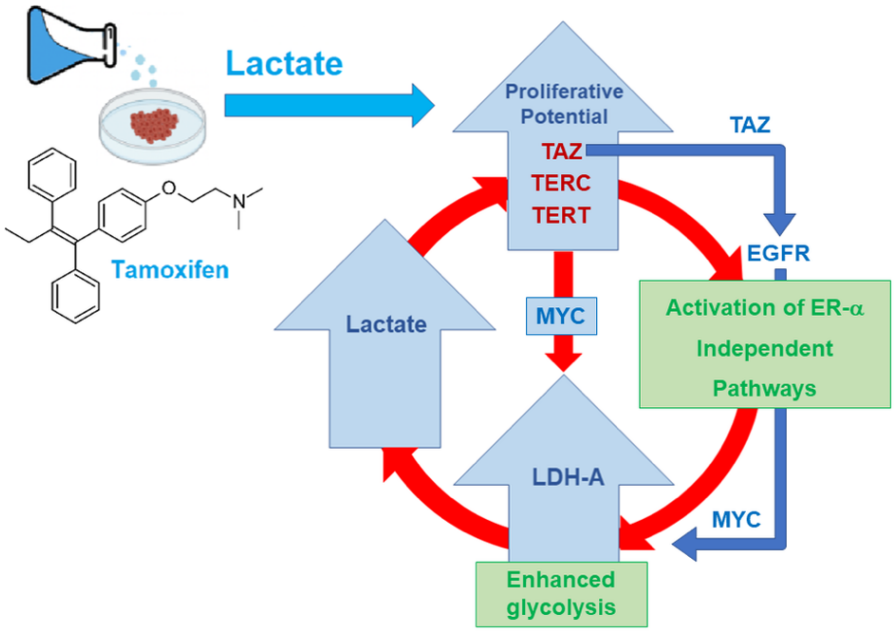

Figure 30. Self-supporting cycle potentially induced by lactate in MCF7 cells. *Increased lactate exposure increases the proliferative potential of MCF7 cells by upregulating the expression of TAZ, TERC and TERT. TAZ overexpression was found to activate EGFR pathway and to increase MYC level, leading to increased LDHA expression/activity. On the basis of our results, we propose that, by causing increased lactate production in cells, the TAM associated metabolic changes could activate ERα-independent pathways, paving the way to a progressive reduction of therapeutic effects.*

[This page is intentionally left blank]

6. SECTION IV

Lactate-induced HBEGF Shedding And EGFR Activation: Paving The Way To a New Anticancer Therapeutic Opportunity

In the concluding phase of this project, based on our findings, we focused our investigation on exploring the potential effect of lactate in promoting the activation of the EGFR pathway.

6.1 Introduction

EGFR (also known as ErbB1/HER1) is one of the members of the ErbB receptor tyrosine kinase family[309]. In cancer cells, its aberrant activation is primarily mediated by gene amplification and gives rise to signalling cascades promoting cell proliferation and playing a key role in cell survival[310]. These findings suggest that EGFR hyperactivation can take active part in the neoplastic change process and in conferring substantial growth and survival advantages to cancer cells. In addition, EGFR-mediated signalling was found to play a fundamental role in the initial steps of the EMT[311,312], while treatment with EGFR inhibitors appeared in some contexts to induce changes in cell morphology, from a spindle shape to a more epithelial phenotype[313].

In light of these data, it is not surprising that in patients with multiple cancer forms elevated EGFR expression revealed to be a strong prognostic feature, usually associated with poor outlook and indicative of reduced recurrence-free or overall survival rates[314]. Conversely, the clinical use of EGFR inhibitors often appeared to produce substantial therapeutic benefits[315].

A common feature of rapidly proliferating cells is the increased level of glycolysis, and activated EGFR pathway was also found to be one of the major regulators of cancer cell metabolism[303]. Stimulation of EGFR by its ligands is known to accelerate glucose consumption and foster the so-called Warburg effect, resulting in increased lactate production by cancer cells[11]. At the molecular level, this metabolic reprogramming was shown to be mediated through the concurrent upregulation of hexokinase-2 (HK2) expression and phosphorylation of pyruvate kinase M2 (PKM2), which alters the oligomerization state of the enzyme and inhibits its activity[316]. These changes cause at the same time an acceleration of the first step of glycolysis, together with a stall at the end of the glycolytic cascade[303]. As a result, an accumulation of metabolic intermediates is generated in cell cytoplasm, with lactate being the prevailing one. Interestingly, lactate was found to further promote glycolytic metabolism by leading to increased MYC and LDHA expression[222].

Based on these premises, the aim of this study was to investigate on a possible role of lactate in fostering the activated state of EGFR pathway. In particular, we first considered the observation that some cancer cells can directly release EGF-like peptides, acquiring the capacity of autocrine stimulation[317]. One of these peptides is the soluble form of heparin-binding EGF (HBEGF). Initially synthesized as a transmembrane precursor protein, HBEGF is cleaved at the cell surface by proteases and is released in a soluble form[318], a process usually referred to as "HBEGF shedding". Released HBEGF was found to be a potent mitogen[319]; furthermore, it was found to be implicated in tumour progression and chemotherapy resistance[320,321].

To test the activation of EGFR by lactate, we used two human cell cultures in which the expression of HBEGF was clearly documented in published studies: MDA-MB-231[322] and HT-29[323]. The first culture is the same that we used for the experiments of Section II: triple-negative breast cancer (MDA-MB-231), meanwhile HT-29 is a representative of clinically relevant tumour form of colon adenocarcinoma. We routinely maintained the two cultures in a medium containing a physiological glucose concentration found in healthy human tissues (1 g/l). By exposing the cultures to a lactate level (20 mM) similar to that detected in the microenvironment of neoplastic tissues, we verified whether this metabolite can play a role in sustaining the HBEGF-mediated EGFR pathway.

6.2 Materials and methods

6.2.1 Cell Cultures and treatments

MDA-MB-231 and HT-29 cells (ATCC) were grown in low-glucose (1 g/l) DMEM (Thermo Fisher Sci.) supplemented with 100 U/ml penicillin/streptomycin, 2 mM glutamine and 10% FBS. All the materials used for cell culture and all the reagents were obtained from Merck, unless otherwise specified. L-lactate was dissolved in culture medium at a 20 mM concentration. Before experiments, both cell cultures were adapted to grow in the lactate-containing medium for at least 3 months. This time interval was found to be necessary for the complete manifestation of the phenotype linked to the epigenetic effects of lactate. MDA-MB-231 cells were found to adequately proliferate in the lactate-containing culture medium without any sign of alteration. HT-29 culture showed delayed substrate adhesion in the presence of lactate; for this reason, in routine cell passages these cells were let to adhere for 16 h to the new substrate before adding lactate to the culture medium. Both cultures were routinely split once a week.

Cisplatin (CPL) (MedChem Express) was dissolved in 0.9% NaCl. CRM197 (Cross Reacting Material 197) was obtained in lyophilized form (Santa Cruz Biotechnology); it was dissolved in ultra-pure water and stored at -80°C. BC11 hydrobromide (Bio-Techne) was dissolved in DMSO (30 mM) and stored at -20°C. Cultures were routinely tested for Mycoplasma contamination and found to be free.

6.2.2 Real-time PCR

RT-PCR was first performed using MDA-MB-231 cells, to compare the gene expression of the lactate-exposed culture with that of the same culture routinely maintained in high-glucose (4 g/l) DMEM. This procedure helped in identifying a small group of genes specifically responsive to lactate, excluding the effects of upregulated glycolysis. Subsequently, the expression of these genes was also evaluated in lactate-exposed HT-29 cells. Exponentially growing cells from T25 flasks were used. RNA was extracted using an RNA isolation kit (Merck) and was quantified spectrophotometrically (ONDA Nano Genius Photometer). Retro-transcription to cDNA was performed as describe in paragraph 4.2.5 of Materials and methods of Section II. RT-PCR procedure and analyses of data were performed as describe in 4.2.5 of Materials and methods of Section II. All the primers used for the PCR experiments were from Merck.

6.2.3 Immunoblotting experiments

These experiments were performed in control and lactate-exposed MDA-MB-231 and HT-29 cells, to confirm the data obtained by RT-PCR and assess the activation state of EGFR. To evaluate the effects of HBEGF and uPA inhibitors in lactate-exposed MDA-MB-231 cells, they were exposed for 24 h to CRM197 (2 μg/ml, corresponding to 32 nM) and BC11 (100 μM).

Cultures (T-25 flasks, at 80% confluence) were harvested and lysed in 50 μl RIPA buffer containing protease and phosphatase inhibitors. Then, 70 μg of protein (determined by using Bradford reagent) was loaded onto precast 4–12% polyacrylamide gels for electrophoresis (Thermo Fisher Sci.) and run at 170 V. The separated proteins were blotted on low-fluorescent PVDF membranes (Cytiva Life Sciences) using the BoltTM transfer system and maintaining 60 mA for 16 h. The blotted membranes were blocked with 5% BSA in TBS-Tween and probed with the primary antibody. Actin was used as a loading control in all experiments. The following primary antibodies were used: rabbit anti-uPa, rabbit anti-GPER1, rabbit anti-ERR-alpha, rabbit anti-phospho-EGFR-Y1068 (all from ABclonal); rabbit anti-EGFR (Cohesion Bioscience); rabbit anti-ERK1/2 and rabbit anti-phospho-ERK1/2 (Thr202/Tyr204) (both from Cell Signaling); mouse anti-PUMA α/β (Santa Cruz); rabbit anti-Actin (Merck).

The secondary antibodies used for binding detection were: goat anti-rabbit-IgG (Cy5-labelled, from Cytiva Life Sciences) and donkey anti-mouse IgG (Alexa Fluor 647-labelled, from Jackson Immuno-Research).

Membranes' fluorescence was assessed with the Pharos FXTM Scanner (Bio-Rad) at a resolution of 100 μm and bands' intensities were evaluated using the ImageJ software (version 1.53a).

6.2.4 ELISA for the detection of HBEGF released in culture medium

Both control and lactate-exposed cells were used; released HBEGF was assessed by applying a commercially available ELISA assay (Thermo Fisher Sci.).

Cells (3×10^5 MDA-MB-231 and 5×10^5 HT-29) were seeded in each well of 6-well plates in 750 μl culture medium and maintained for 24 h in a humidified incubator at 37°C. During this time, lactate-exposed cells were also treated with 100 μM BC11. At the end of treatment, culture medium was recovered, filtered through a 0.22 μm syringe filter and centrifuged for 30 min at 2000 RCF. Samples were then aliquoted and stored at -80°C. The ELISA assay was performed by using 100 μl samples and following the manufacturer instructions. At the end of the procedure, absorbance of

samples was evaluated at 450 nm, with the aid of a Synergy HT–BioTek plate reader (Agilent Technologies). For both cell lines, ELISA procedure was replicated at least 4 times.

6.2.5 Cell proliferation

To evaluate the effect on cell proliferation caused by the different cell culture media and by the used inhibitors, we adopted a procedure based on crystal violet (CV) staining. CV binds to nucleic acids and allows a precise estimate of cell number, which can be calculated with the aid of a calibration curve. At the beginning of each experiment, a plot reporting the CV absorbance values of scalar amounts of cells was obtained. These data were fitted by using the linear regression analysis; the resulting equation was used to calculate the number of cells at the end of experiments (24 h).

Control and lactate-exposed MDA-MB-231 and HT-29 cells (1×10^4 cells/well) were seeded in 96-multiwell plates and let to adhere overnight. Cultures were then exposed to treatments for 24 h. CPL was administered at a dose of 50 μM; CRM197 at 32 nM; BC11 at the doses of 50, 75 and 100 μM. At the end of treatment, medium was removed and the cells were fixed with 1% glutaraldehyde for 20 min. After staining with CV (0.01% in distilled water, 30 min) wells were washed with PBS and CV was solubilized by shaking in 70% ice-cold ethanol for 30 min at room temperature. Absorbance was evaluated at 570 nm by using the Multiskan EX plate reader (Thermo Fisher Sci.). In each experiment and for each treatment, the increase (or decrease) in cell number during the 24 h was calculated.

6.2.6 Assay of lactate levels

Control and lactate-exposed MDA-MB-231 cells were seeded in triplicate in 24-wells plates (2×10^5 cells/well) and let to adhere. They were then treated with 32 nM CRM197 and 100 μM BC11, given individually or in combination for 16 h. Culture medium was then replaced with Krebs-Ringer buffer (300 μl/well). The concentration of lactate released in Krebs-Ringer buffer was evaluated after 5 hours of incubation at 37°C, following the method described in paragraph 4.2.2 of Materials and methods of Section II.

6.2.7 Wound healing assay

For this experiment control and lactate-exposed MDA-MB-231 cells were used. Lactate-exposed cells were also treated with the association of CRM197 (32 nM) and BC11 (100 μM). Cells were

seeded in triplicate in 6-well plates (1.5×10^6 cells/well) and cultured until they had reached 100% confluence. The procedure of this assay is described in paragraph 5.2.7 of Materials and methods of Section III.

The wound areas were captured with an inverted microscope (Primovert, Carl Zeiss Microscopy) at 0, 6, 20, 24 and 30 h and their repopulation were analysed by using the ImageJ software. A similar experiment was performed on HT-29 cells; in this culture, lactate-exposed cells were treated with the single BC11 treatment (100 μM).

6.2.8 Clonogenicity assay

Control and lactate-exposed MDA-MB-231 cells were seeded in duplicate in 6-well plates (5×10^2 cells/well) and let to adhere overnight. Lactate-exposed cells were also treated with the association of CRM197 (32 nM) and BC11 (10 μM). Cell colonies became clearly evident after 8 days; at this time, they were fixed and stained with 6% glutaraldehyde and 0.5% CV in PBS (30 min at room temperature). Stained colonies were dissolved with 10% SDS (400-800 μl). The absorbance of the solutions was measured with the aid of the Multiskan EX plate reader at 570 nm.

A similar experiment was also performed on HT-29 cultures. In this case, lactate-exposed cells were treated only with BC11, given at 10 and 20 μM; colonies became evident after 15 days.

6.2.9 E-Cadherin immunostaining

Lactate-exposed MDA-MB-231 cells were seeded on glass slides posed in the wells of a 6-well plate (1500 cells/well). They were let to adhere and were then treated with 32 nM CRM197 for 8 days, with medium renewal at day 4. After this time cells were fixed with 4% paraformaldehyde and permeabilized with 70% ethanol. Glass slides were then treated with a blocking solution containing 5% BSA and exposed to a mouse monoclonal anti-human E-cadherin antibody (1 ng/ml in BSA 5%, 16 h, at 4°C). Binding was revealed with the aid of a FITC-conjugated anti-mouse polyvalent-(G, A, M)-immunoglobulins, produced in goat (1:400 in BSA 5%, 30 min at room temperature). Glass slides were then mounted with a solution of DAPI (2 μg/mL) and DABCO. Pictures of cells were taken at a 600× magnification, using a Nikon Eclipse-E600 epifluorescence microscope (Nikon Corporation) equipped with filters for FITC and DAPI and with a DXM1200F Nikon digital camera (ACT-2U software).

6.2.10 Statistical analyses

Results were obtained from at least two independent experiments, performed with triplicate samples. Data were analysed using the GraphPad Prism software. For each experiment, the adopted statistical evaluation is described in the corresponding paragraph of the Results section. Data were expressed as mean values ± SE and were calculated using all the results obtained from the independent experiments; the significance level was set at $p < 0.05$.

6.3 Results and discussion

6.3.1 Lactate upregulates urokinase-type plasminogen activator (uPA), leading to HBEGF shedding

To highlight the potential role of lactate in EGFR activation, in the first set of experiments we adopted for MDA-MB-231 cells three different culture conditions: a) maintenance in the presence of physiologic glucose levels (1 g/l, Low-Glc DMEM, control cells); b) maintenance in Low-Glc DMEM supplemented with 20 mM lactate (lactate-exposed cells); c) maintenance in a conventional, high-glucose (4 g/l) DMEM (High-Glc DMEM). The lactate supplementation used in medium (b) is the same used for experiments of Section II and Section III and it matches the level of metabolite detected in the microenvironment of neoplastic tissues[9]. In study described in Section II and Section III was found to cause a significantly increased level of histone-3 acetylation. As specified in paragraph 6.2.1, MDA-MB-231 cells were grown in the above-described conditions for at least three months before beginning the experiments. The same phase of adaptation was adopted for HT-29 cultures, which were maintained in Low-Glc DMEM supplemented with 20 mM lactate.

Before experiments, we compared the proliferation dynamics of the cell cultures in the different media. As shown in Figure 31A, lactate supplementation in Low-Glc DMEM did not affect the proliferation of MDA-MB-231 cells, and both cultures maintained in Low-Glc DMEM almost doubled their cell number in 24 h. On the contrary, a significantly increased cell proliferation (+ ≈35%) was observed in the culture maintained in High-Glc DMEM. A similar experiment performed in the HT-29 culture showed again that lactate supplementation in the Low-Glc medium did not modify cell proliferative potential.

We then analysed by RT-PCR the mRNA level of EGFR and of a small number of proteins involved in its activation and/or having prognostic value in cancer diseases: MMP-2 and -9 [324,325]; uPA[326,327]; G Protein Coupled Receptor 1 (GPER1)[328,329]; Estrogen Related Receptor alpha (ERR-alpha)[330,331]; SRC[332]; LDH-A and -B[333]; HBEGF. The adopted culture conditions helped us in discriminating between the effects specifically ascribable to lactate from those caused by an overactivated glycolytic flux (High-Glc DMEM).

The obtained results are shown in Figure 31B. The genes considered for further experiments were those showing: 1) a ≥50%-increased level and 2) a similar expression in High-Glc DMEM grown and in lactate-exposed cells; differences were statistically evaluated by ANOVA followed by Tukey's post-test. The selected conditions were met by uPA (Low- Glc DMEM vs +Lactate, $p < 0.05$;

Low-Glc DMEM vs High-Glc DMEM, $p < 0.01$; High-Glc DMEM vs Low-Glc DMEM+Lactate, NS), GPER1 and ERR-alpha (for both genes, Low-Glc DMEM vs +Lactate, and vs High-Glc DMEM, $p < 0.01$; High-Glc DMEM vs Low-Glc DMEM+Lactate, NS). Graph 31B also shows increased expression of LDH-A (+55% in lactate exposed cells and +90% in High-Glc DMEM grown cells); this result was not considered since the difference observed between the two culture media suggested a major contribution by enhanced glycolysis rather than by lactate alone. For the same reason, we did not consider the strongly increased level (+ 130%) of SRC, a tyrosine kinase engaged in breast cancer development and progression[332], which was observed only in cells exposed to High-Glc DMEM.

Media containing enhanced glucose levels are routinely used in research laboratories to maintain cell cultures and hasten their proliferation; our results suggest caution in following this procedure, since it showed the potential of changing gene expression, affecting the experimental results.

Interestingly, MMP-9 (a protease usually described as a potential HBEGF activator[324]) was significantly reduced as a consequence of lactate exposure, while MMP-2 expression was not detected in MDA-MB-231 cells. These results were confirmed in HT-29 cultures, adapted to grow in Low-Glc DMEM + 20 mM lactate for a period ≥ 3 months (Figure 31C). In these cells, lactate appeared to exert a much stronger effect on ERR-alpha expression. RT-PCR data obtained in HT-29 cells were evaluated by ANOVA followed by Dunnet's post-test. A highly significant statistical difference was observed for GPER1 and ERR-alpha ($p < 0.01$ and 0.001, respectively). In this experiment, the increase of uPA mRNA did not reach the level of statistical significance (which, however, was observed at the immunoblotting detection of Figure 32B). It is noteworthy that when the expression of HBEGF in the two cultures was compared, MDA-MB-231 showed a more than 10-times higher mRNA level compared to HT-29, suggesting a far lower dependence of these cells on HBEGF-mediated signalling (Figure 31D).

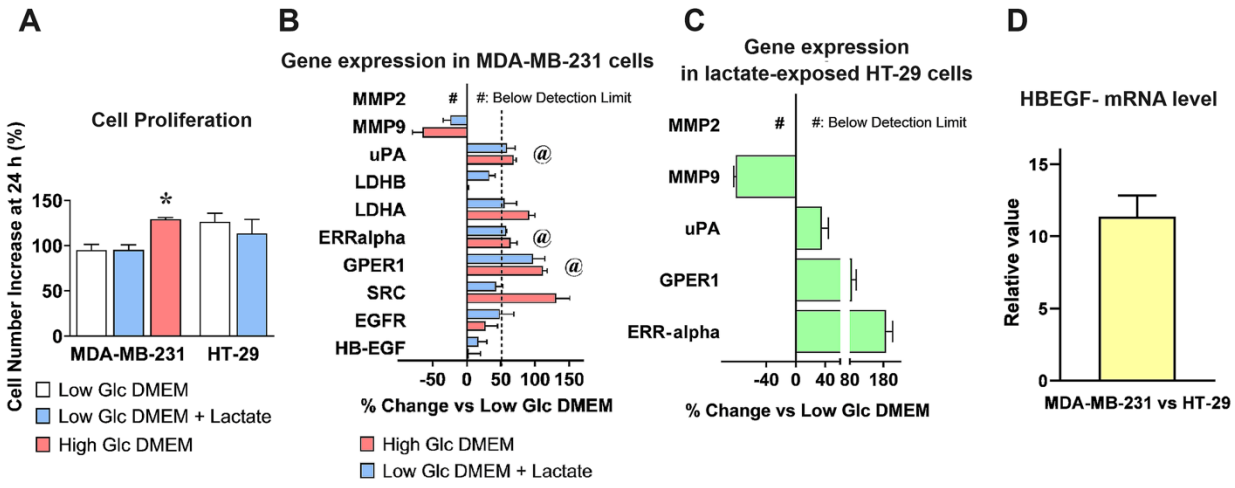

Figure 31. mRNA levels of EGFR and of proteins involved in its activation, assessed by RT-PCR. ***(A)*** *Before experiment, a preliminary evaluation was carried out to verify whether the different DMEM formulations could affect the proliferation dynamics of cell cultures. *, a statistically significant difference with $p < 0.05$ was found in cultures maintained in High-Glc DMEM vs those maintained in the Low-Glc medium (ANOVA followed by Tukey's post-test).* ***(B)*** *mRNA levels in MDA-MB-231 cells grown in Low-Glc DMEM were compared to those detected in High-Glc DMEM maintained cells and in cells exposed to Low-Glc DMEM + lactate. For genes' selection, a threshold at ≥50% increase was set (dotted line). Furthermore, only genes showing no statistically significant difference between High-Glc DMEM grown cells and those exposed to Low-Glc DMEM + lactate were considered. These criteria were met by uPA, ERR-alpha, and GPER1 (@). The selected genes (@) were also studied in HT-29 cells, cultured in Low-Glc DMEM and exposed to lactate* ***(C)****, together with MMP9 and MMP2 (two proteases involved in HBEGF shedding). In these cells, RT-PCR analysis substantially confirmed the data obtained in MDA-MB-231 cultures. The statistical evaluations applied to the data shown in* ***(B)*** *and* ***(C)*** *are detailed in the text.* ***(D)*** *Comparison of HBEGF mRNA levels between the two cell cultures.*

In both cell cultures, the RT-PCR data were validated by the immunoblotting evaluation of uPA, GPER1 and ERR-alpha shown in Figure 32. In this experiment, the strong increase of ERR-alpha detected in HT-29 cells was not confirmed and this protein appeared to be scarcely up-regulated in both the cell cultures; GPER1 protein level was markedly increased in lactate-exposed MDA-MB-231 cells and uPA showed a statistically significant ≈40 % increase in both lactate-exposed cultures.

In both normal and malignant breast cells, GPER1 was found to be involved in HBEGF-mediated EGFR pathway activation[328]; furthermore, endogenously produced uPA was proposed as a major determinant leading to ERK1/2 phosphorylation in MDA-MB-231 cells[334]. Although HBEGF expression was not significantly up-regulated as a result of lactate exposure, following the above-mentioned results we verified whether lactate-exposed MDA-MB-231 and HT-29 cells had acquired

the potential of releasing higher levels of HBEGF in medium, through a uPA-mediated mechanism. To this aim, we recurred to the use of BC11, a specific uPA inhibitor[335].

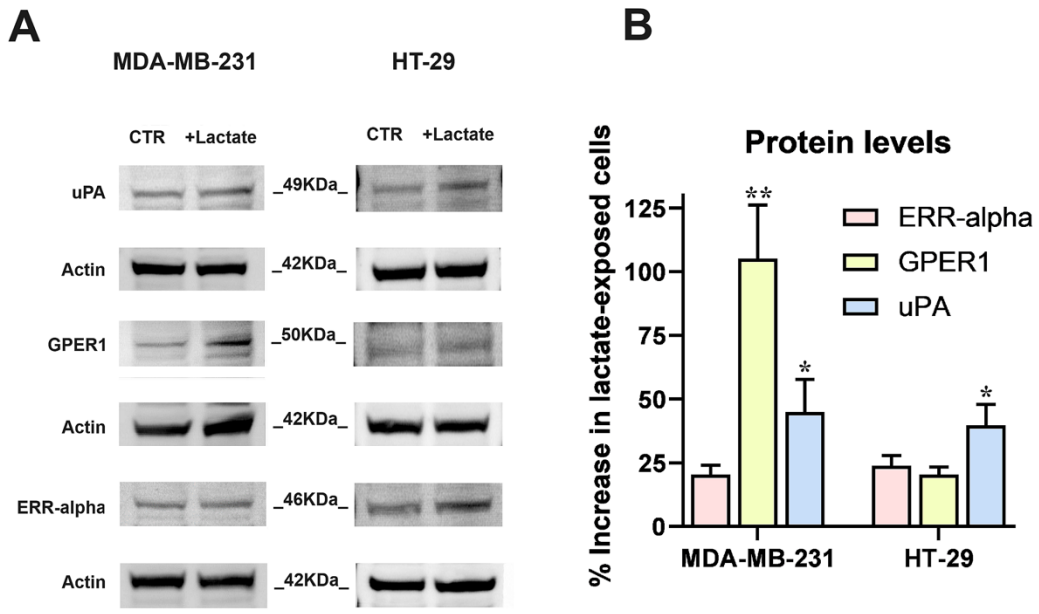

Figure 32. Immunoblotting detection of uPA, GPER1 and ERR-alpha proteins in MDA-MB-231 and HT-29 cells. (A) *Images of the protein bands and of the used internal standard (Actin).* ***(B)*** *The densitometric reading of bands, normalized on Actin levels, was used to calculate the % increase of protein levels in lactate-exposed cells vs control cultures, maintained in Low-Glc DMEM. Because of their limited-extent, the increases of ERR-alpha (in both cell lines) and GPER1 (in HT-29 cultures) were not further considered. The results concerning uPA (in both cell cultures) and GPER1 (only in MDA-MB-231 cells) were analysed by one-sample t-tests; * and ** indicate a statistically significant increase compared to the control cultures, with $p < 0.05$ and 0.01, respectively*

Since BC11 was shown to exert toxic effects on MDA-MB-231 cells[335], in a preliminary experiment we evaluated the tolerability of this compound on the lactate-exposed cultures; results are shown in Figure 33A.

In agreement with published data, BC11 severely affected MDA-MB-231 cell viability in a dose-dependent manner, while HT-29 cells appeared to better tolerate this inhibitor. Interestingly, in lactate-exposed MDA-MB-231 cells the effect of BC11 was drastically reduced and the two lactate-exposed cultures showed to tolerate BC11 similarly, up to 100 μM, 24 h. These conditions were hence adopted to evaluate released HBEGF in medium.

Figure 33B shows the results obtained using a commercially available ELISA, specifically designed for the quantification of HBEGF in its soluble form. In lactate-exposed MDA-MB-231 cultures the level of soluble HBEGF appeared to be 3-fold increased, compared to control cells,

maintained in Low-Glc DMEM; BC11 supplementation almost completely inhibited the effect of lactate supplementation. As expected, in control HT-29 cultures soluble HBEGF was undetectable; it reached the limit of detectability in lactate-exposed cells and, also in this culture, BC11 supplementation was found to reduce the release of the soluble form.

These results clearly demonstrated that the upregulated expression of uPA observed in lactate-exposed cells could play a role in releasing the soluble form of HBEGF.

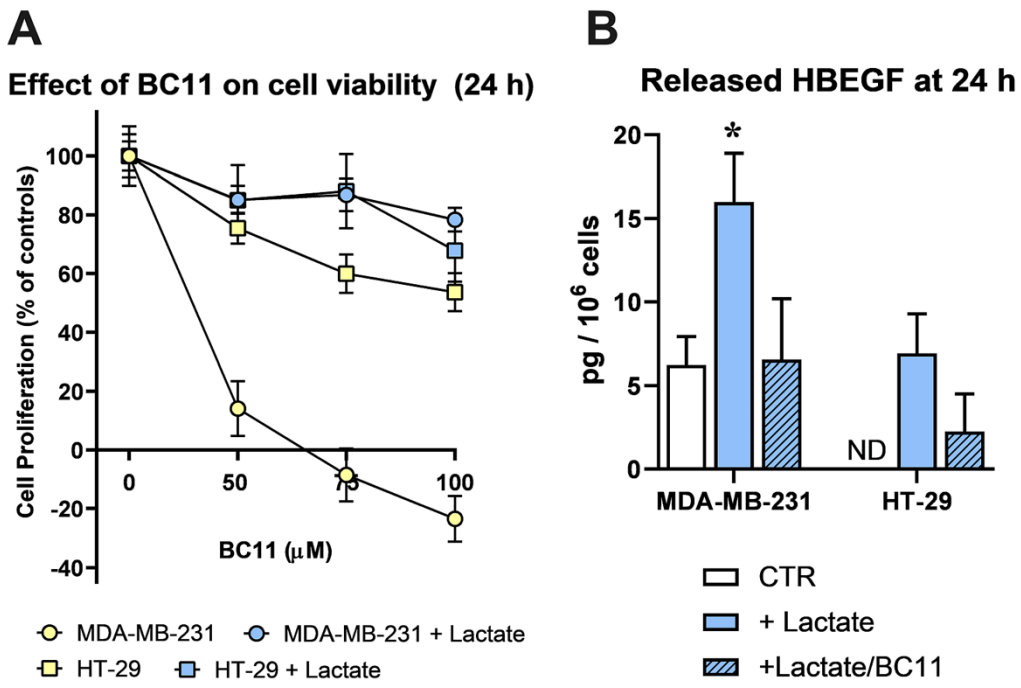

Figure 33. (A) *Effects caused by BC11 (uPA inhibitor) on the proliferation of control (grown in Low-Glc DMEM) and lactate-exposed MDA-MB-231 and HT-29 cells, at 24 h. Lactate was found to drastically reduce the toxic effects of BC11 in MDA-MB-231 culture. No significant difference was observed between the two lactate-exposed cultures at all the tested doses of BC11.* ***(B)*** *Detection of released HBEGF (24 h) in control (Low-Glc DMEM) cultures and in cells exposed to lactate or lactate + BC11 (100 mM). In MDA-MB-231 cultures, lactate significantly increased HBEGF shedding ($p < 0.05$, assessed by ANOVA followed by Dunnett's post-test). In control HT-29 cells released HBEGF was undetectable (ND), but reached the limit of detectability in lactate-exposed cells. In both lactate-exposed cultures, BC11 supplementation reduced the level of released HBEGF and no statistically significant difference was observed between control cells and cells exposed to lactate/BC11.*

6.3.2 Lactate-exposed cells show signatures of activated EGFR pathway and reduced response to cisplatin

To verify whether the uPA-increased HBEGF shedding can result in enhanced activation of EGFR-mediated signalling, we assessed the phosphorylation level of the receptor and of its downstream kinases (ERK1/2) by applying an immunoblotting assay.

The obtained results are shown in Figure 34. The immunoblotting detection of EGFR (Figure 34A) revealed in lactate-exposed MDA-MB-231 cells two bands at a >100 kDa MW level; as previously described[336], these bands are diagnostic of the glycosylated forms of the receptor and indicate the presence of activated EGFR. The higher activated state was also confirmed by the increased level of phospho-EGFR (Tyr1068) and of phospho-ERK1/2 (Thr202/Tyr204) observed in lactate-exposed cells, compared to the control culture.

In lactate-exposed HT-29 cells, the EGFR signal appeared as a single band; however, the immunoblotting evaluation showed enhanced phosphorylation levels of the receptor also in these cells.

For both cultures, the densitometric ratios of the bands for phospho-EGFR/EGFR and phospho-ERK1/2 / ERK1/2 were calculated and are plotted in the bar graph of Figure 34B. The densitometric analysis evidenced a difference between the two cell lines: compared to their respective control cultures, in lactate-exposed MDA-MB-231 cells a significantly higher phosphorylation level was observed in both EGFR and ERK1/2. On the contrary, in lactate-exposed HT-29 cells the phosphorylation of the ERK1/2 downstream kinases was not significantly increased.

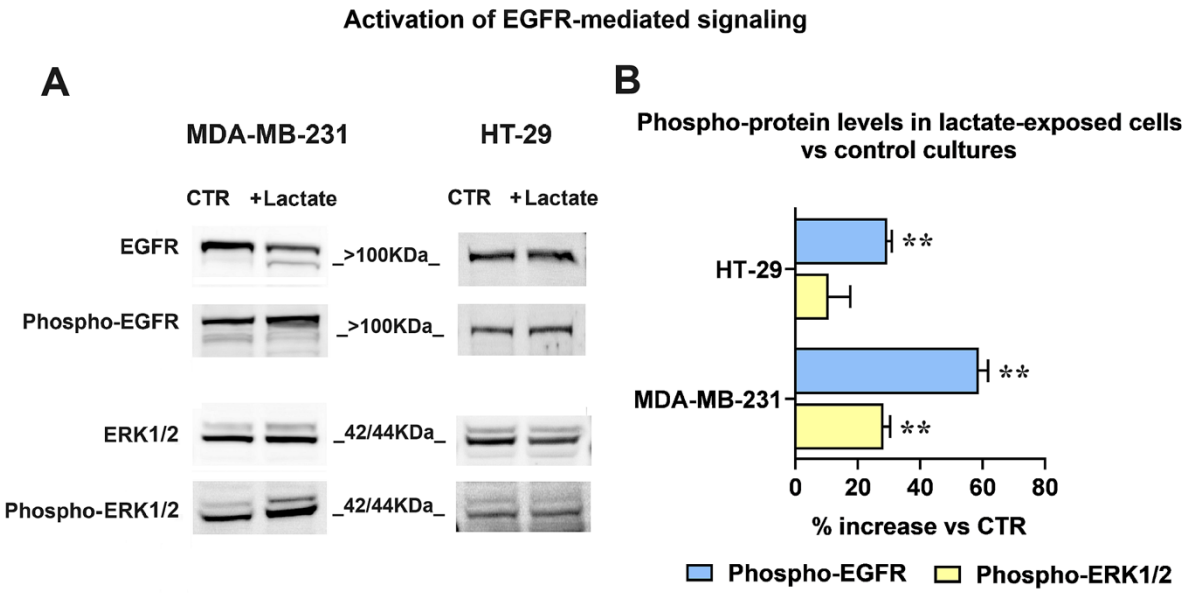

Figure 34. (A) *Immunoblotting detection of EGFR and ERK1/2 phosphorylation. The signal intensity ratios (phospho-protein / protein) were calculated and the obtained values were used to assess the %-increase in phospho-EGFR and phospho-ERK1/2 observed in lactate-exposed cells (B). For both phospho-EGFR / EGFR and phospho-ERK1/2 / ERK1/2 immunoblotting analyses, the same sample was used and was run in parallel experiments; gels and blots were processed in parallel. The data shown in* ***(B)*** *were statistically evaluated by one-sample t-tests. In both cell cultures the increased phosphorylation of EGFR reached the level of statistical significance; on the contrary, phospho-ERK1/2 was significantly increased only in MDA-MB-231 cells. **, $p < 0.01$*

Released HBEGF and the consequent EGFR pathway activation were repeatedly shown to be associated with chemoresistance[321], while EGFR inhibition showed the potential of improving the effects of chemotherapy and radiation therapy[337]. For this reason, in following experiments we evaluated the response of the control and lactate-exposed cultures to cisplatin, a chemotherapeutic agent currently used in the treatment of several neoplastic conditions[338]. In order to define the impact of uPA-induced HBEGF shedding on the antineoplastic action of cisplatin, in these experiments we also used BC11 and CRM197, a well-characterized HBEGF inhibitor[339]. Both cell lines were exposed to 50 μM cisplatin for 24 h; the obtained results are shown in Figure 35.

In MDA-MB-231 cultures (Figure 35A), CRM197 (2 μg/ml, corresponding to 32 nM) did not affect the proliferation of both control and lactate-exposed cells, and the single administration of cisplatin produced in the two cell cultures superimposable effects. When the two compounds were administered in combination, a statistically significant contribution of CRM197 in increasing the effect of cisplatin was observed only in cells maintained in Low-Glc DMEM, suggesting for this

culture higher susceptibility to EGFR pathway inhibition, with a consequently improved drug response[340].

A similar experiment was performed only on the lactate-exposed MDA-MB-231 culture to assess the effects of BC11 supplementation on the combined cisplatin/CRM197 treatment. Results are shown in Figure 35B. When administered in combination with cisplatin, 100 μM BC11 markedly increased the effect of this antineoplastic agent, causing evident cell death (a reduced cell number at 24h, compared to that measured at the beginning of treatment); this antineoplastic effect was further increased by the CRM197 co-administration. Interestingly, the experiment on lactate-exposed cells highlighted a statistically significant difference between the effect of the combination CRM197/BC11 compared to that caused by the single CRM197 treatment; this result was considered for further experiments (see following paragraphs).

Figures 35C, D show the same experiments, replicated on HT-29 cultures. In the culture maintained in Low-Glc DMEM, 50 μM cisplatin significantly impacted on cell proliferation, and a further contribution given by the CRM197 supplementation was not observed. Interestingly, cisplatin susceptibility of lactate-exposed cells appeared to be evidently reduced; this finding is in complete agreement with results obtained in Section I – preliminary data, showing that in a colon adenocarcinoma cell line lactate supplementation significantly reduced the DNA damage signatures caused by this drug. However, also in lactate-exposed HT-29 cells CRM197 supplementation did not affect the antineoplastic action of cisplatin. When the effect of BC11 was examined in lactate exposed HT-29 cells (Figure 35D), this inhibitor did not succeed in increasing cisplatin activity; an improved effect was only observed with the triple combination cisplatin/CRM197/BC11, which, however, did not reach the level of statistically significance, when compared with the single cisplatin treatment.

Taken together, the less marked effects observed in the experiments performed in HT-29 cultures can be easily explained by the lower dependence of these cells on HBEGF-mediated signalling (Figure 31D). For this reason, further studies aimed at characterizing the effect of the CRM197/BC11 combination were performed in lactate-exposed MDA-MB-231 cells; some additional data have also been obtained in the HT-29 culture.

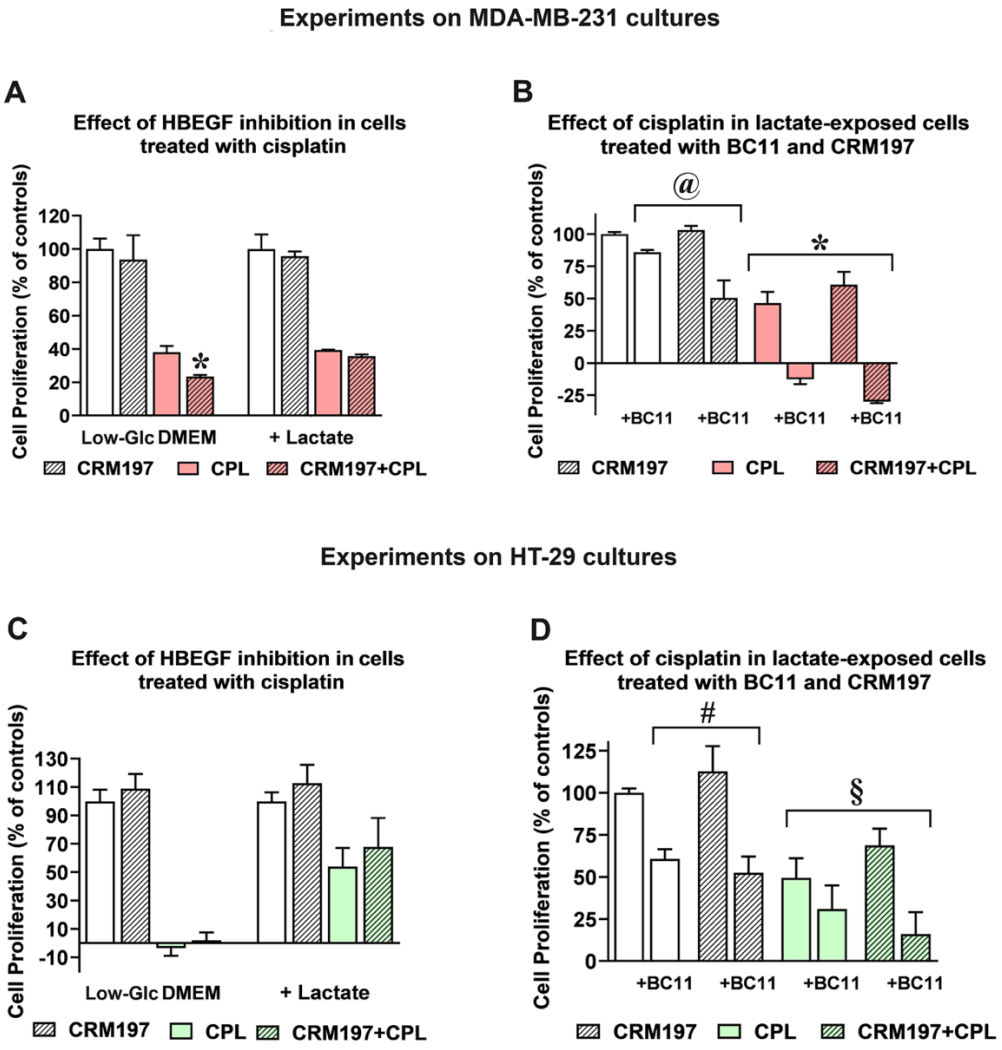

Figure 35. Effect of cisplatin (CPL) in control and lactate-exposed cultures. (A) *In MDA-MB-231 cells grown in Low-Glc DMEM, the antiproliferative effect of 50 mM CPL was increased by CRM197, given at 32 nM (* $p < 0.05$, as assessed by t-test). This effect was not observed in lactate-exposed cells.* ***(B)*** *Lactate-exposed cells were exposed to CPL to evaluate the effect of CRM197 and BC11 on the drug response. Data were analyzed by ANOVA, followed by Tukey's post-test. @: a statistically significant difference was observed between cell samples treated with BC11 and those exposed to BC11+CRM197 ($p < 0.05$). *: BC11 significantly increased the effect of CPL ($p < 0.001$).* ***(C)*** *In HT-29 cells grown in Low-Glc DMEM, the antiproliferative effect of 50 mM CPL was not modified by CRM197. Lactate-exposed cells showed a reduced response to CPL and, again, this effect was not modified by CRM197.* ***(D)*** *The experiments shown in (B) were replicated in HT-29 cultures. #: no statistically significant difference was observed between cell samples treated with BC11 and those exposed to BC11+CRM197. §: the increased antiproliferative effect observed in cell samples exposed to CPL/CRM197/BC11 did not reach the level of statistical significance, when compared to the single CPL treatment. In these experiments, no difference in the proliferation rate was observed between cells maintained in Low Glc DMEM and those cultured in Low Glc DMEM + lactate.*

6.3.3 The combined inhibition of HBEGF shedding and function shows antineoplastic potential in MDA-MB-231 cultures

Taking into account the results of Figure 35B, a further investigation on the effects of the CRM197/BC11 association was performed in lactate-exposed MDA-MB-231 cells (Figure 36). The compounds were always used at the concentrations tested in the previous experiments (32 nM CRM197 and 100 μM BC11). With the experiment of Figure 36A, we evaluated the effect of the two compounds on glycolytic metabolism, assessed by dosing the released lactate. For this experiment, cell cultures were exposed to the two compounds given individually or in association in their routinely used medium for 16 h; after this time, they were maintained in Krebs-Ringer buffer (a lactate-devoid medium allowing glycolysis) for additional 5 h, to assess the level of the released metabolite. As shown in the bar graph of Figure 36A, only the combined treatment CRM197/BC11 caused a statistically significant reduction of lactate release, suggesting impairment of glycolytic metabolism. Since activated glycolytic metabolism is needed to sustain cell proliferation and is associated with poor drug response of cancer cells[340], this effect can be hypothesized to contribute to the strongly increased cisplatin effect observed in lactate-exposed cells exposed to CRM197/BC11 (Figure 35B).

In the experiments of Figure 36B, we replicated the assay of cell proliferation by only including CRM197, BC11 and their combination. Again, the compounds' association caused a statistically significant effect when compared to both CRM197 and BC11 given as single treatments. To better evaluate the power of the CRM197/BC11 combination, we applied to the obtained results a procedure useful to assess synergism between pharmacologically active compounds[341]. According to this procedure, synergism is suggested when the estimate of combination index [cells surviving to CRM197/BC11 / (cells surviving to CRM197 × cells surviving to BC11)] returns a value < 0.8. As reported in Figure 36B, when applied to our experimental data this procedure gave a combination index = 0.46, suggesting a strong advantage given by the compounds' association.

The enhanced power of CRM197/BC11 was also confirmed by the experiments of Figure 36C, which shows EGFR activation and apoptosis, assessed by immunoblotting. Bands' densitometric evaluation is shown in the bar graph. In the untreated and in CRM197-exposed cells, the immunoblotting detection of EGFR showed again the presence of the two bands (see Figure 34) compatible with the activated receptor state, a feature which appeared to be suppressed by BC11. Accordingly, the detection of EGFR-phospho-Tyr1068 was more evidently reduced by BC11 and became barely detectable in cultures exposed to the combined treatment. An exact opposite pattern was observed for the detection of the p53-Upregulated Mediator of Apoptosis (PUMA), which was

not significantly affected by CRM197, was moderately increased by BC11 and appeared to be markedly enhanced following the CRM197/BC11 treatment.

Overall, the obtained results indicate for the CRM197/BC11 combination the potential of leading to a complete inhibition of EGFR pathway, reproducing the effects of the receptor inhibitors used in the clinical practice[211]. Therefore, our data suggest that the administration of CRM197/BC11 could not only empower the efficacy of a chemotherapeutic agent, such as cisplatin, but might also exhibit antineoplastic effects by itself.

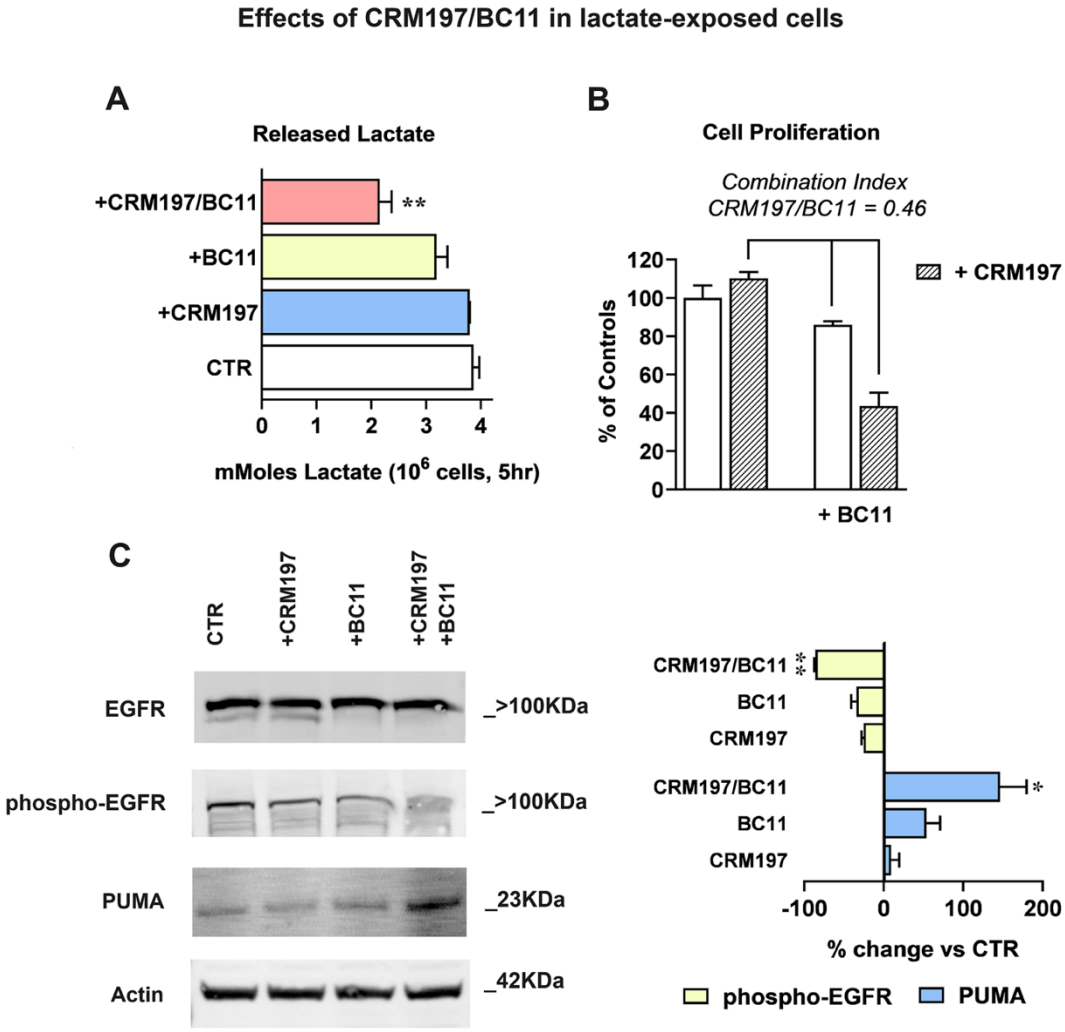

Figure 36. (A) *Glycolysis inhibition, assessed by quantifying the released lactate. Data were analysed by ANOVA followed by Dunnett's post-test; a statistically significant reduction of lactate release was observed in cell samples exposed to the combined CRM197/BC11 treatment, with $p < 0.01$.* ***(B)*** *According to the method described in* [340]*, the antiproliferative effect caused by CRM197/BC11 suggests synergism by the two compounds.* ***(C)*** *Immunoblotting evaluation of EGFR-mediated signalling shutdown and of apoptosis induction (PUMA). Phospho-EGFR band intensities were normalized on the corresponding EGFR signal; for this immunoblotting analysis the same sample was used and was run in parallel experiments; gels and blots were processed in parallel. PUMA band intensities were normalized on the corresponding Actin level. The bar graph shows the effects caused by the two compounds, given individually or in association. Data were analysed by one sample t-tests. The combination CRM197/BC11 significantly reduced phospho-EGFR, which became barely detectable, and markedly increased the level of PUMA. * and ** indicate a statistically significant difference compared to the control cultures, with $p < 0.05$ and 0.01, respectively.*

6.3.4 Effects of the CRM197/BC11 association on infiltrative growth and cell clonogenicity

The antineoplastic potential of CRM197/BC11 was finally characterized by examining the efficacy of the combined treatment in reducing the infiltrative growth and the clonogenic potential of the treated cells. Similar experiments were also performed on HT-29 cultures.

Infiltrative growth was studied by applying a wound-healing assay; the results obtained in MDA-MB-231 cultures are shown in Figure 37. Panel A shows representative pictures of the cell cultures taken at 0, 20 and 30 h after wounding.

Because of the reduced dependence on HBGF-mediated signalling shown by HT-29 cells, in this culture a similar experiment was performed by administering to control and lactate-exposed cells the single BC11 treatment, to assess whether the lactate-induced upregulation of uPA could play a role in increasing cell migration (Figure 38). Figure 38 showing the obtained results in HT-29 cells. In spite of the well-documented role of uPA in facilitating the invasive behaviour of cancer cells[326,342], no evidence of significantly increased repopulation of the wound area was observed in lactate-exposed HT-29 cells and, consequently, the administration of BC11 did not change the experimental outcomes. In our opinion, a possible explanation can be found in the compromised substrate adhesion shown by HT-29 cells when they are exposed to 20 mM lactate (see paragraph 6.2.1 of Materials and methods).

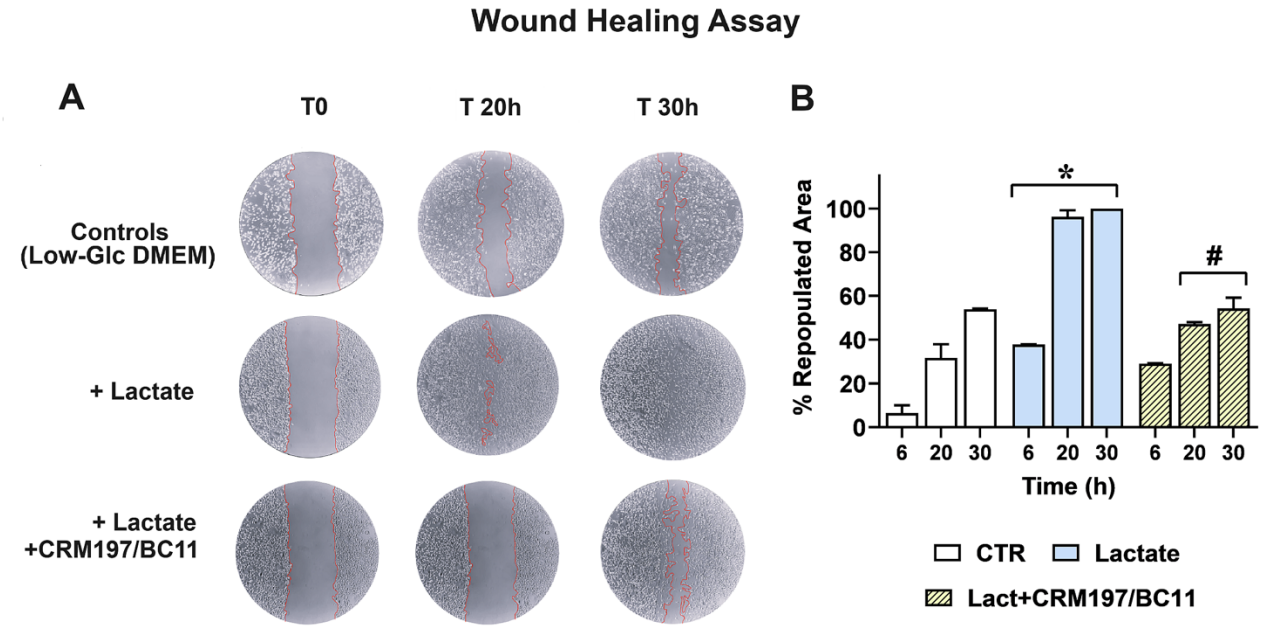

Figure 37. Would healing assay of MDA-MB-231 cells. (A) *Representative pictures of MDA-MB-231 cultures. The limits of the wound area have been outlined in red; the percentage of healed wound over time is reported in (B). Data were analysed by ANOVA followed by Tukey's post-test. *: a statistically significant difference was observed between control and lactate-exposed cultures at all the considered time intervals ($p < 0.01$). #: CRM197/BC11 significantly reduced the effects of lactate at 20 and 30 h ($p < 0.01$). Compared to the control cells maintained in Low-Glc DMEM, lactate-exposed MDA-MB-231 cells exhibited higher infiltrative growth potential, since they were able to almost completely repopulate the wound area after 20 h; this effect appeared to be inhibited by CRM197/BC11.* ***(B)*** *Shows a quantitative estimate of the repopulated area in the three cultures, which also includes the first performed evaluation (6 h). A statistically significant difference was observed between lactate-exposed cells and their parental culture maintained in Low-Glc DMEM at all the considered time intervals (6, 20 and 30 h); the effect caused by CRM197/BC11 in lactate-exposed cells reached the level of statistical significance starting from 20 h after wounding.*

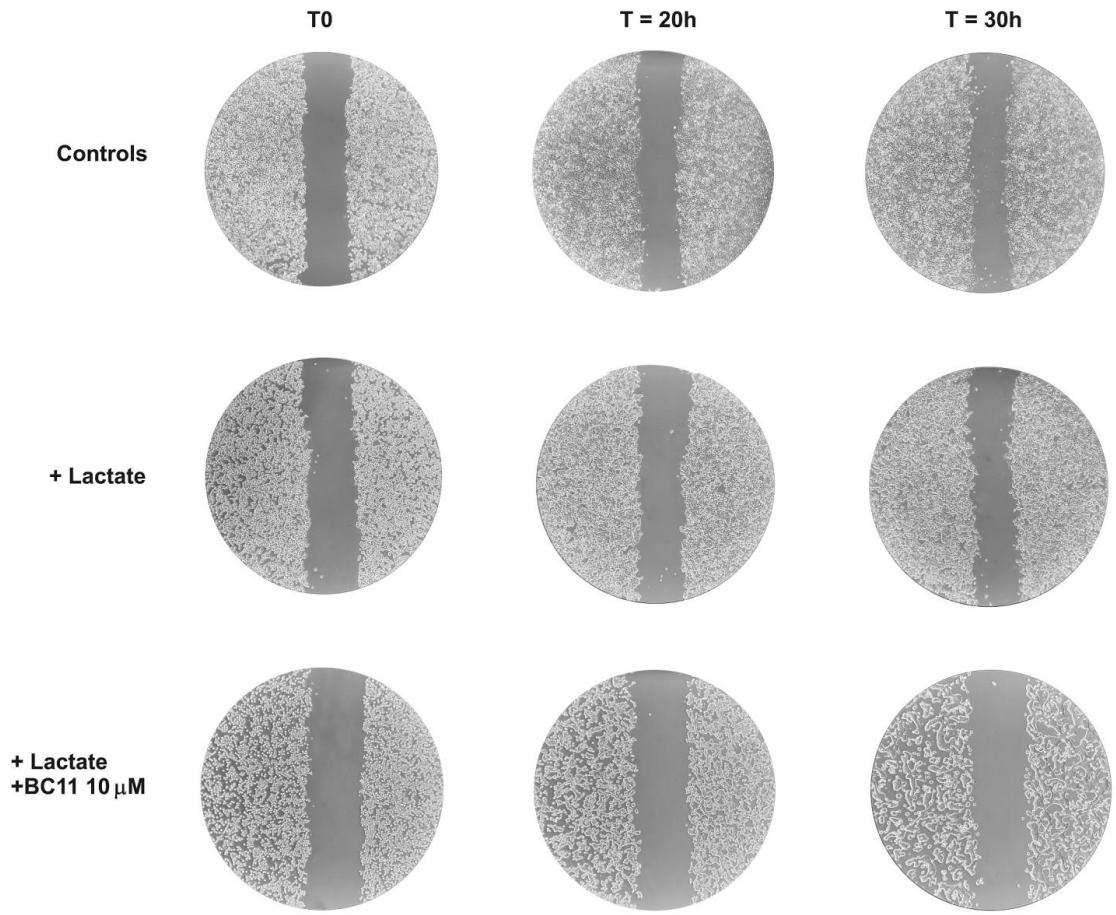

Figure 38. Would healing assay of HT-29 cells. *Representative pictures of HT-29 cultures. No evidence of significantly increased repopulation of the wound area was observed in lactate-exposed HT-29 cells.*

A conclusive experiment was aimed at evaluating the effect of CRM197/BC11 on the clonogenic potential of lactate-exposed MDA-MB-231 cells. In this long-lasting experiment, BC11 concentration was lowered to 10 μM, to reduce the toxicity risk; the obtained results are shown in Figure 39. In this culture, new colonies were clearly evident after 8 days of incubation (Figure 39A); their number and extension were evaluated by colorimetry, after CV staining (Figure 39B).

In lactate-exposed cells a statistically significant, 1.7-fold increased clonogenic power was observed, when compared to the parental culture maintained in Low-Glc DMEM. When administered as individual treatments, both CRM197 and BC11 appeared to significantly reduce the clonogenic power of lactate-exposed cells, which became similar to that observed in Low-Glc DMEM cultured

cells. A further reduction was caused by the compounds' association: this treatment appeared to decrease cell clonogenicity to a level even lower than that observed in Low-Glc DMEM cultured cells. Among all the performed experiments, the clonogenicity assay was the one requiring long-lasting treatments (8 days). This longer exposure to CRM197 and BC11 allowed us to observe changes in MDA-MB-231 cell morphology, which are disclosed in Figure 39C. Pictures of Low-Glc DMEM cultured cells and of the untreated lactate-exposed cells show the typical morphology of the MDA-MB-231 culture, mainly characterized by spindle cells but also including a subpopulation of cells with enlarged cytoplasm[343,344]. In both the shown pictures, one of these enlarged cells can be easily identified. The same pictures also show that, though maintaining the typical spindle morphology, lactate-exposed cells exhibit increased dimensions, probably as a consequence of the lactate-induced changes in gene expression.

Interestingly, treatment with CRM197 was associated with prominent changes in cell morphology, leading to the prevalence of the subpopulation characterized by the enlarged cytoplasm. According to previous studies[341], the two different morphologies of MDA-MB-231 cells are expression of cell subpopulations with different biological properties, with the spindle mesenchymal-like cells exhibiting higher activated glycolysis metabolism and metastatic potential, and the enlarged epithelial-like cells showing oxidative metabolism. Interestingly, these cell phenotypes were found to be plastically modulated by changes in cell energy metabolism[341]. Based on these observations and according to our results, it can be hypothesized that, although lacking direct antineoplastic power, CRM197 treatment could induce a mesenchymal-epithelial transition which should lead to the prevalence of cells with reduced metastatic potential. This hypothesis was confirmed by the E-cadherin (E-CAD) immunostaining shown in Figure 39C: in lactate-exposed cells, no evidence of E-CAD staining was observed, while E-CAD staining became clearly evident after the CRM197 treatment.

Figure 39C also shows that BC11 did not significantly affect MDA-MB-231 cell morphology and that the residual colonies observed following the combined CRM197/BC11 treatment appeared to be smaller and characterized by shrunk cells.

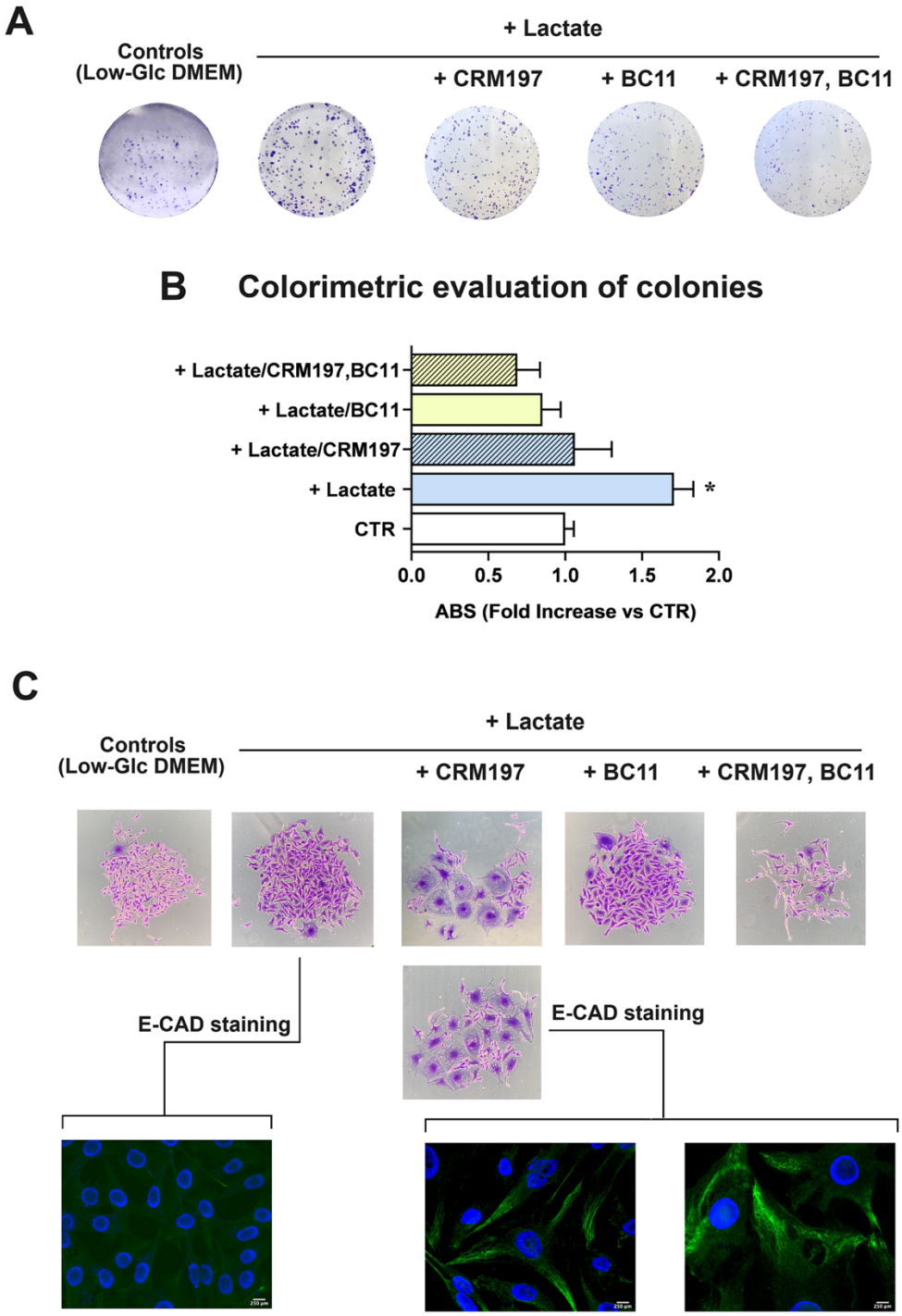

Figure 39. ***(A)*** *Representative pictures of colonies formed by MDA-MB-231 cells, stained with CV.* ***(B)*** *Colorimetric evaluation of colonies. Data were evaluated by ANOVA, followed by Tukey's post-test. *: a statistically significant difference was observed between lactate-exposed cells compared to controls and to all the applied treatments, with p values < 0.01 – 0.001.* ***(C)*** *High magnification pictures of colonies, showing the morphology changes induced by CRM197 (60x) and the immunostaining of E-cadherin (E-CAD) (600x). The green fluorescence indicative of E-CAD positive cells was clearly evident only in cells exposed to CRM197.*

The clonogenicity assay was also performed in HT-29 cultures exposed to the single BC11 treatment, given at 10 and 20 μM; in this case, evident generation of colonies required about 15 days. The obtained results have been included in Figure 40. Compared to the MDA-MB-231 culture, in lactate-exposed HT-29 cells the observed colonies showed smaller dimensions and seemed to be formed by multi-stratified cells, a pattern probably induced by the above-mentioned difficulty in substrate adhesion shown by HT-29 cells when the medium is supplemented with lactate (Figure 40A). The colorimetric detection of colonies showed a small, not statistically significant increase in lactate-exposed cells and a statistically significant reduction of the clonogenic power vs the control and vs lactate-exposed cells when BC11 was administered at 20 μM (Figure 40B).

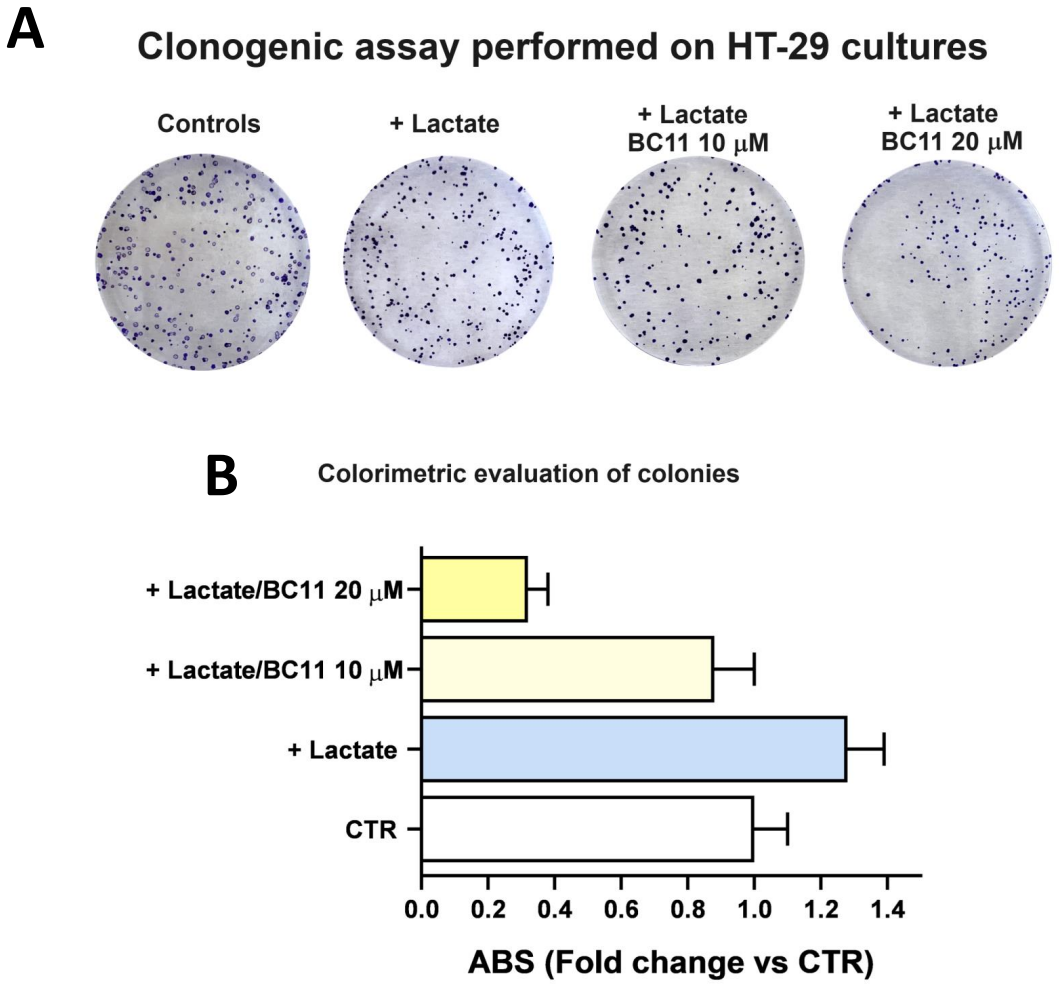

Figure 40. (A) *Representative pictures of colonies formed by HT-29 cells, stained with CV.* ***(B)*** *Colorimetric evaluation of colonies. The colorimetric detection of colonies showed a small, not statistically significant increase in lactate-exposed cells and a statistically significant reduction of the clonogenic power vs the control and vs lactate-exposed cells when BC11 was administered at 20 μM.*

6.4 Conclusion – Section IV

Because of its relevance in a large variety of neoplastic diseases, EGFR has long been considered as an attractive therapeutic target[315,345]. In cancer cells EGFR can be abnormally activated by various mechanisms: receptor overexpression, mutations, ligand-dependent receptor dimerization, ligand-independent activation. Usually, these mechanisms lead to the activation of the intracellular tyrosine kinase domain of the receptor. The consequent autophosphorylation of this domain initiates a cascade of downstream signalling pathways involved in the regulation of cellular proliferation, differentiation and survival.

In the latest decades the introduction of EGFR tyrosine kinase inhibitors produced remarkable clinical results in different cancer forms[346]. Unfortunately, most patients were found to acquire drug resistance over the years and for this reason, second and third generation inhibitors have been introduced in the clinics[347,348]. In spite of these efforts, drug resistance caused by mutations in the EGFR gene or in components of the signal transduction pathways continues to emerge and, recently, novel fourth generation inhibitors have been developed[349,350].

One of best characterized effects of EGFR-mediated signalling is the activation of glycolytic metabolism[303], leading to increased lactate production. The experiments described in this Section suggest that enhanced lactate levels can not only be the consequence of the activated EGFR-mediated signalling, but also take active part in fostering the activated receptor state, generating a vicious feedback loop.

A direct method to dampen this self-sustaining deleterious loop could be the inhibition of LDHA, with consequent block of lactate production. In several experimental settings LDHA inhibition appeared to cause inhibition of EGFR-mediated signalling[351] and, recently, it was also shown to abrogate cancer cell resistance to EGFR tyrosine kinase inhibitors[189].

Our results propose an alternative approach to inhibit EGFR-mediated signalling, which could be considered for those cancer conditions in which receptor activation is mainly triggered by HBEGF. HBEGF is initially synthesized as a transmembrane precursor protein and is then cleaved at the cell surface by the proteases of the ADAM family or by other metalloproteases.

Soluble HBEGF was found to be implicated in the proliferative potential of tumour cells, contributing to tumour aggressiveness, local invasion, metastasis and chemoresistance[321]. Its increased expression, compared to normal cells, was detected in a number of neoplastic diseases usually characterized by dismal prognosis and/or poor treatment response, such as pancreatic, liver, ovarian, gastric cancers and glioblastoma[318,352,353].

CRM197 is a nontoxic mutant of diphtheria toxin which binds to human HBEGF and hinders its mitogenic activity[339]. Since it was found to be ineffective in hindering the effects of other EGFR ligands, it is considered a specific inhibitor of HBEGF[318]. At present, CRM197 is approved for the clinical use as a carrier protein in multiple conjugate vaccines[354]. The antineoplastic activity of CRM197 was investigated in a number of studies which showed the potential of this HBEGF inhibitor mainly in increasing the activity of commonly used anticancer drugs, such as cisplatin, doxorubicin and paclitaxel, in cultured human cancer cells from different neoplastic conditions[355,356,]; in some models, reversion of drug resistance was also observed[357]. Interesting results also came from animal models[358] but, to our knowledge, clinical experience with CRM197 was not encouraging[359]. Remarkably, the difficulties in targeting the EGFR-mediated signalling in cancer have been analysed in[360].

Our data substantially confirmed the limited anticancer potential of CRM197 when administered as a single treatment (Figures 35 and 36). However, the experimental exposure to increased lactate levels, allowed us to identify the protease playing a major role in releasing HBEGF in our cell system. Our experimental results suggest that the association of CRM197 with an inhibitor of the protease primarily involved in HBEGF release is endowed with anticancer potential, since it can lead to the shutdown of EGFR-mediated signalling and apoptosis (Figure 41). In agreement with these data, it also dramatically reduced the cell clonogenic potential and infiltrative growth. Interestingly, this anticancer potential became evident without the administration of chemotherapeutic drugs. Our experiments also evidenced that a single, but sustained exposition to CRM197 can affect cell biology, inducing changes suggesting the reversion of the mesenchymal phenotype; to our knowledge, this effect was never described so far and deserves further investigation.

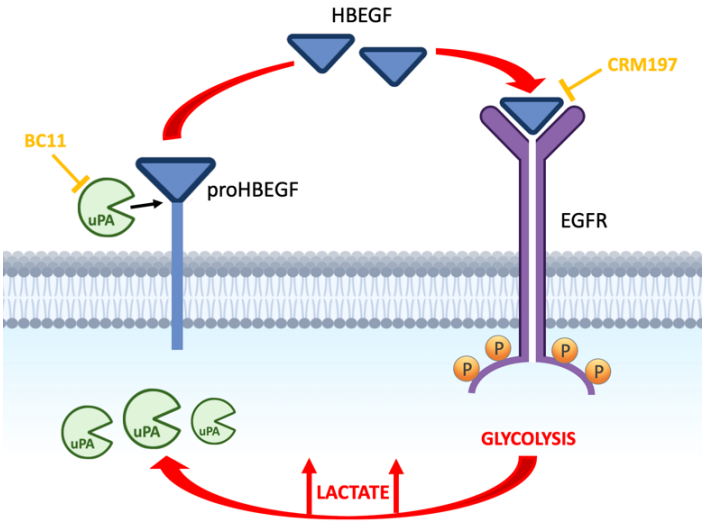

Figure 41. *Schematic representation of results described in Section IV.*

In conclusion, the observations reported in this Section show that at the level reached in the microenvironment of neoplastic tissues, lactate can induce increased levels of uPA, a protease causing HBEGF shedding and EGFR pathway activation. In different neoplastic contexts, other proteases can be involved in HBEGF shedding[361,362]. Protease inhibitors are already under consideration as possible candidates for anticancer treatment[363]; these compounds have also shown the potential of increasing the anticancer activity of chemotherapeutic drugs[364]. The observed antineoplastic effect obtained by the association of CRM197 with the uPA inhibitor suggests the possibility to dampen the EGFR-mediated signalling by adopting a tailored treatment, based on the association of CRM197 with a context-appropriate protease inhibitor. In HBEGF-dependent cancers this alternative approach could be considered to overcome the drug resistance frequently observed following the use of conventional EGFR tyrosine kinase inhibitors.

[This page is intentionally left blank]

7. SECTION V

From The Adverse Effects To a Therapeutic Opportunity

The described studies indicated that lactate can play a significant role in the development of drug resistance. A direct approach to prevent the adverse effects induced by this metabolite should be LDHA inhibition. As explained in the Introduction (paragraph 1.2.2), this enzyme isoform is commonly upregulated in cancer cells; compared to LDHB, it has higher affinity for pyruvate and preferentially converts pyruvate to lactate. During my studies I also joined a research project directed by Professor Alejandro Hochkoeppler, (FaBiT, University of Bologna) and aimed at improving the knowledge of LDHA kinetic properties. These studies also allowed the design of peptides with specific inhibition activity on LDHA. My contribution in this project was to characterize the effects of the peptide inhibitors on the lactate production in cultured cancer cells.

7.1 Introduction

Energy metabolism of cancer cells is primarily focused on glycolysis and lactate production and their intracellular pH (pHi) remains higher than that of normal cells[365]. LDHA exhibits pH sensitivity associated with post-translational modifications, for this reason, the particular phenotype of cancer cells is likely linked to the need to maintain the activity of LDHA[366]. On the contrary, in normal cells, pHi can be induced to decrease during periods of transient or prolonged hypoxia. In the case of skeletal muscle undergoing prolonged fatigue and of cancer cells often exposed to hypoxic conditions, LDHA activity is crucial for energy metabolism[366].

By utilizing human LDHA and rabbit skeletal muscle LDHA, the studies described in [367,368] demonstrate that when exposed to acidic pH, this enzyme undergoes homotropic allosteric transitions induced by pyruvate. In contrast, LDHA exhibits Michaelis-Menten kinetics at pH values of 7.0 or higher. Dynamic light scattering (DLS) experiments indicated that the presence of allosteric kinetics in LDHA corresponds to a stable dissociation of the enzyme tetramer. This suggests that pyruvate facilitates tetramer formation in acidic conditions.

I contributed to this study by performing cell-based experiments. In these experiments we also isolated cells featuring cytosolic pH equal to 7.3 or 6.5, and observed a concomitant decrease in

cytosolic pH and lactate secretion. Overall, these observations suggest negative feedback between lactic acidosis and LDHA activity.

Finally, considering that the activity of LDH is exclusively exerted by the enzyme tetrameric form, peptide inhibitors specifically perturbing the monomers-to-tetramer assembly of human LDHA were developed[369]. My task was to analyse the effects of these peptide inhibitors on cultured cancer cells expressing LDHA and/or LDHB.

7.2 Materials and methods

7.2.1 Study of LDH kinetic properties

Cell Cultures and treatments

For this study we used two cell cultures: HepG2, a human hepatoma cell line, and rabbit skeletal muscle cells (Cell Applications Inc). HepG2 were grown in DMEM, with standard supplementations. Rabbit skeletal muscle cells were grown on their growth medium were obtained from Cell Applications Inc. All the materials used for cell culture and all the reagents were obtained from Merck, unless otherwise specified. Cells were maintained at 37°C in a 5% CO_2 humidified incubator. To determinate the cytosolic pH of cells, we used the fluorescent probe BCECF (2,7-Bis-(2-carboxyethyl)-5-(6)-carboxyfluorescein, acetoxymethyl ester). Cells were washed twice with HBSS (pH 7.3), incubated with 5 μM BCECF for 30 min at room temperature under shaking, and finally washed twice with HBSS (pH 7.3). Cells were washed and incubated in HBSS medium (without bicarbonate and supplemented with HEPES and MES buffers, 10 mM each) at pH 6.5 to induce intracellular acidosis. Control samples were incubated with HBSS medium at pH 7.3. The fluorescence of BCECF was determined using a PerkinElmer (Waltham) Enspire microplate reader, exciting samples at 440 or 490 nm, and evaluating emission at 535 nm. The calibration of BCECF fluorescent response to pH was obtained by exposing cells to a medium containing 0.8 mM $MgSO_4$, 1.8 mM $CaCl_2$, 140 mM KCl, 5 mM glucose, supplemented with MES and HEPES buffers (10mM each), and conditioned at pH values ranging from 5.0 to 8.0. Nigericin (10 μM) was added to cells and they were then incubated for 10 min at room temperature under mild shaking. The fluorescence of BCECF was finally determined as describe above.

Assay of lactate levels

The concentration of lactate released by HepG2 cells and rabbit skeletal muscle cells was determined using two independent methods, relying on colorimetric or enzymatic[370] detection. Cells (5×10^5/well) were seeded in six-well plates and left to adhere overnight. After adhesion, growth medium was replaced with 1ml HBSS (at pH 6.5 or 7.3) containing 20 mM glucose and cells were allowed to equilibrate for 3 h in a 37°C incubator. Medium was then renewed and after 3 h of further incubation at 37°C, HBSS medium was collected from each well to evaluate lactate levels by using

the method described in paragraph 4.2.2 of Materials and Methods of Section II (colorimetric detection).

For the enzymatic assay appropriate volumes of samples were added to a reaction mixture containing 125 mM glycine, 40 mM hydrazine, 10 mM EDTA, 2.5 mM β-NAD+, 105 nM rabbit LDH, pH 9.0 (final concentrations). The increase in absorbance at 340 nm associated with the oxidation of lactate and the simultaneous reduction of β-NAD+ was monitored for 3h, which was found a sufficient time interval to approximate reaction equilibrium. To calculate lactate concentration in samples, a calibration curve was obtained through a series of assays performed in the presence of known concentrations of sodium lactate.

7.2.2 Study of Peptide inhibitors

Cell cultures and treatments

To assess the effectiveness of the peptides in inhibiting LDHA activity in cultured cells, we used two human cell lines: the MCF breast adenocarcinoma (which only express LDHA)[369], and the BxPC3 pancreatic ductal carcinoma (which only express LDHB)[369]. Cell cultures were grown in DMEM (MCF7) or RPMI medium (BxPC3), supplemented with 100 U/mL penicillin/streptomycin, 2 mM glutamine and 10 % (v/v) FBS. All the components of the media used for cell culture were obtained from Merck.

Colorimetric assays of lactate secretion by cultured human cells

We evaluated the ability of peptides to inhibit LDH in cultured cells by measuring the concentration of lactate released by the MCF7 and BxPC3 cell cultures. To this aim, we seeded the cells in duplicate in 24-well plates (2×10^5 cells per well) and allowed them to adhere overnight. The culture medium was then replaced by Krebs-Ringer buffer (300 µL/well). Stock solutions of peptides (8 mM in DMSO) were diluted in Krebs-Ringer buffer to achieve a final concentration of 640 µM and then combined with an equal volume of 4% (v/v, in Krebs-Ringer buffer) Lipofectamine 2000 (Invitrogen). The final solution was mixed and allowed to sit at room temperature for 25 minutes. Subsequently, 100 µl of the solution were added to each well of the plate, resulting in a final peptide concentration of 80 µM. The concentration of lactate released in the Krebs-Ringer buffer was determined after 4 hours of incubation at 37°C, using the method described in paragraph 4.2.2 of Materials and Methods of Section II.

7.3 Results and discussion

7.3.1 Cytosolic pH and LDH-A activity in vivo

In this study we found a dissociation of the LDHA tetramer caused by acidic pH conditions and it indicates that enzyme activity may significantly decline as pH decreases, particularly in environments with low pyruvate concentrations[367]. Thus, we hypothesized that this could result in a moderate production of lactate by cells whose cytosolic pH decreases from the physiological level, typically regarded as 7.2[365]. As mentioned in Materials and methods, we employed two distinct analytical methods to measure the concentration of lactate released by both human HepG2 and rabbit skeletal muscle cells, which are cell lines recognized for primarily expressing LDHA[371,368].

Initially, to assess the cytosolic pH, we quantitatively evaluated the impact of pH on the in vivo fluorescence of the probe BCECF (see paragraph 7.2.1 of Materials and methods). Subsequently, both cell lines had been cultured in their medium were transferred to HBSS medium buffered to pH 7.3 or 6.5.

Figures 42A,C show the time-course of cytosolic pH in HepG2 cells and rabbit skeletal muscle cells respectively, after transferring them to HBSS medium. Based on the observed kinetics, we chose to quantify the lactate released by cells three hours after their transfer to HBSS medium. We quantified the lactate secreted by these cells using two independent analytical methods (colorimetric and enzymatic). Interestingly, regardless of the analytical method employed, the concentration of lactate released into the external medium by cells with lower cytosolic pH was observed to decrease three-fold compared to the lactate concentration secreted by cells exposed to HBSS at pH 7.3 in both cell lines (Figure 42B,D). We interpreted this observation as the result of the in vivo dissociation of the LDHA tetramer, with the dissociated enzyme forms exhibiting low catalytic activity.

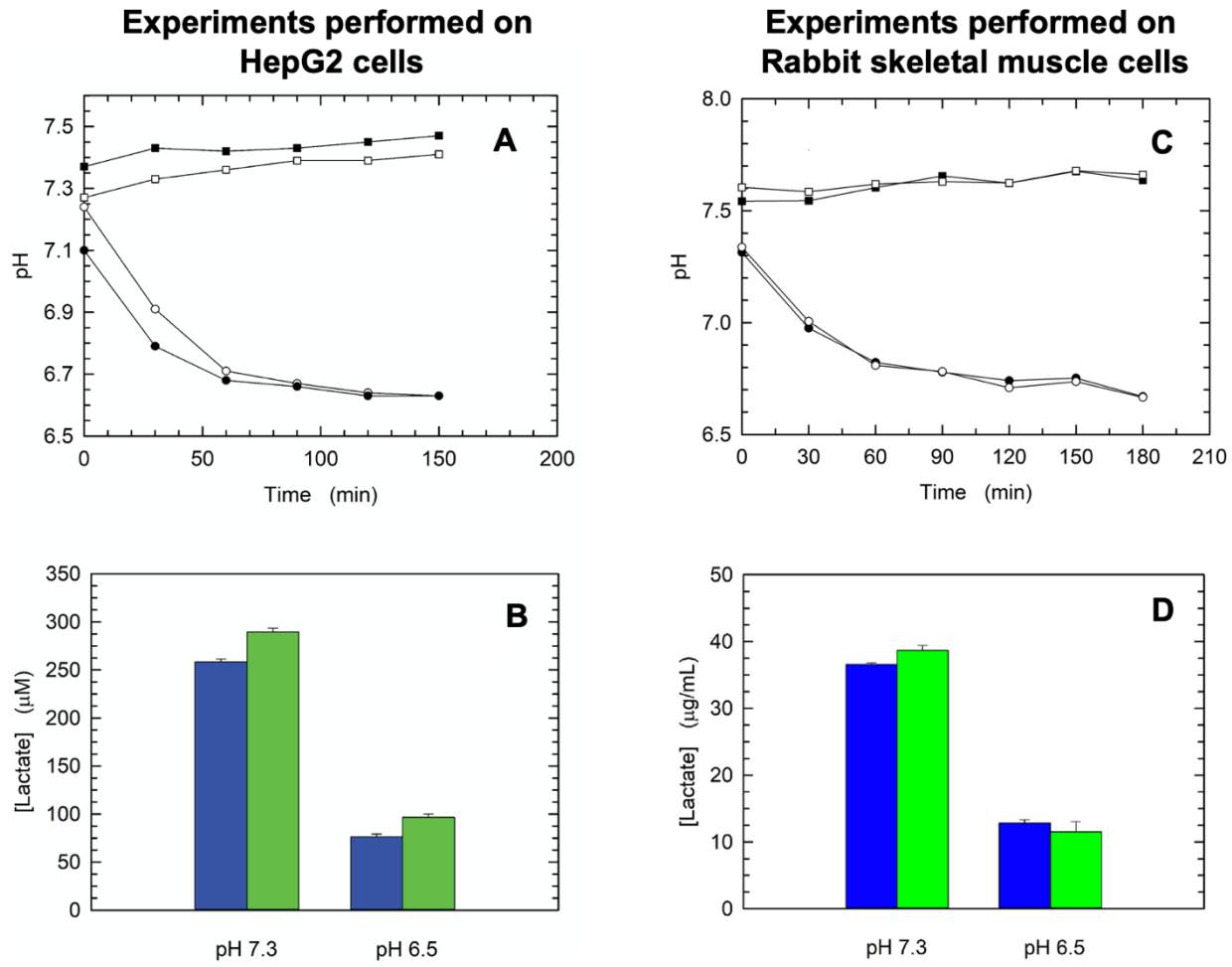

Figure 42. Cytosolic pH of HepG2 cells (left) and of rabbit skeletal muscle cells (right) and generation of lactate. ***(A-C)*** *The cytosolic pH of HepG2 cells and rabbit skeletal muscle after transferring them from HBSS medium at pH 7.3 to the same medium (squares) or to HBSS buffered at pH 6.5 (circles).* ***(B-D)*** *The concentration of lactate released by cells after a 3-hour incubation in HBSS medium at pH 7.3 or 6.5. Lactate levels was measured using a colorimetric (blue bars) and an enzymatic (green bars) analytical method, with two independent samples for each determination. Error bars indicate the standard deviation (n=2).*

7.3.2 Inhibitory action of peptides on lactate production by human cells

In preliminary studies[369] a procedure for the isolation of homogeneous human LDHA in monomeric form was developed. This finding provided a convenient and reliable tool to assay candidate inhibitors directed against the assembly of monomeric human LDHA into the corresponding, catalytically active, tetramer. As a following step, peptides potentially hindering the assembly of LDHA tetrameric form were designed[369]. My contribution in this study was to evaluate the effects of these peptides on lactate production in human cell lines. Specifically, I examined the

effects of the three most effective LDHA peptide inhibitors previously tested on the purified LDHA protein: TH1, TH2, and TH16. These peptides bind the N-terminal region of LDHA, which was found to be involved in the assembly of the enzyme tetrameric form[366].TH1 is an octapeptide showing the primary structure GQNGISDL, the sequence of which is identical to residues 296–303 of the target protein; TH2 is a cyclic tetrapeptide (c[GQN-isoD]) and TH16 is the TH2 peptide in linear form (GQND). These peptides were tested in MCF7 cells (which express only LDHA) and in BxPC3 cultures (which express only LDHB). In preliminary experiments we verified that when peptides are added in the Krebs Ringer buffer used for lactate assay, they elicited minimal and not statistically significant effects on lactate production by MCF7 cells. We hypothesized that this missing effect could be linked to the low solubility of the peptides in the used buffer and, as described in section 7.2.2, repeated the experiment by diluting them in Lipofectamine. Lactate assay was then repeated and in MCF7 cells both the linear TH16 and the cyclic TH2 tetrapeptide were found to cause a statistically significant 20% reduction of metabolite concentration in medium (Figure 43). Conversely, in BxPC3 cells (which express only LDHB) no significant difference in secreted lactate was observed in the cultures exposed to both TH16 and TH2, compared to the untreated controls (Figure 43). Surprisingly enough, the TH1 octapeptide had no significant impact on lactate secretion by MCF7 and BxPC3 cells (Figure 43), in spite of the higher power of LDHA inhibition shown on the purified protein[369]. We can hypothesize that the lack of a detectable effect in cultured cells could again be linked to poor cell penetration, not adequately improved by lipofectamine.

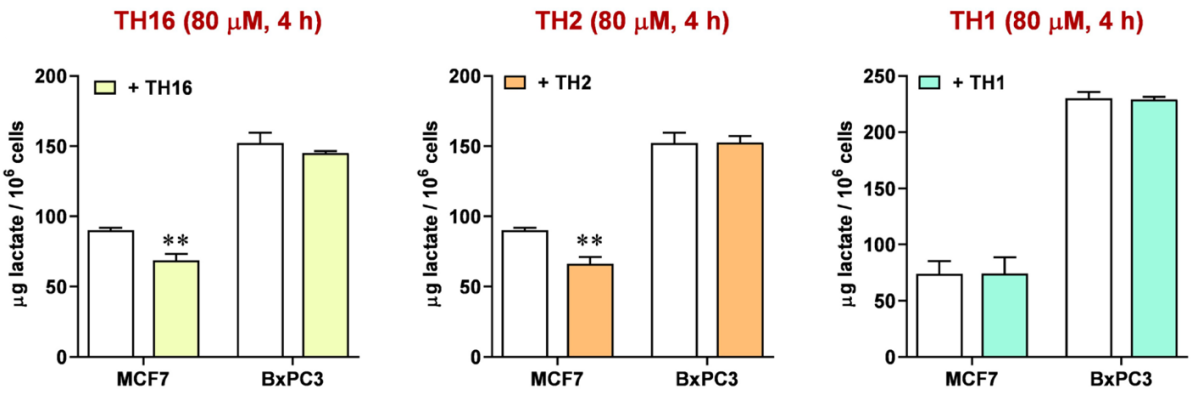

Figure 43. Effect of peptides on the secretion of lactate by human cell lines. *The quantity of lactate secreted by MCF7 and BxPC3 cells without (white bars) or with (yellow, orange and green bars) of different peptides is shown. Error bars represent SD (n = 3). The experimental observations were compared by two-way ANOVA. The ** symbol denote a p value lower than 0.01.*

Although preliminary, these experiments suggest that appropriately designed peptides can exert LDHA inhibitory activity in living cells. Considering the relevance of LDHA in cancer cell biology, we hope that the proceeding of these studies will help in identifying further peptide structures, more efficiently hampering the glycolytic metabolism of cancer cells.

[This page is intentionally left blank]

8. CONCLUSIONS

One of the characteristics that allows malignant cells to sustain tumour growth and progression is metabolic reprogramming[372]. Cancer cells exhibit increased glucose uptake from the extracellular environment[373]. As a result, a significant quantity of glucose is converted into pyruvate, which is subsequently reduced to lactate[374]. This process contributes to supporting the energy demands needed for unrestricted tumour proliferation[374]. Metabolic changes are considered an emerging hallmark of cancer cells[375], and these alterations have been leveraged for clinical applications in the diagnosis of several malignancies through positron emission tomography (PET)[376]. PET is a functional imaging technique used in nuclear medicine that exploits the atypical metabolism of glucose in cancerous cells. The procedure involves the administration of a radiotracer, commonly 2-fluoro-2-deoxy-glucose (^{18}F-FDG), a glucose analogue labelled with the ^{18}F radioisotope, able to emit positrons detectable by PET. This radioactive tracer is absorbed by human cells and then, like normal glucose, is phosphorylated by hexokinase (HK), which ensures ^{18}F-FDG cell trapping. Differently to glucose, which undertakes the glycolytic pathway, ^{18}F-FDG cannot be further metabolized as it lacks the hydroxyl group at the 2–carbon[377]. Thus, high ^{18}F-FDG signals, typical of cells showing high glucose consumption, are positively correlated with the presence of primary tumour or metastasis. In this way, it is possible to localize neoplastic lesions with extremely high precision[376].

As mentioned above, this altered metabolic pattern leads to the production of elevated levels of lactate. Once considered a metabolic waste product, lactate was recently shown to play a role in regulating gene expression and in promoting the unlimited growth of cancer cells[45]. Initially, it was demonstrated that lactate influences gene expression by inhibiting histone deacetylases[14]; more recently it was shown that lactate promotes an open chromatin structure through a histone modification process called lactylation[142]. This modification enhances the access of transcription complexes to DNA. Consequently, lactate can function as a sensor able to transduce metabolic changes into stable gene expression patterns.

As well known, an energy metabolism based on activated glycolysis with consequent increased lactate production also characterizes embryonic tissues. By increasing histone lactylation, high levels of lactate might contribute to changes in gene expression, supporting proliferation and safeguarding DNA integrity[182]. These lactate-induced effects are coherent with the role of glycolytic metabolism in supporting embryonic tissues' development.

The described research project was aimed at characterizing the effects of lactate signalling in cancer cells, with particular attention to the potential role of this metabolite in modifying the response

of cancer cells to chemotherapeutic treatments and in promoting the onset of drug resistance. The experiments described in this thesis have elucidated that lactate can induce drug resistance through pathways that may differ according to the cell types.

The preliminary experiments described in Section I showed for the first time a direct effect of lactate on the expression of genes required for mismatch and nucleotide excision DNA repair, which appeared to compromise the antineoplastic efficacy of cisplatin. The reduced response to cisplatin caused by lactate was associated with decreased signatures of DNA damage and upregulated expression of repair pathways' genes usually involved in the management of DNA alterations caused by this drug.

Following the results obtained with this preliminary study, we evaluated the effects of lactate on the antineoplastic action of DOXO in breast cancer cells. DOXO is a member of the anthracyclines class and is the first-choice therapy for a variety of solid malignancies. In this context, by using DOXO, we found that increased lactate levels did not affect TOP2A poisoning, the main antineoplastic mechanism of the drug. Interestingly, this metabolite significantly reduced drug-induced oxidative damage. Oxidative damage is not considered relevant to the antineoplastic action of DOXO, but it appears to play a major role in the cardiac toxicity caused by this drug. These findings suggest that a short-term exposure to lactate prior to DOXO treatment might help in reducing the oxidative damage in cardiomyocytes without compromising the antineoplastic efficacy of chemotherapeutics in cancer cells.

In ER+ breast cancer cells (MCF7 culture), we further investigated the potential role of lactate in promoting resistance to TAM. TAM is a widely used oestrogen receptor inhibitor, whose clinical success is limited by the development of acquired resistance. Interestingly, this compound was found to inhibit mitochondrial function probably at the level of complex I, and the administration of TAM is associated with an increase in lactate production. In this model, we observed that elevated lactate levels can reduce the efficacy of TAM, promoting drug resistance. This effect was found to be linked to the induction of an enhanced proliferative potential of breast cancer cells caused by TAZ, TERC and TERT upregulation. TAZ overexpression was also found to activate the EGFR pathway, leading to increased LDHA expression/activity.

EGFR hyperactivation can play a crucial role in the neoplastic change process and in conferring survival advantages to cancer cells. In patients with multiple cancer forms, elevated activation of EGFR pathway revealed to be a strong prognostic feature[310]. In the concluding phase of this project, we assessed the potential role of lactate in promoting the activation of EGFR pathway. Through these experiments, we observed that increased lactate levels can induce EGFR activation by stimulating HBEGF shedding, an EGF-like peptide with potent mitogenic activity[319]. This effect was found to be

linked to the lactate-induced release of uPA, a protease promoting HBEGF shedding. We observed that the administration of CRM197 (a specific HBEGF inhibitor) in association with a uPA inhibitor caused dampening of EGFR-mediated signalling and apoptosis induction. Overall, this study highlighted that the increased lactate production can foster the activated state of EGFR receptor and suggested that in cancer cells expressing HBEGF, the inhibition of EGFR-mediated signalling can be attempted by means of CRM197 administered with an appropriate protease inhibitor.

This project allowed us to identify various effects linked to lactate signalling in cancer cells. An intriguing mechanism revealed by our studies is that, at the level reached in the microenvironment of neoplastic tissues, lactate can induce self-sustaining deleterious loops, favouring tumour growth. For example, by activating EGFR pathway, lactate leads to an increase of LDHA expression and activity, resulting in elevated glycolytic metabolism, with further increased lactate production. This phenomenon can fire up an important self-feeding loop where lactate can promote epigenetic changes ultimately resulting in the amplification of its generation. This mechanism can contribute to reduce the efficacy of chemotherapeutic drugs, leading to therapeutic failure.

In accordance with these findings, it would be essential to inhibit the production of lactate in order to disrupt the self-feeding loops that contribute to drug resistance. Additionally, hindering glycolytic metabolism in cancer cells is a crucial strategy in cancer therapy, aimed at improving patient outcomes.

To directly inhibit lactate production, numerous molecules have been developed that target the enzyme responsible for its synthesis: LDH. Hindering the glycolytic metabolism of cancer cells via LDH inhibition was found to overcome the resistance to chemotherapeutic agents[195]. In spite of extensive research aimed at identifying LDH inhibitors, none of these molecules was approved for clinical use in cancer patients[196]. Some years ago, an inhibitor potentially active in *vivo* was identified[75]. Although active, this compound showed no specificity for LDHA and, for this reason, exhibited toxic effects potentially limiting its therapeutic window. The administration of this compound in mice was found to cause haemolysis, presumably associated with the inhibition of LDHB in red blood cells[75]. It can be hypothesized that this side effect could be mitigated through the development of drugs that specifically target and inhibit LDHA. Based on these evidences, and considering that LDHA is the major enzyme isoform in cancer cells, there is a necessity to develop new small-molecule LDHA inhibitors that exhibit enhanced selectivity for cancer cells[58].

While waiting the development of these inhibitors, an alternative approach to inhibit glycolytic metabolism could be the use of EGFR inhibitors. The introduction of EGFR tyrosine kinase inhibitors in clinics has produced significant results in various cancer types[346]. While these drugs demonstrated significant effectiveness in cancer treatment, mutations in the EGFR gene or in components of the

signal transduction pathways have become a major obstacle for their efficacy[346]. For these reasons, most patients were found to acquire drug resistance over the years, leading to the recent introduction of fourth generation inhibitors.

Another important strategy to inhibit glycolytic metabolism and hamper the progression of cancer cells could be the administration of PI3K pathway inhibitors[186]. The PI3K pathway plays a pivotal role in the regulation of cell survival, growth, proliferation, and metabolism. Aberrant activation of this pathway is a hallmark of many cancers and contributes to tumorigenesis and metastasis[183]. In the last twenty years, there has been a significant increase in the number of PI3K inhibitors explored in preclinical studies, with different compounds advancing to clinical trials as new anticancer drugs[185]. However, their considerable toxicity and insufficient selectivity have hindered their use and approval in clinical settings. Adverse events associated with these inhibitors, including hyperglycaemia, pneumonitis, stomatitis, rashes, and diarrhoea, were found to significantly affect patients' quality of life, resulting in a high rate of treatment discontinuation[185].

The final part of my thesis describes experiments aimed at studying the efficacy of peptides that selectively target and inhibit LDHA. These peptides were developed thanks to the collaboration with Professor Alejandro Hochkoeppler, (FaBiT, University of Bologna) and Professor Luca Gentilucci, (CHIM, University of Bologna). I contributed to this study by performing the cell-based experiments. The identified inhibitory peptides proved to be selective for LDHA and effective in reducing lactate production of cultures cancer cells, but showed reduced potency. Experiments are is still ongoing; further studies are aimed at improving the efficacy of the peptide inhibitors and their delivery to cancer cells.

[This page is intentionally left blank]

9. BIBLIOGRAPHY

1. Papadaki S, Magklara A. Regulation of Metabolic Plasticity in Cancer Stem Cells and Implications in Cancer Therapy. Cancers 2022; doi: 10.3390/cancers14235912.

2. Akram M. Mini-review on Glycolysis and Cancer. J Canc Educ 2013;28(3):454–457; doi: 10.1007/s13187-013-0486-9.

3. Chaudhry R, Varacallo M. Biochemistry, Glycolysis. In: StatPearls StatPearls Publishing: Treasure Island (FL); 2023.

4. Granchi C, Bertini S, Macchia M, et al. Inhibitors of Lactate Dehydrogenase Isoforms and their Therapeutic Potentials. Current Medicinal Chemistry n.d. 2010; doi: 10.2174/092986710790416263

5. Dai X, Wei W. Lactate fuels mitosis. Molecular Cell 2023; doi: 10.1016/j.molcel.2023.04.013.

6. Desbats MA, Giacomini I, Prayer-Galetti T, et al. Metabolic Plasticity in Chemotherapy Resistance. Front Oncol 2020; doi: 10.3389/fonc.2020.00281.

7. Kes MMG, Van den Bossche J, Griffioen AW, et al. Oncometabolites lactate and succinate drive pro-angiogenic macrophage response in tumors. Biochim Biophys Acta Rev Cancer 2020; doi: 10.1016/j.bbcan.2020.188427.

8. Ma L-N, Huang X-B, Muyayalo KP, et al. Lactic Acid: A Novel Signaling Molecule in Early Pregnancy? Front Immunol 2020; doi: 10.3389/fimmu.2020.00279.

9. de la Cruz-López KG, Castro-Muñoz LJ, Reyes-Hernández DO, et al. Lactate in the Regulation of Tumor Microenvironment and Therapeutic Approaches. Front Oncol 2019; doi: 10.3389/fonc.2019.01143.

10. Barba I, Carrillo-Bosch L, Seoane J. Targeting the Warburg Effect in Cancer: Where Do We Stand? Int J Mol Sci 2024; doi: 10.3390/ijms25063142.

11. Menchikov LG, Shestov AA, Popov AV. Warburg Effect Revisited: Embodiment of Classical Biochemistry and Organic Chemistry. Current State and Prospects. Biochemistry Moscow 2023; doi: 10.1134/S0006297923140018.

12. Kocianova E, Piatrikova V, Golias T. Revisiting the Warburg Effect with Focus on Lactate. Cancers 2022; doi: 10.3390/cancers14246028.

13. Weinhouse S. On Respiratory Impairment in Cancer Cells. Science 1956; doi: 10.1126/science.124.3215.267.

14. Latham T, Mackay L, Sproul D, et al. Lactate, a product of glycolytic metabolism, inhibits histone deacetylase activity and promotes changes in gene expression. Nucleic Acids Research 2012; doi: 10.1093/nar/gks066.

15. Hammad N, Rosas-Lemus M, Uribe-Carvajal S, et al. The Crabtree and Warburg effects: Do metabolite-induced regulations participate in their induction? Biochimica et Biophysica Acta (BBA) - Bioenergetics 2016; doi: 10.1016/j.bbabio.2016.03.034.

16. Cai M, Wan J, Cai K, et al. Understanding the Contribution of Lactate Metabolism in Cancer Progress: A Perspective from Isomers. Cancers 2022; doi: 10.3390/cancers15010087.

17. Koppenol WH, Bounds PL, Dang CV. Otto Warburg's contributions to current concepts of cancer metabolism. Nat Rev Cancer 2011; doi: 10.1038/nrc3038.

18. Jia D, Park JH, Jung KH, et al. Elucidating the Metabolic Plasticity of Cancer: Mitochondrial Reprogramming and Hybrid Metabolic States. Cells 2018; doi: 10.3390/cells7030021.

19. Mathupala SP, Ko YH, Pedersen PL. The Pivotal Roles of Mitochondria in Cancer: Warburg and Beyond and Encouraging Prospects for Effective Therapies. Biochim Biophys Acta 2010; doi: 10.1016/j.bbabio.2010.03.025.

20. Vander Heiden MG, Cantley LC, Thompson CB. Understanding the Warburg Effect: The Metabolic Requirements of Cell Proliferation. Science 2009; doi: 10.1126/science.1160809.

21. Liberti MV, Locasale JW. The Warburg Effect: How Does it Benefit Cancer Cells? Trends Biochem Sci 2016; doi: 10.1016/j.tibs.2015.12.001.

22. DeBerardinis RJ, Lum JJ, Hatzivassiliou G, et al. The biology of cancer: metabolic reprogramming fuels cell growth and proliferation. Cell Metab 2008; doi: 10.1016/j.cmet.2007.10.002.

23. Gillies RJ, Robey I, Gatenby RA. Causes and consequences of increased glucose metabolism of cancers. J Nucl Med 2008; doi: 10.2967/jnumed.107.047258.

24. Wu Y, Ma W, Liu W, et al. Lactate: a pearl dropped in the ocean—an overlooked signal molecule in physiology and pathology. Cell Biology International 2023; doi: 10.1002/cbin.11975.

25. Zhang Y, Song H, Li M, et al. Histone lactylation bridges metabolic reprogramming and epigenetic rewiring in driving carcinogenesis: Oncometabolite fuels oncogenic transcription. Clin Transl Med 2024; doi: 10.1002/ctm2.1614.

26. Poole DC, Rossiter HB, Brooks GA, et al. The anaerobic threshold: 50+ years of controversy. The Journal of Physiology 2021; doi: 10.1113/JP279963.

27. Haas R, Smith J, Rocher-Ros V, et al. Lactate Regulates Metabolic and Pro-inflammatory Circuits in Control of T Cell Migration and Effector Functions. PLoS Biol 2015; doi: 10.1371/journal.pbio.1002202.

28. Manosalva C, Quiroga J, Hidalgo AI, et al. Role of Lactate in Inflammatory Processes: Friend or Foe. Front Immunol 2021; doi: 10.3389/fimmu.2021.808799.

29. Levitt MD, Levitt DG. Quantitative Evaluation of D-Lactate Pathophysiology: New Insights into the Mechanisms Involved and the Many Areas in Need of Further Investigation. Clin Exp

Gastroenterol 2020; doi: 10.2147/CEG.S260600.

30. Hasegawa H, Fukushima T, Lee J-A, et al. Determination of serum d-lactic and l-lactic acids in normal subjects and diabetic patients by column-switching HPLC with pre-column fluorescence derivatization. Anal Bioanal Chem 2003; doi: 10.1007/s00216-003-2108-6.

31. Rossi V, Govoni M, Di Stefano G. Lactate Can Modulate the Antineoplastic Effects of Doxorubicin and Relieve the Drug's Oxidative Damage on Cardiomyocytes. Cancers (Basel) 2023; doi: 10.3390/cancers15143728.

32. Sun S, Li H, Chen J, et al. Lactic Acid: No Longer an Inert and End-Product of Glycolysis. Physiology 2017; doi: 10.1152/physiol.00016.2017.

33. Rabinowitz JD, Enerbäck S. Lactate: the ugly duckling of energy metabolism. Nat Metab 2020; doi: 10.1038/s42255-020-0243-4.

34. Vernon C, LeTourneau JL. Lactic Acidosis: Recognition, Kinetics, and Associated Prognosis. Critical Care Clinics 2010; doi: 10.1016/j.ccc.2009.12.007.

35. Kane DA. Lactate oxidation at the mitochondria: a lactate-malate-aspartate shuttle at work. Front Neurosci 2014; doi: 10.3389/fnins.2014.00366.

36. Lin Y, Wang Y, Li P. Mutual regulation of lactate dehydrogenase and redox robustness. Front Physiol 2022; doi: 10.3389/fphys.2022.1038421.

37. Cruzat V, Macedo Rogero M, Noel Keane K, et al. Glutamine: Metabolism and Immune Function, Supplementation and Clinical Translation. Nutrients 2018; doi: 10.3390/nu10111564.

38. DeBerardinis RJ, Mancuso A, Daikhin E, et al. Beyond aerobic glycolysis: Transformed cells can engage in glutamine metabolism that exceeds the requirement for protein and nucleotide synthesis. Proc Natl Acad Sci U S A 2007; doi: 10.1073/pnas.0709747104.

39. Anderson NM, Mucka P, Kern JG, et al. The emerging role and targetability of the TCA cycle in cancer metabolism. Protein Cell 2018; doi: 10.1007/s13238-017-0451-1.

40. Bennis Y, Bodeau S, Batteux B, et al. A Study of Associations Between Plasma Metformin Concentration, Lactic Acidosis, and Mortality in an Emergency Hospitalization Context. Crit Care Med 2020; doi: 10.1097/CCM.0000000000004589.

41. Jha MK, Lee I-K, Suk K. Metabolic reprogramming by the pyruvate dehydrogenase kinase-lactic acid axis: Linking metabolism and diverse neuropathophysiologies. Neurosci Biobehav Rev 2016; doi: 10.1016/j.neubiorev.2016.05.006.

42. Luengo A, Li Z, Gui DY, et al. Increased demand for NAD+ relative to ATP drives aerobic glycolysis. Mol Cell 2021; doi: 10.1016/j.molcel.2020.12.012.

43. Li X, Yang Y, Zhang B, et al. Lactate metabolism in human health and disease. Signal Transduct Target Ther 2022; doi: 10.1038/s41392-022-01151-3.

44. Ippolito L, Morandi A, Giannoni E, et al. Lactate: A Metabolic Driver in the Tumour Landscape. Trends in Biochemical Sciences 2019; doi: 10.1016/j.tibs.2018.10.011.

45. Baltazar F, Afonso J, Costa M, et al. Lactate Beyond a Waste Metabolite: Metabolic Affairs and Signaling in Malignancy. Front Oncol 2020; doi: 10.3389/fonc.2020.00231.

46. Feng Y, Xiong Y, Qiao T, et al. Lactate dehydrogenase A: A key player in carcinogenesis and potential target in cancer therapy. Cancer Med 2018; doi: 10.1002/cam4.1820.

47. Blanco A, Zinkham WH. Lactate Dehydrogenases in Human Testes. Science 1963; doi: 10.1126/science.139.3555.601.

48. Woodford MR, Chen VZ, Backe SJ, et al. Structural and functional regulation of lactate dehydrogenase-A in cancer. Future Med Chem 2020; doi: 10.4155/fmc-2019-0287.

49. Adeva-Andany M, López-Ojén M, Funcasta-Calderón R, et al. Comprehensive review on lactate metabolism in human health. Mitochondrion 2014; doi: 10.1016/j.mito.2014.05.007.

50. Liang X, Liu L, Fu T, et al. Exercise Inducible Lactate Dehydrogenase B Regulates Mitochondrial Function in Skeletal Muscle. J Biol Chem 2016; doi: 10.1074/jbc.M116.749424.

51. Dawson DM, Goodfriend TL, Kaplan NO. Lactic dehydrogenases: functions of the two types rates of synthesis of the two major forms can be correlated with metabolic differentiation. Science 1964; doi: 10.1126/science.143.3609.929.

52. Castonguay Z, Auger C, Thomas SC, et al. Nuclear lactate dehydrogenase modulates histone modification in human hepatocytes. Biochemical and Biophysical Research Communications 2014; doi: 10.1016/j.bbrc.2014.10.071.

53. Miao P, Sheng S, Sun X, et al. Lactate dehydrogenase a in cancer: A promising target for diagnosis and therapy. IUBMB Life 2013; doi: 10.1002/iub.1216.

54. Khajah MA, Khushaish S, Luqmani YA. The effect of lactate dehydrogenase inhibitors on proliferation, motility and invasion of breast cancer cells *in vitro* highlights a new role for lactate. Molecular Medicine Reports 2024; doi: 10.3892/mmr.2023.13135.

55. Chen L, Xing X, Zhu Y, et al. Palmitoylation alters LDHA activity and pancreatic cancer response to chemotherapy. Cancer Lett 2024; doi: 10.1016/j.canlet.2024.216696.

56. Sheng SL, Liu JJ, Dai YH, et al. Knockdown of lactate dehydrogenase A suppresses tumor growth and metastasis of human hepatocellular carcinoma. The FEBS Journal 2012; doi: 10.1111/j.1742-4658.2012.08748.x.

57. Bok R, Lee J, Sriram R, et al. The Role of Lactate Metabolism in Prostate Cancer Progression and Metastases Revealed by Dual-Agent Hyperpolarized 13C MRSI. Cancers (Basel) 2019; doi: 10.3390/cancers11020257.

58. Sharma D, Singh M, Rani R. Role of LDH in tumor glycolysis: Regulation of LDHA by small molecules for cancer therapeutics. Seminars in Cancer Biology 2022; doi:

10.1016/j.semcancer.2022.11.007.

59. Liu C, Jin Y, Fan Z. The Mechanism of Warburg Effect-Induced Chemoresistance in Cancer. Front Oncol 2021; doi: 10.3389/fonc.2021.698023.

60. Zhao Y, Liu H, Liu Z, et al. Overcoming Trastuzumab Resistance in Breast Cancer by Targeting Dysregulated Glucose Metabolism. Cancer Research 2011; doi: 10.1158/0008-5472.CAN-11-0127.

61. Balboni A, Govoni M, Rossi V, et al. Lactate dehydrogenase inhibition affects homologous recombination repair independently of cell metabolic asset; implications for anticancer treatment. Biochimica et Biophysica Acta (BBA) - General Subjects 2021; doi: 10.1016/j.bbagen.2020.129760.

62. Ye Y, Chen M, Chen X, et al. Clinical Significance and Prognostic Value of Lactate Dehydrogenase Expression in Cervical Cancer. Genetic Testing and Molecular Biomarkers 2022; doi: 10.1089/gtmb.2021.0006.

63. Jin L, Chun J, Pan C, et al. Phosphorylation-mediated activation of LDHA promotes cancer cell invasion and tumour metastasis. Oncogene 2017; doi: 10.1038/onc.2017.6.

64. Xing B-C, Wang C, Ji F-J, et al. Synergistically suppressive effects on colorectal cancer cells by combination of mTOR inhibitor and glycolysis inhibitor, Oxamate. Int J Clin Exp Pathol 2018; doi: 11(9):4439–4445.

65. Altinoz MA, Ozpinar A. Oxamate targeting aggressive cancers with special emphasis to brain tumors. Biomedicine & Pharmacotherapy 2022; doi: 10.1016/j.biopha.2022.112686.

66. Valvona CJ, Fillmore HL. Oxamate, but Not Selective Targeting of LDH-A, Inhibits Medulloblastoma Cell Glycolysis, Growth and Motility. Brain Sci 2018; doi: 10.3390/brainsci8040056.

67. Koukourakis M, Tsolou A, Pouliliou S, et al. Blocking LDHA glycolytic pathway sensitizes glioblastoma cells to radiation and temozolomide. Biochem Biophys Res Commun 2017; doi: 10.1016/j.bbrc.2017.07.138.

68. An J, Zhang Y, He J, et al. Lactate dehydrogenase A promotes the invasion and proliferation of pituitary adenoma. Sci Rep 2017; doi: 10.1038/s41598-017-04366-5.

69. El-Sisi AE, Sokar SS, Abu-Risha SE, et al. Oxamate potentiates taxol chemotherapeutic efficacy in experimentally-induced solid ehrlich carcinoma (SEC) in mice. Biomedicine & Pharmacotherapy 2017; doi: 10.1016/j.biopha.2017.09.090.

70. Judge JL, Lacy SH, Ku W-Y, et al. The Lactate Dehydrogenase Inhibitor Gossypol Inhibits Radiation-Induced Pulmonary Fibrosis. Radiat Res 2017; doi: 10.1667/RR14620.1.

71. Rellinger EJ, Craig BT, Alvarez AL, et al. FX11 inhibits aerobic glycolysis and groth of neuroblastoma cells. Surgery 2017; doi: 10.1016/j.surg.2016.09.009.

72. Billiard J, Dennison JB, Briand J, et al. Quinoline 3-sulfonamides inhibit lactate

dehydrogenase A and reverse aerobic glycolysis in cancer cells. Cancer Metab 2013; doi: 10.1186/2049-3002-1-19.

73. Fiume L, Vettraino M, Carnicelli D, et al. Galloflavin prevents the binding of lactate dehydrogenase A to single stranded DNA and inhibits RNA synthesis in cultured cells. Biochem Biophys Res Commun 2013; doi: 10.1016/j.bbrc.2012.12.013.

74. Oshima N, Ishida R, Kishimoto S, et al. Dynamic Imaging of LDH Inhibition in Tumors Reveals Rapid In Vivo Metabolic Rewiring and Vulnerability to Combination Therapy. Cell Rep 2020; doi: 10.1016/j.celrep.2020.01.039.

75. Yeung C, Gibson AE, Issaq SH, et al. Targeting Glycolysis through Inhibition of Lactate Dehydrogenase Impairs Tumor Growth in Preclinical Models of Ewing Sarcoma. Cancer Res 2019; doi: 10.1158/0008-5472.CAN-19-0217.

76. Hu L, Huang S, Chen G, et al. Nanodrugs Incorporating LDHA siRNA Inhibit M2-like Polarization of TAMs and Amplify Autophagy to Assist Oxaliplatin Chemotherapy against Colorectal Cancer. ACS Appl Mater Interfaces 2022; doi: 10.1021/acsami.2c05841.

77. Lin J, Liu G, Chen L, et al. Targeting lactate-related cell cycle activities for cancer therapy. Semin Cancer Biol 2022; doi: 10.1016/j.semcancer.2022.10.009.

78. Merezhinskaya N, Fishbein WN. Monocarboxylate transporters: past, present, and future. Histol Histopathol 2009; doi: 10.14670/HH-24.243.

79. Halestrap AP, Price NT. The proton-linked monocarboxylate transporter (MCT) family: structure, function and regulation. Biochem J 1999; doi: 343(Pt 2):281–299.

80. Halestrap AP, Meredith D. The SLC16 gene family-from monocarboxylate transporters (MCTs) to aromatic amino acid transporters and beyond. Pflugers Arch - Eur J Physiol 2004; doi: 10.1007/s00424-003-1067-2.

81. Liu X, Zhang Y, Li W, et al. Lactylation, an emerging hallmark of metabolic reprogramming: Current progress and open challenges. Front Cell Dev Biol 2022; doi: 10.3389/fcell.2022.972020.

82. Li Z, Wang Q, Huang X, et al. Lactate in the tumor microenvironment: A rising star for targeted tumor therapy. Front Nutr 2023; doi: 10.3389/fnut.2023.1113739.

83. Chambers AF, Matrisian LM. Changing Views of the Role of Matrix Metalloproteinases in Metastasis. JNCI: Journal of the National Cancer Institute 1997; doi: 10.1093/jnci/89.17.1260.

84. Cui N, Hu M, Khalil RA. Biochemical and Biological Attributes of Matrix Metalloproteinases. Prog Mol Biol Transl Sci 2017; doi: 10.1016/bs.pmbts.2017.02.005.

85. Arpino V, Brock M, Gill SE. The role of TIMPs in regulation of extracellular matrix proteolysis. Matrix Biol 2015; doi: 10.1016/j.matbio.2015.03.005.

86. Gatenby R, Gawliski A, Kaylor B, Gillies RJ. Acid-Mediated Tumor Invasion: A Multidisciplinary Study. Cancer Research. 2006; doi: 10.1158/0008-5472.CAN-05-4193.

87. San-Millán I, Brooks GA. Reexamining cancer metabolism: lactate production for carcinogenesis could be the purpose and explanation of the Warburg Effect. Carcinogenesis 2017; doi: 10.1093/carcin/bgw127.

88. Wang Z-H, Peng W-B, Zhang P, et al. Lactate in the tumour microenvironment: From immune modulation to therapy. EBioMedicine 2021; doi: 10.1016/j.ebiom.2021.103627.

89. Calcinotto A, Filipazzi P, Grioni M, et al. Modulation of microenvironment acidity reverses anergy in human and murine tumor-infiltrating T lymphocytes. Cancer Res 2012; doi: 10.1158/0008-5472.CAN-11-1272.

90. Lardner A. The effects of extracellular pH on immune function. J Leukoc Biol 2001; doi: 69(4):522–530.

91. Fukumura D, Xu L, Chen Y, et al. Hypoxia and acidosis independently up-regulate vascular endothelial growth factor transcription in brain tumors in vivo. Cancer Res 2001; doi: 61(16):6020–6024.

92. Romero-Garcia S, Moreno-Altamirano MMB, Prado-Garcia H, et al. Lactate Contribution to the Tumor Microenvironment: Mechanisms, Effects on Immune Cells and Therapeutic Relevance. Front Immunol 2016; doi: 10.3389/fimmu.2016.00052.

93. Zhao Y, Li M, Yao X, et al. HCAR1/MCT1 Regulates Tumor Ferroptosis through the Lactate-Mediated AMPK-SCD1 Activity and Its Therapeutic Implications. Cell Reports 2020; doi: 10.1016/j.celrep.2020.108487.

94. Pu F, Chen F, Zhang Z, et al. Ferroptosis as a novel form of regulated cell death: Implications in the pathogenesis, oncometabolism and treatment of human cancer. Genes Dis 2020; doi: 10.1016/j.gendis.2020.11.019.

95. Zhou Q, Meng Y, Li D, et al. Ferroptosis in cancer: From molecular mechanisms to therapeutic strategies. Sig Transduct Target Ther 2024; doi: 10.1038/s41392-024-01769-5.

96. Mukai Y, Yamaguchi A, Sakuma T, et al. Involvement of SLC16A1/MCT1 and SLC16A3/MCT4 in l-lactate transport in the hepatocellular carcinoma cell line. Biopharm Drug Dispos 2022; doi: 10.1002/bdd.2329.

97. Watson MJ, Vignali PDA, Mullett SJ, et al. Metabolic support of tumour-infiltrating regulatory T cells by lactic acid. Nature 2021; doi: 10.1038/s41586-020-03045-2.

98. Payen VL, Hsu MY, Rädecke KS, et al. Monocarboxylate Transporter MCT1 Promotes Tumor Metastasis Independently of Its Activity as a Lactate Transporter. Cancer Research 2017; doi: 10.1158/0008-5472.CAN-17-0764.

99. Oparaugo NC, Ouyang K, Nguyen NPN, et al. Human Regulatory T Cells: Understanding the Role of Tregs in Select Autoimmune Skin Diseases and Post-Transplant Nonmelanoma Skin Cancers. Int J Mol Sci 2023; doi: 10.3390/ijms24021527.

100. Hong CS, Graham NA, Gu W, et al. MCT1 modulates cancer cell pyruvate export and growth

of tumors that co-express MCT1 and MCT4. Cell Rep 2016; doi: 10.1016/j.celrep.2016.01.057.

101. Payen VL, Mina E, Van Hée VF, et al. Monocarboxylate transporters in cancer. Mol Metab 2020; doi: 10.1016/j.molmet.2019.07.006.

102. Brooks GA. Cell–cell and intracellular lactate shuttles. J Physiol 2009; doi: 10.1113/jphysiol.2009.178350.

103. Park SJ, Smith CP, Wilbur RR, et al. An overview of MCT1 and MCT4 in GBM: small molecule transporters with large implications. Am J Cancer Res 2018; doi: 8(10):1967–1976.

104. Medel V, Crossley N, Gajardo I, et al. Whole-brain neuronal MCT2 lactate transporter expression links metabolism to human brain structure and function. Proceedings of the National Academy of Sciences 2022; doi: 10.1073/pnas.2204619119.

105. Gallagher-Colombo S, Maminishkis A, Tate S, et al. Modulation of MCT3 Expression during Wound Healing of the Retinal Pigment Epithelium. Invest Ophthalmol Vis Sci 2010; doi: 10.1167/iovs.09-5028.

106. Zhu S, Goldschmidt-Clermont PJ, Dong C. Inactivation of monocarboxylate transporter MCT3 by DNA methylation in atherosclerosis. Circulation 2005; doi: 10.1161/circulationaha104.519025.

107. Felmlee MA, Jones RS, Rodriguez-Cruz V, et al. Monocarboxylate Transporters (SLC16): Function, Regulation, and Role in Health and Disease. Pharmacol Rev 2020; doi: 10.1124/pr.119.018762.

108. Husted AS, Trauelsen M, Rudenko O, et al. GPCR-Mediated Signaling of Metabolites. Cell Metab 2017; doi: 10.1016/j.cmet.2017.03.008.

109. Colucci ACM, Tassinari ID, Loss E da S, et al. History and Function of the Lactate Receptor GPR81/HCAR1 in the Brain: A Putative Therapeutic Target for the Treatment of Cerebral Ischemia. Neuroscience 2023; doi: 10.1016/j.neuroscience.2023.06.022.

110. Kuei C, Yu J, Zhu J, et al. Study of GPR81, the lactate receptor, from distant species identifies residues and motifs critical for GPR81 functions. Mol Pharmacol 2011; doi: 10.1124/mol.111.074500.

111. Brown TP, Ganapathy V. Lactate/GPR81 signaling and proton motive force in cancer: Role in angiogenesis, immune escape, nutrition, and Warburg phenomenon. Pharmacology & Therapeutics 2020; doi: 10.1016/j.pharmthera.2019.107451.

112. Ahmed K, Tunaru S, Tang C, et al. An autocrine lactate loop mediates insulin-dependent inhibition of lipolysis through GPR81. Cell Metab 2010; doi: 10.1016/j.cmet.2010.02.012.

113. Roland CL, Arumugam T, Deng D, et al. Cell surface lactate receptor GPR81 is crucial for cancer cell survival. Cancer Res 2014; doi: 10.1158/0008-5472.CAN-14-0319.

114. Lee YJ, Shin KJ, Park S-A, et al. G-protein-coupled receptor 81 promotes a malignant

phenotype in breast cancer through angiogenic factor secretion. Oncotarget 2016; doi: 10.18632/oncotarget.12286.

115. Ishihara S, Hata K, Hirose K, et al. The lactate sensor GPR81 regulates glycolysis and tumor growth of breast cancer. Sci Rep 2022; doi: 10.1038/s41598-022-10143-w.

116. Feng J, Yang H, Zhang Y, et al. Tumor cell-derived lactate induces TAZ-dependent upregulation of PD-L1 through GPR81 in human lung cancer cells. Oncogene 2017; doi: 10.1038/onc.2017.188.

117. Handy DE, Castro R, Loscalzo J. Epigenetic Modifications: Basic Mechanisms and Role in Cardiovascular Disease. Circulation 2011; doi: 10.1161/circulationaha.110.956839.

118. Berger SL, Kouzarides T, Shiekhattar R, et al. An operational definition of epigenetics. Genes Dev 2009; doi: 10.1101/gad.1787609.

119. Al Aboud NM, Tupper C, Jialal I. Genetics, Epigenetic Mechanism. In: StatPearls StatPearls Publishing: Treasure Island (FL); 2024.

120. Yang J, Xu J, Wang W, et al. Epigenetic regulation in the tumor microenvironment: molecular mechanisms and therapeutic targets. Sig Transduct Target Ther 2023; doi: 10.1038/s41392-023-01480-x.

121. Chen C, Wang Z, Qin Y. Connections between metabolism and epigenetics: mechanisms and novel anti-cancer strategy. Front Pharmacol 2022; doi: 10.3389/fphar.2022.935536.

122. Fendt S-M, Frezza C, Erez A. Targeting metabolic plasticity and flexibility dynamics for cancer therapy. Cancer Discov 2020; doi: 10.1158/2159-8290.CD-20-0844.

123. Fan J, Krautkramer K, Feldman J, Denu H. Metabolic Regulation of Histone Post-Translational Modifications. ACS Chem. Biol. 2015; doi: 10.1021/cb500846u.

124. Bassal MA. The Interplay between Dysregulated Metabolism and Epigenetics in Cancer. Biomolecules 2023; doi: 10.3390/biom13060944.

125. An YJ, Jo S, Kim J-M, et al. Lactate as a major epigenetic carbon source for histone acetylation via nuclear LDH metabolism. Exp Mol Med 2023; doi: 10.1038/s12276-023-01095-w.

126. Liu X-S, Little JB, Yuan Z-M. Glycolytic metabolism influences global chromatin structure. Oncotarget 2015; doi: 6(6):4214–4225.

127. Mariño-Ramírez L, Kann MG, Shoemaker BA, et al. Histone structure and nucleosome stability. Expert Rev Proteomics 2005; doi: 10.1586/14789450.2.5.719.

128. Sokolova V, Sarkar S, Tan D. Histone variants and chromatin structure, update of advances. Comput Struct Biotechnol J 2022; doi: 10.1016/j.csbj.2022.12.002.

129. Xie Y, Hu H, Liu M, et al. The role and mechanism of histone lactylation in health and diseases. Front Genet 2022; doi: 10.3389/fgene.2022.949252.

130. Bannister AJ, Kouzarides T. Regulation of chromatin by histone modifications. Cell Res 2011; doi: 10.1038/cr.2011.22.

131. Shahbazian MD, Grunstein M. Functions of site-specific histone acetylation and deacetylation. Annu Rev Biochem 2007; doi: 10.1146/annurev.biochem.76.052705.162114.

132. Gong F, Miller KM. Mammalian DNA repair: HATs and HDACs make their mark through histone acetylation. Mutat Res 2013; doi: 10.1016/j.mrfmmm.2013.07.002.

133. Van der Knaap JA, Verrijzer CP. Undercover: gene control by metabolites and metabolic enzymes. Genes Dev 2016; doi: 10.1101/gad.289140.116.

134. Bhatt AN, Chauhan A, Khanna S, et al. Transient elevation of glycolysis confers radio-resistance by facilitating DNA repair in cells. BMC Cancer 2015; doi: 10.1186/s12885-015-1368-9.

135. Van Vugt MATM. Shutting down the power supply for DNA repair in cancer cells. J Cell Biol 2017; doi: 10.1083/jcb.201701026.

136. Wang Z, Hao D, Zhao S, et al. Lactate and Lactylation: Clinical Applications of Routine Carbon Source and Novel Modification in Human Diseases. Molecular & Cellular Proteomics 2023; doi: 10.1016/j.mcpro.2023.100641.

137. Racey LA, Byvoet P. Histone acetyltransferase in chromatin: Evidence for in vitro enzymatic transfer of acetate from acetyl-coenzyme A to histones. Experimental Cell Research 1971; doi: 10.1016/0014-4827(71)90089-9.

138. Wagner W, Ciszewski WM, Kania KD. L- and D-lactate enhance DNA repair and modulate the resistance of cervical carcinoma cells to anticancer drugs via histone deacetylase inhibition and hydroxycarboxylic acid receptor 1 activation. Cell Communication and Signaling 2015; doi: 10.1186/s12964-015-0114-x.

139. Legoff L, Dali O, De La Mata Santaella E, et al. Histone deacetylase inhibition leads to regulatory histone mark alterations and impairs meiosis in oocytes. Epigenetics Chromatin 2021; doi: 10.1186/s13072-021-00413-8.

140. Castaño-Cerezo S, Bernal V, Post H, et al. Protein acetylation affects acetate metabolism, motility and acid stress response in Escherichia coli. Mol Syst Biol 2014; doi: 10.15252/msb.20145227.

141. Certo M, Llibre A, Lee W, et al. Understanding lactate sensing and signalling. Trends Endocrinol Metab 2022; doi: 10.1016/j.tem.2022.07.004.

142. Zhang D, Tang Z, Huang H, et al. Metabolic regulation of gene expression by histone lactylation. Nature 2019; doi: 10.1038/s41586-019-1678-1.

143. Moreno-Yruela C, Zhang D, Wei W, et al. Class I histone deacetylases (HDAC1–3) are histone lysine delactylases. Sci Adv n.d. 2022; doi: 10.1126/sciadv.abi6696.

144. Chen A-N, Luo Y, Yang Y-H, et al. Lactylation, a Novel Metabolic Reprogramming Code: Current Status and Prospects. Front Immunol 2021; doi: 10.3389/fimmu.2021.688910.

145. Cui H, Xie N, Banerjee S, et al. Lung Myofibroblasts Promote Macrophage Profibrotic Activity through Lactate-induced Histone Lactylation. Am J Respir Cell Mol Biol 2021; doi: 10.1165/rcmb.2020-0360OC.

146. Hu Y, He Z, Li Z, et al. Lactylation: the novel histone modification influence on gene expression, protein function, and disease. Clinical Epigenetics 2024; doi: 10.1186/s13148-024-01682-2.

147. Minami E, Sasa K, Yamada A, et al. Lactate-induced histone lactylation by p300 promotes osteoblast differentiation. PLoS One 2023; doi: 10.1371/journal.pone.0293676.

148. Wang T, Ye Z, Li Z, et al. Lactate-induced protein lactylation: A bridge between epigenetics and metabolic reprogramming in cancer. Cell Proliferation 2023; doi: 10.1111/cpr.13478.

149. Niu Z, Chen C, Wang S, Lu C, Wu Z et al. HBO1 Catalyzes Lysine Lactylation and Mediates Histone H3K9la to Regulate Gene Transcription. Nature Communications. 2024; 10.1038/s41467-024-47900-6

150. Figlia G, Willnow P, Teleman AA. Metabolites Regulate Cell Signaling and Growth via Covalent Modification of Proteins. Dev Cell 2020; doi: 10.1016/j.devcel.2020.06.036.

151. Hu X, Huang X, Yang Y, et al. Dux activates metabolism-lactylation-MET network during early iPSC reprogramming with Brg1 as the histone lactylation reader. Nucleic Acids Research 2024; doi: 10.1093/nar/gkae183.

152. Phillips DM. The presence of acetyl groups of histones. Biochem J 1963; doi: 10.1042/bj0870258.

153. Jo C, Park S, Oh S, et al. Histone acylation marks respond to metabolic perturbations and enable cellular adaptation. Exp Mol Med 2020; doi: 10.1038/s12276-020-00539-x.

154. Shang S, Liu J, Hua F. Protein acylation: mechanisms, biological functions and therapeutic targets. Signal Transduct Target Ther 2022; doi: 10.1038/s41392-022-01245-y.

155. Hagihara H, Shoji H, Otabi H, et al. Protein lactylation induced by neural excitation. Cell Rep 2021; doi: 10.1016/j.celrep.2021.109820.

156. Zhang Y, Peng Q, Zheng J, et al. The function and mechanism of lactate and lactylation in tumor metabolism and microenvironment. Genes & Diseases 2023; doi: 10.1016/j.gendis.2022.10.006.

157. Gao M, Zhang N, Liang W. Systematic Analysis of Lysine Lactylation in the Plant Fungal Pathogen Botrytis cinerea. Front Microbiol 2020; doi: 10.3389/fmicb.2020.594743.

158. Yu X, Yang J, Xu J, et al. Histone lactylation: from tumor lactate metabolism to epigenetic regulation. Int J Biol Sci 2024; doi: 10.7150/ijbs.91492.

159. Izzo LT, Wellen KE. Histone lactylation links metabolism and gene regulation. Nature 2019; doi: 10.1038/d41586-019-03122-1.

160. Gaffney DO, Jennings EQ, Anderson CC, et al. Non-enzymatic Lysine Lactoylation of Glycolytic Enzymes. Cell Chem Biol 2020; doi: 10.1016/j.chembiol.2019.11.005.

161. Yang K, Fan M, Wang X, et al. Lactate promotes macrophage HMGB1 lactylation, acetylation, and exosomal release in polymicrobial sepsis. Cell Death Differ 2022; doi: 10.1038/s41418-021-00841-9.

162. Jiang P, Ning Y, Shi Y, Liu C, Mo S. FSL-Kla: A Few-Shot Learning-Based Multi-Feature Hybrid System for Lactylation Site Prediction. Comput Struct Biotechnol J; 2021; doi: 10.1016/j.csbj.2021.08.013.

163. Yu J, Chai P, Xie M, et al. Histone lactylation drives oncogenesis by facilitating m6A reader protein YTHDF2 expression in ocular melanoma. Genome Biol 2021; doi: 10.1186/s13059-021-02308-z.

164. Wang X, Fan W, Li N, Ma Y, Yao M. YY1 Lactylation in Microglia Promotes Angiogenesis through Transcription Activation-Mediated Upregulation of FGF2. Genome Biol; 2023; doi: 10.1186/s13059-023-02931-y.

165. Galle E, Wong C-W, Ghosh A, et al. H3K18 lactylation marks tissue-specific active enhancers. Genome Biol 2022; doi: 10.1186/s13059-022-02775-y.

166. Offermans K, Jenniskens JC, Simons CC, et al. Expression of proteins associated with the Warburg-effect and survival in colorectal cancer. J Pathol Clin Res 2022; doi: 10.1002/cjp2.250.

167. Li Y, Ma H. circRNA PLOD2 promotes tumorigenesis and Warburg effect in colon cancer by the miR-513a-5p/SIX1/LDHA axis. Cell Cycle 2022; doi: 10.1080/15384101.2022.2103339.

168. Yang Z, Yan C, Ma J, et al. Lactylome analysis suggests lactylation-dependent mechanisms of metabolic adaptation in hepatocellular carcinoma. Nat Metab 2023; doi: 10.1038/s42255-022-00710-w.

169. Zhang W, Zhang K, Shi J, et al. The impact of the senescent microenvironment on tumorigenesis: Insights for cancer therapy. Aging Cell 2024; doi: 10.1111/acel.14182.

170. Wei S, Zhang J, Zhao R, et al. Histone lactylation promotes malignant progression by facilitating USP39 expression to target PI3K/AKT/HIF-1α signal pathway in endometrial carcinoma. Cell Death Discov 2024; doi: 10.1038/s41420-024-01898-4.

171. Jiang J, Huang D, Jiang Y, et al. Lactate Modulates Cellular Metabolism Through Histone Lactylation-Mediated Gene Expression in Non-Small Cell Lung Cancer. Front Oncol 2021; doi: 10.3389/fonc.2021.647559.

172. Kitamura F, Semba T, Yasuda-Yoshihara N, et al. Cancer-associated fibroblasts reuse cancer-derived lactate to maintain a fibrotic and immunosuppressive microenvironment in pancreatic cancer. JCI Insight 2023; doi: 10.1172/jci.insight.163022.

173. Wu J, Hu M, Jiang H, et al. Endothelial Cell-Derived Lactate Triggers Bone Mesenchymal Stem Cell Histone Lactylation to Attenuate Osteoporosis. Adv Sci (Weinh) 2023; doi: 10.1002/advs.202301300.

174. Huang Z-W, Zhang X-N, Zhang L, et al. STAT5 promotes PD-L1 expression by facilitating histone lactylation to drive immunosuppression in acute myeloid leukemia. Signal Transduct Target Ther 2023; doi: 10.1038/s41392-023-01605-2.

175. Zha J, Zhang J, Lu J, et al. A review of lactate-lactylation in malignancy: its potential in immunotherapy. Front Immunol 2024; doi: 10.3389/fimmu.2024.1384948.

176. Xiong J, He J, Zhu J, et al. Lactylation-driven METTL3-mediated RNA m6A modification promotes immunosuppression of tumor-infiltrating myeloid cells. Mol Cell 2022; doi: 10.1016/j.molcel.2022.02.033.

177. Rong Y, Dong F, Zhang G, et al. The crosstalking of lactate-Histone lactylation and tumor. Proteomics Clin Appl 2023; doi: 10.1002/prca.202200102.

178. Qu J, Li P, Sun Z. Histone lactylation regulates cancer progression by reshaping the tumor microenvironment. Front Immunol 2023; doi: 10.3389/fimmu.2023.1284344.

179. Fan M, Yang K, Wang X, et al. Lactate promotes endothelial-to-mesenchymal transition via Snail1 lactylation after myocardial infarction. Sci Adv 2023; doi: 10.1126/sciadv.adc9465.

180. Xu H, Li L, Wang S, et al. Royal jelly acid suppresses hepatocellular carcinoma tumorigenicity by inhibiting H3 histone lactylation at H3K9la and H3K14la sites. Phytomedicine 2023; doi: 10.1016/j.phymed.2023.154940.

181. Govoni M, Rossi V, Di Stefano G, et al. Lactate Upregulates the Expression of DNA Repair Genes, Causing Intrinsic Resistance of Cancer Cells to Cisplatin. Pathol Oncol Res 2021; doi: 10.3389/pore.2021.1609951.

182. Chen S, Xu Y, Zhuo W, et al. The emerging role of lactate in tumor microenvironment and its clinical relevance. Cancer Letters 2024; doi: 10.1016/j.canlet.2024.216837.

183. He Y, Sun MM, Zhang GG, et al. Targeting PI3K/Akt signal transduction for cancer therapy. Signal Transduct Target Ther 2021; doi: 10.1038/s41392-021-00828-5.

184. Elstrom R, Bauer DE, Buzzai M, Karnauskas R, Harris MH et al. Akt Stimulates Aerobic Glycolysis in Cancer Cells. Cancer Research; 2004; 10.1158/0008-5472.CAN-03-2904.

185. Sirico M, D'Angelo A, Gianni C, et al. Current State and Future Challenges for PI3K Inhibitors in Cancer Therapy. Cancers (Basel) 2023; doi: 10.3390/cancers15030703.

186. Belli C, Repetto M, Anand S, et al. The emerging role of PI3K inhibitors for solid tumour treatment and beyond. Br J Cancer 2023; doi: 10.1038/s41416-023-02221-1.

187. Park S, Chang C-Y, Safi R, et al. ERRα-Regulated Lactate Metabolism Contributes to Resistance to Targeted Therapies in Breast Cancer. Cell Rep 2016; doi:

10.1016/j.celrep.2016.03.026.

188. Barnes EME, Xu Y, Benito A, et al. Lactic acidosis induces resistance to the pan-Akt inhibitor uprosertib in colon cancer cells. Br J Cancer 2020; doi: 10.1038/s41416-020-0777-y.

189. Apicella M, Giannoni E, Fiore S, et al. Increased Lactate Secretion by Cancer Cells Sustains Non-cell-autonomous Adaptive Resistance to MET and EGFR Targeted Therapies. Cell Metab 2018; doi: 10.1016/j.cmet.2018.08.006.

190. Dong Q, Zhou C, Ren H, et al. Lactate-induced MRP1 expression contributes to metabolism-based etoposide resistance in non-small cell lung cancer cells. Cell Communication and Signaling 2020; doi: 10.1186/s12964-020-00653-3.

191. Chen H, Li Y, Li H, et al. NBS1 lactylation is required for efficient DNA repair and chemotherapy resistance. Nature 2024; doi: 10.1038/s41586-024-07620-9.

192. Pan L, Feng F, Wu J, et al. Demethylzeylasteral targets lactate by inhibiting histone lactylation to suppress the tumorigenicity of liver cancer stem cells. Pharmacol Res 2022; doi: 10.1016/j.phrs.2022.106270.

193. Vaidya FU, Sufiyan Chhipa A, Mishra V, et al. Molecular and cellular paradigms of multidrug resistance in cancer. Cancer Rep (Hoboken) 2020; doi: 10.1002/cnr2.1291.

194. Hammoudi N, Ahmed KBR, Garcia-Prieto C, et al. Metabolic alterations in cancer cells and therapeutic implications. Chin J Cancer 2011; doi: 10.5732/cjc.011.10267.

195. Le A, Cooper CR, Gouw AM, et al. Inhibition of lactate dehydrogenase A induces oxidative stress and inhibits tumor progression. Proc Natl Acad Sci U S A 2010; doi: 10.1073/pnas.0914433107.

196. El Hassouni B, Franczak M, Capula M, et al. Lactate dehydrogenase A inhibition by small molecular entities: steps in the right direction. Oncoscience 2020; doi: 10.18632/oncoscience.519.

197. DeBerardinis RJ, Chandel NS. Fundamentals of cancer metabolism. Sci Adv 2016; doi: 10.1126/sciadv.1600200.

198. Bui T, Thompson CB. Cancer's sweet tooth. Cancer Cell 2006; doi: 10.1016/j.ccr.2006.05.012.

199. Bhattacharya B, Mohd Omar MF, Soong R. The Warburg effect and drug resistance. Br J Pharmacol 2016; doi: 10.1111/bph.13422.

200. Fiume L, Manerba M, Vettraino M, et al. Inhibition of lactate dehydrogenase activity as an approach to cancer therapy. Future Med Chem 2014; doi: 10.4155/fmc.13.206.

201. Fiume L, Vettraino M, Manerba M, et al. Inhibition of lactic dehydrogenase as a way to increase the anti-proliferative effect of multi-targeted kinase inhibitors. Pharmacol Res 2011; doi: 10.1016/j.phrs.2010.12.005.

202. Manerba M, Di Ianni L, Fiume L, et al. Lactate dehydrogenase inhibitors sensitize lymphoma cells to cisplatin without enhancing the drug effects on immortalized normal lymphocytes. Eur J Pharm Sci 2015; doi: 10.1016/j.ejps.2015.04.022.

203. Boukouris AE, Zervopoulos SD, Michelakis ED. Metabolic Enzymes Moonlighting in the Nucleus: Metabolic Regulation of Gene Transcription. Trends Biochem Sci 2016; doi: 10.1016/j.tibs.2016.05.013.

204. Fan Q, Yang L, Zhang X, et al. Autophagy promotes metastasis and glycolysis by upregulating MCT1 expression and Wnt/β-catenin signaling pathway activation in hepatocellular carcinoma cells. J Exp Clin Cancer Res 2018; doi: 10.1186/s13046-018-0673-y.

205. Sprowl-Tanio S, Habowski A, Pate K, McQuade M, Wang K et al. Lactate/Pyruvate Transporter MCT-1 Is a Direct Wnt Target That Confers Sensitivity to 3-Bromopyruvate in Colon Cancer. Cancer Metab; 2016; 10.1186/s40170-016-0159-3.

206. Repetto G, del Peso A, Zurita JL. Neutral red uptake assay for the estimation of cell viability/cytotoxicity. Nat Protoc 2008; doi: 10.1038/nprot.2008.75.

207. Kubo K, Ide H, Wallace SS, et al. A novel, sensitive, and specific assay for abasic sites, the most commonly produced DNA lesion. Biochemistry 1992; doi: 10.1021/bi00129a020.

208. Green MR, Sambrook J. Precipitation of DNA with Ethanol. Cold Spring Harb Protoc 2016; doi: 10.1101/pdb.prot093377.

209. Sharma A, Singh K, Almasan A. Histone H2AX phosphorylation: a marker for DNA damage. Methods Mol Biol 2012; doi: 10.1007/978-1-61779-998-3_40.

210. Papaconstantinou J, Colowick SP. The role of glycolysis in the growth of tumor cells. I. Effects of oxamic acid on the metabolism of Ehrlich ascites tumor cells in vitro. J Biol Chem 1961; doi: 236:278–284.

211. Basu A, Krishnamurthy S. Cellular responses to Cisplatin-induced DNA damage. J Nucleic Acids 2010; doi: 10.4061/2010/201367.

212. Wagner W, Kania KD, Ciszewski WM. Stimulation of lactate receptor (HCAR1) affects cellular DNA repair capacity. DNA Repair (Amst) 2017; doi: 10.1016/j.dnarep.2017.02.007.

213. Liska DJ. The detoxification enzyme systems. Altern Med Rev 1998; 3(3):187–198.

214. Stoimenov I, Helleday T. PCNA on the crossroad of cancer. Biochem Soc Trans 2009; doi: 10.1042/BST0370605.

215. Wang S-C. PCNA: a silent housekeeper or a potential therapeutic target? Trends Pharmacol Sci 2014; doi: 10.1016/j.tips.2014.02.004.

216. Rodríguez N, Peláez A, Barderas R, et al. Clinical implications of the deregulated TP73 isoforms expression in cancer. Clin Transl Oncol 2018; doi: 10.1007/s12094-017-1802-3.

217. Loh C-Y, Chai JY, Tang TF, et al. The E-Cadherin and N-Cadherin Switch in Epithelial-to-

Mesenchymal Transition: Signaling, Therapeutic Implications, and Challenges. Cells 2019; doi: 10.3390/cells8101118.

218. Sun X, Kaufman PD. Ki-67: more than a proliferation marker. Chromosoma 2018; doi: 10.1007/s00412-018-0659-8.

219. Katoh M. Network of WNT and Other Regulatory Signaling Cascades in Pluripotent Stem Cells and Cancer Stem Cells. Current Pharmaceutical Biotechnology 2011; 10.2174/138920111794295710.

220. Liu X, Tan N, Liao H, et al. High GSTP1 inhibits cell proliferation by reducing Akt phosphorylation and is associated with a better prognosis in hepatocellular carcinoma. Oncotarget 2018; doi: 10.18632/oncotarget.23420.

221. Vassalli G. Aldehyde Dehydrogenases: Not Just Markers, but Functional Regulators of Stem Cells. Stem Cells Int 2019; doi: 10.1155/2019/3904645.

222. San-Millán I, Julian CG, Matarazzo C, et al. Is Lactate an Oncometabolite? Evidence Supporting a Role for Lactate in the Regulation of Transcriptional Activity of Cancer-Related Genes in MCF7 Breast Cancer Cells. Front Oncol 2019; doi: 10.3389/fonc.2019.01536.

223. Walenta S, Mueller-Klieser WF. Lactate: mirror and motor of tumor malignancy. Semin Radiat Oncol 2004; doi: 10.1016/j.semradonc.2004.04.004.

224. Wilson BE, Jacob S, Yap ML, et al. Estimates of global chemotherapy demands and corresponding physician workforce requirements for 2018 and 2040: a population-based study. Lancet Oncol 2019; doi: 10.1016/S1470-2045(19)30163-9.

225. Sritharan S, Sivalingam N. A comprehensive review on time-tested anticancer drug doxorubicin. Life Sci 2021; doi: 10.1016/j.lfs.2021.119527.

226. Carvalho C, Santos RX, Cardoso S, et al. Doxorubicin: the good, the bad and the ugly effect. Curr Med Chem 2009; doi: 10.2174/092986709788803312.

227. Nicoletto RE, Ofner CM. Cytotoxic mechanisms of doxorubicin at clinically relevant concentrations in breast cancer cells. Cancer Chemother Pharmacol 2022; doi: 10.1007/s00280-022-04400-y.

228. Yang F, Teves SS, Kemp CJ, et al. Doxorubicin, DNA torsion, and chromatin dynamics. Biochim Biophys Acta 2014; doi: 10.1016/j.bbcan.2013.12.002.

229. Pang B, Qiao X, Janssen L, et al. Drug-induced histone eviction from open chromatin contributes to the chemotherapeutic effects of doxorubicin. Nat Commun 2013; doi: 10.1038/ncomms2921.

230. Pilco-Ferreto N, Calaf GM. Influence of doxorubicin on apoptosis and oxidative stress in breast cancer cell lines. Int J Oncol 2016; doi: 10.3892/ijo.2016.3558.

231. Berthiaume JM, Wallace KB. Adriamycin-induced oxidative mitochondrial cardiotoxicity. Cell Biol Toxicol 2007; doi: 10.1007/s10565-006-0140-y.

232. Sobczuk P, Czerwińska M, Kleibert M, et al. Anthracycline-induced cardiotoxicity and renin-angiotensin-aldosterone system—from molecular mechanisms to therapeutic applications. Heart Fail Rev 2022; doi: 10.1007/s10741-020-09977-1.

233. Colombo R, Dalle Donne I, Milzani A. Metal ions modulate the effect of doxorubicin on actin assembly. Cancer Biochem Biophys 1990; 11(3):217–226.

234. Gomes A, Fernandes E, Lima JLFC. Fluorescence probes used for detection of reactive oxygen species. J Biochem Biophys Methods 2005; doi: 10.1016/j.jbbm.2005.10.003.

235. Valavanidis A, Vlachogianni T, Fiotakis C. 8-Hydroxy-2' -Deoxyguanosine (8-OHdG): A Critical Biomarker of Oxidative Stress and Carcinogenesis. J Environ Sci Health C Environ Carcinog Ecotoxicol Rev; 2009; doi: 10.1080/10590500902885684.

236. Livak KJ, Schmittgen TD. Analysis of relative gene expression data using real-time quantitative PCR and the 2(-Delta Delta C(T)) Method. Methods 2001; doi: 10.1006/meth.2001.1262.

237. Nitiss JL, Soans E, Rogojina A, et al. Topoisomerase assays. Curr Protoc Pharmacol 2012; doi: 10.1002/0471141755.ph0303s57.

238. Anampa J, Makower D, Sparano JA. Progress in adjuvant chemotherapy for breast cancer: an overview. BMC Med 2015; doi: 10.1186/s12916-015-0439-8.

239. Alkaraki A, Alshaer W, Wehaibi S, Gharaibeh L et al. Enhancing Chemosensitivity of Wild-Type and Drug-Resistant MDA-MB-231 Triple-Negative Breast Cancer Cell Line to Doxorubicin by Silencing of STAT 3, Notch-1, and β-Catenin Genes. Breast Cancer; 2020; doi: 10.1007/s12282-020-01098-9.

240. Shields AF, Lange LM, Zalupski MM. Phase II study of liposomal doxorubicin in patients with advanced colorectal cancer. Am J Clin Oncol 2001; doi: 10.1097/00000421-200102000-00019.

241. Hamanaka RB, Chandel NS. Cell biology. Warburg effect and redox balance. Science 2011; doi: 10.1126/science.1215637.

242. Schwab M, Thunborg K, Azimzadeh O, et al. Targeting Cancer Metabolism Breaks Radioresistance by Impairing the Stress Response. Cancers (Basel) 2021; doi: 10.3390/cancers13153762.

243. Schwab M, Multhoff G. A Low Membrane Hsp70 Expression in Tumor Cells With Impaired Lactate Metabolism Mediates Radiosensitization by NVP-AUY922. Front Oncol 2022; doi: 10.3389/fonc.2022.861266.

244. Yang Y, Chong Y, Chen M, et al. Targeting lactate dehydrogenase a improves radiotherapy efficacy in non-small cell lung cancer: from bedside to bench. J Transl Med 2021; doi: 10.1186/s12967-021-02825-2.

245. Azzam EI, Jay-Gerin J-P, Pain D. Ionizing radiation-induced metabolic oxidative stress and

prolonged cell injury. Cancer Lett 2012; doi: 10.1016/j.canlet.2011.12.012.

246. Dejeans N, Glorieux C, Guenin S, et al. Overexpression of GRP94 in breast cancer cells resistant to oxidative stress promotes high levels of cancer cell proliferation and migration: implications for tumor recurrence. Free Radic Biol Med 2012; doi: 10.1016/j.freeradbiomed.2011.12.019.

247. Kurashova NA, Madaeva IM, Kolesnikova LI. Expression of heat shock proteins HSP70 under oxidative stress. Adv Gerontol 2019; doi: 32(4):502–508.

248. Matassa DS, Amoroso MR, Maddalena F, et al. New insights into TRAP1 pathway. Am J Cancer Res 2012; doi: 2(2):235–248.

249. Albakova Z, Mangasarova Y, Albakov A, et al. HSP70 and HSP90 in Cancer: Cytosolic, Endoplasmic Reticulum and Mitochondrial Chaperones of Tumorigenesis. Front Oncol 2022; doi: 10.3389/fonc.2022.829520.

250. Buc Calderon P, Sennesael A-L, Glorieux C. Glucose-regulated protein of 94 kDa contributes to the development of an aggressive phenotype in breast cancer cells. Biomed Pharmacother 2018; doi: 10.1016/j.biopha.2018.05.106.

251. Boldinova EO, Khairullin RF, Makarova AV, et al. Isoforms of Base Excision Repair Enzymes Produced by Alternative Splicing. Int J Mol Sci 2019; doi: 10.3390/ijms20133279.

252. Liu Y-Y, Hill RA, Li Y-T. Ceramide glycosylation catalyzed by glucosylceramide synthase and cancer drug resistance. Adv Cancer Res 2013; doi: 10.1016/B978-0-12-394274-6.00003-0.

253. Liu Y-Y, Yu JY, Yin D, et al. A role for ceramide in driving cancer cell resistance to doxorubicin. FASEB J 2008; doi: 10.1096/fj.07-092981.

254. Riccio AA, Schellenberg MJ, Williams RS. Molecular mechanisms of topoisomerase 2 DNA-protein crosslink resolution. Cell Mol Life Sci 2020; doi: 10.1007/s00018-019-03367-z.

255. Deweese JE, Osheroff N. The DNA cleavage reaction of topoisomerase II: wolf in sheep's clothing. Nucleic Acids Res 2009; doi: 10.1093/nar/gkn937.

256. Burgess DJ, Doles J, Zender L, et al. Topoisomerase levels determine chemotherapy response in vitro and in vivo. Proc Natl Acad Sci U S A 2008; doi: 10.1073/pnas.0803513105.

257. Takahashi DT, Gadelle D, Agama K, et al. Topoisomerase I (TOP1) dynamics: conformational transition from open to closed states. Nat Commun 2022; doi: 10.1038/s41467-021-27686-7.

258. Pérez-Tomás R, Pérez-Guillén I. Lactate in the Tumor Microenvironment: An Essential Molecule in Cancer Progression and Treatment. Cancers (Basel) 2020; doi: 10.3390/cancers12113244.

259. Zhu H, Sarkar S, Scott L, et al. Doxorubicin Redox Biology: Redox Cycling, Topoisomerase Inhibition, and Oxidative Stress. React Oxyg Species (Apex) 2016; doi:

10.20455/ros.2016.835.

260. Dallons M, Schepkens C, Dupuis A, et al. New Insights About Doxorubicin-Induced Toxicity to Cardiomyoblast-Derived H9C2 Cells and Dexrazoxane Cytoprotective Effect: Contribution of In Vitro 1H-NMR Metabonomics. Front Pharmacol 2020; doi: 10.3389/fphar.2020.00079.

261. Jiang Y, Zhang Q. Catalpol ameliorates doxorubicin-induced inflammation and oxidative stress in H9C2 cells through PPAR-γ activation. Exp Ther Med 2020; doi: 10.3892/etm.2020.8743.

262. Varum S, Rodrigues AS, Moura MB, et al. Energy metabolism in human pluripotent stem cells and their differentiated counterparts. PLoS One 2011; doi: 10.1371/journal.pone.0020914.

263. Seshadri G, Che PL, Boopathy AV, et al. Characterization of Superoxide Dismutases in Cardiac Progenitor Cells Demonstrates a Critical Role for Manganese Superoxide Dismutase. Stem Cells Dev 2012; doi: 10.1089/scd.2012.0191.

264. Lu P. Monitoring cardiac function in patients receiving doxorubicin. Semin Nucl Med 2005; doi: 10.1053/j.semnuclmed.2005.02.005.

265. Green PS, Leeuwenburgh C. Mitochondrial dysfunction is an early indicator of doxorubicin-induced apoptosis. Biochim Biophys Acta 2002; doi: 10.1016/s0925-4439(02)00144-8.

266. Minotti G, Menna P, Salvatorelli E, et al. Anthracyclines: molecular advances and pharmacologic developments in antitumor activity and cardiotoxicity. Pharmacol Rev 2004; doi: 10.1124/pr.56.2.6.

267. Zhang P, Lu H, Wu Y, et al. COX5A Alleviates Doxorubicin-Induced Cardiotoxicity by Suppressing Oxidative Stress, Mitochondrial Dysfunction and Cardiomyocyte Apoptosis. Int J Mol Sci 2023; doi: 10.3390/ijms241210400.

268. Al-Kenany SA, Al-Shawi NN. Protective effect of cafestol against doxorubicin-induced cardiotoxicity in rats by activating the Nrf2 pathway. Front Pharmacol 2023; doi: 10.3389/fphar.2023.1206782.

269. Hu C, Fan L, Cen P, et al. Energy Metabolism Plays a Critical Role in Stem Cell Maintenance and Differentiation. Int J Mol Sci 2016; doi: 10.3390/ijms17020253.

270. Jaiyesimi IA, Buzdar AU, Decker DA, et al. Use of tamoxifen for breast cancer: twenty-eight years later. J Clin Oncol 1995; doi: 10.1200/JCO.1995.13.2.513.

271. Osborne CK. Tamoxifen in the treatment of breast cancer. N Engl J Med 1998; doi: 10.1056/NEJM199811263392207.

272. Ring A, Dowsett M. Mechanisms of tamoxifen resistance. Endocr Relat Cancer 2004; doi: 10.1677/erc.1.00776.

273. Gradishar WJ. Tamoxifen--what next? Oncologist 2004; doi: 10.1634/theoncologist.9-4-378.

274. García-Becerra R, Santos N, Díaz L, et al. Mechanisms of resistance to endocrine therapy in breast cancer: focus on signaling pathways, miRNAs and genetically based resistance. Int J Mol Sci 2012; doi: 10.3390/ijms14010108.

275. Goetz MP, Rae JM, Suman VJ, et al. Pharmacogenetics of tamoxifen biotransformation is associated with clinical outcomes of efficacy and hot flashes. J Clin Oncol 2005; doi: 10.1200/JCO.2005.03.3266.

276. Manavalan TT, Teng Y, Appana SN, et al. Differential expression of microRNA expression in tamoxifen-sensitive MCF-7 versus tamoxifen-resistant LY2 human breast cancer cells. Cancer Lett 2011; doi: 10.1016/j.canlet.2011.08.018.

277. Araki K, Miyoshi Y. Mechanism of resistance to endocrine therapy in breast cancer: the important role of PI3K/Akt/mTOR in estrogen receptor-positive, HER2-negative breast cancer. Breast Cancer 2018; doi: 10.1007/s12282-017-0812-x.

278. Woo YM, Shin Y, Lee EJ, et al. Inhibition of Aerobic Glycolysis Represses Akt/mTOR/HIF-1α Axis and Restores Tamoxifen Sensitivity in Antiestrogen-Resistant Breast Cancer Cells. PLOS ONE 2015; doi: 10.1371/journal.pone.0132285.

279. He M, Jin Q, Chen C, et al. The miR-186-3p/EREG axis orchestrates tamoxifen resistance and aerobic glycolysis in breast cancer cells. Oncogene 2019; doi: 10.1038/s41388-019-0817-3.

280. Varghese E, Samuel SM, Líšková A, et al. Targeting Glucose Metabolism to Overcome Resistance to Anticancer Chemotherapy in Breast Cancer. Cancers (Basel) 2020; doi: 10.3390/cancers12082252.

281. Moreira PI, Custódio J, Moreno A, et al. Tamoxifen and estradiol interact with the flavin mononucleotide site of complex I leading to mitochondrial failure. J Biol Chem 2006; doi: 10.1074/jbc.M510249200.

282. Daurio NA, Tuttle SW, Worth AJ, et al. AMPK Activation and Metabolic Reprogramming by Tamoxifen through Estrogen Receptor-Independent Mechanisms Suggests New Uses for This Therapeutic Modality in Cancer Treatment. Cancer Res 2016; doi: 10.1158/0008-5472.CAN-15-2197.

283. Dehdashti F, Flanagan FL, Mortimer JE, et al. Positron emission tomographic assessment of "metabolic flare" to predict response of metastatic breast cancer to antiestrogen therapy. Eur J Nucl Med 1999; doi: 10.1007/s002590050359.

284. Farabegoli F, Vettraino M, Manerba M, et al. Galloflavin, a new lactate dehydrogenase inhibitor, induces the death of human breast cancer cells with different glycolytic attitude by affecting distinct signaling pathways. Eur J Pharm Sci 2012; doi: 10.1016/j.ejps.2012.08.012.

285. Pinto TNC, Fernandes JR, Arruda LB, et al. Cost-Effective Trap qPCR Approach to Evaluate Telomerase Activity: an Important Tool for Aging, Cancer, and Chronic Disease Research. Clinics (Sao Paulo) 2021; doi: 10.6061/clinics/2021/e2432.

286. Hou M, Xu D, Björkholm M, et al. Real-time quantitative telomeric repeat amplification

protocol assay for the detection of telomerase activity. Clin Chem 2001;47(3):519–524.

287. Farabegoli F, Barbi C, Lambertini E, et al. (-)-Epigallocatechin-3-gallate downregulates estrogen receptor alpha function in MCF-7 breast carcinoma cells. Cancer Detect Prev 2007; doi: 10.1016/j.cdp.2007.10.018.

288. Cordenonsi M, Zanconato F, Azzolin L, et al. The Hippo transducer TAZ confers cancer stem cell-related traits on breast cancer cells. Cell 2011; doi: 10.1016/j.cell.2011.09.048.

289. White SM, Avantaggiati ML, Nemazanyy I, et al. YAP/TAZ Inhibition Induces Metabolic and Signaling Rewiring Resulting in Targetable Vulnerabilities in NF2-Deficient Tumor Cells. Dev Cell 2019; doi: 10.1016/j.devcel.2019.04.014.

290. Knudsen KA, Wheelock MJ. Cadherins and the mammary gland. Journal of Cellular Biochemistry 2005; doi: 10.1002/jcb.20419.

291. Vesuna F, Lisok A, Kimble B, et al. Twist modulates breast cancer stem cells by transcriptional regulation of CD24 expression. Neoplasia 2009; doi: 10.1593/neo.91084.

292. Olsson E, Honeth G, Bendahl P-O, et al. CD44 isoforms are heterogeneously expressed in breast cancer and correlate with tumor subtypes and cancer stem cell markers. BMC Cancer 2011; doi: 10.1186/1471-2407-11-418.

293. Soule HD, Maloney TM, Wolman SR, et al. Isolation and characterization of a spontaneously immortalized human breast epithelial cell line, MCF-10. Cancer Res 1990;50(18):6075–6086.

294. Wang H, Zhang S, Zhang Y, et al. TAZ is indispensable for c-MYC-induced hepatocarcinogenesis. J Hepatol 2022; doi: 10.1016/j.jhep.2021.08.021.

295. Dang CV, Le A, Gao P. MYC-induced Cancer Cell Energy Metabolism and Therapeutic Opportunities. Clin Cancer Res 2009; doi: 10.1158/1078-0432.CCR-09-0889.

296. Wang Z, Kyo S, Maida Y, et al. Tamoxifen regulates human telomerase reverse transcriptase (hTERT) gene expression differently in breast and endometrial cancer cells. Oncogene 2002; doi: 10.1038/sj.onc.1205463.

297. Lu L, Zhang C, Zhu G, et al. Telomerase expression and telomere length in breast cancer and their associations with adjuvant treatment and disease outcome. Breast Cancer Res 2011; doi: 10.1186/bcr2893.

298. Hurd C, Khattree N, Dinda S, et al. Regulation of tumor suppressor proteins, p53 and retinoblastoma, by estrogen and antiestrogens in breast cancer cells. Oncogene 1997; doi: 10.1038/sj.onc.1201233.

299. Britton DJ, Hutcheson IR, Knowlden JM, et al. Bidirectional cross talk between ERα and EGFR signalling pathways regulates tamoxifen-resistant growth. Breast Cancer Res Treat 2006; doi: 10.1007/s10549-005-9070-2.

300. Massarweh S, Osborne CK, Creighton CJ, et al. Tamoxifen resistance in breast tumors is driven by growth factor receptor signaling with repression of classic estrogen receptor genomic function. Cancer Res 2008; doi: 10.1158/0008-5472.CAN-07-2707.

301. Rojas M, Yao S, Lin YZ. Controlling epidermal growth factor (EGF)-stimulated Ras activation in intact cells by a cell-permeable peptide mimicking phosphorylated EGF receptor. J Biol Chem 1996; doi: 10.1074/jbc.271.44.27456.

302. Jung K-H, Lee EJ, Park JW, et al. EGF receptor stimulation shifts breast cancer cell glucose metabolism toward glycolytic flux through PI3 kinase signaling. PLoS One 2019; doi: 10.1371/journal.pone.0221294.

303. Lim S-O, Li C-W, Xia W, et al. EGFR Signaling Enhances Aerobic Glycolysis in Triple-Negative Breast Cancer Cells to Promote Tumor Growth and Immune Escape. Cancer Res 2016; doi: 10.1158/0008-5472.CAN-15-2478.

304. Hamadneh L, Al-Lakkis L, Alhusban AA, et al. Changes in Lactate Production, Lactate Dehydrogenase Genes Expression and DNA Methylation in Response to Tamoxifen Resistance Development in MCF-7 Cell Line. Genes (Basel) 2021; doi: 10.3390/genes12050777.

305. Das CK, Parekh A, Parida PK, et al. Lactate dehydrogenase A regulates autophagy and tamoxifen resistance in breast cancer. Biochim Biophys Acta Mol Cell Res 2019; doi: 10.1016/j.bbamcr.2019.03.004.

306. Kashkin KN, Chernov IP, Stukacheva EA, et al. Cancer Specificity of Promoters of the Genes Involved in Cell Proliferation Control. Acta Naturae 2013;5(3):79–83.

307. Yang N, Morrison CD, Liu P, et al. TAZ induces growth factor-independent proliferation through activation of EGFR ligand amphiregulin. Cell Cycle 2012; doi: 10.4161/cc.21386.

308. Guo L, Zheng J, Zhang J, et al. Knockdown of TAZ modifies triple-negative breast cancer cell sensitivity to EGFR inhibitors by regulating YAP expression. Oncol Rep 2016; doi: 10.3892/or.2016.4875.

309. Wang Z. ErbB Receptors and Cancer. Methods Mol Biol 2017; doi: 10.1007/978-1-4939-7219-7_1.

310. Roskoski R. The ErbB/HER family of protein-tyrosine kinases and cancer. Pharmacological Research 2014; doi: 10.1016/j.phrs.2013.11.002.

311. Appert-Collin A, Hubert P, Crémel G, et al. Role of ErbB Receptors in Cancer Cell Migration and Invasion. Front Pharmacol 2015; doi: 10.3389/fphar.2015.00283.

312. Al Moustafa A-E, Achkhar A, Yasmeen A. EGF-receptor signaling and epithelial-mesenchymal transition in human carcinomas. Front Biosci (Schol Ed) 2012; doi: 10.2741/s292.

313. Lorch JH, Klessner J, Park JK, et al. Epidermal growth factor receptor inhibition promotes desmosome assembly and strengthens intercellular adhesion in squamous cell carcinoma cells. J Biol Chem 2004; doi: 10.1074/jbc.M405123200.

314. Nicholson RI, Gee JM, Harper ME. EGFR and cancer prognosis. Eur J Cancer 2001; doi:

10.1016/s0959-8049(01)00231-3.

315. Sabbah DA, Hajjo R, Sweidan K. Review on Epidermal Growth Factor Receptor (EGFR) Structure, Signaling Pathways, Interactions, and Recent Updates of EGFR Inhibitors. Curr Top Med Chem 2020; doi: 10.2174/1568026620666200303123102.

316. Alquraishi M, Puckett DL, Alani DS, et al. Pyruvate kinase M2: A simple molecule with complex functions. Free Radic Biol Med 2019; doi: 10.1016/j.freeradbiomed.2019.08.007.

317. Kuo P-L, Huang M-S, Cheng D-E, et al. Lung cancer-derived galectin-1 enhances tumorigenic potentiation of tumor-associated dendritic cells by expressing heparin-binding EGF-like growth factor. J Biol Chem 2012; doi: 10.1074/jbc.M111.321190.

318. Miyamoto S, Yagi H, Yotsumoto F, et al. Heparin-binding epidermal growth factor-like growth factor as a novel targeting molecule for cancer therapy. Cancer Sci 2006; doi: 10.1111/j.1349-7006.2006.00188.x.

319. Raab G, Klagsbrun M. Heparin-binding EGF-like growth factor. Biochim Biophys Acta 1997; doi: 10.1016/s0304-419x(97)00024-3.

320. Van Hiep N, Sun W-L, Feng P-H, et al. Heparin binding epidermal growth factor-like growth factor is a prognostic marker correlated with levels of macrophages infiltrated in lung adenocarcinoma. Front Oncol 2022; doi: 10.3389/fonc.2022.963896.

321. Wang F, Liu R, Lee SW, et al. Heparin-binding EGF-like growth factor is an early response gene to chemotherapy and contributes to chemotherapy resistance. Oncogene 2007; doi: 10.1038/sj.onc.1209999.

322. Yotsumoto F, Yagi H, Suzuki SO, et al. Validation of HB-EGF and amphiregulin as targets for human cancer therapy. Biochem Biophys Res Commun 2008; doi: 10.1016/j.bbrc.2007.11.015.

323. Rivetti S, Lauriola M, Voltattorni M, et al. Gene expression profile of human colon cancer cells treated with cross-reacting material 197, a diphtheria toxin non-toxic mutant. Int J Immunopathol Pharmacol 2011; doi: 10.1177/039463201102400310.

324. Carroll MJ, Kapur A, Felder M, et al. M2 macrophages induce ovarian cancer cell proliferation via a heparin binding epidermal growth factor/matrix metalloproteinase 9 intercellular feedback loop. Oncotarget 2016; doi: 10.18632/oncotarget.13474.

325. Zhou ZN, Sharma VP, Beaty BT, et al. Autocrine HBEGF expression promotes breast cancer intravasation, metastasis and macrophage-independent invasion in vivo. Oncogene 2014; doi: 10.1038/onc.2013.363.

326. Tang L, Han X. The urokinase plasminogen activator system in breast cancer invasion and metastasis. Biomed Pharmacother 2013; doi: 10.1016/j.biopha.2012.10.003.

327. Sarno F, Goubert D, Logie E, et al. Functional Validation of the Putative Oncogenic Activity of PLAU. Biomedicines 2022; doi: 10.3390/biomedicines11010102.

328. Lappano R, De Marco P, De Francesco EM, et al. Cross-talk between GPER and growth factor signaling. J Steroid Biochem Mol Biol 2013; doi: 10.1016/j.jsbmb.2013.03.005.

329. Scaling AL, Prossnitz ER, Hathaway HJ. GPER mediates estrogen-induced signaling and proliferation in human breast epithelial cells and normal and malignant breast. Horm Cancer 2014; doi: 10.1007/s12672-014-0174-1.

330. Ye S, Xu Y, Wang L, et al. Estrogen-Related Receptor α (ERRα) and G Protein-Coupled Estrogen Receptor (GPER) Synergistically Indicate Poor Prognosis in Patients with Triple-Negative Breast Cancer. Onco Targets Ther 2020; doi: 10.2147/OTT.S265372.

331. Cai Q, Lin T, Kamarajugadda S, et al. Regulation of Glycolysis and the Warburg Effect by Estrogen-related Receptors. Oncogene 2013;32(16):2079–2086; doi: 10.1038/onc.2012.221.

332. Luo J, Zou H, Guo Y, et al. SRC kinase-mediated signaling pathways and targeted therapies in breast cancer. Breast Cancer Res 2022; doi: 10.1186/s13058-022-01596-y.

333. Zhou Y, Tao L, Qiu J, et al. Tumor biomarkers for diagnosis, prognosis and targeted therapy. Signal Transduct Target Ther 2024; doi: 10.1038/s41392-024-01823-2.

334. Ma Z, Webb DJ, Jo M, et al. Endogenously produced urokinase-type plasminogen activator is a major determinant of the basal level of activated ERK/MAP kinase and prevents apoptosis in MDA-MB-231 breast cancer cells. J Cell Sci 2001; doi: 10.1242/jcs.114.18.3387.

335. Longo A, Librizzi M, Chuckowree IS, et al. Cytotoxicity of the Urokinase-Plasminogen Activator Inhibitor Carbamimidothioic Acid (4-Boronophenyl) Methyl Ester Hydrobromide (BC-11) on Triple-Negative MDA-MB231 Breast Cancer Cells. Molecules 2015; doi: 10.3390/molecules20069879.

336. Licitra L, Perrone F, Tamborini E, et al. Role of EGFR family receptors in proliferation of squamous carcinoma cells induced by wound healing fluids of head and neck cancer patients. Ann Oncol 2011; doi: 10.1093/annonc/mdq756.

337. Dutta PR, Maity A. Cellular responses to EGFR inhibitors and their relevance to cancer therapy. Cancer Lett 2007; doi: 10.1016/j.canlet.2007.02.006.

338. Kopacz-Bednarska A, Król T. Cisplatin — properties and clinical application. Oncology in Clinical Practice 2022; doi: 10.5603/OCP.2022.0020.

339. Mitamura T, Higashiyama S, Taniguchi N, et al. Diphtheria Toxin Binds to the Epidermal Growth Factor (EGF)-like Domain of Human Heparin-binding EGF-like Growth Factor/Diphtheria Toxin Receptor and Inhibits Specifically Its Mitogenic Activity (∗). Journal of Biological Chemistry 1995; doi: 10.1074/jbc.270.3.1015.

340. Peng J, Cui Y, Xu S, et al. Altered glycolysis results in drug-resistant in clinical tumor therapy. Oncol Lett 2021; doi: 10.3892/ol.2021.12630.

341. Breitinger H-G. Drug Synergy – Mechanisms and Methods of Analysis. In: Toxicity and Drug Testing IntechOpen; 2012; doi: 10.5772/30922.

342. Ryu J, Yoon NA, Lee YK, et al. Tristetraprolin inhibits the growth of human glioma cells through downregulation of urokinase plasminogen activator/urokinase plasminogen activator receptor mRNAs. Mol Cells 2015; doi: 10.14348/molcells.2015.2259.

343. Hapach LA, Carey SP, Schwager SC, et al. Phenotypic Heterogeneity and Metastasis of Breast Cancer Cells. Cancer Res 2021; doi: 10.1158/0008-5472.CAN-20-1799.

344. Schwager SC, Mosier JA, Padmanabhan RS, et al. Link between glucose metabolism and epithelial-to-mesenchymal transition drives triple-negative breast cancer migratory heterogeneity. iScience 2022; doi: 10.1016/j.isci.2022.105190.

345. Levantini E, Maroni G, Del Re M, et al. EGFR signaling pathway as therapeutic target in human cancers. Semin Cancer Biol 2022; doi: 10.1016/j.semcancer.2022.04.002.

346. Abourehab MAS, Alqahtani AM, Youssif BGM, et al. Globally Approved EGFR Inhibitors: Insights into Their Syntheses, Target Kinases, Biological Activities, Receptor Interactions, and Metabolism. Molecules 2021; doi: 10.3390/molecules26216677.

347. Uribe ML, Marrocco I, Yarden Y. EGFR in Cancer: Signaling Mechanisms, Drugs, and Acquired Resistance. Cancers (Basel) 2021; doi: 10.3390/cancers13112748.

348. Cooper AJ, Sequist LV, Lin JJ. Third-generation EGFR and ALK inhibitors: mechanisms of resistance and management. Nat Rev Clin Oncol 2022; doi: 10.1038/s41571-022-00639-9.

349. Shi K, Wang G, Pei J, et al. Emerging strategies to overcome resistance to third-generation EGFR inhibitors. J Hematol Oncol 2022; doi: 10.1186/s13045-022-01311-6.

350. Mansour MA, AboulMagd AM, Abbas SH, et al. Insights into fourth generation selective inhibitors of (C797S) EGFR mutation combating non-small cell lung cancer resistance: a critical review. RSC Adv n.d.; doi: 10.1039/d3ra02347h.

351. Han JH, Lee E-J, Park W, et al. Natural compounds as lactate dehydrogenase inhibitors: potential therapeutics for lactate dehydrogenase inhibitors-related diseases. Front Pharmacol 2023; doi: 10.3389/fphar.2023.1275000.

352. Mishima K, Higashiyama S, Asai A, et al. Heparin-binding epidermal growth factor-like growth factor stimulates mitogenic signaling and is highly expressed in human malignant gliomas. Acta Neuropathol 1998; doi: 10.1007/s004010050901.

353. Kobrin MS, Funatomi H, Friess H, et al. Induction and expression of heparin-binding EGF-like growth factor in human pancreatic cancer. Biochem Biophys Res Commun 1994; doi: 10.1006/bbrc.1994.2131.

354. Shinefield HR. Overview of the development and current use of CRM(197) conjugate vaccines for pediatric use. Vaccine 2010; doi: 10.1016/j.vaccine.2010.04.072.

355. Wang L, Wang P, Liu Y, et al. Regulation of cellular growth, apoptosis, and Akt activity in human U251 glioma cells by a combination of cisplatin with CRM197. Anticancer Drugs 2012; doi: 10.1097/CAD.0b013e32834b9b72.

356. Kunami N, Yotsumoto F, Ishitsuka K, et al. Antitumor effects of CRM197, a specific inhibitor of HB-EGF, in T-cell acute lymphoblastic leukemia. Anticancer Res 2011; doi: 31(7):2483–2488.

357. Tang X-H, Li M, Deng S, et al. Cross-reacting material 197, a heparin-binding EGF-like growth factor inhibitor, reverses the chemoresistance in human cisplatin-resistant ovarian cancer. Anticancer Drugs 2014; doi: 10.1097/CAD.0000000000000155.

358. Dateoka S, Ohnishi Y, Kakudo K. Effects of CRM197, a specific inhibitor of HB-EGF, in oral cancer. Med Mol Morphol 2012; doi: 10.1007/s00795-011-0543-6.

359. Fiorentini G, Banfi R, Dentico P, et al. Clinical experience of treatment of metastatic melanoma and solid tumours adopting a derivative of diphtheria toxin: cross-reacting material 197. In Vivo 2013; doi: 27(2):197–202.

360. Seshacharyulu P, Ponnusamy MP, Haridas D, et al. Targeting the EGFR signaling pathway in cancer therapy. Expert Opin Ther Targets 2012; doi: 10.1517/14728222.2011.648617.

361. Tanida S, Joh T, Itoh K, et al. The mechanism of cleavage of EGFR ligands induced by inflammatory cytokines in gastric cancer cells. Gastroenterology 2004; doi: 10.1053/j.gastro.2004.05.017.

362. Takenobu H, Yamazaki A, Hirata M, et al. The stress- and inflammatory cytokine-induced ectodomain shedding of heparin-binding epidermal growth factor-like growth factor is mediated by p38 MAPK, distinct from the 12-O-tetradecanoylphorbol-13-acetate- and lysophosphatidic acid-induced signaling cascades. J Biol Chem 2003; doi: 10.1074/jbc.M211835200.

363. Kataoka H. EGFR ligands and their signaling scissors, ADAMs, as new molecular targets for anticancer treatments. J Dermatol Sci 2009; doi: 10.1016/j.jdermsci.2009.10.002.

364. Hedemann N, Rogmans C, Sebens S, et al. ADAM17 inhibition enhances platinum efficiency in ovarian cancer. Oncotarget 2018;9(22):16043–16058; doi: 10.18632/oncotarget.24682.

365. White KA, Grillo-Hill BK, Barber DL. Cancer cell behaviors mediated by dysregulated pH dynamics at a glance. J Cell Sci 2017; doi: 10.1242/jcs.195297.

366. Read JA, Winter VJ, Eszes CM, et al. Structural basis for altered activity of M- and H-isozyme forms of human lactate dehydrogenase. Proteins 2001; doi: 10.1002/1097-0134(20010501)43:2<175::aid-prot1029>3.0.co;2-#.

367. Pasti AP, Rossi V, Di Stefano G, et al. Human lactate dehydrogenase A undergoes allosteric transitions under pH conditions inducing the dissociation of the tetrameric enzyme. Biosci Rep 2022; doi: 10.1042/BSR20212654.

368. Iacovino LG, Rossi M, Di Stefano G, et al. Allosteric transitions of rabbit skeletal muscle lactate dehydrogenase induced by pH-dependent dissociation of the tetrameric enzyme. Biochimie 2022; doi: 10.1016/j.biochi.2022.03.008.

369. Stefan A, Gentilucci L, Ruffolo F, et al. Peptides inhibiting the assembly of monomeric human l-lactate dehydrogenase into catalytically active homotetramer decrease the synthesis of

lactate in cultured cells. Protein Sci 2024; doi: 10.1002/pro.5161.

370. Engel PC, Jones JB. Causes and elimination of erratic blanks in enzymatic metabolite assays involving the use of NAD+ in alkaline hydrazine buffers: improved conditions for the assay of L-glutamate, L-lactate, and other metabolites. Anal Biochem 1978; doi: 10.1016/0003-2697(78)90447-5.

371. Wan X, Liu Y, Zhao Y, et al. Orexin A affects HepG2 human hepatocellular carcinoma cells glucose metabolism via HIF-1α-dependent and -independent mechanism. PLoS One 2017; doi: 10.1371/journal.pone.0184213.

372. Lin X, Xiao Z, Chen T, et al. Glucose Metabolism on Tumor Plasticity, Diagnosis, and Treatment. Front Oncol 2020; doi: 10.3389/fonc.2020.00317.

373. Pavlova NN, Zhu J, Thompson CB. The hallmarks of cancer metabolism: Still emerging. Cell Metabolism 2022; doi: 10.1016/j.cmet.2022.01.007.

374. Cunha A, Silva PMA, Sarmento B, et al. Targeting Glucose Metabolism in Cancer Cells as an Approach to Overcoming Drug Resistance. Pharmaceutics 2023; doi: 10.3390/pharmaceutics15112610.

375. Yang J, Shay C, Saba NF, et al. Cancer metabolism and carcinogenesis. Experimental Hematology & Oncology 2024; doi: 10.1186/s40164-024-00482-x.

376. Feng H, Wang X, Chen J, et al. Nuclear Imaging of Glucose Metabolism: Beyond 18F-FDG. Contrast Media Mol Imaging 2019; doi: 10.1155/2019/7954854.

377. Yu S. Review of 18F-FDG Synthesis and Quality Control. Biomed Imaging Interv J 2006; doi: 10.2349/biij.2.4.e57.

[This page is intentionally left blank]